CONTENTS

List of Figures

Chapter 1

List of Abbreviations

°C	Degrees celcius
µl	Microlitre
µM	Micromolar
AMV	Avian myeloblastosis virus
ANOVA	Analysis of variance
APAH	Associated pulmonary arterial hypertension
ARNT	Aryl hydrocarbon nuclear translocator
ATP	Adenosine tri-phosphate
BMP	Bone morphogenetic protein
BMPR2	Bone morphogenetic protein type 2 receptor
BSA	Bovine serum albumin
CBP	CREB binding protein
CO_2	Carbon dioxide
CTEPH	Chronic thromboembolic pulmonary hypertension
DAB	Diacylglycerol
DAG	3, 3'-diaminobenzidine
DAPI	Diamino-2-phenylindole
DHEA	Dehydroepiandrosterone
DMOG	Dimethyloxalylglycine
Dvl	Dishevelled
EC-PC	Endothelial cell progenitor cell
ELISA	Enzyme-linked immunosorbant assay
EPO	Erythropoietin
ET-1	Endothelin-1
FCS	Foetal calf serum
FIH	Factor inhibiting HIF
FITC	Fluorescein isothiocynate
FIZZ1	Found in the inflammatory zone 1
FSC	Forward scatter
GAPDH	Glyceraldehyde-3-phosphate dehydrogenase
GM-CSF	Granulocyte macrophage colony stimulating factor
GSK3β	Glycogen synthase kinase-3 beta
HETE	Hydroeicosatetraenoic acid
HIF	Hypoxia inducible factor
HIMF	Hypoxia induced mitogenic factor
HIV	Human immunodeficiency virus
HLA	Human leukocyte antigen
HRE	Hypoxia response element
HRP	Horseradish peroxidase
IFNγ	Interferon gamma
IL-1	Interleukin-1
IL-10	Interleukin-10
IL-1R1	Interleukin-1 type 1 receptor
IL-1ra	Interleukin-1 receptor antagonist

IL-6	Interleukin-6
IL-8	Interleukin-8
IP3	Inositoltrisphosphate
IPAH	Idiopathic pulmonary arterial hypertension
IRAK	Interleukin- 1 associated kinase 1
kg	Kilogram
kPa	Kilopascal
LPS	Lipopolysaccharide
MCP-1	Monocyte chemotactic protein- 1
MCT	Monocrotaline
mg	Milligram
mins	Minutes
ml	Millilitre
mM	Millimolar
mmHg	Millimeters of Mercury
MMP	Matrix metalloproteinase
n	Number of experiments
NADPH	Nicotinamide adenine dinucleotide phosphate
ng	Nanogram
nm	Nanometer
NO	Nitric oxide
O_2	Oxygen
Oct-04	Octamer-binding 4
OPG	Osteoprotegerin
P/S	Penicillin G and streptomycin
PAH	Pulmonary arterial hypertension
PBMC	Peripheral blood mononuclear cells
PBS	Phosphate buffered saline
pCO_2	Partial pressure of carbon dioxide
PCR	Polymerase chain reaction
PDGF	Platelet derived growth factor
PE	Phycoerythrin
PHD	Prolyl hydroxylase
PI3K	Phosphoinositide-3 kinase
PKC	Protein kinase C
pO_2	Partial pressure of oxygen
PPH	Primary pulmonary hypertension
PPP	Platelet poor plasma
RANK	Receptor activator of nuclear factor- κB
RANTES	Regulated and normal T cell expressed and secreted
RISC	RNAi induced silencing complex
ROS	Reactive oxygen species
rpm	Rotations per minute
SEM	Standard error of mean
SMC	Smooth muscle cell
SSC	Side scatter

SSc	Systemic sclerosis
TGF-β	Transforming growth factor- beta
TLR	Toll-like receptor
TNFα	Tumour necrosis factor alpha
TRAIL	TNF- related apoptosis inducing ligand
TUNEL	Terminal deoxynucleotidyl transferase dUTP nick end labelling
UV	Ultraviolet
VEGF	Vascular endothelial growth factor
vWF	Von Willebrand factor
WHO	World health organisation

1. GENERAL INTRODUCTION

In order to enable effective oxygen distribution to the body, our circulation consists of systemic circulation and a pulmonary circulatory loop. The pulmonary circulation's primary role is to enable gas exchange and reoxygenate oxygen poor systemic blood and return its oxygenated form to the heart. The pulmonary circulation involves an intricate network of thinly walled arteries with low luminal pressure and high flow rates. Each pulmonary artery is composed of several layers including the adventitia, the media and the intima with each individual layer made up of specific cell types: fibroblasts, smooth muscle cells (SMCs) and endothelial cells respectively surrounded by extracellular matrix components. The adventitia also contains a population of progenitor cells which have the ability to differentiate into SMCs (Torsney et al., 2005). In the pulmonary circulation, the media layer is very thin compared to the systemic vasculature with the distal pulmonary arteries having little or no SMCs.

Pulmonary arterial hypertension (PAH) is a potentially devastating disease characterised by the occlusion and narrowing of the pulmonary arteries, leading to increased vascular resistance and right ventricular pressure and eventual right heart failure. Diseased vessels have been shown to have a dramatically thickened medial layer and lesions characteristic to pulmonary hypertension display excessive SMC deposition. Much work has been done to try and understand the structural pathogenesis of the disease but it is still little understood what is driving the vascular remodelling process. Inflammatory cells are thought to have a role and there is evidence of immune cell infiltrates in diseased vessels in both animal models of PAH and in PAH patient lung sections. Within these immune cell infiltrates, the monocyte is of particular interest. Monocytes have been shown to be present in a variety of animal models of PH and have been shown to be actively entering pulmonary vessels in rats prior to the development of monocrotaline (MCT) induced PH. Also monocytes have been found in plexiform lesions of pulmonary arteries isolated from children with the sporadic form of the disease but not in left heart disease

associated forms of pulmonary hypertension. Moreover, with systemic pro-inflammatory cytokine expression found to be altered in PAH and monocytes being a major source of cytokines, the monocyte is a very interesting cell type to study in relation to PAH.

Interestingly, the hypoxia inducible transcription factor, HIF, has also been found within diseased vessels. HIF is essential for myeloid cell function therefore perhaps there is a related role of the monocytes and HIF in the remodelled vessels. HIF can also be an indirect indicator of hypoxia, although the exact oxygen tensions of these areas are yet to be established. The effect of hypoxia on SMCs is controversial but there is a body of data suggesting that hypoxia induces SMC proliferation. Therefore my hypothesis is that hypoxia can induce SMC proliferation which monocytes can alter via the HIF pathway and this is different in PAH.

1.1 PULMONARY ARTERIAL HYPERTENSION

Haemodynamically, pulmonary hypertension is characterized by an elevated mean pulmonary artery pressure ≥ 25 mmHg (mm Mercury) at rest, compared to normal resting pressure of 15-20 mmHg (Simonneau et al., 2009). Pulmonary hypertension has many different forms with various aetiologies. The umbrella of pulmonary hypertension can be divided into PAH, previously known as primary pulmonary hypertension (PPH), pulmonary hypertension and left heart disease, pulmonary hypertension and lung disease and /or hypoxia, chronic thromboembolic pulmonary hypertension (CTEPH) and pulmonary hypertension with unclear multifactorial mechanisms (Table 1.1) (Simonneau, 2009). In 2008 at the Dana Point 4th World Health Organisation (WHO) symposium on pulmonary hypertension, PAH was sub-divided into the following categories: idiopathic PAH (IPAH), heritable PAH, drug- and toxin-induced PAH, associated with (APAH) including connective tissue disease APAH, HIV APAH and congenital heart disease APAH and persistent pulmonary

hypertension of the newborn (McGlothlin, 2012). The 5th WHO symposium on pulmonary hypertension is set to take place in Nice in 2013.

The severity of the disease can be further assessed in accordance to the New York heart association classification which is used when deciding on treatments. The classifications describe the limitations on the patient with least severe functional class (Class I) being pulmonary hypertension patients without limitations to ordinary physical activity and the most severe functional class (Class IV) being patients with the inability to perform any physical activity without dyspnoea and /or fatigue (Table 1.2). Patients presenting with early stage disease tend to show general symptoms or are even asymptomatic. Initial indicators are dyspnoea, fatigue, syncope, peripheral oedema and chest pain. Further diagnosis is usually made by physical examinations, chest radiographs and electrocardiogram examination followed by computed tomography and eventual confirmation by right heart catheter. Although if left untreated prognosis is poor, recent developments in treatments and better understanding have extended prognosis by more than 10 years (McLaughlin et al., 2004).

The PAH group, which can all be characterised by vascular remodelling processes during the development of the disease, is of particular interest as it is a deadly form which, if left untreated, gives rise to a median survival of only 2 ½ years (Gaine and Rubin, 1998). Females have a predisposition of 2:1 to males of contracting the idiopathic form of PAH (Barst et al., 2012). Interestingly, more than 60 % of people with IPAH have a germline mutation in bone morphogenetic protein receptor 2 (BMPR2) (Aldred et al., 2006) (Cogan et al., 2006) but surprisingly only 20 % of all people with this mutation develop the disease (Cogan et al., 2012). However, mutations in the gene for BMPR2 are recognised as being responsible for 80 % cases of heritable PAH (Machado et al., 2006). This receptor and its ligand are part of transforming growth factor β (TGF- β) family and their role in PAH is expanded below with regards to SMC proliferation.

1. Pulmonary Arterial Hypertension

1.1 Idiopathic pulmonary hypertension
1.2 Heritable
1.2.1 BMPR2
1.2.2 ALK1. endoglin
1.2.3 Unknown
1.3 Drug- and toxin- induced
1.4 Associated with
1.4.1 Connective tissue diseases
1.4.2 HIV Infection
1.4.3 Portal hypertension
1.4.4 Congenital heart diseases
1.4.5 Schistosomiasis
1.4.6 Chronic hemolytic anaemia
1.5 Persistent pulmonary hypertension of the newborn

1'. Pulmonary venoocclusive disease (PVOD) and /or pulmonary capillary hemangiomatosis (PCH)

2. Pulmonary hypertension owing to left heart disease

2.1 Systolic dysfunction
2.2 Diastolic dysfunction
2.3 Valvular disease

3. Pulmonary hypertension owing to lung diseases and /or hypoxia

3.1 Chronic obstructive pulmonary disease
3.2 Interstitial lung disease

3.3 Other pulmonary diseases with mixed restrictive and obstructive pattern
3.4 Sleep disordered breathing
3.5 Alveolar hypoventilation disorders
3.6 Chronic exposure to high altitude
3.7 Developmental abnormalities

4. Chronic thromboembolic pulmonary hypertension (CTEPH)

5. Pulmonary hypertension with unclear multifactorial mechanisms

5.1 Hematologic disorders
5.2 Systemic disorders
5.3 Metabolic disorders
5.4 Others

Table 1.1 World Health Organisation clinical classification of pulmonary hypertension as described in Dana Point, 2008.

Rewritten from Journal of the American College of Cardiology, Simonneau, G. *et al*, Updated Clinical Classification of Pulmonary Hypertension, S43-S54, copyright (2009) with permission from Elsevier.

Class I	Patients with disease but without limitation of physical activity. Ordinary physical activity does not cause undue dyspnea or fatigue or chest pain.
Class II	Patients with disease resulting in slight limitation of physical activity. Comfortable at rest but ordinary physical activity causes undue dyspnea or fatigue or chest pain.
Class III	Patients with disease resulting in marked limitation of physical activity. Comfortable at rest but less than ordinary activity causes undue dyspnea or fatigue or chest pain.
Class IV	Patients with disease with the inability to carry out any physical activity without symptoms. Patients present signs of heart failure. Dyspnea and/or fatigue may even be present at rest.

Table 1.2 World Health Organisation and New York Heart Association classification of functional class of patients with pulmonary hypertension

Rewritten from CHEST, Rubin L. J., Introduction; Diagnosis and Management of Pulmonary Arterial Hypertension: ACCP Evidence-Based Clinical Practice Guidelines, 126, 1S, copyright (2004) with permission from the American College of Chest Physicians.

The pathogenesis of PAH is still poorly understood, however, it has previously been demonstrated that all three layers of the vasculature, intima, media and adventitia, are involved in arterial remodelling in PAH patients (Chazova et al., 1995) (Stenmark et al., 2006). Endothelial cell apoptosis is thought to be the trigger inducing SMC proliferation in the vascular remodelling process (Cool et al., 1999) as the intimal layer plays a role in mediating homeostasis, aiding adhesion, maintaining the balance between vasodilators and vasoconstrictors and interacting with cells in the blood (Davies, 1986). A leaky intima due to endothelial cell apoptosis can lead to vasoconstriction, causing dedifferentiated SMCs to proliferate (Cool et al., 1999). The media contains both fully differentiated contractile SMCs which are resistant to proliferative stimuli and an inter-dispersed dedifferentiated synthetic population which readily proliferate (Frid et al., 1997). The adventitia also contains a diverse population of cells consisting of both fibroblasts and dedifferentiated SMCs which not only influence expression of extracellular matrix proteins (Stenmark et al., 2006) but also have a role in regulating vascular tone in response to ROS and injury (Irani et al., 1997) (Touyz and Schiffrin, 2004).

During the vascular remodelling process both obliterative concentric and plexiform lesions can form (Figure 1.1). Muscularisation of the pulmonary arteries from excess SMC proliferation leads to medial hypertrophy and loss of precapillaries, followed by neointima and plexiform lesion formation (Atkinson et al., 2002) (Rubin, 1997). Neointima formation describes the infiltration of dedifferentiated SMCs and extracellular matrix components between the endothelium and internal lamina preventing vessel elasticity. Altered proliferation and survival of endothelium contributes to the formation of plexiform lesions (Sakao et al., 2006). Each lesion consists of opened channels separated by proliferating SMCs and endothelial cells embedded in a cellular matrix (Atkinson et al., 2002) (Cool et al., 1999). Prevalence of lesions is increased in IPAH where endothelial cells tend to be deficient in genes for endothelial growth suppressors such as TGF-β (Humbert et al., 2004) (Stenmark et al., 2006).

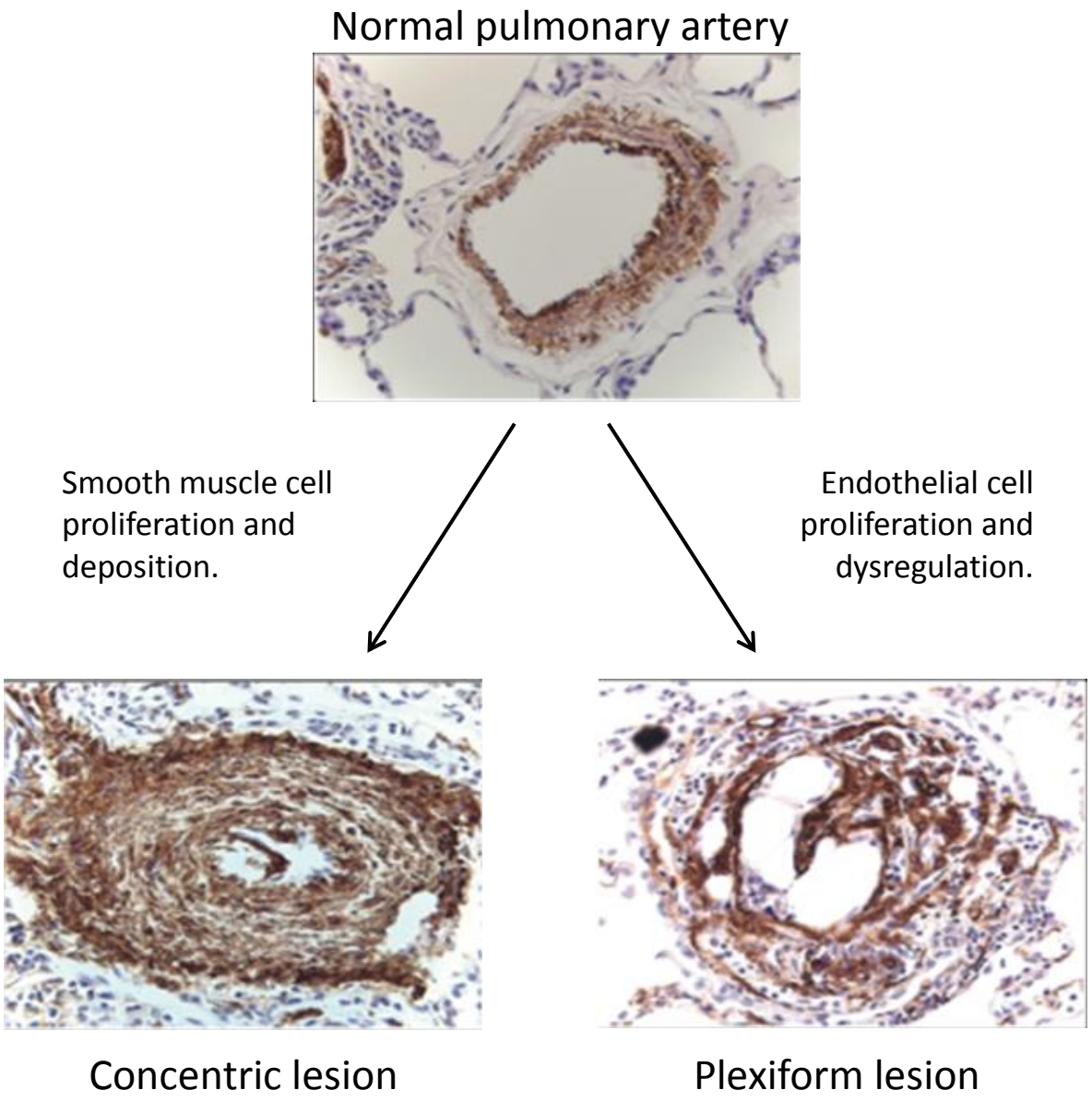

Figure 1.1 Lesion formation in pulmonary hypertension

Images are of human lung tissue samples stained for smooth muscle actin. They illustrate how normal pulmonary arteries have thin SMC walls that are dramatically thickened in PAH. In disease, pulmonary artery SMCs proliferate and swell decreasing lumen size and increasing vascular resistance. Plexiform lesion formation occurs by endothelial cell dysregulation and aberrant growth therefore SMC walls remain relatively thin with neointima formation.

1.2 SMOOTH MUSCLE CELL PROLIFERATION

One protein which has been linked to PAH and SMC proliferation is a member of the TGF-β super-family, BMPR2. Bone morphogenetic protein (BMP) ligands exert their effects through heterodimerization and phosphorylation of BMP receptor 1a or b (BMPR1a /ALK-3 or BMPR2b /ALK6) and BMPR2 on the cell surface (Chen et al., 2004). Receptor activation leads to phosphorylation of SMAD 1 /5 /8 proteins before binding the co-SMAD, SMAD4, and translocating to the nucleus where the SMAD complex regulates gene expression (Yoshida et al., 2000) (Humbert et al., 2004). BMPs are synthesised by cells in the pulmonary vasculature and maintain the balance of apoptosis and proliferation in these cells. BMPs inhibit growth, downregulate Bcl-2 (an anti-apoptotic protein) in SMCs and promote endothelial cell survival. In pulmonary hypertension, the roles of BMPs are reversed causing SMC proliferation and survival followed by endothelial death (Yuan et al., 1998). The BMPR2 gene encodes a TGF- β type II receptor, which is involved in apoptosis and cell cycle. Mutations in this gene lead to impaired SMC signalling and cell death (Yoshida et al., 2000). TGF-β itself acts on SMC proliferation by binding its type 1 and type 2 receptors. Once bound the receptors dimerise inducing phosphorylation of the regulatory SMAD proteins, SMAD2 and SMAD3. These phosphorylated proteins then bind the co-SMAD, SMAD4, and translocate to the nucleus where they form complexes with DNA binding proteins to induce transcription of cell cycle mediators such as c-Myc (Figure 1.2). More specifically this pathway has been shown to be upregulated in SMCs from IPAH patient lung explants coupled with dysregulation of the related BMPR2 pathway emphasising its importance in vascular remodelling (Morrell et al., 2001).

Similarly, SMCs from pulmonary hypertensive patients have also been shown to have altered growth response to growth factors such as VEGF and PDGF. Interestingly, expression of both VEGF itself and the type 1 receptor, Flt-1, is also increased in SMCs from pulmonary hypertension patients compared to controls (Hirose et al., 2000). Moreover, lungs from patients with pulmonary hypertension have been shown to have an increase PDGF as well enhanced

proliferation in response to the growth factor compared to healthy SMCs (Berg, 1998). Both VEGF and PDGF receptors contain kinase domains which upon ligand binding, dimerise and activate the protein kinase C (PKC) and phosphoinositide-3 kinase (PI3K) pathways. During receptor activation, intracellular calcium ion concentrations are regulated by the calcium binding protein calmodulin via PKC. Intracellular calcium influx directly modulates SMC proliferation. The PI3K pathway also regulated cell proliferation by kinase cascade from protein kinase B (also known as AKT) cascade culminating in mammalian target of rapamycin (mTOR) activity leading to transcription of genes inducing cellular proliferation (Figure 1.2).

Another pathway thought to regulate SMC proliferation is the IL- 1 pathway with IL- 1β being shown to directly induce SMC proliferation (Lawrie et al., 2011). Moreover, increased IL- 1 protein and RNA expression is found in lesions of IPAH patients as well as an increase in circulating levels when compared to healthy donors (Wong et al., 1996) (Fartoukh et al., 1998). Binding of IL- 1 to its type 1 receptor (IL- 1R1) and its accessory protein MyD88 leads to a phosphorylation cascade. IL- 1 associated kinase 1 (IRAK 1) and IRAK 4 are subsequently activated leading to downstream release of the transcription factor NF-κB. Degradation of inhibitor of κB (IκB) allows nuclear NK-κB translocation and transcription of genes such as cyclin D which regulate cell cycle progression (Figure 1.2). All these pathways contribute to SMC proliferation and are highly regulated in healthy SMCs. In disease many of these pathways are dysregulated either by increased ligand availability, receptor dysfunction or alterations to downstream pathway mediators. By fully understanding these processes new therapeutics can be developed in the hope to prevent or reverse vascular remodelling.

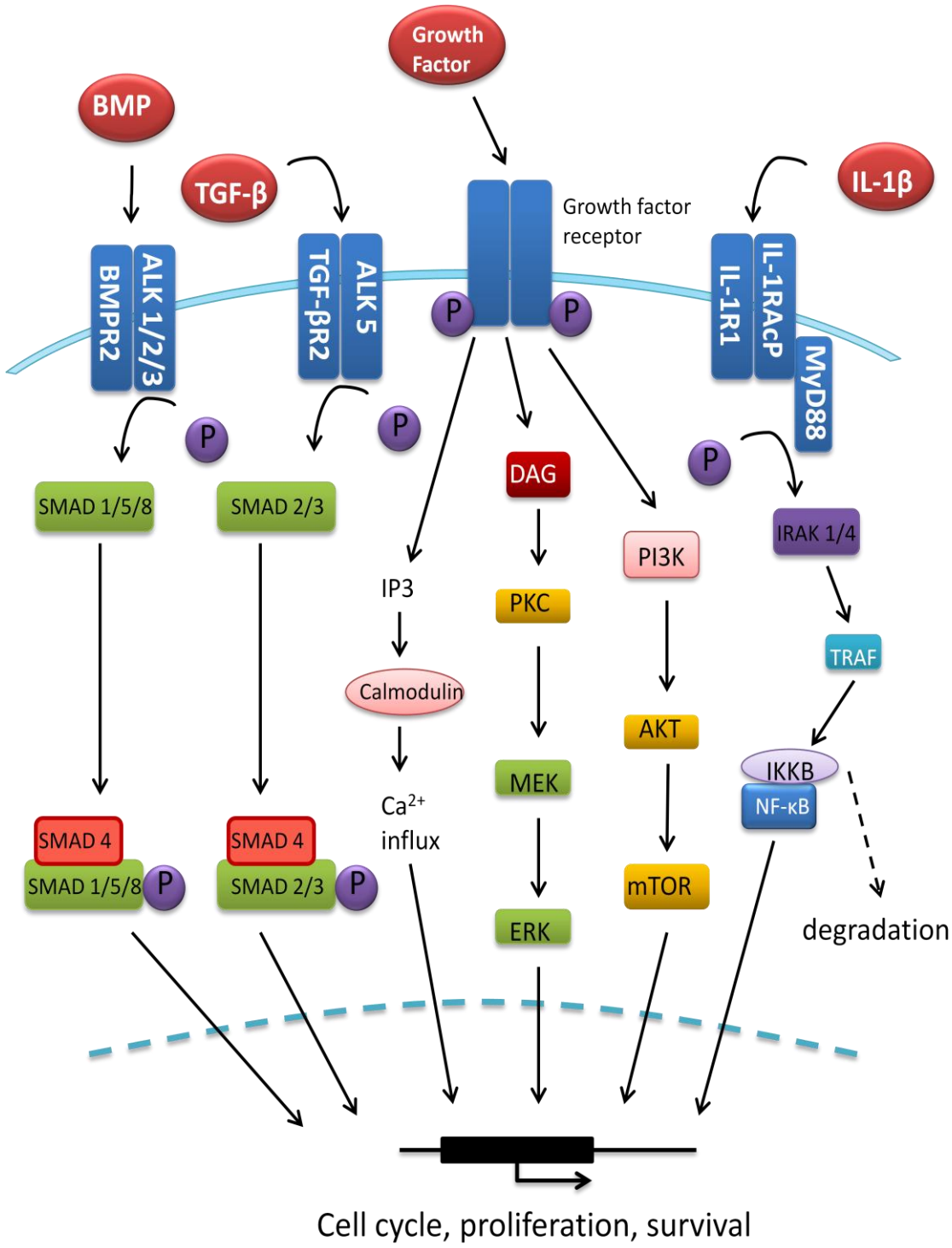

Figure 1.2 Summary of pathways influencing smooth muscle cell proliferation

A schematic depicting transforming growth factor β (TGF-β), bone morphogenetic protein (BMP), growth factors and interleukin- 1 (IL- 1) signalling pathways. Upon ligand binding each receptor induces a phosphorylation reaction and activation of separate pathway members culminating in SMC proliferation.

1.3 PULMONARY ARTERY CELLS AND HYPOXIA

Local hypoxia has been implicated as a potential initiating factor for PAH with hypoxia exposure causing proliferation of both SMCs and fibroblasts *in vitro*. In humans systemic hypoxia exposure can directly induce pulmonary hypertension as seen in Dana Point classification group 3. Although the pathogenesis of hypoxia induced pulmonary hypertension is different from PAH we can gain insights into a role of hypoxia in the disease. Altitude studies by Maggiorini and Penazola showed that residents at high altitudes and low oxygen bioavailability had increased pulmonary arterial pressures than those at sea level. Also newcomers to high altitude were more susceptible to developing pulmonary hypertension but this phenomenon was reversed upon maintained residence at altitudes close to sea level (Maggiorini, 2003) (Penaloza and Arias-Stella, 2007). Exact oxygen tensions of the pulmonary artery vessel wall are unknown but perhaps the local oxygen mismatch could be an initiating trigger for SMC proliferation in both hypoxia induced PH and PAH.

Further evidence that hypoxia may be a trigger for disease progression comes in the form of pulmonary hypertension mammalian models. Many pulmonary hypertension murine models have used incubation in hypoxia along with a secondary stimulus to induce the diseased state (Beppu et al., 2004) (Liu et al., 2005) (Eddahibi et al., 1999) (Steiner et al., 2009) (Frid et al., 2009). Hypoxia has also been shown to affect the vascular cells directly but this is controversial. Whilst some *in vitro* studies show that 3-5 kPa oxygen in the media can induce pulmonary artery SMC proliferation in both human derived cells (Cooper and Beasley, 1999) (Yang et al., 1997) (Tamm et al., 2004) and bovine SMCs (Hassoun et al., 1989) others have shown an anti-proliferative phenotype of SMCs in oxygen tensions of 0-3 kPa oxygen (Dempsey et al., 1991) (Eddahibi et al., 1999). The controversy surrounding SMC proliferation in hypoxia is compounded by the fact that within the same paper Frid et al. have shown a dual proliferative phenotype of SMCs exposed to 3 kPa oxygen but with different serum concentrations (Frid et al., 1997). However, seeing as none of these papers used the same culture conditions or SMCs derived from the same

sourse it is difficult to determine the effect of hypoxia on SMC proliferation. Despite the controversy, most papers suggest that in 5-10 % serum and 3-5 kPa oxygen in the media, SMCs proliferate. However, the method by which hypoxia induces SMC proliferation is still unknown. An *in vivo* study using auto antibodies against potassium voltage-gated channels found that hypoxia can inhibit potassium channels and initiate vasoconstriction in rat vascular SMCs (Archer et al., 1998). Further to this potassium channels were found to be inhibited in human SMC incubated under 5 % hypoxia (Post et al., 1992). These data give us insights into potential mechanisms by which hypoxia can induce the diseased state but it is still unknown how hypoxia can induce SMC proliferation.

1.4 MONOCYTES IN DISEASE

Monocytes are short lived circulating phagocytes that can live between 1 to 3 days in the circulation and represent approx. 10 % of the total mononuclear cell population (Fogg et al., 2006). Although few in number these cells have important pro-inflammatory roles and are a major source of cytokines. Further to this, monocytes have patrolling roles in the circulation allowing interactions with antigen presenting cells thus activating the adaptive immune response and the complement cascade targeting pathogens for degradation and killing. Moreover, monocytes are able to aid margination of neutrophils into tissues from the circulation (Kreisel et al., 2010) and can themselves migrate into damaged or injured tissues.

The monocyte population can be divided into groups based on their differentiation state (Thomas and Lipsky, 1994). Circulating monocyte populations consist of the more common cluster of differentiation 14 positive ($CD14^+$) monocyte and the more mature cluster of differentiation 16 positive ($CD16^+$) monocyte (Ziegler-Heitbrock et al., 1988) (Sunderkotter et al., 2004). $CD16^+$ monocytes are a longer lived subset (Hilgendorf and Swirski, 2012) but only form 20- 30 % of total monocyte populations (Passlick et al., 1989).

Analysis of both subsets found upon stimulation both were able to induce respiratory burst but $CD16^+$ showed less phagocytosis or adhesion molecule expression (Passlick et al., 1989). Moreover $CD16^+$ monocytes lack the monocyte chemotactic protein- 1 (MCP-1) receptor so are thought not to be the first cell type to be recruited to sites of inflammation and have a more regulatory and patrolling role in the vasculature (Weber et al., 2000). Therefore my work has explored the role of the $CD14^+$ 'classical' monocyte also known as the 'pro-inflammatory' monocyte due to its large contribution to ROS and inflammatory cytokine expression upon activation.

In relation to PAH, monocyte infiltration seems to occur prior to disease onset. For example, the monocrotaline (MCT) rat model of PAH shows monocyte and lymphocyte infiltration into the pulmonary vasculature from 1-24 hours post injection prior to vascular remodelling (Voelkel and Tuder, 1994). The insult of MCT may cause the monocytes to alter their protective phenotype to allow severe vascular remodelling. Perivascular monocytes have been shown to increase expression of many stress markers such as nitrotyrosine upon MCT injection (Dorfmuller et al., 2011) which may induce a phenotypic alteration preventing monocytes from being able to maintain vascular tone. Further evidence for a role of immune cells in the pathogenesis of PAH have been provided in humans by work from Klein *et al*. who have shown the predominance of leukocytes in lung tissue from treatment naive children with IPAH. These sections were compared to normal post-mortem child lung sections and those from children with congenital heart disease associated pulmonary hypertension of which both had considerably less leukocyte presence (Hall et al., 2009). Moreover, Voelkel's group described aggregations of macrophages within the plexiform lesions themselves from seven of ten severe PAH patient lung tissue isolates. Interestingly T cells and macrophages were seen invading the vascular wall of pulmonary arteries with early signs of remodelling (Tuder et al., 1994). It is postulated that these immune cells have a direct role in the pathogenesis of PAH by influencing vascular remodelling (Dorfmuller et al., 2003). This theory is strengthened by the fact that myeloid cells have been shown to be present in the vasculature during the remodelling

process from lung sections of patients with PAH compared to unaffected explanted lung (Cool et al., 1999) (Frid et al., 2006). Moreover, in the hypoxic murine model of PH depletion of circulating leukocytes prevented remodelling in pulmonary arteries. However, these data are descriptive and the actual role of these immune cells in the pathogenesis of PAH is yet to be established.

Not only are monocytes themselves thought to be involved in the pathogenesis of PAH but also cytokines produced from these cells. In pulmonary hypertension, circulating serum concentrations of both IL- 1 and IL- 6 pro-inflammatory cytokines are upregulated compared to healthy controls. IL- 1 acts on both vascular cells (endothelial cells and SMCs) and monocytes inducing proliferation and migration of vascular cells and exacerbating inflammation (Humbert et al., 2004) Although not in pulmonary SMCs it is known that IL- 1 signalling has been shown to modulate systemic artery remodelling. Work by Chamberlain *et al*. showed that mice deficient in IL- 1 receptor type 1 (IL-1R1$^{-/-}$) had decreased neointima formation upon vascular injury by ligation of the carotid artery compared to IL- 1R1$^{+/+}$ control mice after 14 days (Chamberlain et al., 2006). Furthermore, IL- 1R1 antagonist (IL- 1ra) fed pigs also had reduced neointima formation after injury from oversized stents in coronary arteries compared to control pigs which were injured but not administered IL-1ra (Morton et al., 2005). Extrapolating from this data perhaps the IL- 1 pathway also plays a role in pulmonary arterial remodelling. In relation to pulmonary hypertension monocrotaline (MCT) treated rats, which develop severe pulmonary hypertension, were administered twice daily injections of 2 mg /kg IL- 1ra or PBS. Rats administered with IL- 1ra had significantly reduced pulmonary hypertension progression after 3 weeks as determined by hemodynamic analysis compared to controls (Voelkel et al., 1994). Taken together, these data and the knowledge that IL- 1β can directly influence pulmonary artery SMC migration and proliferation (Lawrie et al., 2011) implicate a role of IL- 1 in PAH progression, however, the mechanism is yet to be established.

Another important proinflammatory cytokine in disease is IL- 6, it is consistently increased in the serum and lungs of patients with IPAH and

rheumatoid arthritis (Humbert et al., 1995) (Nishimaki et al., 1999). Moreover, lung specific IL-6 over expressing mice showed significant vascular remodelling as seen in progressed PAH. Interestingly, 5 % hypoxia progressed remodelling of pulmonary vessels further (Steiner et al., 2009). Previous work in rats with MCT induced pulmonary hypertension showed proinflammatory cytokines highly expressed in remodelled pulmonary arteries than compared to those resistant to remodelling (Voelkel et al., 1994). Interestingly, immunosuppressant therapy has been shown to reduce PAH progression in mice with hypoxia induced PAH again showing the importance of inflammation in PAH progression (Dorfmuller et al., 2003). Overall, although most of these data are descriptive both the presence of monocytes in remodelling vessels and the fact that they are a major source of cytokines involved in the disease strengthen the argument that these cells are important in PAH.

1.4.1 MONOCYTE RECRUITMENT

Cross talk between inflammatory immune cells and vascular tissue cells may play an important role in IPAH. Cell and tissue interactions are essential for chemotaxis, inflammation and myeloid cell invasion into tissue. For example, endothelial cells produce platelet activating factor that induces myeloid cell adherence in hypoxia (Milhoan et al., 1992). Endothelial cells also express E- and P- selectins, vascular cell adhesion molecules, MCP-1 and chemokines which is essential for recruitment of circulating myeloid cells. Monocytes can in turn activate endothelial cells via cytokines such as tumour necrosis factor α (TNF α) enabling them to recruit more circulating lymphocytes and monocytes (Tsouknos et al., 2003).

Monocyte recruitment involves several steps namely capture, rolling, slow rolling, adhesion and finally transmigration through the endothelium. The capture process involves transient interactions between Selectin proteins and their transmembrane glycoprotein ligands. Selectin mediated low affinity binding is strengthened by chemokine activation leading to rolling of the

leukocyte along the endothelium. The transit time of leukocyte recruitment depends on chemokine stimulation. Chemokine signalling aids high affinity integrin binding, this allows slow rolling of leukocytes along the endothelium and finally adhesion with the aid of the immunoglobulins intercellular adhesion molecule- 1 (ICAM- 1) and vascular cell adhesion molecule- 1 (VCAM- 1) (Chavakis et al., 2009). With respect to PAH, expression of these immunoglobulins is decreased in diseased vessels proportionally to vessel damage by monocrotaline particularly in the case of platelet/ endothelial cell adhesion molecule-1 (PECAM-1) (Huang et al., 2012). By blocking this leukocyte recruitment in endothelial cell specific BMPR2 knockout mice, PAH is significantly reduced both heamodynamically and pathologically (Burton et al., 2011). These findings reflect work using anti-inflammatory drugs to reduce the progression of PAH in these same mice and mice with hypoxia induced PH (Dorfmuller et al., 2006). Incidentally, also in the endothelial cell specific BMPR2 knockout mice, it was shown that the increased circulating levels of endothelin- 1 (ET- 1) in mice with PH was not only due to endothelial derived ET- 1 but also monocytes themselves were adding to ET- 1 secretion (Talati et al., 2010). ET -1 is a potent vasoconstrictor which is thought to contribute directly to vascular remodelling, these data suggest that monocytes may be driving the remodelling either by systemically secreting ET- 1 or expressing ET-1 locally once recruited and thus driving the remodelling process.

Expression profiles of adhesion molecules, with regards to integrins, are increased in pulmonary hypertension compared to healthy controls in humans. This is true for both vascular cell expression and circulating cell expression (Larsen et al., 2011). This means that not only are more cells recruited to pulmonary vessels but also the circulating cells themselves are expressing more adhesion molecules and are more ready to infiltrate the pulmonary artery. It has also been found that chemokine stimulation induces this increase in integrin expression on circulating cells emphasising the important role of chemokine in monocyte recruitment (Larsen et al., 2011). Moreover, many of the chemokines have been shown to be increased in murine models of PAH. For example, macrophage migration inhibitory factor which is an early

inflammatory cytokine has been found to be increased in lungs of rats with hypoxia induced pulmonary hypertension. Subsequent investigation identified that migration inhibitory factor specifically induces pulmonary artery SMC proliferation via activation of the ERK phosphorylation cascade (Zhang et al., 2011). Also in the rat, MCP- 1 inhibition by intramuscular injection of a deletion mutant MCP- 1 gene significantly reduced vascular remodelling when compared to non-injected controls. In humans, patients with developed PAH have been found to have significant increases in circulating levels of the chemokine regulated and normal T cell expressed and secreted (RANTES) (Dorfmuller et al., 2007), the CX(3)C chemokine fractalkine (Balabanian et al., 2002) and the chemokine macrophage inflammatory protein- 1α (Fartoukh et al., 1998) compared to healthy controls. It was proposed that the chemokines and cytokines produced by the inflammatory cells may, in fact, encourage pulmonary artery SMC proliferation (Cool et al., 1999).

Chemokine or Adhesion molecule	Secreted by	Studied in	Reference
Increased			
E- Selectin P- Selectin PAF	EC EC EC	porcine *in vivo*	Milhoan, 1992
TNFα	monos	human *in vitro*	Tsouknos, 2003
ET-1	EC	murine *in vivo*	Talati, 2010
CX3CL1	circulating	human *in vivo*	Larsen, 2011
MIF	circulating	rat *in vivo*	Zhang, 2011
RANTES	circulating	human *in vivo*	Dorfmuller, 2007
Fractalkine	circulating	human in vivo	Fartoukh, 1998
Decreased			
ICAM-1 VCAM-1 PECAM-1	EC EC EC	rat *in vivo*	Huang, 2012
CCR7	leukocytes	murine *in vivo*	Larsen, 2011

Table 1.3 Adhesion molecule and chemokine changes in pulmonary arterial hypertension.

A table illustrating the changes in chemokine and adhesion molecule expression found in the literature with regards to pulmonary arterial hypertension.

1.5 HYPOXIA

Ambient oxygen tension is in the region of 150 mmHg, however, biologically cells rarely see such high tensions. High oxygen tensions can dramatically affect cell homeostasis, for example, exposure to ambient oxygen tension directly effects human endothelial cell expression of plasminogen activator inhibitor, an important protein in clot breakdown *in vitro* (Gertler et al., 1993) and isolated islets of Langerhans release of insulin (Kuhtreiber et al., 1993). Human body oxygen tensions are about 40 mmHg in liver, 30 mmHg in muscle, 20 mmHg in tissue but much lower at sites of inflammation (Wiener et al., 1982) (Lund et al., 1995). Mammalian cells utilise oxygen for energy production by aerobic mitochondrial respiration. Critically, once the Pasteur point of oxygen is reached, human cells revert to energy production by anaerobic glycolysis. The ability of myeloid cells to function in inflamed areas depends on their capacity to utilise glycolysis, as opposed to mitochondrial respiration, as an energy source. Myeloid cells use the anaerobic glycolysis pathway for their ATP production independent of oxygen tensions. When glycolysis is inhibited in neutrophils and macrophages their functional capacity is rapidly impaired (Cramer et al., 2003), but the same is not seen if mitochondrial inhibitors are used (Borregaard and Herlin, 1982), indicating the importance of glycolysis and also suggesting that these cells evolved very early in phylogeny prior to our symbiotic relationship to mitochondria. All human cells have the innate ability to sense oxygen, which is controlled by oxygen sensitive hydroxylases and their influence upon hypoxia inducible transcription factor (HIF). HIF activation leads to transcription of many essential genes for host defence, disease susceptibility and glycolysis.

1.5.1 HIF PATHWAY

HIF is a hypoxia induced transcription factor and is found in all metazoans. Greg Semenza's group discovered the HIF protein and over 1-4 % genome is directly HIF regulated (Ahmed, 2010). HIF proteins are basic-helix-loop-helix (bHLH) – PAS proteins (containing sequence homology to the Drosophila Per-ARNT-AHR-Sim domains) as determined by genetic screening and protein microsequence analysis (Wang et al., 1995). HIF is a heterodimer comprising of HIF- 1α and HIF- 1β subunits. The HIF- 1β subunit (also known as aryl hydrocarbon nuclear translocator (ARNT)) is constitutively expressed in all cells while the HIF- 1α subunit is precisely regulated by cellular oxygen (Semenza, 2000). HIF α subunit has 3 isoforms: HIF- 1α, HIF- 2α and HIF- 3α. The expression patterns of these isoforms differ in various tissues. HIF expression is also altered by hypoxia shown by rats having increased mRNA levels of HIF- 1α, -2α and -3α after 12 days incubation in hypoxia (Chen et al., 2006). Little is known about HIF- 3α, other than that multiple splice variants can inhibit HIF- 1 (Makino et al., 2002). HIF- 3α has a low expression profile in most cells except lung epithelial cells where it is found in abundance and increased further in response to 1 % oxygen in comparison to HIF- 1α expression (Li et al., 2006). HIF- 2α is not found in all cell types but has large sequence homology to HIF- 1α. Despite their similarities, HIF- 1α and HIF- 2α have not been proven to have functional redundancy (Gleadle et al., 2006). Being the most abundant isoform, HIF- 1α is the best studied of the three isoforms and is found in all cell types.

HIF is regulated by two post-translational mechanisms: by the oxygen sensing prolyl hydroxylases (PHD) and by factor inhibiting HIF (FIH). These enzymes are dependent on iron uptake into their core for activation. Iron chelators can effectively inhibit both PHD and FIH function (Semenza, 2004). There are three PHD enzymes that directly control HIF, named PHD 1, PHD 2 and PHD 3. In oxygen abundant conditions, these enzymes hydrolyse HIF- 1α at proline-402 and proline-564 residues in the oxygen dependant degradation domain (ODDD) using oxygen available from tissue (Pugh, 1997), thus targeting it to the von Hippel Lindau (VHL) tumour suppressor protein (a subunit of E3 ubiquitin

ligase) for ubiquitination and subsequent degradation (Percy et al., 2006). Disruption of proline-402 and proline-564 residues in HIF- 1α prevents VHL binding. The binding efficiency of VHL to HIF- 1 is increased 1000 times following proline hydroxylation showing the important role PHD enzymes have in HIF regulation (Chowdhury et al., 2009). FIH also regulates HIF but to a lesser extent than the PHDs. FIH exerts its effects by hydroxylating asparagine-803 residue on HIF- 1α to reduce its affinity to co-activators CREB binding protein (CBP) and p300. This reduces its binding to hypoxia response elements (HREs) in promoters of target genes (Masson et al., 2012) (Figure 1.3).

In reduced oxygen tensions, stabilised HIF- 1α binds HIF- 1β subunits allowing transcription of genes containing HREs in their promoters including the genes for PHD 2 and PHD 3 which negatively feedback upon HIF protein expression (Figure 1.4). Discovery of genes with HRE in their promoters has a constant turnover with the latest being identified as early as this year. This gene was KCNMB1 which encodes for the β-1 subunit of large conductance calcium dependant potassium channels. These channels are tetramer complexes consisting of four α subunits that interact with β-1 subunits (Wu, 2003). Expression of the β-1 subunits have been found to be increased in hypoxia and further examination identified two HREs in the promoter of KCNMB1 (Ahn et al., 2012).

In some cases, HIF can also be regulated in an oxygen independant manner. For example, Nizet's group showed that HIF-1 alpha expression at the transcriptional level can be regulated in a TLR4 dependant fashion by the TLR4 agonist LPS in myeloid cells (Peyssonnaux, 2007). How bacterial stimuli can induce HIF-1 expression in myeloid cells is yet to be explored as does the effect of hypoxia on monocyte HIF expression and monocyte function. However, the effect of hypoxia on monocyte-derived macrophages has been looked at. It has been shown that monocyte-derived macrophages exposed to hypoxia have increased expression of HIF-1 both *in vitro* and in those located at sites of tumours in mice (Burke et al., 2003) (Elbarghati et al., 2008).

Although HIF is primarily regulated by oxygen tension and by bacterial stimuli in myeloid cells, there is also evidence of indirect HIF regulation by growth factors such as PDGF and VEGF involving cross-talk with the NF-κB pathway (Tsapournioti et al., 2013) (ten Freyhaus et al., 2011). It is unknown how both the NF-κB and the HIF pathway interact but Ruis *et al*. have shown that the interaction of HIF and the NF-κB pathway member IKKβ is important in innate cell function *in vitro* and in mice (Ruis et al., 2008). Further to this, in the field of cancer, much data supports a differential regulation of HIF-1 and HIF-2 (Wu et al., 2011)(Raghavan et al., 2012). Perhaps this is also true of vascular cells and myeloid cells but it is an area that is yet to be explored.

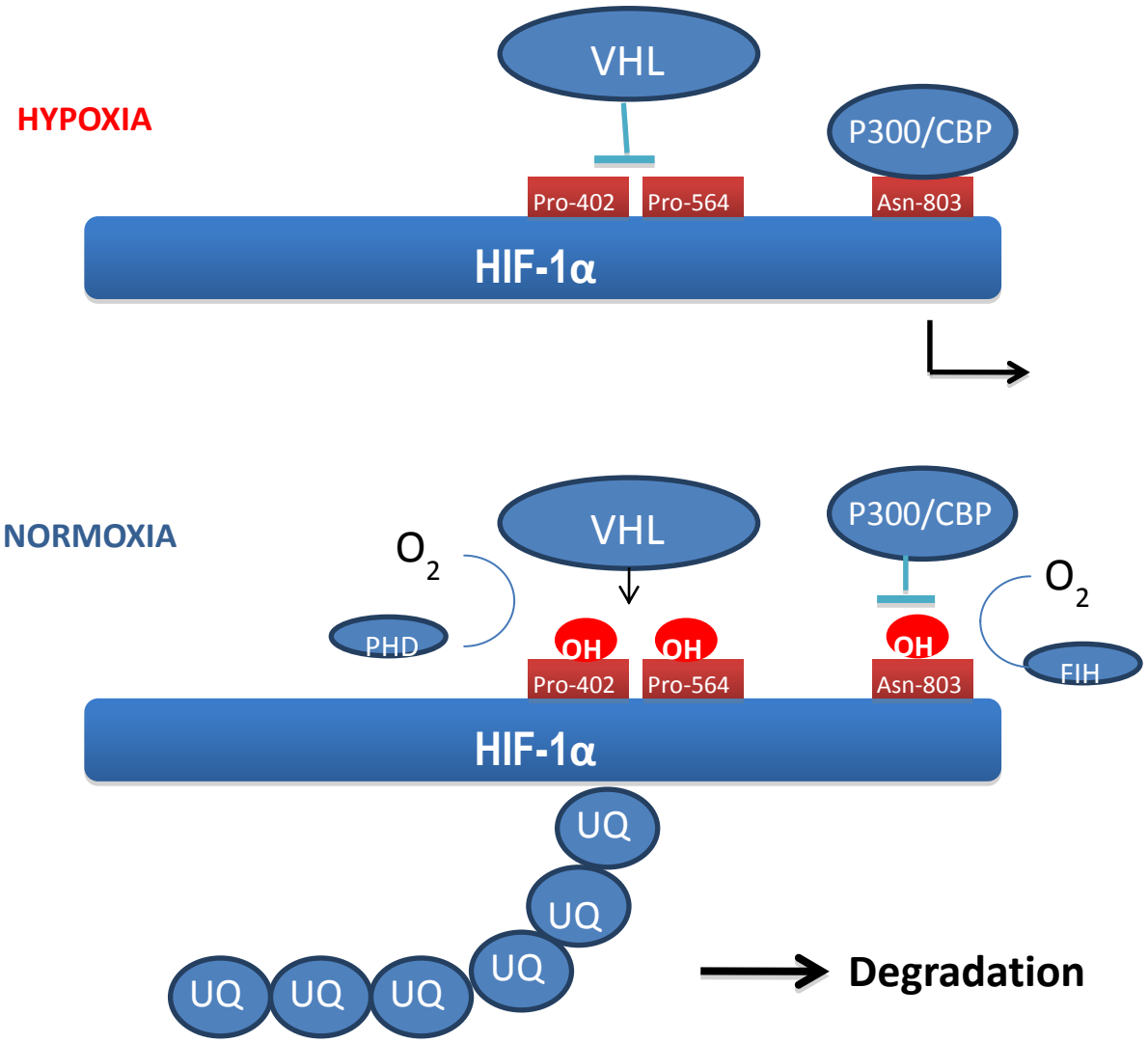

Figure 1.3 HIF oxygen dependant regulation

The HIF- 1α subunit of HIF is regulated by two oxygen sensitive hydroxylases. In hypoxia the HIF- 1α subunit is stabilised and is able to bind to its co-factors p300 and CREB binding protein (CBP) allowing transcription. When cellular oxygen concentrations are high, prolyl hydroxylase domain proteins (PHDs) use oxygen to hydroxylate proline-402 and proline-564 residues allowing binding of von Hippel Lindau tumour suppressor protein. This is an E3 ubiquitin ligase protein targeting HIF-1α for degradation. Furthermore, factor inhibiting HIF (FIH) hydroxylates aspargaine-803 reducing its affinity to p300 and CBP. Based on diagram from Semenza, (2004) Hydroxylation of HIF-1: oxygen sensing at the molecular level, Physiology, 19, 176-182.

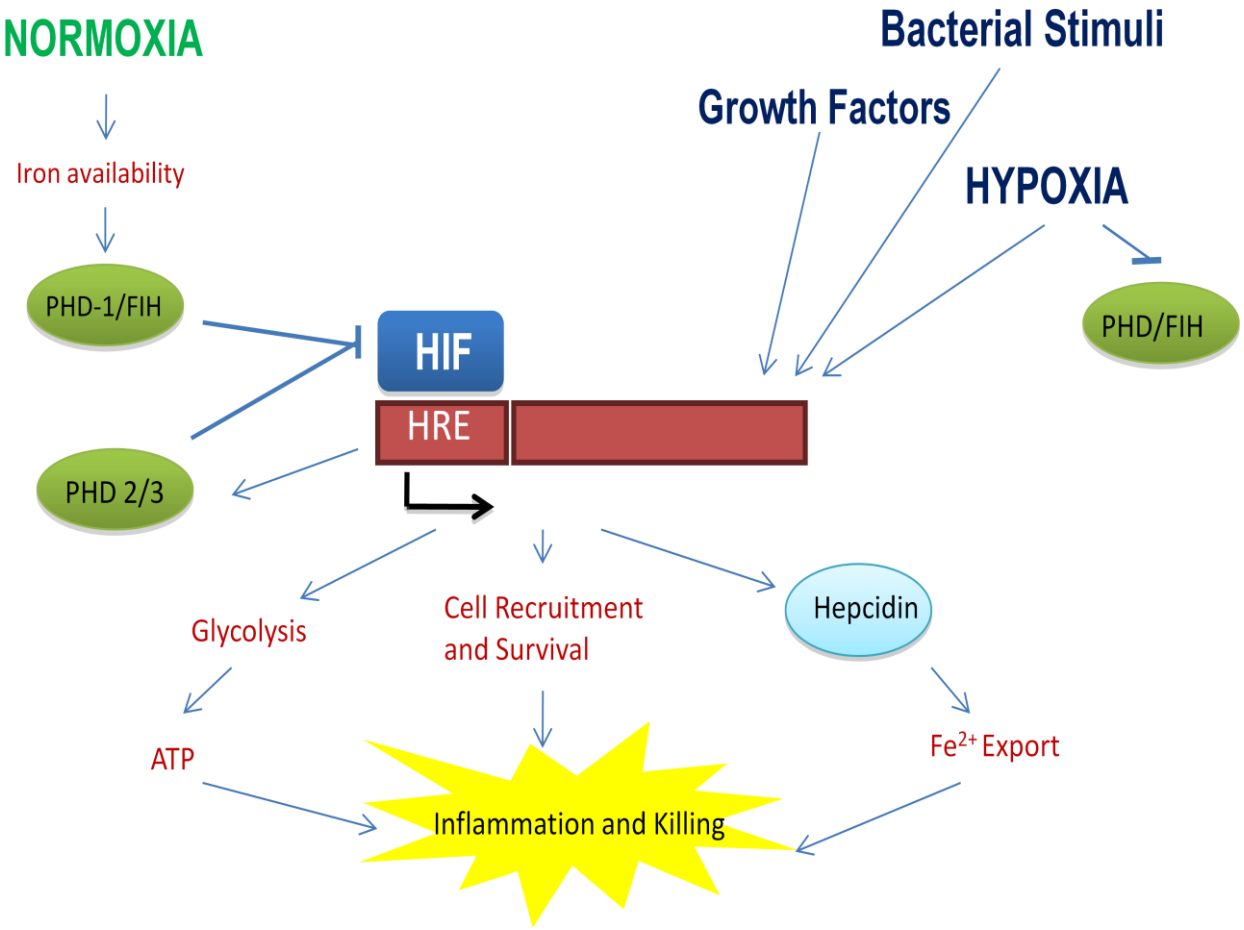

Figure 1.4 The HIF pathway

HIF-1 is a transcription factor regulated by oxygen sensitive hydroxlases. In normoxia and iron replete conditions the oxygen sensitive prolyl hydroxylase proteins-1, -2, -3 (PHD-1, -2, -3) and factor inhibiting HIF (FIH) prevent HIF downstream effects. Hypoxia and bacterial stimuli such as LPS, stabilises HIF allowing it to bind to hypoxia response elements (HRE) in promoters of varies genes. HIF activated genes include glycolytic enzymes enabling anaerobic energy production, myeloid cell pro-survival proteins and enzymes for iron export.

Better understanding is needed to fully elucidate the role of hypoxia and the HIF pathway in pulmonary hypertension. It is known that prolonged hypoxia in murine models induces pulmonary hypertension (James and Thomas, 1968) (Meyrick and Reid, 1978) but the mechanism of disease progression is unclear. Hypoxia is also used as a secondary stimulus to induce pulmonary hypertension in mice. For example, the VEGF receptor inhibitor, Sugen- 5416, causes mild increases in pulmonary arterial pressures but when administered to hypoxic rats it caused a severe pulmonary hypertension phenotype with vascular remodelling (Taraseviciene-Stewart et al., 2001) (Laird et al., 2002). Also mice heterozygous for BMPR2 have been shown to develop pulmonary hypertension but vascular remodelling is progressed further with exposure to chronic hypoxia (Beppu et al., 2004). Chronic hypoxic mice which develop pulmonary hypertension have been found to have pulmonary vascular infiltrates of fibocytes which are circulating precursor cells of monocyte lineage. During vascular injury fibroblasts and fibrocytes are first recruited to pulmonary arteries. Here they contribute to neointima formation by proliferating and inducing deposition of extracellular matrix proteins. This suggests that hypoxia helps initiate neointima formation in diseased arteries (Frid et al., 2006).

As previously mentioned, oxygen depletion leads to impaired potassium channel function in SMCs, the resulting cell membranes depolarise giving intracellular calcium ion influx. Increased intracellular calcium concentrations lead to vasoconstriction and cell proliferation. Humbert *et al* have shown that hypoxia depolarises vascular membranes at sites of vascular remodelling in rats (Humbert et al., 2004). The proliferative effects of hypoxia have been difficult to replicate *in vitro* giving contradictory data as to the effects of hypoxia on vascular cells. In spite of this, it has been shown that hypoxia increases proliferation of SMC and endothelial cells by inhibition of anti-mitogenic factors and production of mitogenic stimuli, which in turn induces extracellular matrix protein production (Pak et al., 2007).

Interestingly, when explants from PAH patients were investigated, HIF- 1α was found at both the mRNA and protein level in the plexiform lesions of diseased pulmonary vessels (Tuder et al., 2001). Expression of HIF is highly regulated by

oxygen sensing enzymes which are very responsive to iron availability. Unsurprisingly, iron prevalence modifies pulmonary arterial pressure in hypoxia. To further investigate the effects of iron in the pulmonary vessel response to hypoxia, Smith *et al*, carried out *in vivo* studies on healthy subjects. The group gave intra venous iron or iron chelator over several weeks to patients followed by 8 hours sustained hypoxia. Results showed lower pulmonary arterial systolic pressure in hypoxia from subjects given iron supplements compared to non-administered controls (Smith et al., 2008). This further strengthens the view that hypoxia is important in the development of pulmonary hypertension and understanding of the mechanisms involved could potentially aid defence against disease progression.

Work from Celeste Simon's group implicated a role for HIF itself in the pathogenesis of pulmonary hypertension using a murine model of Chuvash polycythemia. The Chuvash form of erythrocytosis is a rare form found locally in Chuvashia hence its name. The disease results from an autosomal recessive mutation in the VHL protein. Similar to human disease, mice with a homozygous mutation for arginine substitution to tryptophan at residue 200 of VHL ($VHL^{R/R}$) are susceptible to spontaneously develop pulmonary hypertension. Lungs from $VHL^{R/R}$ mice with pulmonary hypertension were found to have substantial vascular remodelling and macrophage infiltration characteristic to pulmonary hypertensive diseased vessels but also increased endothelial cell expression HIF- 2α protein (Hickey et al., 2010). HIF- 2 target genes as well as HIF- 2 protein itself has also been shown to be increased in pulmonary artery endothelial cells from lung sections of mice exposed to hypoxia (Krotova et al., 2010). Furthermore, loss of function experiments in $VHL^{R/R}$ HIF- $2\alpha^{+/-}$ mice showed delayed onset of pulmonary hypertension when compared to $VHL^{R/R}$ mice with fully competent HIF- 2 (Hickey et al., 2010). Together with the fact that dominant active mutations in HIF- 2α are linked with development of severe pulmonary hypertension (Gale et al., 2008) a potential role for the HIF pathway in pulmonary hypertension pathogenesis is postulated. Further investigation could identify potential therapeutic interventions targeting the HIF pathway for reduction in the development of pulmonary hypertension.

1.6 RATIONALE AND AIMS

IPAH is a devastating disease characterised by the narrowing and occlusion of the pulmonary arteries leading to increase right ventricular pressure and eventual failure. Inflammation has been linked as a contributor to the vascular remodelling process which occurs in this disease however, the mechanism by which it contributes is unknown. Within the characteristic lesions of the disease, there is a predominance of innate immune cells but the relevance of this is still to be established. Pulmonary arterial SMCs have been shown *in vivo* to proliferate to hypoxia and plexiform lesions from IPAH patients stain positive for the hypoxia inducible factor HIF-1. Despite the exact oxygen tensions of these areas being unknown a role for hypoxia and the HIF pathway in IPAH is postulated.

Therefore my hypothesis is that hypoxia induces pulmonary artery SMC proliferation which monocytes can inhibit in a HIF dependant manner and this is altered in disease.

In order to prove my hypothesis I hope:

- To culture SMCs in normoxia (19 kPa) and hypoxia (3 kPa) and measure SMC proliferation
- To use a co-culture model to investigate monocyte and SMC interactions both in normoxia (19 kPa) and hypoxia (3 kPa) and discover if monocytes can regulate SMC proliferation
- If monocytes have a role in SMC proliferation regulation, identify if this is dependant on the HIF pathway
- To ascertain if monocytes or SMCs from IPAH patients alter my observed phenotype.

2. METHODS

2.1 WHITE BLOOD CELL ISOLATION AND PURIFICATION

2.1.1 WHITE BLOOD CELL ISOLATION BY THE OPTIPREP™ METHOD

Peripheral blood was taken from healthy volunteers or PAH patients with informed consent in accordance with the South Sheffield Local Research Ethics Committee or the Sheffield Cardiovascular Biomedical Research Unit Ethics respectively. Sterile technique and good lab practice was carried out throughout to avoid infection or activation of cells. Centrifuge spins were carried out at room temperature and reagents warmed to 37 °C in a pre-warmed water bath. Whole blood was decanted into a 50 ml conical tube (SARSTEDT AG & Co) containing 4.4 ml 3.8 % tri sodium citrate (Martindale Pharmaceuticals) per 50 mls blood to prevent coagulation. The blood was spun at 1200 rpm for 20 mins to give two phases of upper platelet rich plasma (PRP) and lower cell rich phase. The upper phase was transferred to a clean 50 ml conical tube and spun at 2000 rpm for 20 mins leaving platelet poor plasma (PPP) supernatant and a hard platelet rich pellet. The supernatant was poured into a clean 50 ml conical tube to avoid resuspension of the platelet pellet. To the lower cell rich phase 6 mls 6 % dextran (Sigma-Aldrich Ltd) was added and topped up to 50 mls with 0.9 % saline (Baxter Healthcare Ltd). Gentle inversion was used to mix the tube and all air bubbles removed with a Pasteur pipette (Greiner bio-one). The lid was loosened and erythrocytes left to sediment for 20 mins in a warm incubator at 37 °C after which the upper phase removed and spun at 1000 rpm for 6 mins.

Gradients were prepared for cell separation by an adapted protocol using OptiPrep™ (Axis-shield, Alere), a 60 % iodixanol in water solution. OptiPrep™ can be used in conjunction with 80 % 1 x Hanks' Balanced Salt Solution (Gibco, Life Technologies) and 20 % PPP (buffer) to make a gradient suitable for immune cell separation. Before making the gradient, OptiPrep™ must be shaken to disrupt the naturally forming density layers. The gradient is formed on a soft

cell pellet resuspended in 4 ml OptiPrep™ and 6 ml buffer. OptiPrep™ 1.095 % (8.036 ml buffer and 3 ml OptiPrep™) was carefully overlaid on the cell layer followed by OptiPrep™ 1.080 % (10.435 ml buffer + 3 ml OptiPrep™) and finally 10 ml buffer. The gradients were spun at 1978 rcf for 30 mins with no brake to avoid disturbing the layers. Three populations of cells were observed (erythrocytes, polymorphonuclear cells and peripheral blood mononuclear cells) and the peripheral blood mononuclear cells (PBMC) isolated (Figure 2.1). Haemocytometer counts were then performed on the washed isolated cells.

2.1.2 MONOCYTE ISOLATION BY MAGNETIC NEGATIVE SELECTION

Monocytes were obtained from a mixed PBMC population isolated by OptiPrep™ density gradient sedimentation using negative magnetic selection (Figure 2.1). Macs Monocyte Isolation Kit II (Miltenyi Biotec) and magnetic columns (Miltenyi Biotec) were used according to the manufacturer's instructions. The antibody cocktail contained anti- CD3, CD7, CD16, CD56, CD123 and Glycophorin A antibodies for depletion of T cell, NK cell, macrophage, B cell, dendritic cell, basophil and erythrocyte contaminants. Column buffer was made up by adding 200 µl EDTA (Gibco, Invitrogen) and 250 µl foetal calf serum (FCS) (Autogen Bioclear, Source BioScience) to 50 ml sterile 1 x phosphate buffered saline (PBS) (Biowhittaker, Lonza). Columns were washed by the addition of 9 ml column buffer and discarding flow through. Careful preparation was used throughout and care taken to ensure sterile conditions. For every 10 million PBMCs 30 µl column buffer, 10 µl FCR blocking agent and 10 µl biotin conjugated antibody cocktail was added. The cell suspension was transferred to clean 1.5 ml microcentrifuge tube (SARSTEDT AG & Co) and incubated at 4 °C for 10 mins. Following incubation, 20 µl vortexed anti- biotin magnetic beads and 30 µl column buffer were added and incubated again for 15 mins at 4 °C. The cells were then spun at 1000 g for 2 mins in a microcentrifuge to pellet cells and the supernatant discarded. The pellet was resuspended in 500 µl column buffer and applied to the washed column. Pure unlabelled monocytes were obtained by depletion of the

magnetically labelled unwanted cells. Haemocytometer counts were carried out and cells resuspended in RPMI 1640 (Gibco, Life Technologies), 10 % FCS and 1 % penicillin G and streptomycin (P/S) (Gibco, Invitrogen) at 1 x 10^6 /ml.

2.1.3 CALCULATING MONOCYTE PURITY

Monocyte purity was assessed by CD14 positivity on a FACS Calibur flow cytometer (Becton Dickenson, Oxford) as CD16 positive monocytes will have been depeted by the antibody cocktail used for monocyte isolation. Negative selected monocytes were resuspended at 1 x 10^6 /ml in RPMI, 10 % FCS and 1 % P/S. Then 0.5 x 10^6 monocytes added into two clean 0.5 ml microcentrifuge tubes (SARSTEDT AG & Co). Tubes were spun at 2000 rpm for 2 mins in a microcentrifuge to pellet the cells. Supernatants were discarded, pellets washed with PBS and resuspended in either 2.5 µl phycoerythrin (PE) conjugated CD14 (eBioscience) or 2.5 µl PE conjugated immunoglobulin G1 kappa (IgG1κ) isotype (eBioscience) in a total volume of 25 µl with PBS. Samples were incubated at 4 °C in the dark for 20 mins. After incubation, samples were spun again at 2000 rpm for 2 mins, supernatants discarded and pellets resuspended in 250 µl 1 x cell fix (BD Biosciences) and stored at 4 °C until transferred to FACS tubes (BD Biosciences) and run on the FACS Calibur flow cytometer. PE positivity was measured on the FL-2 parameter, cell size by the forward scatter (FSC) and granulation by the side scatter (SSC). The results were calculated using FlowJo 8.7.1 software (Tree Star, Inc.) (Figure 2.2). Monocyte populations were determined by their FSC and SSC properties. From this population, histograms of FL-2 intensity were generated. Using the bisector tool IgG1 peaks were isolated to identify negative CD14+ population. Intensities above this were used as readouts of purity (percentage CD14+ positive).

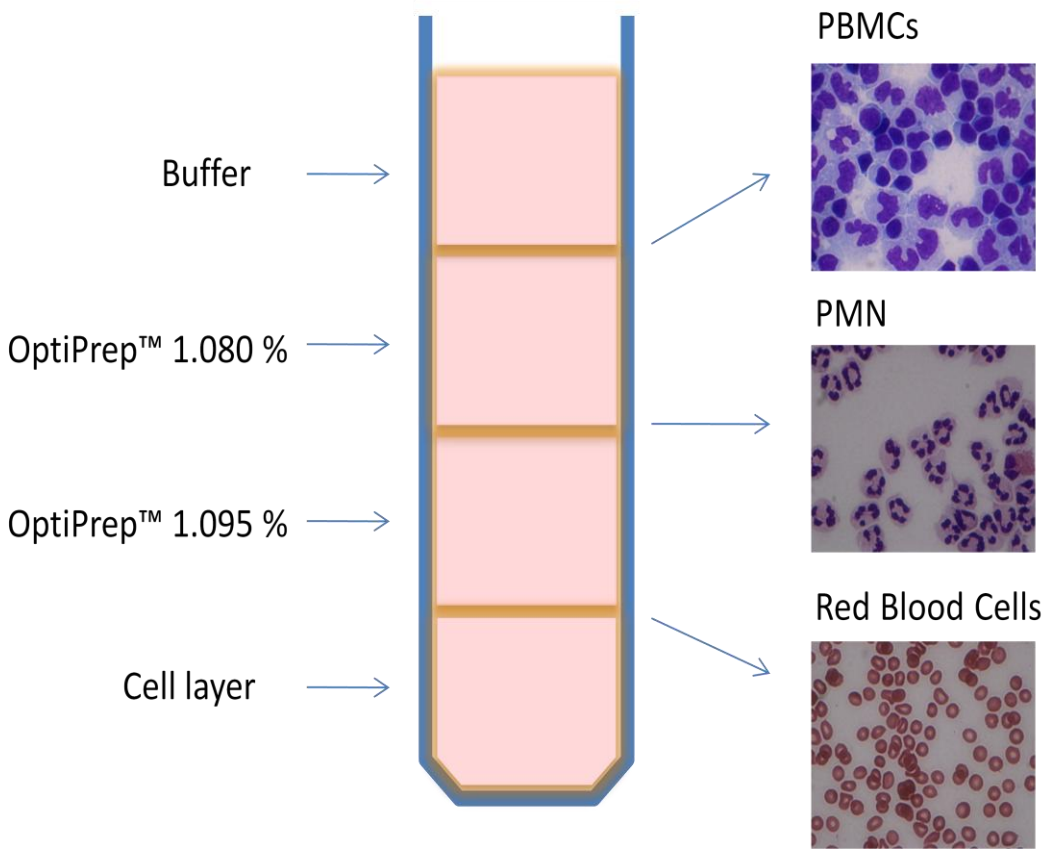

Figure 2.1. OptiPrep™ density gradients

OptiPrep™ is a density gradient medium ideal for isolating cells and organelles. Using a modified protocol established from manufacturers' instructions, peripheral blood mononuclear cells (PBMCs) and polymorphonuclear leukocytes (PMN) were isolated from whole blood. Cell pellets were resuspended in Hanks' Balanced Salts Solution containing 20 % platelet poor plasma (buffer) and OptiPrep™. To make the gradient OptiPrep™ 1.095 % contained 8 ml buffer and 3 ml 60 % OptiPrep™ and OptiPrep™ 1.080 % contained 10.5 ml buffer and 3 ml 60 % OptiPrep™. This was spun at 1978 rcf for 30 mins to obtain cell layers shown above.

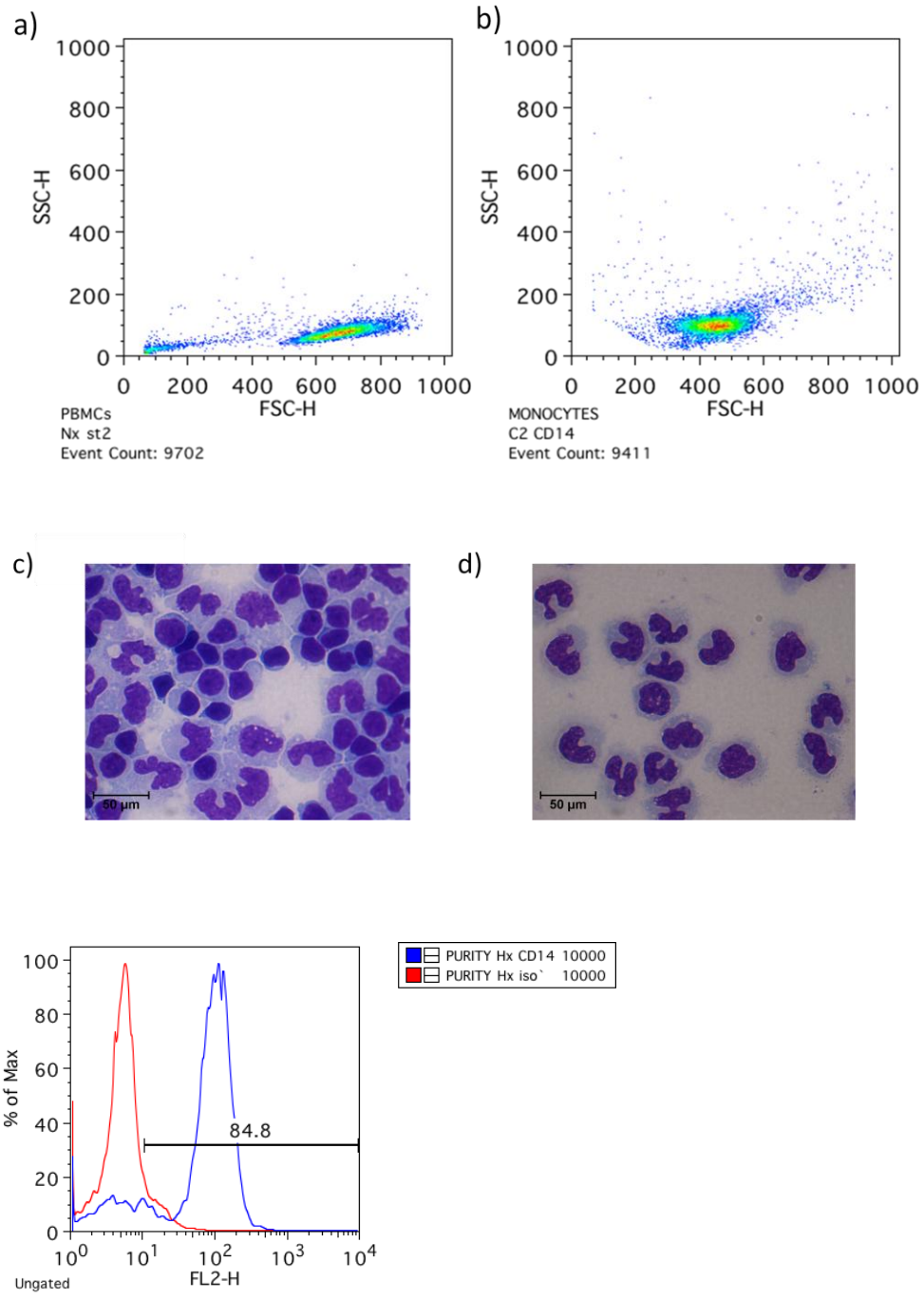

Figure 2.2 Calculating monocyte purity

Representative forward scatter (FSC) and side scatter (SSC) flow plots for a) mixed PBMC population and b) CD14 purified monocytes. To further illustrate the difference in cell samples representative cytospins of c) mixed PBMC population and d) CD14 positive monocytes are shown. Purity was measured by CD14 positivity as seen on the above histogram compared to isotype controls. Purity values ranged from 86.7 to 97.9 % with average purity being 89.8 % +/- 3.5 % (n=23).

2.2 CULTURING LEUKOCYTES IN HYPOXIA

In order to confirm the effect of hypoxia on monocytes in my culture conditions, RPMI 1640, 10 % FCS and 1 % P/S was placed into a Ruskin InVivo$_2$ 400 hypoxic workstation (Ruskin Technology Ltd, Bridgend) overnight. The gas settings were pre-set with 1 % oxygen (O_2) and 5 % carbon dioxide (CO_2) and the pO_2, pCO_2 and pH measured by an NPT7 automated blood gas analyser (Radiometer Copenhagen) (n=4) (Figure 2.3).

Isolated monocytes were spun at 1500 rpm and supernatants discarded. Pellets were taken into the hypoxic chamber and resuspended in pre-equilibrated media at 0.1 x 10^6 monocytes /ml. Cells were plated out and 250,000 cells /condition were left to equilibrate for 1 hour then incubated with and without 10 ng /ml LPS (Alexis Corporation, Enzo Life Sciences) for 4 and 20 hours. Normoxic conditions were carried out in parallel using a room air 37 °C incubator supplemented with 5 % CO_2.

a)

Media Readings	Mean Value	SEM
ρO_2	3.21 kPa	0.05
ρCO_2	4.66 kPa	0.15
pH	7.42	0.23

b)

Media Readings	Mean Value	SEM
ρO_2	19.02 kPa	0.17
ρCO_2	4.66 kPa	0.16
pH	7.38	0.03

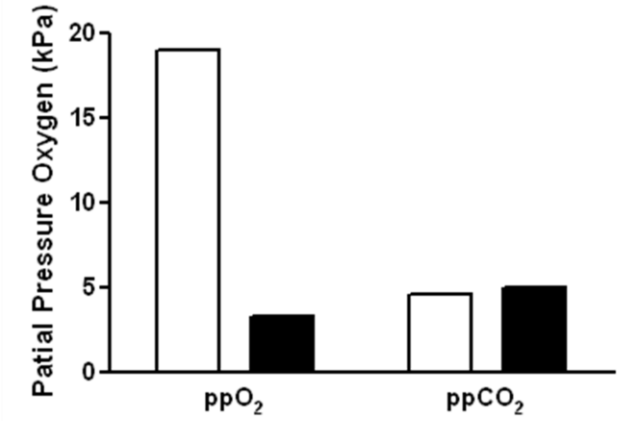

Figure 2.3 Culturing cells in hypoxia

Mean partial pressure and pH readings from a) hypoxic pre-equilibrated media n=4 and b) normoxic media n=4. Graph to show partial pressures of oxygen and carbon dioxide in both normoxic (19 kPa) (open bars) media and hypoxic (3 kPa) (closed bars) media. Bars represent mean +/- SEM, n=4.

2.3 PRIMARY CELL CULTURE

2.3.1 GROWING PRIMARY HUMAN PULMONARY ARTERY SMOOTH MUSCLE CELLS

Cryopreserved primary human pulmonary artery SMCs were purchased at passage three from Cascade Biologics now Life Technologies (catalogue number: C-009-5C). Each vial contains more than 500,000 viable cells isolated from the medial portion of healthy pulmonary arteries from unused donor lungs. Each section of the artery was confirmed to have no vasculopathies by a pathologist before cells were harvested. All reagents were warmed to 37 °C in a pre- warmed water bath and sterile technique used throughout in a laminar air flow culture hood. The cells were maintained according to the manufacturer's recommendations using basal Medium 231 (Gibco, Life Technologies), growth serum (catalogue number: S00725, Gibco, Life Technologies) and P/S. The growth serum contains basic fibroblast growth factor, insulin, epidermal growth factor, heparin, FCS and bovine serum albumin optimal for SMC growth. Each vial was used from passage 4 – 9 and each flask grown to 90 % confluence.

Vials were removed from nitrogen storage and left to defrost in a water bath for 30 secs. Once thawed the cells were immediately agitated using a sterile 1 ml pipette tip. Dye exclusion was used to check cell viability. Trypan blue (Sigma-Aldrich Ltd) was used at a 1:10 ratio of trypan blue to cell suspension in media. The dye does not enter healthy cells but can enter dead and dying cells. The dye allows visualisation of blue dead and clear live cells under a light microscope.

Viable cells were counted by haemocytometer and diluted to 1.25×10^4 cells /ml in supplemented media. The cells were then seeded in 25 cm^2 flasks (SARSTEDT AG & Co.) at approximately 6.25×10^4 and gently rocked to ensure even distribution of cells. Each flask was then incubated undisturbed for at least 24 hours in 37 °C cell culture incubators conditioned with 5 % CO_2 and 95 % air.

2.3.2 *GROWING IPAH PATIENT PULMONARY ARTERY SMOOTH MUSCLE CELLS*

Explant lung tissue was obtained from patients with confirmed IPAH diagnosis in accordance with Papworth Tissue Bank Ethics REC 08/H0304/56. SMCs were isolated from the medial portion of pulmonary arteries by micro-dissection. Following isolation, all samples were genotyped to identify BMPR2 or ALK1 mutations. The vial of pulmonary artery SMCs corresponding to patient 74mps was a kind gift from Professor Nicholas Morrell, Cambridge University. The vial contained cells with a known mutation in BMPR2, the leucine at residue 401 being replaced with a serine.

The cells were grown as described above and maintained using DMEM (Gibco, Life Technologies) containing 10 % FCS and 1 % P/S. The vial was used from passage 4 – 9 and each flask grown to 90 % confluence at which time cells were either maintained in 75 cm^2 flasks at 0.8 x 10^5 cell /ml or used in experiments. Flasks were incubated at 37 °C in incubators conditioned with 5 % CO_2 and room air.

2.3.3 *GROWING PRIMARY HUMAN AORTIC VASCULAR SMOOTH MUSCLE CELLS*

Cyropreserved human aortic vascular SMCs were obtained from Cambrex Bioscience at passage 4. The vial contained approx. 450,000 viable cells from a single donor. Before growing up the vial all reagents were left to warm to 37 °C in a heated water bath and sterile technique used throughout. Cells were maintained in Medium 231 containing SMC growth serum and P/S as above (2.3.1). Cells were only used to passage 9 and each culture flask split once cells reached 90 % confluence.

The vial was left to thaw in a water bath heated to 37 °C before manual agitation using a sterile 1 ml pipette tip. Trypan blue (Sigma-Aldrich Ltd) exclusion was used as above to calculate viable cell numbers and haemocytometer counts performed. Cells were diluted to 1.25 x 10^4 cells /ml and seeded in 25 cm^2

flasks with approximately 6.25 x 10^4 cells /flask as above. Flasks were incubated undisturbed for 24 hours in 37 °C cell culture incubators conditioned with 5 % CO_2 and 95 % air before experimental use.

2.3.4 MAINTAINING AND SUB CULTURING PRIMARY CELLS

Primary cells were grown and maintained in 75 cm^2 flasks in Medium 231 containing SMC growth serum and 1 % P/S or DMEM with 10 % FCS and 1 % P/S. Once cells were grown to approximately 90 % confluence, they were washed with Dulbecco's PBS (Gibco, Invitrogen). Flasks were then incubated with 1 ml 0.25 % Trypsin /EDTA solution (Gibco, Invitrogen) /flask for 2 mins in 37 °C incubator. Fully supplemented media was used to stop the reaction (5 ml /flask) and cell number determined by manual haemocytometer counts. Cells were then seeded in 75 cm^2 flasks at 0.8 x 10^5 cell /ml or used in experiments. Flasks were incubated at 37 °C, sterile technique was used throughout.

2.3.5 FREEZING DOWN CELLS

Cryopreservation medium was made with basal medium DMEM containing 10 % FCS and 10 % DMSO (Sigma-Aldrich Ltd). A manual cooling chamber (Mr. Frosty, Sigma-Aldrich Ltd) was filled with 200 ml clean isopropanol (Fisher Scientific) and vial holder placed on top. Cell suspensions were made by lifting adherent cells using 0.25 % trypsin /EDTA solution. Cell number was determined by haemocytometer counts and cells spun at 100 *g* for 5 minutes. Cells were resuspended at 1 x 10^6 /ml in cryopreservation medium and 1 ml placed in each 1.5 ml cryovial (SARSTEDT AG & Co.). Vials were left in a Mr. Frosty vial holder and lid tightened. Each Mr. Frosty was placed in -80 ^oC freezer overnight to cool -1 ^oC / min allowing dehydration before freezing before all vials were transferred to liquid nitrogen.

2.4 GROWING SMOOTH MUSCLE CELLS IN NORMOXIA AND HYPOXIA

Prior to establishing PA-SMC and monocyte co-cultures, cell viability and number was defined in both hypoxic monoculture (3 kPa) and normoxic monoculture (19 kPa). Cell viability was measured by reduction of cell permeable alamarBlue® (Invitrogen), an indicator of metabolic activity (2.4.2). A Coulter counter (Z-1 series, Beckman Coulter Ltd.) was used to calculate total cell numbers (2.4.1).

To determine the optimal seeding densities for co-culture experiments, pulmonary artery SMCs were seeded in 24 well Costar plates (Corning Incorporated) at 10,000 to 35,000 cells /well at 5,000 cell increments. Plates were then cultured for 24, 48 and 72 hours. After seeding, plates were left to equilibrate in either normoxia (19 kPa) or hypoxia (3 kPa) for 24 hours. All hypoxic experiments and incubations were carried out in a Ruskin InVivo$_2$ 400 hypoxic workstation pre-set to supply 1 % O_2 and 5 % CO_2 and sterile technique used throughout. All hypoxic media was left to pre-equilibrate for at least 24 hours prior to experimental use. All normoxic experiments were carried out in a laminar air flow culture hood. Normoxic incubations were carried out at 37 °C in incubators supplemented with 5 % CO_2 and 95 % air.

After 24 hours of equilibration in each oxygen tension, plates were then serum starved in DMEM containing 0.2 % FCS and 1 % P/S for 48 hours. Plates were then washed in PBS and replaced with 500 µl RPMI with 10 % FCS and 1 % P/S for either 24, 48 or 72 hours.

2.4.1 TOTAL CELL COUNTS IN SMOOTH MUSCLE CELL MONOCULTURES

Total SMC number /well was calculated by use of a Coulter counter; each well was washed with PBS and cells lifted by incubation with 500 µl non enzymatic cell dissociation solution (Gibco, Invitrogen) for 5 mins to allow cell detachment. Detachment was confirmed visually under the microscope and the

lifted solution was added to 9.5 ml Isoton (BD Biosciences), an electrolyte solution, in a cell counter chamber (Becton Dickinson, Oxford). The counter works using the Coulter principle allowing small molecule number and size to be determined in a solution by electrolyte flux. Micro channels pass a small aliquot of the cell suspension through two charged chambers. Cells are non-conducting causing a temporary drop in current, the size of the change is proportional to the size of the particle. The machine detects the changes in electrolyte flux indicating presence of non- conducting particles. Settings were altered to measure all items between 0.5 to 10 μm. The number of particles diluted in the Isoton are expressed on the machine and manually recorded. Total cell counts from each sample are then calculated and the mean for each used to establish the period of time and seeding density used for co-culture (Figure 2.4).

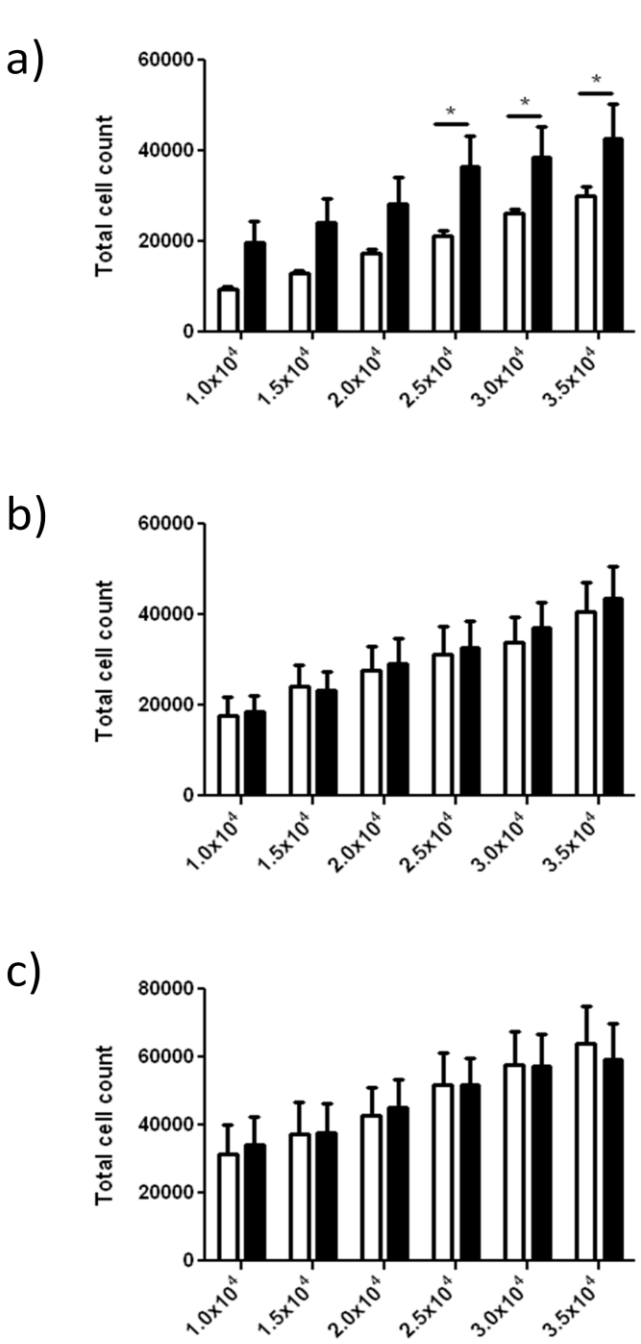

Figure 2.4 Growing pulmonary arterial smooth muscle cells in normoxia and hypoxia

To establish the best baseline for our co-culture experiments, SMCs were seeded between 10,000 and 35,000 cells /well in 24 well plates. Cells were incubated in pre-equilibrated RPMI containing 10 % FCS and 1 % P/S for a) 24, b) 48 and c) 72 hours in normoxia (19 kPa) (open bars) or hypoxia (3 kPa) (closed bars). Coulter counts were then performed and bars represent mean +/- SEM, *P<0.05, cells from 2 seperate vials studied n=8, two-way ANOVA with Bonferonni post test.

2.4.2 RELATIVE METABOLIC ACTIVITY IN SMOOTH MUSCLE CELL MONOCULTURES

AlamarBlue® (Invitrogen) has a low redox potential allowing its non fluorescent blue compound called Resazurin to be readily reduced to its fluorescent red counterpart called Resorufin without disturbing respiration in living cells. Reduction of the dye is mediated by oxidative respiration so was used to show relative metabolic activity of SMCs thus indirectly showing viability. Cycloheximide (Sigma-Aldrich Ltd.) at a final concentration of 1 ng/ ml was used as a positive control. Cycloheximide is a protein synthesis inhibitor and acts specifically on the 60S subunit of ribosomes. SMCs were grown in 24 well Costar plates, left to oxygen equilibrate for 24 hours and serum starved for a further 48 hours in basal DMEM containing 0.2 % FCS and 1 % P/S. After 20 hour culture in RPMI containing 10 % FCS and 1 % P/S wells were washed and replaced with fresh media. Each well was incubated for 4 hours with 50 µl alamarBlue® and positive controls with cycloheximide then cell free supernatants analysed in triplicate on 96 well Costar plates (Corning Incorporated) by flourecence plate reader set to excitation limit 544 nm and emission limit 590 nm. For each sample a fluorescence ratio (sample flourecence: cycloheximide killed sample fluorescence) was calculated:

$$\text{Fluorescence ratio} = \frac{\chi \text{ fluorescence}}{\text{killed } \chi \text{ fluorescence}}$$

Triplicate flourescnece ratios were averaged to give mean fluorescence ratios, also expressed as relative metabolic activity (Figure 2.5). Mean relative metabolic activity values were then normalised for cell number and used to determine the effects of oxygen tension on metabolic activity (Figure 2.6).

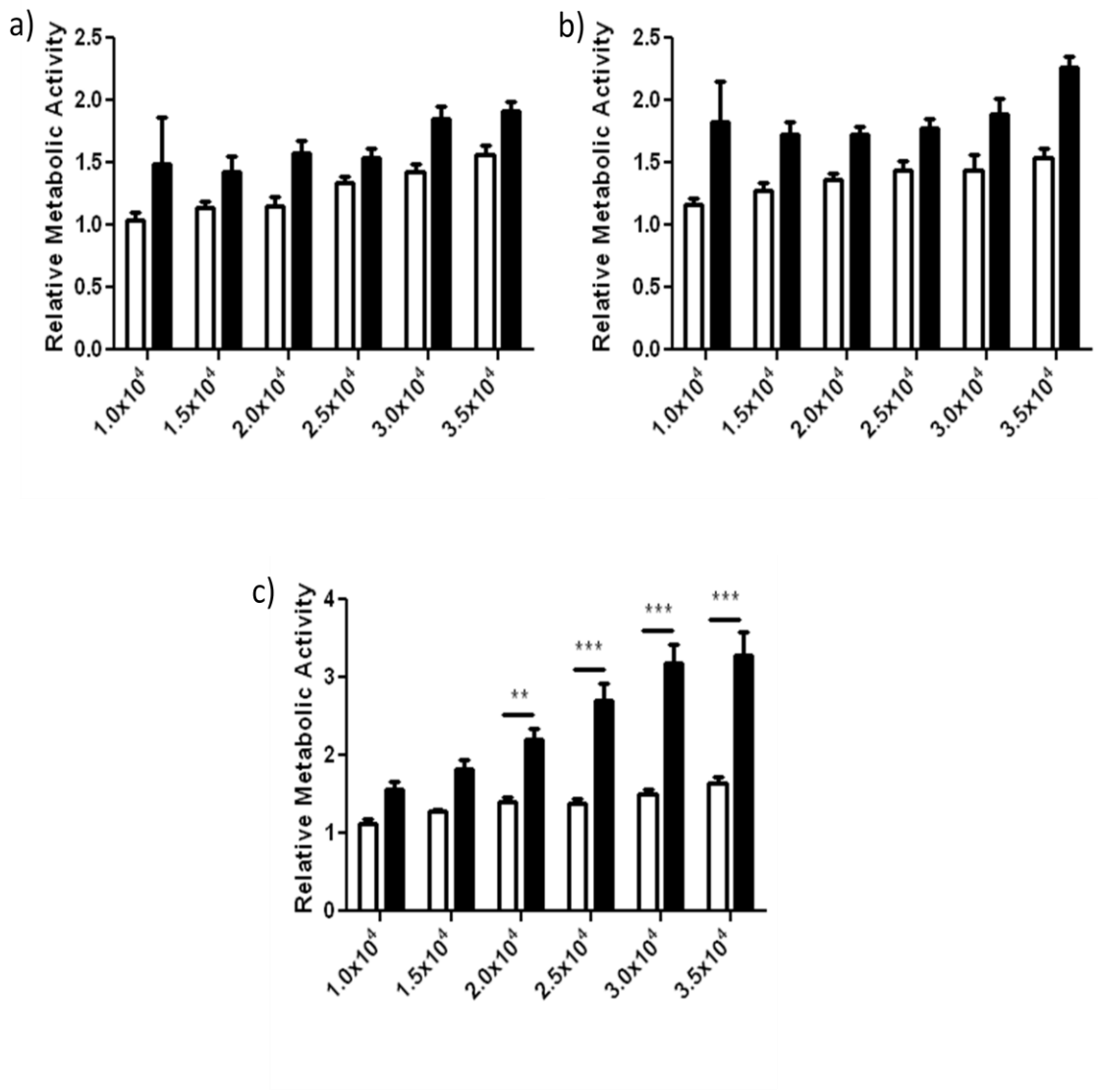

Figure 2.5 Calculating metabolic activity of normoxic and hypoxic smooth muscle cells

To measure changes in metabolic activity SMCs were seeded from 10,000 to 35,000 cells /well in 24 well plates. Cells were cultured in pre-equilibrated RPMI containing 10 % FCS and 1 % P/S in normoxia (19 kPa) (open bars) or hypoxia (3 kPa) (closed bars) for a) 24, b) 48 and c) 72 hours. AlamarBlue® was added in the last 4 hours of culture with and without 1 μg/ ml cycloheximide. Graphs show relative metabolic activity when compared to matched cycloheximide killed controls. Bars represent mean +/- SEM, **P<0.01, ***P<0.001, cells from 2 seperate vials studied n=8, two-way ANOVA with Bonferonni post test. Please note scales bars for graph a) and b) are different from graph c).

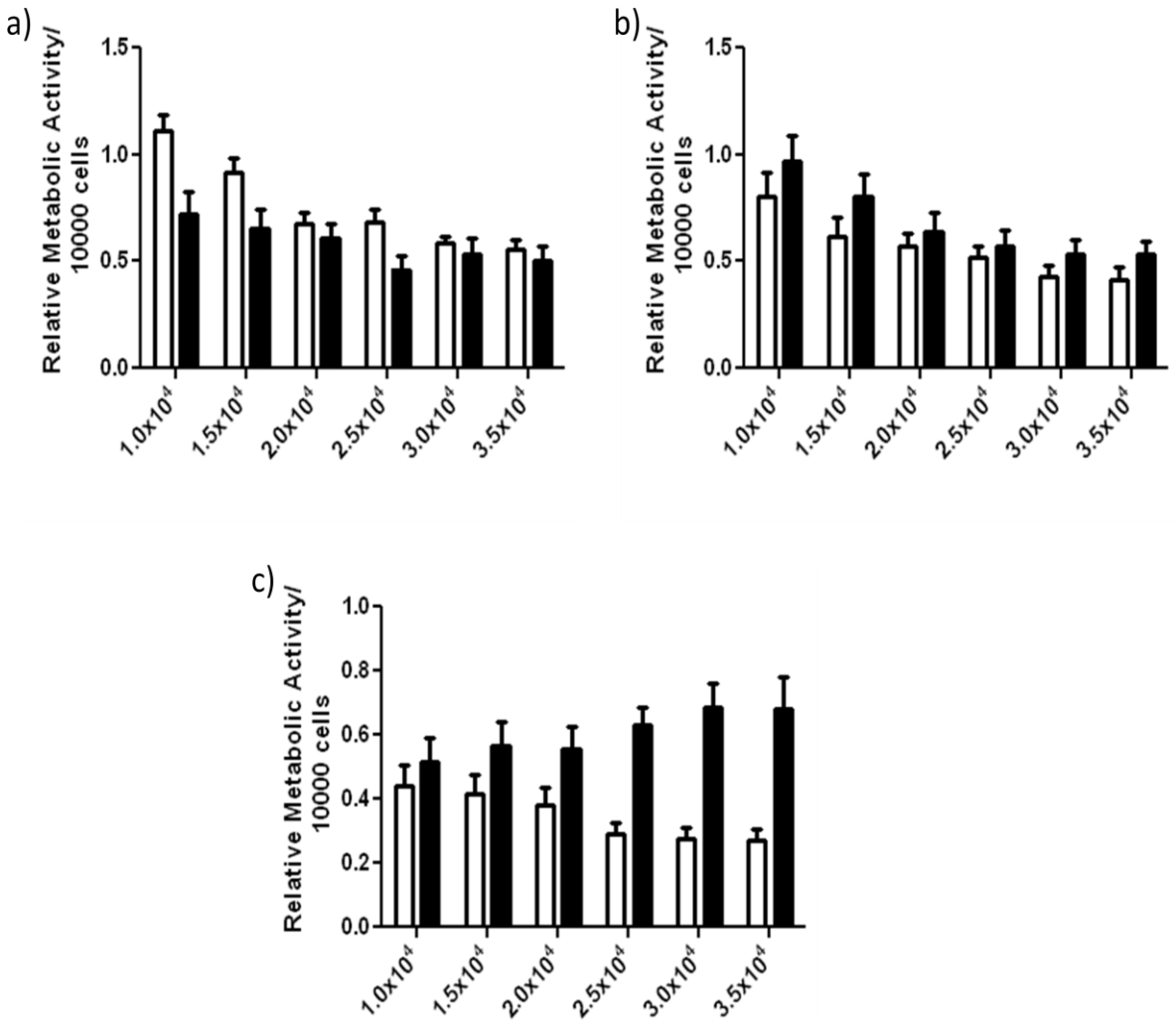

Figure 2.6 Relative metabolic activity corrected for smooth muscle cell number

Metabolic activity was measured at each SMC density from 10,000 to 35,000 cells /well in 24 well plates. Cells were cultured in pre-equilibrated RPMI containing 10 % FCS and 1 % P/S in normoxia (19 kPa) (open bars) or hypoxia (3 kPa) (closed bars) for a) 24, b) 48 and c) 72 hours. AlamarBlue® was added in the last 4 hours of culture with and without 1 µg /ml cycloheximide and cell counts performed. Graphs show relative metabolic activity normalised to total cell number at each density. Bars represent mean +/- SEM, cells from 2 seperate vials studied n=8. Please note scales for graph a) and b) are different from graph c).

2.5 CO-CULTURE MODELS

A seeding density of 25,000 SMCs /well and an incubation period of 24 hours was selected because SMC metabolic activity was preserved and monocyte survival was unaffected over this time. Moreover, 24 hours allowed us to directly compare our co-culture system to the established model used in Professor Sabroe's laboratory (Morris *et al.*) (Figure 2.7).

To set up co-cultures of SMC and monocytes, 24 well Costar plates were seeded at 25,000 cells /well in an overall volume of 500 µl with SMC between passage 4 and 9. All hypoxic media was allowed to equilibrate in hypoxia at least 24 hours prior to use and sterile technique used throughout. Plates were equilibrated in normoxia and hypoxia for 24 hours and serum starved for a further 48 hours in DMEM, 0.2 % FCS and 1 % P/S. Plates were washed in PBS and then fresh RPMI with 10 % FCS and 1 % P/S was added to each well with and without freshly isolated monocytes at a ratio of 1:5 monocytes to SMC (Figure 2.7). Monocytes were added either directly into wells or into transwell inserts (0.2 µm pore size) (Corning Incorporated) in an overall volume of 500 µl. At this point cells were stimulated with either 10 ng /ml LPS; 5 ng /ml or 10 ng /ml recombinant PDGF (Sigma-Aldrich Ltd.); 1 µM, 10 µM, 100 µM or 1 mM pan hydroxylase inhibitor DMOG (Sigma-Aldrich Ltd.); 0.75 ng /ml, 1.5 ng /ml, 3 ng /ml, 6 ng /ml, 12.5 ng /ml 25 ng /ml or 50 ng /ml IL- 1 receptor antagonist (Amgen Ltd.); 3 ng /ml or 50 ng /ml IL-1 receptor antagonist placebo (Amgen Ltd.); 1 mM, 10 mM, 100 mM or 1 M vitamin E analogue Trolox (Calbiochem, Merek Millipore).

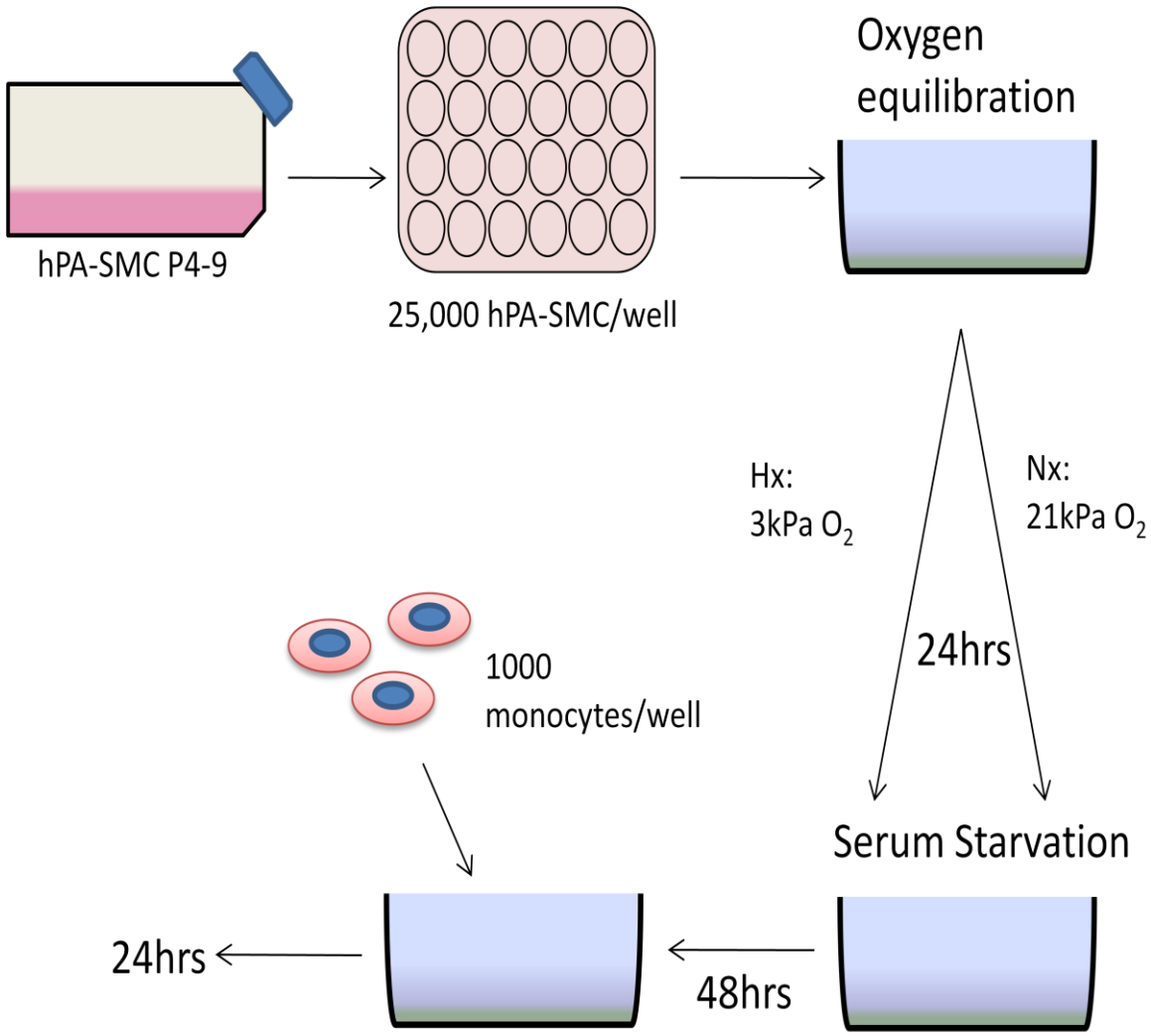

Figure 2.7 Flow diagram illustrating co-culture model set up

SMCs from passage 4-9 were grown in Medium 213 with full growth supplement and P/S in T75 cm^2 flasks until 90 % confluence. Flasks were then washed with PBS, incubated with 0.25 % Trypsin/ EDTA and total cell number calculated by haemocytometer. Plates were seeded with 25,000 SMC /well. After 24 hour oxygen equilibration in either normoxia (19 kPa) or hypoxia (3 kPa) and serum starvation, purified monocytes were obtained from peripheral blood and added to each well at 1000 monocytes /well. After 24 hour incubation, total cell countes were performed, relative metabolic activity calculated and cell free supernatants were obtained and stored at -80 ^oC for analysis by ELISA.

2.5.1. SUPERNATANT TRANSFER EXPERIMENTS

Monocytes were cultured in normoxia (19 kPa) or hypoxia (3 kPa) in 24 well plates for 24 hours. Monocytes were cultured at 0.1 x 10^6 cells /ml in pre-equilibrated RPMI containing 10 % FCS and 1 % P/S. All subsequent steps were carried out in sterile laminar flow hoods (normoxia) or Ruskin $InVivo_2$ 400 chamber (hypoxia). Upon removal from sterile areas all tubes were kept on ice.

Cell-free supernatants were collected by transferring media from monocyte wells into sterile 1.5 ml microcentrifuge tubes and spinning tubes at 2000 rpm for 2 mins in a microcentrifuge. Supernatants were then transferred to clean 1.5 ml microcentrifuge tubes and stored at -80 °C until needed. Before use, supernatants were thawed on ice. SMCs were grown as above, seeded at 25,000 cells /well in 24 well plates and left to equilibrate in normoxia (19 kPa) and hypoxia (3 kPa) for 24 hours. Following 48 hour serum starvation, cells were washed with PBS and wells replaced with either 500 µl pre- equilibrated RPMI containing 10 % FCS and 1 % P/S or 500 µl normoxic or hypoxic cell-free supernatant. Plates were incubated for a further 24 hours prior to total cell counts being performed.

2.6 STAINING PROTOCOLS

2.6.1 IMMUNOCYTOCHEMISTRY

To ensure SMCs were maintaining their phenotype over our culture period and in each oxygen tension, SMCs were stained for beta- smooth muscle cell actin using the VECTASTAIN Elite ABC kit and DAB substrate kit (Vector Laboratories Ltd.). The VECTOR kits are used to amplify primary antibody signal by binding of biotinylated secondary antibody and subsequent binding of avidin /biotinylated enzyme complexes. Protocol dictates to be diluted in equal measure both avidin and biotinylated peroxidase which are left for 30 mins to

make complexes. After incubation and washing 3, 3'-diaminobenzidine (DAB) substrate was added where it was oxidised to give a brown colour.

SMCs were grown in 4 well chamber slides (Lab-Tek, Thermo Scientific) at 0.2 x 10^6 cells /chamber under the same conditions as 24 well Costar plates. After incubation the slides were washed in PBS and fixed with 1 % paraformaldehyde (Sigma-Aldrich Ltd.) on ice for 10 mins. Immediately following this slides were stained for beta- smooth muscle cell actin (AbCam ab5694), CD31 (AbCam ab24590) and Von Willebrand factor (AbCam ab6994). Desired SMC populations were positive for beta- smooth muscle cell actin but negative for the endothelial and differentiation markers CD31 and Von Willebrand factor. Chambers were removed and slides labelled in pencil then protocol was carried out as advised in data sheet. A 1 % solution of Marvel (Premier International Foods (UK) Ltd) in PBS was used to block and make up antibody solutions. Non-sterile PBS was used for all wash steps. Endogenous peroxidase activity was quenched by incubation in 1 % hydrogen peroxide solution (Fisher Scientific) in water for 30 mins at room temp before blocking. All other incubation steps were carried out in a humidified chamber for 1 hour. Primary antibodies were used at 1:200 dilution and secondary antibodies at 1:1000. After staining with DAB, slides were counterstained with nuclear dye haematoxylin (Reagena Oy Ltd) and fixed with coverslips (Thermo Scientific) using DPX (Fisher Scientific).

2.7 APOPTOSIS ASSAYS

2.7.1 DETERMINING CELL DEATH BY MORPHOLOGY

Cells undergoing apoptosis have many distinct characteristics including cell shrinkage, membrane blebbing and chromatin condensation which can be observed morphologically. Monocytes and PBMC were lifted by gentle agitation and transferred to a clean 1.5 ml microcentrifuge tube. Samples were then spun at 2000 rpm for 2 mins in a microcentrifuge and the supernatants discarded. The pellets were resuspended in 100 µl RPMI and applied to a cytospin funnel

clamped to a slide and blotting paper (Thermo Scientific). The slides were spun at 3000 rpm for 3 mins in a cytospin machine (Thermo Shandon Cytospin 3) and clamps dismantled allowing slides to air dry. Once dried, slides were fixed by ice cold methanol (VWR International Ltd.). Fixed slides were then dual stained with the acidic cytoplasmic dye eosin (Reagena Oy Ltd.) and basic nuclear stain haematoxylin before covering with coverslips using the xylene containing fixative DPX. Ultraviolet (UV) killed PBMC and monocytes were used as positive controls. These were incubated under a UV cross linker (Hoefer Scientific Instruments) for 10 mins at 10 kJ prior to culturing. Apoptosis was calculated as a percentage by morphological change:

$$\frac{\text{Number apoptotic cells}}{\text{Total cells}} \times 100 = \%\ \text{Apoptotic cells}$$

2.7.2 QUANTIFYING CELL SURVIVAL BY FLOW CYTOMETRY

To verify the obsevered survival phenotype of monocytes and PBMC, these cells were stained with the fluorescent necrosis indicator dye TO-PRO-3 iodide (Molecular Probes, Life technologies) and fluorescently conjugated annexin V (BD Pharmagen) and observed by flow cytometry. TO-PRO-3 is a very effective indicator of membrane integrity; as such it is used in a 1: 10000 dilution in 1 x annexin binding buffer (BD Pharmagen) to denote necrotic cells. Annexin binds negatively charged phosphotidyl serine which is externalised upon activation of apoptosis pathway. For use on flow cytometry, phycoerythrin (PE) conjugated annexin was used. Positive controls were made either by pre-incubating cells for 10 mins under a 10 kJ UV cross-linker or co-incubation with 100 ng /ml cycloheximide 1 hour prior to lifting cells.

Monocytes and PBMCs were lifted by gentle agitation and transferred to a clean 1.5 ml microcentrifuge tube, these were then spun at 2000 rpm for 2 mins in a

microcentrifuge and washed with ice cold PBS. Cell pellets were resuspended in 50 µl 1 x annexin binding buffer and 2.5 µl annexin-PE added to relevant samples. These were then incubated in the dark for 10 mins on ice before addition of 250 µl TO-PRO-3 or 250 µl PBS. Before reading on the FACS Calibur flow cytometer, samples were transferred to clean labelled FACS tubes (Figure 2.8). FlowJo 8.7.1 software was used to analyse data from the FACS Calibur.

PBMC populations were isolated according to size and granulation and then gated into four quadrants. This separation was then superimposed onto all samples and each quadrant analysed. Quadrant a showed a necrotic population (TO-PRO-3 positive only), quadrant b signifies late apoptotic and early necrotic population (TO-PRO-3 and annexin positive), quadrant d represents apoptotic populations (annexin positive only) and quadrant c is the viable population (annexin and TO-PRO-3 negative) (Figure 2.8). Results are expressed as the percentage necrotic and apoptotic cells. This was calculated by:

$$\% \text{ Necrosis} = \frac{(\text{Counts FL-2 } -\text{ve}/\text{ FL-4 } +\text{ve})}{\text{Total event count}} \times 100$$

$$\% \text{ Apoptosis} = \frac{(\text{Counts FL-2 } +\text{ve}/\text{FL-4 } -\text{ve}) + (\text{Counts FL-2 } +\text{ve}/\text{FL-4 } +\text{ve})}{\text{Total event count}} \times 100$$

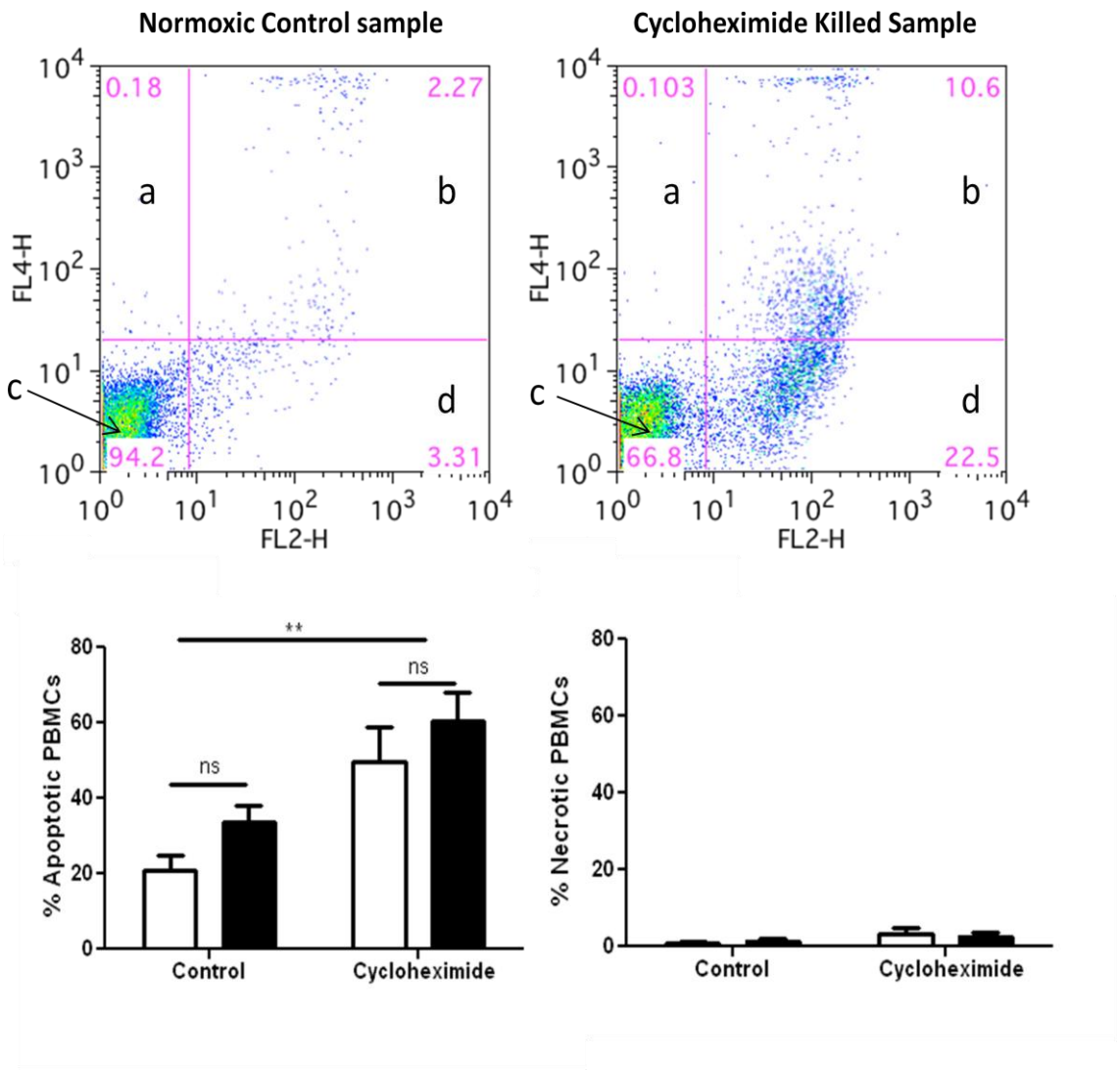

Figure 2.8 Calculating PBMC survival by flow cytometry

PBMCs were isolated and cultured in normoxia (19 kPa) (open bars) or hypoxia (3 kPa) (closed bars) for 24 hours with and without cycloheximide (1 µg /ml). Cells were labelled with both the apoptosis label annexin and the necrosis indicator TO-PRO-3. Samples were then run on FACS Calibur to allow for analysis by FlowJo 8.7.1. software. The PBMC populations were identified by size and granulation. This was then gated into four quadrants and superimposed to all samples. Quadrant a is necrotic population, quadrant b signifies late apoptotic and early necrotic population, quadrant d represents apoptotic populations and quadrant c is the viable population. Graphs represent mean +/- SEM, **P<0.01, ns= not significant, n=8, two-way ANOVA with Bonferonni post test.

2.7.3 ASSAYING APOPTOSIS BY TUNEL

A TUNEL (terminal deoxynucleotidyl transferase dUTP nick end labelling) assay was used to determine apoptosis in cells by labelling DNA fragmentation. The principle behind this assay was first described by Garvrieli *et al.* (Garvrieli, 1992). When cells undergo programmed cell death the genome becomes fragmented. In order to detect nuclear DNA fragmentation cells need to be permeabilised. Following this, both the enzyme terminal deoxynucleotidyl transferase and fluorescein conjugated dUTPs are added in excess to catalyse the reaction between the nick ends of fragmented DNA and the labelled dUTPs allowing direct detection of apoptotic cells by fluorescent microscopy.

TUNEL kits were purchased (Millipore, Merck Millipore) and SMCs and monocytes were analysed as described by the manufacturer's protocols. SMCs were cultured with or without monocytes in transwell inserts as described above. Cycloheximide (100 μM) killed cells were used as positive controls and all samples carried out in duplicate. Washes were carried out between each step using PBS for 5 mins on a plate rocker and repeated three times. All solutions were added drop wise across each well to ensure even coverage and incubation at room temperature unless stated otherwise. After 24 hour culture in both normoxia and hypoxia plates were removed from their sterile environment and were fixed using 4 % paraformaldehyde for 10 mins on the bench. Paraformaldehyde was the preferred fixative as its cross linking properties are thought to anchor chromatin in the cells. The fixative was then replaced with PBS, at this point plates were either stored at 4 °C or rest of staining protocol carried out.

In order to permealize the cells a mix of ethanol and acetic acid (2:1) was used for 5 mins at -20 °C. To optimise the sample pH levels, 13 μl equilibration buffer was added to each well for 10 secs. All excess was removed by pipette and cells incubated with 11 μl working strength TdT enzyme and reaction buffer mix containing digoxigenin labelled deoxynucleotides for 1 hour. The reaction was stopped by addition of 100 μl working strength stop wash buffer /well for 10

secs. Each well was then fluorescently labelled by addition of 8 µl anti-digoxigenin fluorescein isothiocynate (FITC) conjugate for 30 mins in the dark.

Samples were counterstained with cell permeable fluorescent DNA label 4'6-diamino-2-phenylindole (DAPI) (Gibco, Life Technologies) and examined under a fluorescent microscope. Approximately 300 total cells were counted from 3 different fields. The blue channel was counted first for DAPI positive cells then the FITC/ TUNEL positive green channel. Images were taken of each and then overlaid for dual fluorescent counts. Results were expressed as percentage TUNEL positive from total cell counts.

2.8 ELISA ANALYSIS

Cell free supernatants were prepared by centrifugation (2000 rpm, 2mins) following 24 hour culture and stored at -80 ^{o}C. For all samples cytokine generation was determined by DuoSet® sandwich enzyme-linked immunosorbent assay (ELISA) (DuoSet®, R&D Systems Inc.), the following factors were analysed:

IL- 1β, IL- 1 receptor antagonist (IL-1ra), interleukin-8 (IL-8), interleukin-6 (IL-6), interleukin-10 (IL-10), interferon- gamma (IFN-γ) and Regulated upon Activation, Normal T-cell Expressed and Secreted (RANTES), BMP4, OPG, endothelin-1, VEGF and soluble VEGF receptor (sFlt-1).

The method was carried out according to the manufacturer's specifications using 96-well Costar plates (Corning Incorporated) and standards diluted to recommendations in protocol (appendix I). Blocking was carried out using 5 % bovine serum albumin (BSA) (Sigma-Aldrich Ltd) in PBS while all washes and antibody dilutions using PBS and 0.05 % Tween-20 (Fisher Scientific). Plates were washed between each step until addition of colour substrate. To prevent desiccation, plates were wrapped in cling film until addition of streptavidin-horse radish peroxidase (HRP) (R&D Systems Inc.) where foil was used to avoid

cleavage of the light sensitive HRP conjugate. 100µl solution was added / well unless otherwise stated.

Coating antibodies were added to plates and left overnight at room temperature on the bench before plates were blocked for 1 hour. After blocking, standards and samples were each applied in duplicate and plates incubated for 1 ½ hours on a rotating platform. Samples were diluted appropriately to fit within linear portions of a log (concentration) / linear (optical density) standard curve as recommended. Biotinylated antibodies were then applied to plates to be incubated for 1 ½ hours on a rotating platform and subsequent addition of 1:20 HRP for 20 mins in the dark on a rotator. A 1:1 ratio of hydrogen peroxide and tetramethylbenzidine (R&D Systems Inc.) was then mixed and added to the plate. This solution undergoes a colour change when it interacts with peroxidase on the plate. The reaction was stopped by the addition of 50 µl 1 M sulphuric acid (Fisher Scientific), turning the solution yellow which was then analysed on a 96 well plate reader by reading absorbance at 450 nm. Values were calculated from linear values of standard curves (Figure 2.9).

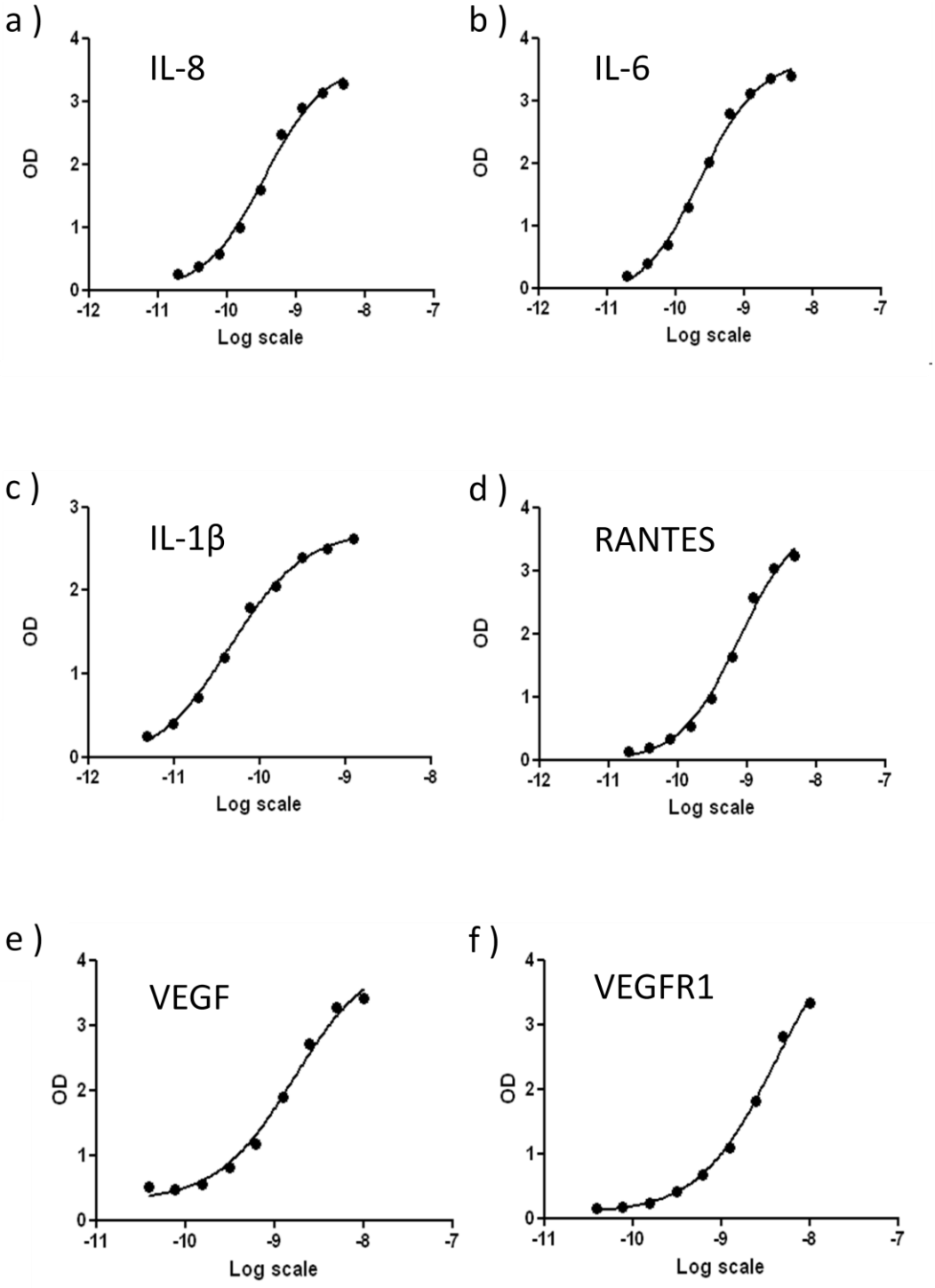

Figure 2.9 ELISA standard curves

Representative standard curves created for ELISA analysis of a) IL-8, b) IL-6, c) IL-1 β, d) RANTES, e) VEGF and f) VEGFR1 as calculated by transformation of standard concentrations by x = log (x).

2.9 RNA ANALYSIS

2.9.1 RNA PRODUCTION

TRI reagent is a commercially available solution used for RNA isolation. Guanidinium thiocynate- phenol- chloroform isolation was used as previously described (Chomcynski, 1987). Cells were spun in 1.5 ml microcentrifuge tubes and lysed using 1 ml TRI Reagent (Sigma-Aldrich Ltd.). TRI Reagent is a guanidinium thiocynate and phenol denaturing solution which is used with chloroform to produce three separate phases of organic protein, DNA and RNA according to the manufacturer's protocol.

2.9.2 RNA ISOLATION

SMCs and monocytes were lifted, transferred to 1.5 ml microcentrifuge tubes and spun at 2000 rpm for 2 mins. Supernatants were discarded and for every 10 million monocytes or 35,000 SMCs, 1 ml of TRI Reagent was added. Throughout all RNA preparations RNase and DNase free pipette tips (ART, Sigma-Aldrich Ltd.), water and microcentrifuge tubes were used and all surfaces and equipment carefully cleaned with 10 % IMS to reduce RNase or DNase contamination. Pellets were dislodged by vigorous pippetting and then inverted to mix. At this point samples could be stored at -80 °C or progressed to RNA isolation.

To each microcentrifuge tube 200 µl chloroform (VWR International) was added, mixed by inversion and left to settle at room temperature for 5 mins. Water saturated phenol is insoluble in chloroform leading to separation into 2 phases. Samples were spun at 14,000 rcf for 15 mins at 4 °C giving an upper clear aqueous phase, a white precipitate and a lower pink aqueous phase. The upper clear phase contains soluble RNA, a DNA precipitate in the inter-phase and the lower pink organic phase with dissolved lipids. The aqueous clear layer

was transferred to a clean labelled 1.5 ml microcentrifuge tube and the remainder discarded in the fume hood. Aqueous RNA was left to form a precipitate by the addition of 500 µl sterile isopropanol (Fisher Scientific) to each tube. Samples were inverted to mix and then incubated at room temperature for 10 mins before spinning at 14000 rcf for 8 mins at 4 °C. Small RNA pellets were purified by carefully removing supernatants and addition of 1 ml 75 % ethanol without mixing. Tubes were spun at 9000 rcf for 5 mins at 4 °C and supernatants carefully removed. Air dried pellets were then resuspended in 10 µl RNase-free water (B. Braun, Melsungen) before quantifying on a ND-1000 spectrophotometer (Nanodrop, Thermo Scientific).

2.9.3 RNA PURIFICATION BY DNA DIGESTION

DNA contamination was removed by treatment with DNase I enzyme (Ambion, Invitrogen). Throughout RNase and DNase free pipette tips, water and microcentrifuge tubes were used and all surfaces and equipment carefully cleaned with 10 % IMS. Each sample was diluted with RNase-free water to give an overall concentration of 200 ng /µl nucleic acid and for every 200 ng /µl nucleic acid, 1 µl 1 x DNase I buffer was added. To each microcentrifuge tube 1 µl DNase I enzyme was added and samples mixed by gently shaking on a vortex. Samples were subsequently incubated for 30 mins at 37 °C prior to removal of divalent cations and inactivation of the DNase enzyme by addition of 2 µl DNase Inactivation reagent at a 1: 10 dilution. In order to pellet the inactivation beads, tubes were spun at 10,000 rcf for 90 secs at 4 °C. Without disturbing the beads, tubes were taken to a ND-1000 spectrophotometer to quantify RNA suspended in the supernatant. Samples were then stored at -80 °C or converted to cDNA immediately.

2.9.4 cDNA SYNTHESIS BY PROMEGA AMV-REVERSE TRANSCRIPTASE

Avian myeloblastosis virus (AMV) reverse transcriptase transcribes single stranded RNA to single stranded complementary DNA sequence (cDNA). This property was manipulated to obtain stable cDNA sequences from instable RNA solutions. All reagents used were purchased from Promega and thawed on ice prior to use.

Aliquots of 1 µg RNA were made up to 12.4 µl with RNase free water in clean labelled 0.5 ml microcentrifuge tubes. To each 1 µg RNA: 8 µl 5 x AMV buffer containing 50mM Tris-HCl (pH 8.3), 40mM KCl, 8.75mM $MgCl_2$, 10mM DTT and 0.1 mg/ml acetylated BSA; 1.6 µl 100 mM deoxycytosine triphosphate (dCTP); 1.6 µl 100 mM deoxythymidine triphosphate (dTTP); 1.6 µl 100 mM deoxyadenosine triphosphate (dATP); 1.6 µl 100 mM deoxyguanine triphosphate (dGTP); 1.2 µl recombinant ribonuclease inhibitor (RNasin); 1.2 µl random primers; 1.2 µl AMV- reverse transcriptase and 9.6 µl RNase and DNase free water was added. Samples were vortexed to mix, centrifuged at 2000 rpm for 2 mins in a microcentrifuge and then run on a thermal cycler with heated lid (GS1, G-Storm). Samples were run at 23 °C for 5 mins, 42 °C for 2 hours and heated to 99 °C to deactivate the enzyme before cooling to 4 °C until manually stopped. Samples were then stored at -20 °C until needed.

2.9.5 Measuring RNA quantity and integrity by Nanodrop ND-1000 spectrophotometer

Quantification of RNA solutions was needed to establish protocols for DNase treatment and generation of cDNA. Samples were kept on ice and taken to a Nanodrop ND-1000 spectrophotometer. The machine measures 1 µl aliquots of samples using surface tension to hold the sample in place. It reads between 220 and 750 nm so can be used to measure both concentration and integrity of nucleic acids.

The sampler was cleaned with alcohol wipes (AZO wipes, Cravenmount Ltd.) and Nanodrop software opened on the computer. To initiate the programme 1 µl of RNase-free water was loaded onto the pedestal. After each reading the pedestal was wiped with clean laboratory tissue. Blank measurements were made using 1 µl RNase free water and RNase free tips (ART, Sigma-Aldrich Ltd.) used throughout. Each reading measured DNA contamination using 260:280 nm ratios, chemical contamination using 260:230 nm ratios and concentration as ng /µl.

2.10 PCR amplification protocol

Polymerase chain reaction (PCR) is a technique for amplifying DNA using Taq DNA polymerase to amplify samples. Specific primers can be used to amplify a gene of interest or random hexamer primers to amplify all DNA. Samples are fed through a cycle of temperatures; 95 °C to denature cDNA complexes to single stranded structures, 40-60 °C to allow annealing of primers to the DNA, 72 °C the optimum temperature for the Taq DNA polymerase to work and then cooled to 4 °C to stop the reaction. The PCR products can then be run on agarose electrophoresis gels for visualisation. All samples and reagents were incubated on ice when not used. RNase and DNase free tips, microcentrifuge tubes and water were used throughout. All PCR reagents were purchased from Promega

unless stated otherwise. Each reagent was vortexed thoroughly and spun in a microcentrifuge at 2000 rpm for 2 mins prior to use. All primers were created by request from Eurogentec.

2.10.1 PCR AMPLIFICATION AND VISUALISATION

Glyceraldehyde-3-phosphate dehydrogenase (GAPDH) is an ubiquitiously enzyme which catalyses the convertion of glyceraldehydes-3-phosphate to D-glycerate 1,3-bisphosphate in glycolysis. Integrity of cDNA was established by polymerase chain reaction (PCR) using primers for GAPDH (Figure 2.10). Also, in order to optimise the protocol for siRNA transfection of SMCs, cyclophilin B siRNA was used. Transfection efficiency was determined by PCR using primers to cyclophilin B compared to GAPDH loading controls. The primer sequences for GAPDH and cyclophilin B were:

GAPDH forward primer: 5'- ACTTTGGTATCGTGGAAGGAC- 3',
GAPDH reverse primer: 5'- TGGTCGTTGAGGGCAATC- 3'.

Cyclophilin B forward primer: 5'- CTTCCCCGATGAGAACTTCA- 3',
Cyclophilin B reverse primer: 5'- CTGTGGAATGTGAGGGGAGT- 3'.

To each 2 µl aliquot of cDNA, 23 µl of PCR master mix was added. The master mix was made up of: 5 µl 5 x green GoTaq Flexi buffer; 1.5 µl 25 mM magnesium chloride solution; 1 µl 10 mM dNTP mix; 13.85 µl RNase and DNase free water; 0.7 µl forward primer; 0.7 µl reverse primer and 0.25 µl 5 U /µl GoTaq Flexi DNA polymerase /sample. A thermal cycler (GS1, G-Storm) was used to perform the PCR on each sample using the following settings: 1 cycle of 92 °C for 2 mins; 25 cycles of 94 °C for 30 secs, 60 °C for 1 min, 72 °C for 30 secs; 1

cycle of 72 °C for 2 mins and then hold at 4 °C until manually stopped. Samples were then stored at -20 °C until ran on an agarose electrophoresis gel.

Both GAPDH and cyclophilin B PCR products were in the region of 400 bp so were run on a 1.5 % agarose (Sigma-Aldrich Ltd.) gel made in 1 x TAE buffer with a 1000 bp ladder (Bioline). Ethidium bromide (VWR International) was added for visualisation at 1 µl /100 mls 1.5 % agarose in 1 x TAE buffer. Samples were run at 100 V for 40 mins after which gels were exposed on ChemiDoc MP imaging system (Si Laboratories Ltd.).

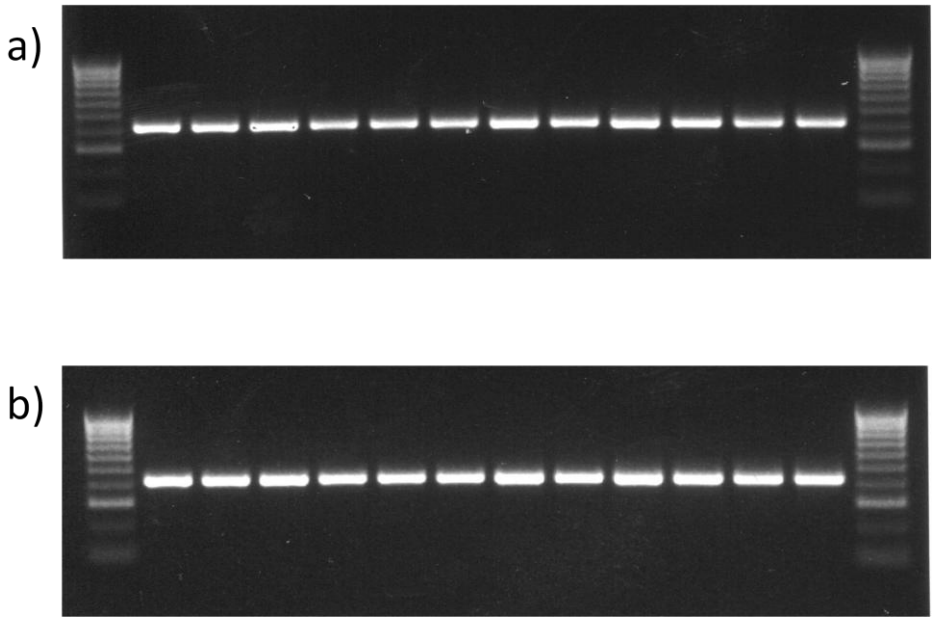

Figure 2.10 GAPDH PCR blots to confirm cDNA integrity

PCR gel electrophoresis was performed on amplified cDNA samples from primary human pulmonary artery SMCs. 1 µl of each 1 µg sample was amplified with primers to GAPDH to confirm cDNA integrity. PCR gels were run as hyperladder IV, 12 different SMC cDNA samples and hyperladder IV. Blots a) and b) are from two separate dates where RNA from human SMCs was isolated and converted to cDNA. Both blots show maintained GADDH expression across all samples which suggests good cDNA quality.

2.10.2 REAL-TIME PCR BY TAQMAN

Real time PCR allows the reaction to be monitored as it progresses using TaqMan hydrolysis probes enabling relative quantification. Specific cyclers with fluorescent resonance energy transfer (FRET) light source are used to excite flourophores. The method relies on Taq polymerase to cleave dual-labelled TaqMan probes which bind at a specific site in the primer amplification region. The probes have 6-carboxyfluorescein (FAM) fluorescent reporters covalently bound to the 5'- end of the probe and a non- fluorescent 6-carboxytetramethylrhodamine (TAMRA) quencher at the 3'- end. As the Taq polymerase extends the 5'- primer it degrades the probe releasing the reporter from the quencher. Hence fluorescence is detected as the reaction progresses and is proportional to the amount of DNA.

All samples and reagents were incubated on ice when not used. RNase and DNase free tips, microcentrifuge tube and water were used throughout. All probes were purchased from Applied Biosystems unless stated otherwise. Each reagent was vortexed thoroughly and spun in a microcentrifuge at 2000 rpm for 2 mins prior to use. New standard curves were generated for each primer probe set measured using seven 1 in 4 or 1 in 2 serial dilutions of time 0 commercial SMC cDNA in water. Before use all samples were diluted 1 in 4 and each standard and sample was applied to 384 well plates (Greiner Bio-One GmbH) in duplicate. Plates were covered with Microseal 'B' adhesive seals (Bio-Rad Laboratories) and agitated before spinning at 1200 rpm for 2 mins to remove air bubbles and ensure all solutions are in the bottom of the wells. Each experiment was run on ABI 7900HT Real-time PCR system (Applied Biosystems, Life Technologies) using 384 well plate block. Total reaction volumes of 20 µl /well were used containing 1 µl cDNA and 19 µl reaction master mix.

Commercially available TaqMan primer probe sets (Applied Biosystems, Life Technologies) were used against β actin, HIF-1, HIF-2 and BMPR2. The assay ID for each was hs01060665_g1, hs00153153_m1, hs01026149_m1 and hs00176148_m1 respectively. The reaction master mix consisted of: 1 µl

TaqMan primer probe containing both forward and reverse primers as well as the TaqMan probes; 10 µl 2 x qRT-PCR Master Mix (Eurogentec) containing HotGoldStar Taq enzyme, dNTPs, $MgCl_2$, and ROX passive reference which is a fluorescent dye which maintains its intensity used to eliminate well to well variations; 8 µl water. Once completed data was analysed by SDS 2.2.1. Software.

2.10.3 Analysis of real-time PCR

All standards were labelled and given an arbitrary value corresponding with the dilution series. Undiluted cDNA was given the value of 10,000 and water was used as the negative control. From these standards, amplification plots were generated and Ct values assigned. Standard curve plots and amplification plots were generated for samples as well as standards (Figure 2.11). Threshold values were decided upon by determining the linear portion of each standard and sample amplification plot. The point at which each amplification plot crossed the threshold (Ct value) was compared between duplicates. Duplicates with large variation in Ct values were discarded. Ct values for each sample were read off the amplification plot and arbitrary values generated by comparing to the standard curve. Ratios of gene of interest compared to actin were generated in Microsoft Office 7 EXCEL (Microsoft):

$$\text{Ratio gene of interest to actin} = \frac{\text{mean quantity gene of interest}}{\text{mean quantity actin for each sample}}$$

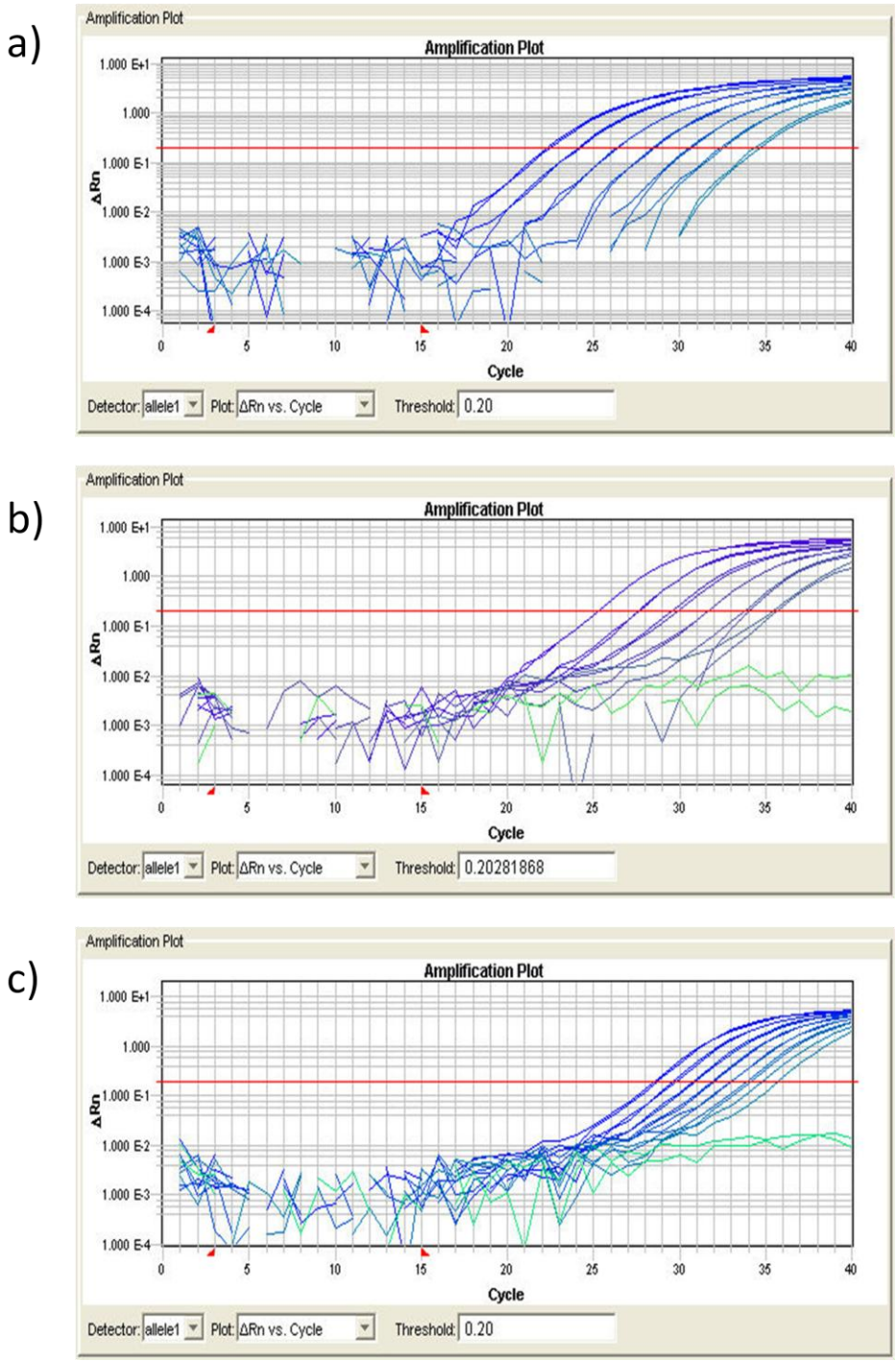

Figure 2.11 Representative amplification plots obtained from real-time PCR standards

Representative amplification plots for human SMC a) actin standards diluted 1 in 4, b) HIF-1 α standard diluted 1 in 4, c) HIF-2 α standard diluted 1 in 2 and d) BMPR2 standard diluted 1 in 4.

2.11 PROTEIN LYSIS

Plates were seeded at 25,000 cells /well and monocytes incubated at 0.1 x 10^6 cells /ml at a ratio of 5 SMCs: 1 monocyte. After 24 hour culture in normoxia (19 kPa) or hypoxia (3 kPa), cells were lysed using sodium orthovanadate lysis buffer. All plates were incubated on ice when removed from sterile culture environments.

2.11.1 SODIUM ORTHOVANADATE LYSIS METHOD

Aliquots of sodium orthovanadate lysis buffer (appendix II) were boiled at 95 °C in a heat block (Unitek HBS-130, Life systems designs) for 10 mins. SMC wells were washed with pre-equilibrated PBS and all excess PBS removed with a sterile P1000 pipette tip. Plates were removed from sterile conditions on ice and 50 µl of hot lysis buffer added to each well for 5 mins. Cells were scraped using a blunt P200 tip and lysate transferred to a clean labelled 1.5 ml microcentrifuge tube. Lysates were boiled at 95 °C in a heat block for 5 mins before being spun at 14,000 rpm for 10 mins at 4 °C. Supernatants were transferred to clean labelled 1.5 ml microcentrifuge tubes and stored at -80 °C to be run on SDS-PAGE gels.

2.12 QUANTIFYING PROTEIN

2.12.1 DC ASSAY

DC assay (Bio-Rad Laboratories) is a colorimetric assay used to quantify proteins and is readily compatible with detergents as well as EDTA and Tris. The DC reagents contain alkaline copper tartrate solution and folin reagent which react with proteins to give a colour change.

Samples and standards were run on a clear bottom 96 well plates to be read on an absorbance plate reader. Assay reagents were prepared by addition of 20 µl reagent S to every 1 ml reagent A in a clean bijoux tube (BD Biosciences). This solution was called reagent A' and 25 µl added to each well containing standards or samples. Standard curves were generated based on readings from BSA diluted in sodium orthovanadate lysis buffer. BSA was diluted from 16 µg /ml to 0 µg /ml by 1 in 2 serial dilutions and 20 µl of each standard loaded onto the plate in triplicate. Samples were run in duplicate and 20 µl of sample was used in each duplicate. To all wells 200 µl reagent B was added before plates were left to develop for 15 mins on the bench. After incubation plates were agitated and absorbance at 630 nm read on an absorbance plate reader. Values were expressed as µg /ml and volumes needed to load 30 µg or 50 µg protein/ lane on SDS-PAGE gels calculated.

2.13 WESTERN BLOT ANALYSIS OF PROTEIN EXPRESSION

Protein samples were heated to 95 °C for 10 mins prior to running on 8 % SDS-PAGE gels (appendix III) and separated by electrophoresis. Geneflow electrophoresis kits were assembled (Geneflow Ltd.), plates secured and structure lowered into western tank. Gaskets were filled to the top with 1 x SDS Running buffer (appendix IV) and rest of tank filled halfway. Combs were removed and wells cleared with a 0.7 gauge needle (BD Microlance) attached to 1 ml syringe (BD Plastipak). Either 30 µg or 50 µg protein from each sample was loaded into wells along with 5 µl ColourPlus Protein ladder (New England Biolabs). Gels were run at 120 V for 20 mins (Bio-Rad Laboratories) or until the dye front passed through the stacking gel after which voltage was raised to 200 V. Power packs were stopped when the dye front ran off the bottom of the gel.

Separated proteins were then transferred to PVDF membranes (Millipore, Merck Millipore) pre activated with methanol. Transfer tanks were filled with 1 x transfer buffer (appendix V) then sponges (Geneflow Ltd.) and blotting paper (Scientific Laboratory Supplies) submerged in 1 x transfer buffer. Cassettes

were opened and assembled as: 2 x sponges, 1 x blotting paper, SDS-PAGE gel, PVDF membrane, 1 x blotting paper and 2 x sponges. Careful layering to avoid air bubbles was carried out before cassettes were re-assembled. Tanks were kept in ice and transfers were run at 180 V for 90 mins. The transfer efficiency was checked by soaking membranes in 1 in 10 Ponceau S (Sigma-Aldrich Ltd.). After membranes were rinsed in water, blots were blocked with 5 % Marvel in 1 x TBS for 1 hour at room temperature on a rocker. Membranes were then incubated overnight at 4 °C on a rotating platform in primary antibodies (appendix VI), washed 3 x 15 min in TBS and 0.1 % Tween-20 before incubating for 1 hour with filtered HRP- conjugated secondary antibody at room temperature on a rotating platform. Membranes were washed again as above and developed with Enhanced Chemilluminescent Reagent, EZ-ECL (Geneflow Ltd.) and visualised either in the dark room using photographic film (GE Healthcare Ltd.) or read on the ChemiDoc MP imaging system (Bio-Rad Laboratories).

2.13.1 DENSITOMETRY

All western images and films were scanned using Canon scanner (Canon (UK) Ltd.) and saved as a new .TIFF file. Images were opened using Image J and boxes transformed across bands. The programme can then be used to calculate the optical density across the area and values expressed as a histogram. The area under the graph was recorded for each sample and all values were normalised to corresponding actin densitometry values.

2.14 SIRNA TRANSFECTION OF PULMONARY ARTERY SMOOTH MUSCLE CELLS

Small interfering RNAs can be used in cell culture to knock down expression of target genes. This technique manipulates eukaryotic cells' RNAi pathway. To do this specifically designed 20-25 base pair complementary sequences with 2-3

nucleotide overhangs are introduced into a cell. Once entered, the double stranded RNA unwinds and is incorporated into RNAi induced silencing complex (RISC). The RISC containing the antisense sequence is then active to target its complimentary mRNA leading to its degradation.

Designed siRNA sequences against cyclophilin B, HIF- 1 α, HIF- 2 α and BMPR2 mRNA were transfected into primary pulmonary artery SMCs using the chemical agent DharmaFECT2 (Dharmacon, Thermo Scientific). For each transfection 1 µl DharmaFECT2 was used with OptiMEM I (Gibco, Life Technologies) to transfect 2 µM siRNA for every 35,000 SMCs.

After transfection total cell counts were performed and transfection efficiency measured by PCR electrophoresis or real-time PCR. Sterile technique was used throughout.

Each siRNA was bought from Dharmacon (Thermo Scientific). Cyclophilin B siRNA sequences were pre designed targeting accession number NM_000942 (siSTABLE Cyclophilin B siRNA, D-001710-02-05) whereas HIF-1 α, HIF-2 α and BMPR2 sequences were custom designed:

HIF-1 α: sense 5'- CUGAUGACCAGCAACUUGAdTdT -3'

antisense 5'- UCAAGUUGCUGGUCAUCAGdTdT -3'

HIF-2 α: sense 5'- CAGCAUCUUUGAUAGCAGUdTdT -3'

antisense 5'- ACUGCUAUCAAAGAUGCUGdTdT -3'

BMPR2: sense 5'- CAUGUAUGCUCUUGGACUAUUdTdT -3'

antisense 5'- UAGUCCAAGAGCAUACAUGUUdTdT -3'

The day before transfection, SMCs were seeded into 24 well plates at a concentration of 70 million cells /ml in a total well volume of 500 µl. Plates were incubated overnight at 37 °C in a normoxic (19 kPa) incubator supplemented with 5 % CO_2. On the day of transfection 2 µM siRNA solutions were made up in RNase free water from 20 µM reconstituted stocks. For each well two tubes of solutions were created:

Tube 1- 25 µl 2 µM siRNA + 25 µl OptiMEM I

Tube 2- 1 µl DharmaFECT2 + 49 µl OptiMEM I

For mock infected controls 25 µl OptiMEM I was used instead of 2 µM siRNA. Each tube was mixed and incubated for 5 mins at room temperature. Both tubes were then combined and mixed by carefully pipetting up and down before incubating for 30 mins at room temperature to allow formation of chemical complexes containing siRNA sequences. During the incubation media was removed from each well, cells washed with PBS and 400 µl OptiMEM I without antibiotics or supplements added. After incubation 100 µl siRNA complexes were applied to each well for a total transfection time of 12 hours at 37 °C in normoxic incubators supplemented with 5 % CO_2.

After incubation complexes were removed by gentle pipetting and cells washed with PBS. Media was then replaced with DMEM containing 0.2 % FCS and 1 % P/S. Immediately following cells left to recover for a further 12 hours at 37 °C as above. After recovery plates were washed with PBS and media replaced with fresh DMEM containing 0.2 % FCS and 1 % P/S. Plates were incubated for a further 24 hours either in normoxia as above or a Ruskin InVivo$_2$ 400 hypoxic workstation pre-set with 1 % O_2 and 5 % CO_2. Following this wells were washed with PBS and either lifted by the addition of 500 µl 0.25 % Trypsin/ EDTA solution for Coulter counts to be performed or lysed with 1 ml TRI Reagent.

This protocol was first optimised using siRNA to cyclophillin B, which is an abundantly expressed mRNA (Figure 2.12). Knock down of cyclophilin B does not affect cell viability so it is often used as a positive control. Initially cells and complexes were incubated for 6 hours leading to inefficient knockdown of cyclophillin B (Figure 2.12a). However, a transfection time of 12 hours was both effective and reproducible (Figure 2.12b).

2.15 STATISTICS

All statistics were performed using GraphPad Prism 5.0 (GraphPad Software Inc.). All data is expressed as mean +/- standard error of mean (SEM) of a number of independent experiments (n). Parametric statistical tests were chosen when normal distribution of data was observed. One-way analysis of variance (ANOVA) was used when comparing several samples with Bonferonni post test to compare means of all samples. Two-way ANOVA was used when comparing two variables such as oxygen tension and culture conditions with Bonferonni post test to compare interactions of each variable. Where only two samples were being compared a students' *t*-test was used. Data was considered significant if $P<0.05$.

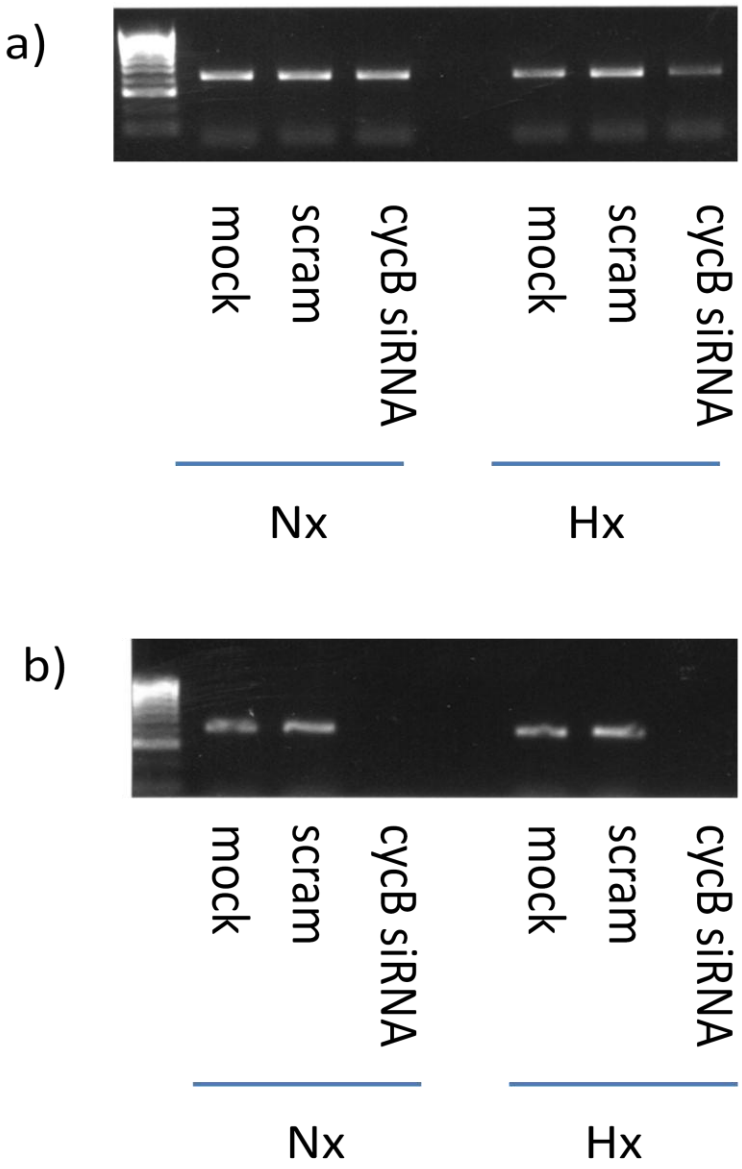

Figure 2.12 Confirming knock-down of cyclophillin B in smooth muscle cells using PCR gel electrophoresis

In brief SMCs were either mock infected (mock), transfected with 0.5 μM scrambled siRNA (scram) or with 0.5 μM siRNA targeting cyclophilin B (cycB siRNA) by chemical transfection for a) 6 hours or b) 12 hours. Samples were washed and incubated in either normoxia (Nx) (19 kPa) or hypoxia (Hx) (3 kPa) for a further 24 hours. Samples were lysed using TRI Reagent and RNA converted to cDNA. Samples were amplified with cyclophilin B primers and run on 1 % agarose gels with ethidium bromide for visualisation. Representative blots of n=3.

3. MONOCYTE REGULATION OF HYPOXIC SMOOTH MUSCLE CELL PROLIFERATION

3.1 INTRODUCTION

The vascular remodelling events which occur in the pulmonary artery leading to disease progression are driven by excessive SMC proliferation. SMC deposition is characteristic of concentric lesion formation and a dysregulated media is also seen in plexiform lesions. An important property of SMCs leading to vascular remodelling is the pleotrophic nature of the cell type. In healthy pulmonary arteries, small non-muscularised vessels are composed of fully differentiated contractile SMC whereas during vascular remodelling the cells switch to a synthetic phenotype (Dempsey et al., 1998). It is still unknown how this switch is initiated, however, the two distinct sub-types each play a role in the development of PAH. Both SMC types can be defined by their differential growth and cell surface expression as identified by isolating both cell types from pulmonary arteries and examining there growth and expression *in vitro.* Synthetic SMC were shown to have a more proliferative phenotype in comparison to their contractile counterparts which resembled a senescent population (Frid et al., 1997). The differential cell surface expression patterns were exemplified by co-culture of SMC and tumour necrosis factor-α stimulated vascular endothelial cells. Synthetic SMC and endothelial cell co-culture caused increased ICAM-1 and VCAM-1 expression and NF-κB translocation but senescent contractile SMC and endothelial cell co-culture had the converse effect (Wallace and Truskey, 2010). Primary SMCs isolated from pulmonary arteries of neonatal calves with hypoxia induced pulmonary hypertension displayed increased motility associated with upregulation of the Ca^{2+} binding protein S100A4 compared to healthy controls. With prolonged hypoxic exposure these SMC dedifferentiated to a more synthetic phenotype where they expressed the myofibroblast maker α- smooth muscle cell actin and showed increased [^{3}H]-thymidine and BrdU incorporation. More work is needed to identify why SMC change phenotype, however, this work by Stenmark *et al*

suggests hypoxia may be a contributing factor (Frid et al., 2009). Although some data suggest the contrary, the main body of data suggests hypoxia is a proliferative stimulus. For example within the same paper, Cooper *et al* show SMCs cultured in 5 % 0_2 and 10 % FCS proliferate after 24 hours as determined by BrdU incorporation and total cell counts. However, when these cells were cultured in 1 % 0_2 for 24 hours no proliferation was seen by the same detection methods (Cooper and Beasley, 1999). 10 % hypoxia has also been used as a secondary stimulus to stabilise a PAH phenotype in a variety of mouse models (Eddahibi et al., 2000) (Beppu et al., 2004) (Lui et al., 2005) (Steiner et al., 2009). A more reliable rat model of PAH uses 10 % hypoxia and Sugen 5416 injected rats to induce vascular remodelling which has traditionally been difficult to replicate in animal models but it is important to note that there is a significant difference in directly cellular exposure of oxygen between 10 % inhaled oxygen and 10 % oxygen *in vitro* (Abe et al., 2010).

The exact oxygen tensions of diseased vessels are unknown, however, indirect evidence that these lesions are hypoxic was provided by lungs from patients presenting with severe PAH. These patients expressed the hypoxia inducible transcription factor (HIF) both at the protein and mRNA level in both plexiform and concentric lesions (Tuder et al., 2001). HIF is a heterodimeric transcription factor composed of constitutively expressed β subunit and one of three oxygen sensitive α subunits. During oxygen availability, hydroxylated HIF- α is ubiquitinated and degraded by the E3 ubiquitin ligase complex containing the tumor suppressor protein Von Hippel- Lindau (VHL). Its presence therefore is an indirect marker of regional hypoxia. Another murine model for PAH is the $VHL^{R/R}$ mouse, these mice are homozygous for a specific mutation R200W affecting HIF degradation and have been shown to develop spontaneous PAH as determined by elevated systolic PA pressures of >25 mmHg. Moreover, the $VHL^{R/R}$ mice have increased mRNA expression of many HIF target genes specific to the HIF-2α subunit e.g. endothelin-1 (ET-1) thus a role for HIF-2α in the development of IPAH has been postulated (Hickey et al., 2010). In humans this specific mutation is associated with developing Chuvash Polycythemia. Patients with this disease are susceptible to developing spontaneous PAH making these

mice a potentially strong animal model for PAH and strengthening the link between HIF activity and PAH progression.

The presence of monocytes have also been shown in lung sections of patients with PAH (Hall et al., 2009) (Tuder et al., 1994) (Dorfmuller et al., 2003) (Frid et al., 2006) and in various animal models (Ikeda et al., 2002) (Voelkel and Tuder, 1994) (Dorfmuller et al., 2011), however, the role of these cell infiltrates is yet to be determined. Moreover, at sites of inflammation in the pulmonary vasculature there is evidence of neutophils invading tissue by extravating the endothelium of blood vessels. An essential leukocyte in facilitating neutrophil margination is the monocyte (Maus et al., 2003). Monocytes are circulating phagocytes with a patrolling role in tissues. Once in tissues they have the potential to differentiate into either tissue resident macrophages or dentritic cells. The importance of monocytes is strengthened by the fact that these cells are a major source of cytokines and very few cells can lead to a large biological effect (Morris et al., 2005). These are key cells in driving the inflammatory process, not only do they induce ROS production but this in turn increases pro-inflammatory cytokine release in plasma and further leukocyte recruitment to the pulmonary artery thus the association of inflammation and progression of PAH is strengthened.

Another inflammatory artefact which has been shown to be altered in pulmonary hypertension is systemic cytokine expression with the pro-inflammatory cytokines IL- 1β and IL-6 been shown to be increased 40 fold and 4 fold respectively in serum from patients with severe PPH, now known as PAH, compared with healthy control serum or those with pulmonary hypertension secondary to chronic obstructive pulmonary disease (Martin et al., 2002) (Hall et al., 2009). Circulating plasma levels of monocyte chemokines tumour necrosis factor-α (TNF-α) and MCP-1 have also been shown to be increased in the early stages of IPAH when compared to plasma of healthy controls (Itoh et al., 2006). Not only is IL- 1 been found to be increased in disease but also it is known that IL- 1β and IL- 1α are potent SMC proliferative stimuli (Ikeda et al., 1990), however, the mechanism by which they act is still under investigation. There is evidence that NF-κB pathway activation is needed for IL- 1β to exert its

proliferative effects on SMC. When exposed to 1 ng/ ml IL- 1β, SMC showed more nuclear translocation of the NK-κB pathway member p65 in cells expressing the proliferative marker Ki67 compared to non proliferating SMC (Sasu and Beasley, 2000). Furthermore, SMC transfection with dominant active IL- 1α precursor or full length protein transcript displayed enhanced SMC proliferation as measured by BrdU incorporation (Beasley, 1999). IL- 1 type 1 receptor (IL- 1R1) transduction involves the adaptor protein MyD88. Although not shown in pulmonary hypertension, the interaction of IL- 1 and the MyD88 pathway is evident in many other cardiovascular diseases such as atherosclerosis. Homozygous MyD88 deficient mice ($MyD88^{-/-}$) show significantly less neointima formation in response to vascular injury. This was reduced further by administration of an IL- 1R1 blocking antibody (Saxena et al., 2011) implicating a role for innate signalling in vascular repair. Taken together these data show an important role of the IL- 1 pathway in SMC proliferation.

The IL- 1 pathway also interacts with PAH diseased linked factors such as PDGF. PDGF is a potent proliferative stimulus for SMCs and induces proliferation via PI3K and Akt phosphorylation. Antibodies against PDGF inhibit IL-1 induced proliferation in smooth SMC as detected in mice by decreased tritiated leucine incorporation (Ikeda et al., 1990). Moreover, *in vitro* migration assays showed PDGF antibodies can inhibit IL-1 induced mitogenesis (Raines et al., 1989). The interaction of both these pathways is supported by work from Jiang *et al* who found SMC co-stimulated with 10 ng/ ml IL-1 β and 25 ng/ ml PDGF upregulating contractile markers such as myosin heavy chain and calponin at the protein level after 24 hours causing proliferation (Jiang et al., 2002). Membrane fractions from SMC stimulated with either PDGF or IL-1 β have shown an interaction of both PDGF receptor and IL-1R1 by co-immunoprecipitation. This interaction was explored further showing PDGF receptor β phosphorylation is inhibited by the addition of 10 ng/ ml IL-1 receptor antagonist (IL-1ra) (Cho et al., 2013).

A further growth factor associated with SMC proliferation and vascular remodelling in disease is VEGF. This cytokine is a HIF target gene and has been

demonstrated to be important in angiogenesis during embryonic development in particular. Evidence for this has been provided *in vivo* by homozygous and heterozygous VEGF knock out mice being embryonic lethal with abnormal blood vessel formation (Carmeliet et al., 1996) (Ferrara et al., 1996). VEGF is also known to be a potent pro survival and proliferation stimulus for endothelial cells and has more recently been shown to be upregulated in PAH vascular lesions (Geiger et al., 2000). Moreover, recent work also links soluble VEGF receptor secretion to stimulated monocytes. The group found HIF-2α mediated soluble VEGF receptor (Flt-1) production was increased in monocytes cultured in 0.5 % O_2 with GM-CSF stimulation (Eubank et al., 2011). The levels of Flt-1 in my co-culture supernatants will be investigated in my work.

I propose to study the interactions of vascular SMCs and monocytes using co-culture models with particular regard to total cell counts. I will investigate the potential role of local hypoxia on SMC proliferation and I want to establish both a normoxic (19 kPa) and hypoxic (3 kPa) comparative co-culture model with and without direct cell contact. Furthermore, due to changes in circulating levels of IL-6, IL-1, TNF- α, MCP-1, MIP-1 cytokines in patients with pulmonary hypertension and in monocrotaline rat models of the disease it will be important to establish whether cytokine profiles are modified with hypoxic stimulation and/ or the addition of monocytes.

3.2 RESULTS

3.2.1 PULMONARY ARTERY SMOOTH MUSCLE CELL NUMBER IS INCREASED IN HYPOXIA COMPARED TO NORMOXIA BUT METABOLIC ACTIVITY IS PRESERVED

Due to the controversy surrounding the effect of hypoxia on pulmonary arterial SMC proliferation it was important to establish the effect of hypoxia on SMC number in my model. Based on preliminary experiments investigating non diseased SMC numbers over a range of seeding densities (Chapter 2.4.1), a seeding density of 25,000 SMCs /well was selected. Moreover, to attempt to resemble physiological oxygen tensions 3 kPa of oxygen in the media was also selected. To ensure all findings were robust each experiment was carried out using at least 2 separate vials of cells over different passage numbers.

Commercially available healthy pulmonary arterial SMCs were grown alone in hypoxia (3 kPa) or normoxia (19 kPa) for 24 hours after 48 hours quiescence. Post-culture, cells were lifted and total cell counts were calculated by Coulter counter. SMC numbers were significantly increased in hypoxia compared to normoxia (n=16) (Figure 3.1 a).

To eliminate the possibility of the difference in SMC number at each oxygen tension being due to a change in cell viability in either culture condition, reduction of alamarBlue® was used as an indirect measure of cell viability. AlamarBlue® acts as a terminal electron acceptor in the electron transport chain in viable cells. Reduction of alamarBlue® leads to a colour change in the compound, this can then be read on a spectrophotometer. The results were compared to matched killed controls using 1 µg/ ml, protein synthesis inhibitor, cycloheximide. Cell free supernatant samples of healthy SMC cultured in hypoxia or normoxia were compared with cell free supernatants of matched killed controls. Results are expressed as arbitrary units /10,000 SMC (Figure 3.1

b). When corrected for cell number there was no significant difference in relative metabolic activity in either oxygen tension (n=8).

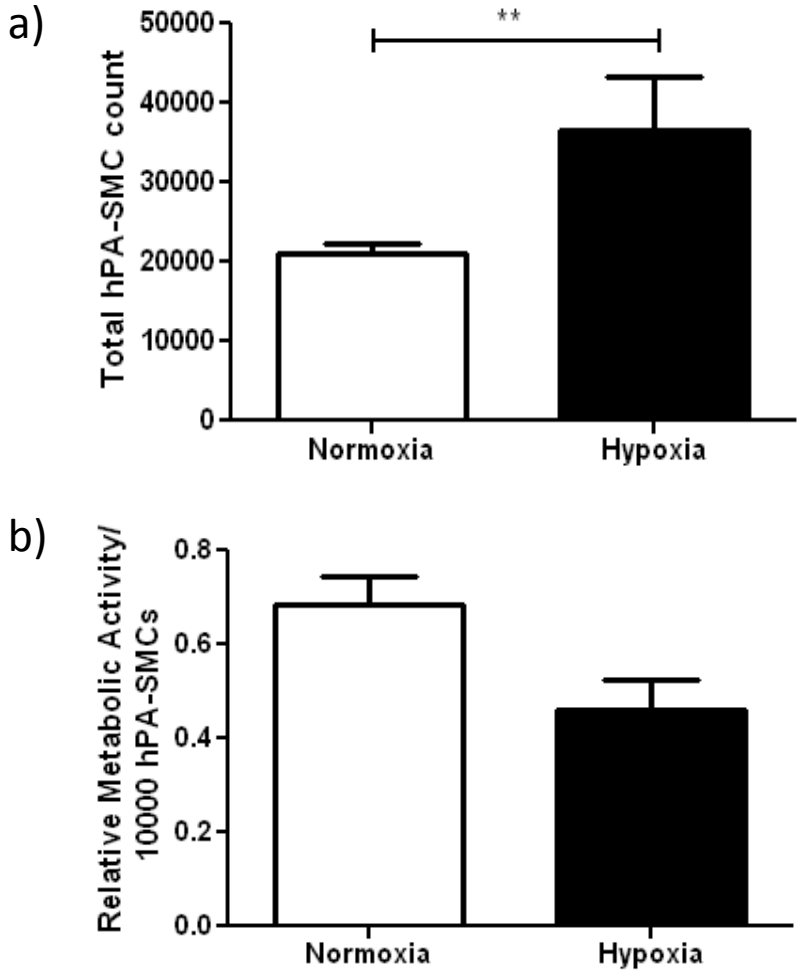

Figure 3.1 Pulmonary artery smooth muscle cell number is increased in hypoxia compared to normoxia but metabolic activity is preserved

SMCs were seeded in 24 well plates at 25,000 cells /well for 24 hours in normoxia (19 kPa) (open bars) and hypoxia (3 kPa) (closed bars) following 24 hours oxygen equilibration and 48 hours in low serum. a) Total cell numbers were calculated by Coulter counter. Bars represent mean +/- SEM, **P<0.01, cells from 6 seperate vials studied n=16, one-way ANOVA with Bonferonni post test. b) Relative metabolic activity

was measured by alamarBlue® reduction and expressed as arbitrary units /10,000 cells. Bars represent mean +/- SEM, cells from 2 seperate vials studied n=8.

3.2.2 PULMONARY ARTERY SMOOTH MUSCLE CELLS RETAIN THEIR PHENOTYPE IN HYPOXIA COMPARED TO NORMOXIA

Synthetic SMCs have been shown to de-differentiate when undergoing cell stress. The de-differentiated state has been shown to express more endothelial-like markers in comparison to the contractile SMCs (Dempsey et al., 1999). To ensure both hypoxic (3 kPa) and normoxic (19 kPa) SMC preserved their phenotype in the experimental model, they were fixed post- oxygen equilibration, serum starvation and 24 hour culture with 4 % paraformaldehyde for immunocytochemistry (ICC) to be performed. To ensure all findings were robust each experiment was carried out using at least 2 separate vials of cells over different passage numbers. Cells were analysed for smooth muscle cell β actin (a SMC marker), CD31 and Von Willebrand factor (both endothelial cell markers) using standard ICC protocols (Chapter 2.6.1).

Both normoxic and hypoxic SMCs were positive for smooth muscle cell β actin and negative for Von Willebrand factor and CD31. Secondary antibody only controls were negative for all three labels showing SMCs were maintaining their phenotype in the culture conditions (Figure 3.2).

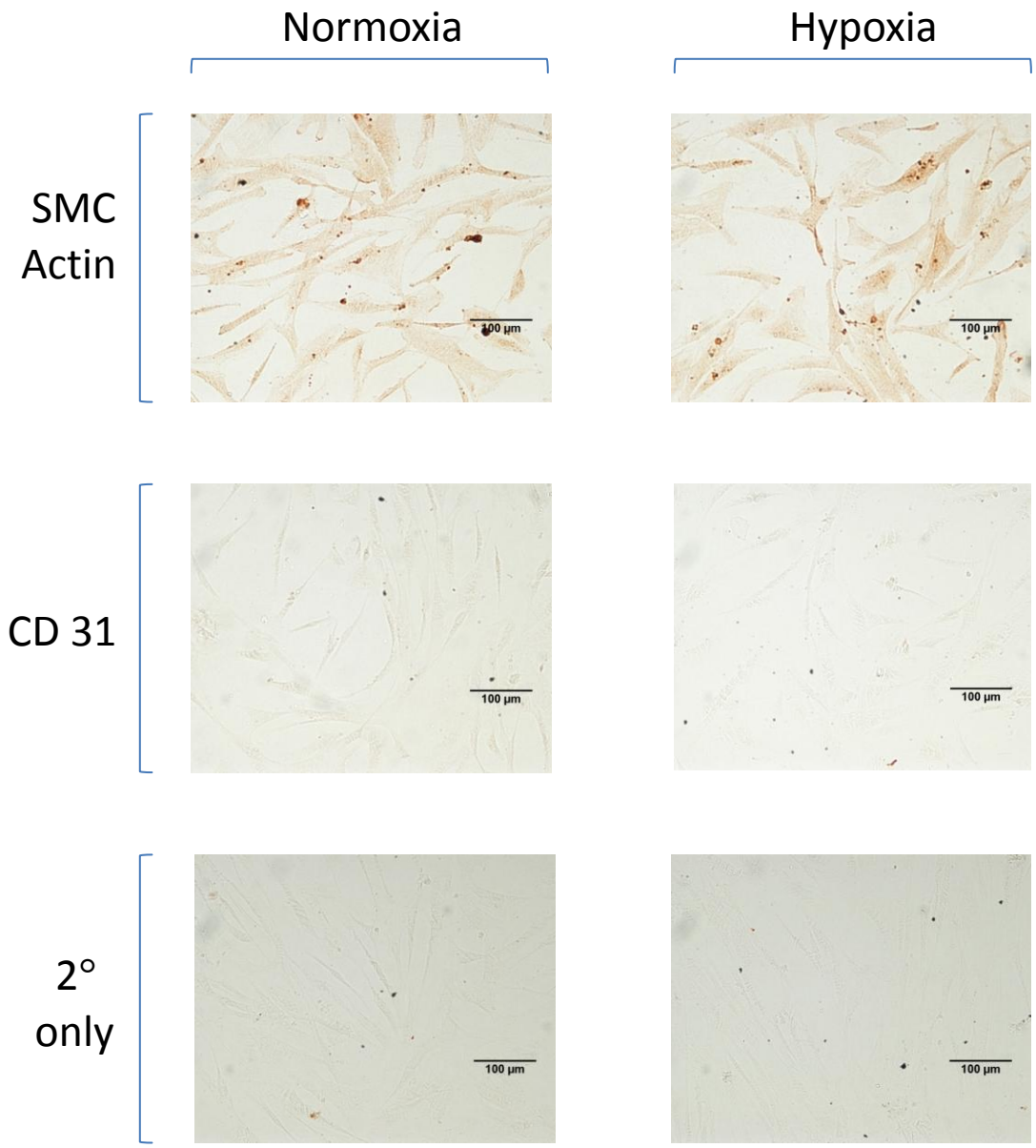

Figure 3.2 Smooth muscle cells retain their phenotype in hypoxia compared to normoxia

To establish if commercial SMCs were maintaining their phenotype in the culture system, cells were stained for the SMC marker, smooth muscle cell β actin and endothelial markers CD31 and Von Willebrand factor. Both normoxic and hypoxic SMC were positive for smooth muscle cell β actin. These cells were also negative for CD31 in

each oxygen tension. Secondary antibody only controls were negative for all three labels. Images were taken using the x 100 objective.

3.2.3 MONOCYTES HAVE INCREASED SURVIVAL AND MAINTAINED METABOLIC ACTIVITY IN HYPOXIA

Having found a difference in SMC behaviour in each oxygen tension, the effect of hypoxia (3 kPa) on monocytes was investigated. It has been shown in neutrophils that hypoxia acts as an anti-apoptotic stimulus (Walmsley et al., 2005), however, it is unknown whether this is true of other myeloid cells therefore survival was measured in each oxygen tension. Monocytes were obtained from healthy volunteers by OptiPrep™ density gradient separation. Only suspensions of purity 85 % or higher were used for experiments. Monocytes were cultured in both normoxia and hypoxia for 24 hours in pre-equilibrated RPMI containing 10 % FCS and 1 % P/S.

To investigate if hypoxia regulates monocyte survival, apoptosis was assessed by annexin-PE positivity seen on the FL-2 parameter on a FACS Calibur flow cytometer (Figure 3. 3 a). Monocytes alone showed a significant increase apoptosis at 24 hours in normoxia compared to hypoxia (n=4). The protein synthesis inhibitor cycloheximide (1 μg /ml) was used as a positive control, treated samples had significantly higher apoptosis compared to untreated samples (n =4). Membrane integrity was used to indicate necrosis. In these data necrosis is described as ToPro-3 positive, annexin -PE negative cells as detected on the FL-4 parameter of the FACS Calibur flow cytometer. There was no difference between rates of necrosis in either normoxia or hypoxia (n=4) or killed controls (n=4) (Figure 3.3 b).

Having shown that relative metabolic activity was unaffected in SMCs in either oxygen tension, the effect of hypoxia on relative metabolic activity of monocytes was subsequently investigated (Figure 3.3 d). Results are expressed as relative metabolic activity per 1000 monocytes. Metabolic activity was preserved in normoxia (19 kPa) versus hypoxia (3 kPa) (n=6). Cells were also stimulated with 10 ng /ml LPS to mimic an inflammatory insult as it is a potent TLR4

agonist, however, it had no additive effect on relative metabolic activity (n=6) (Figure3.3 c).

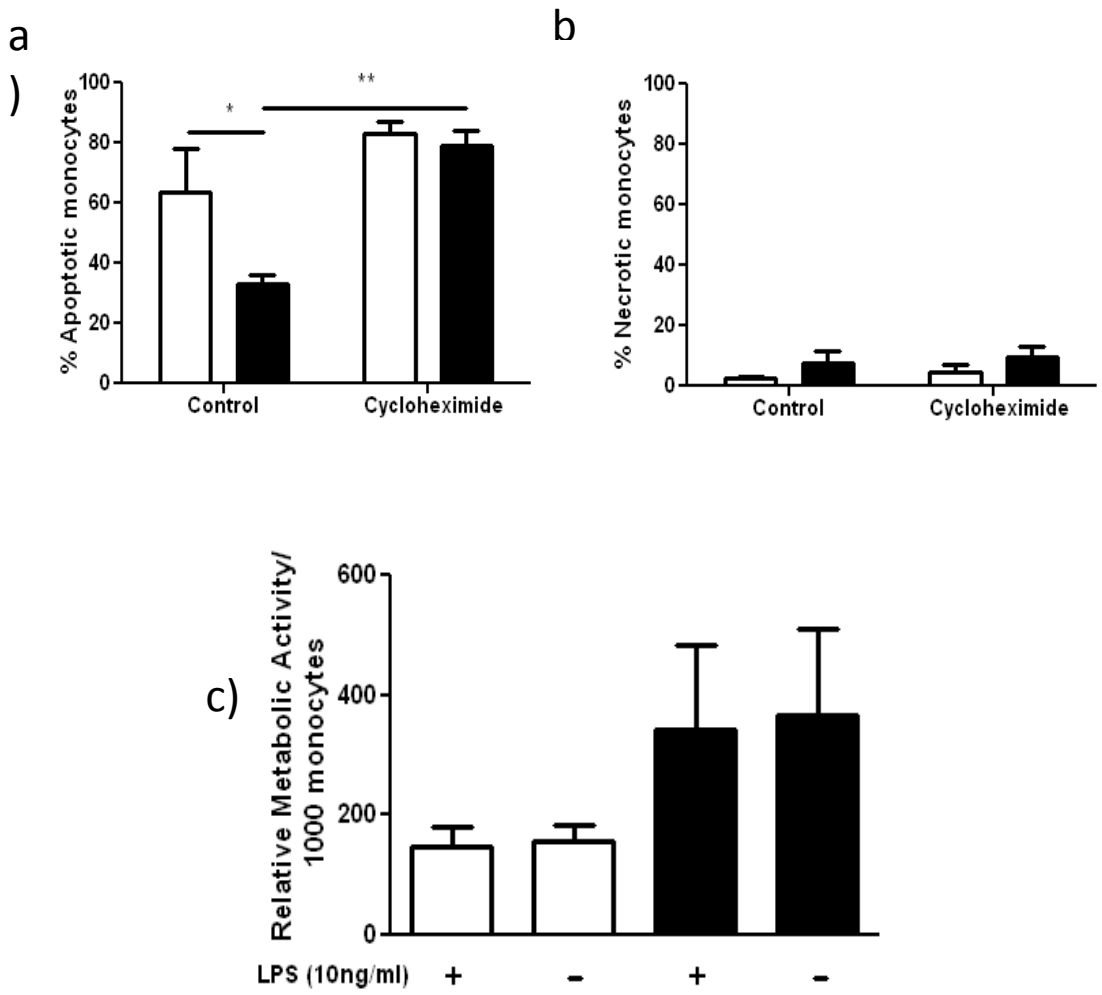

Figure 3.3 Monocytes have increased survival and preserved metabolic activity in hypoxia compared to normoxia

Monocytes were isolated from venous blood and cultured in normoxia (19 kPa) (open bars) or hypoxia (3 kPa) (closed bars) in parallel for 24 hours. a) Percentage apoptosis was calculated by annexin-PE positivity and b) necrosis by ToPro-3 positivity. Monocytes were directly compared to matched killed controls using 1 µg/ ml cycloheximide. Bars represent mean +/- SEM, *P<0.05, **P<0.01, n=4, two-way ANOVA with Bonferonni post test. c) Relative metabolic activity was measured in monocytes cultured for 24 hours with and without 10 ng /ml LPS by reduction of alamarBlue®.

Results are expressed as arbitrary units and normalised for monocyte cell number. Bars represent mean +/- SEM. Results shown as relative metabolic activity /1000 monocytes, n=6.

3.2.4 MONOCYTES CAN ABOLISH HYPOXIC SMOOTH MUSCLE CELL INCREASE IN CELL NUMBER

Having defined each cell type independently in normoxia and hypoxia a co-culture model was established. SMCs were seeded at 25,000 cell /well in each oxygen tension. In order to reflect physiological conditions a ratio of 1 monocyte: 5 SMCs was selected based on previous work on aortic SMC and monocyte co-cultures by Professor Sabroe's group (Morris et al., 2005). Plates were cultured for 24 hours with or without the addition of monocytes (5000 /well). The experiment was carried out using at least 4 separate vials of cells over different passages. Total cell counts were obtained by Coulter counter as previously shown (2.4.1). Total cell counts for SMCs in hypoxia were significantly higher than in normoxia (n=10). Our key finding was that the addition of monocytes (1:5) to SMC had no effect on normoxic SMC number but inhibited hypoxic increase in SMC number (n=10) (Figure 3. 4).

3.2.5 MONOCYTE INHIBITION OF HYPOXIC SMOOTH MUSCLE CELL PROLIFERATION IS NOT DUE TO INCREASED SMOOTH MUSCLE CELL APOPTOSIS

Monocyte induced reduction in hypoxic SMC number could be mediated by inhibition of SMC proliferation or increased SMC death. The latter was investigated using fluorescent TUNEL SMC labelling following mono- and co-culture. The fluorescent nuclear dye DAPI was used to focus samples and overlays with FITC positive TUNEL used for manual counts (Figure 3. 5). Results are expressed as percentage apoptotic from total cells with at least three hundred cells from three different fields counted. Hypoxic and normoxic SMC alone showed less than 5 % apoptosis after 24 hours (n=3). The addition of monocytes had no effect on apoptosis rates in either oxygen tension (n=3). Unstained negative controls showed only DAPI positivity. Positive controls

were carried out by pre-incubation with 1 μg /ml cycloheximide. Cycloheximide significantly increased apoptosis in both normoxic and hypoxic SMC alone compared to their untreated counterparts (n=3).

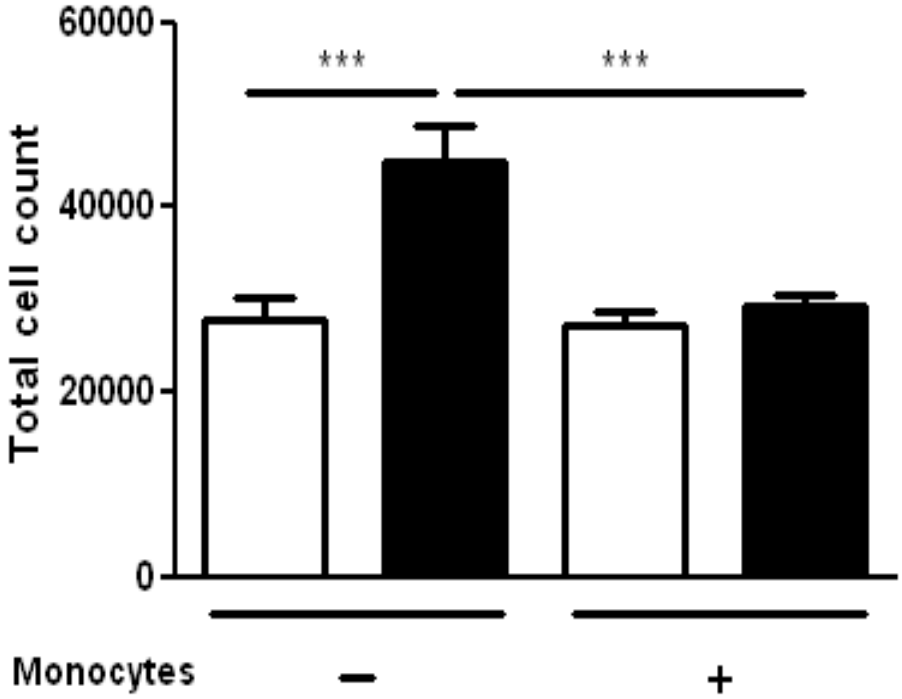

Figure 3.4 Monocytes can abolish hypoxic smooth muscle cell increase in cell number

SMCs were grown in both normoxia (19 kPa) (open bars) and hypoxia (3 kPa) (closed bars) for 24 hours after serum starvation and oxygen equilibration with and without monocytes purified from venous blood. Monocytes were co-cultured at a ratio of 1 monocyte: 5 SMC. Bars represent mean +/- SEM, ***P<0.001, cells from 2 seperate vials studied n=10, one-way ANOVA with Bonferonni post test.

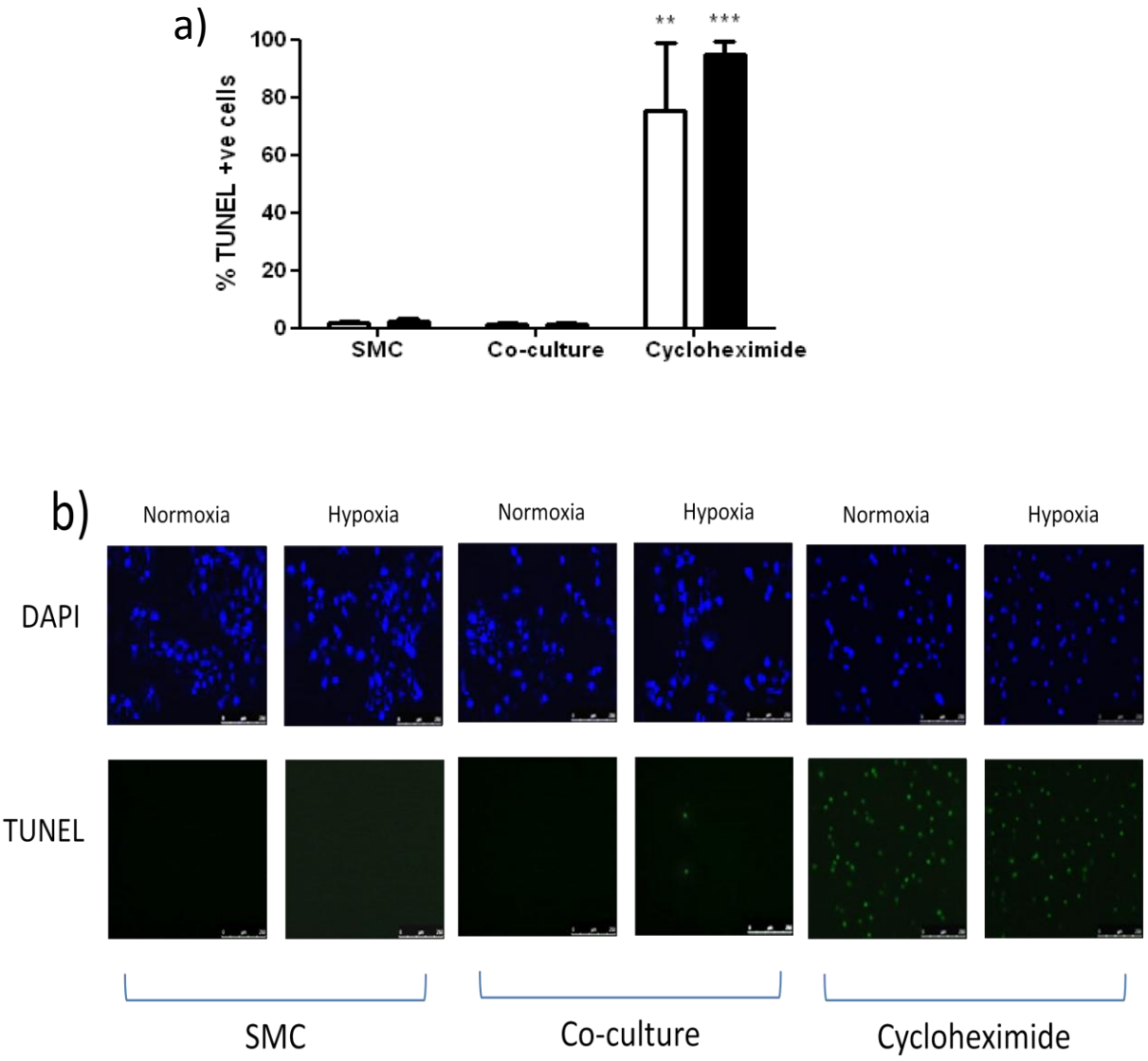

Figure 3.5 Monocyte inhibition of hypoxic smooth muscle cell proliferation is not due to increased apoptosis

SMCs were cultured with and without monocytes for 24 hours in either normoxia (19 kPa) (open bars) or hypoxia (3 kPa) (closed bars). TUNEL assay flourescin labelled apoptotic nuclei. Positive controls were pre-incubated with 1 μg/ ml cycloheximide. a) Percentage apoptotic cells from total cell population in at least 300 cells from 3 different fields. Bars represent mean +/- SEM, **P<0.01, ***P<0.001, n=3, one-way ANOVA with Bonferonni post test. b) Representative FITC positive TUNEL images of normoxic and hypoxic monoculture, co-culture and cycloheximide treated SMC and DAPI positive images. Images were magnified x1000.

3.2.6 AORTIC VASCULAR SMOOTH MUSCLE CELLS HAVE ALTERED GROWTH RESPONSES COMPARED TO PULMONARY ARTERIAL SMOOTH MUSCLE CELLS

The pulmonary vasculature is thought to be unique and possess different properties to the systemic vasculature. Not only due to it being a high pressure and high resistance system but it has also been shown to express different adhesion molecules in comparison to the rest of the circulation. Bearing this in mind both pulmonary artery SMCs and aortic vascular SMCs were compared in the same culture system. Aortic vascular SMCs were seeded at 25,000 cells /well prior to 24 hour oxygen equilibration in either normoxia (19 kPa) or hypoxia (3 kPa) and 48 hour serum starvation. Cells were cultured for a further 24 hours with and without the addition of monocytes at a ratio of 1 monocyte: 5 SMCs as above (Figure 3.6). Instead of finding hypoxic induced proliferation of aortic SMCs, hypoxia had no effect on total cell numbers compared to their normoxic counterparts (n=4). Moreover no change in cell number was observed by the addition of monocytes in either oxygen tension compared to monoculture baseline numbers (n=4). These data suggest hypoxic uplift in SMC number and monocyte inhibition of SMC proliferation is specific to pulmonary artery SMCs.

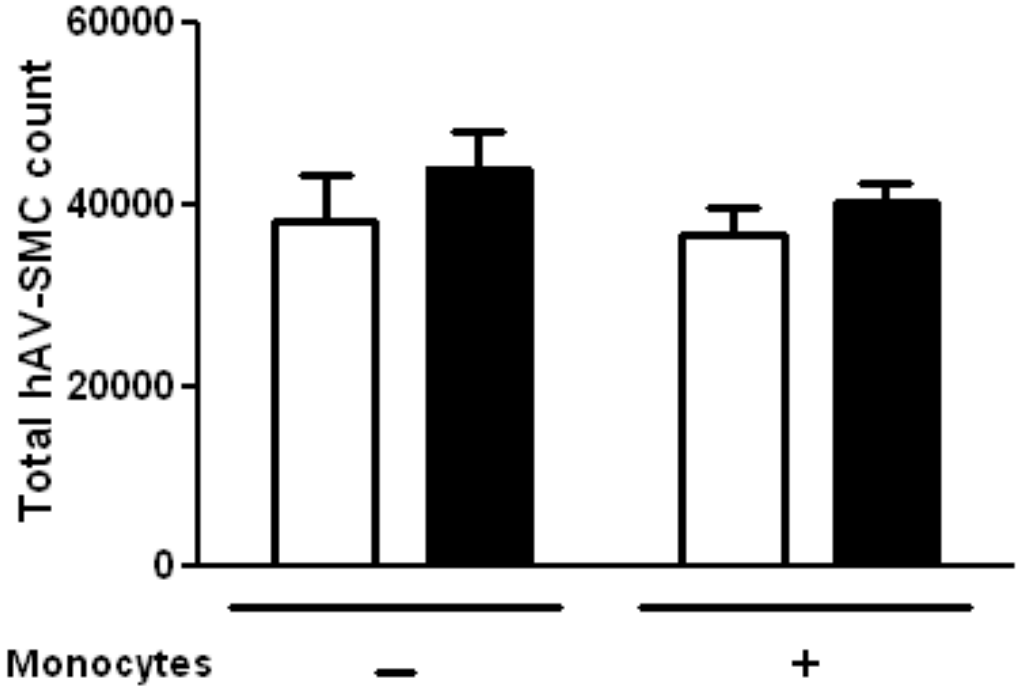

Figure 3.6 Aortic vascular smooth muscle cells have altered growth responses compared to pulmonary arterial smooth muscle cells

Aortic SMCs were seeded at 25,000 cells/ well and left to oxygen equilibrate for 24 hours then left in quiescent media for 48 hours. Cells were then cultured with and without monocytes (1 monocyte: 5 SMC) for 24 hours in both normoxia (19 kPa) (open bars) and hypoxia (3 kPa) (closed bars). Post culture washed trypsinised wells were counted by Coulter counter. Bars represent mean +/- SEM, n=4.

3.2.7 MONOCYTE INHIBITION OF HYPOXIC SMOOTH MUSCLE CELL PROLIFERATION IS INDEPENDANT OF DIRECT CELL CONTACT AND TRANSFERABLE

Having shown that pulmonary artery SMC and monocyte co-culture can modulate SMC proliferation, the importance of direct cell contact was investigated. To do this, co-cultures were carried out as above using 0.4 μm pore transwells to separate monocytes from SMC. To ensure all findings were robust each experiment was carried out using at least 2 separate vials of cells over different passage numbers. Total cell counts were measured by Coulter counter after 24 hour culture. Again hypoxia significantly increased SMC number compared to normoxia (n=6) and addition of monocytes in transwells significantly reduced hypoxic increase in total cell number (n=6) (Figure 3.7 a).

To further explore the importance of direct cell contact, monocytes were cultured for 24 hours in normoxia and hypoxia and cell free supernatants (SN) saved. Total SMC counts were calculated by Coulter counter after 24 hour incubation with monocyte SN. Both normoxic and hypoxic monocyte SN had no effect on normoxic total SMC counts (n=4). However, hypoxic SMC proliferation was significantly inhibited not only by normoxic monocyte supernatants but also by hypoxic monocyte SN to a similar order of magnitude (n=4) (Figure 3.7 b). This experiment shows that monocyte inhibition of hypoxic SMC proliferation is a transferable effect and it is independent of monocyte hypoxia.

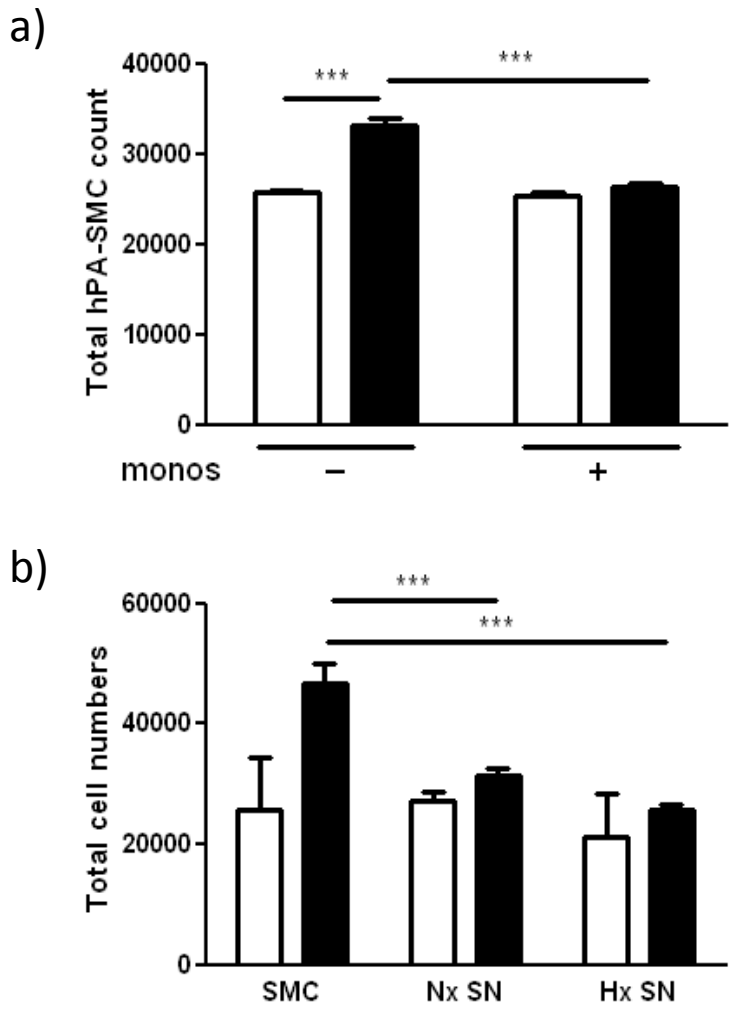

Figure 3.7 Monocyte inhibition of hypoxic smooth muscle cell proliferation is independent of direct cell contact and transferable

SMCs were seeded at 25,000 cells /well in normoxia (19 kPa) (open bars) and hypoxia (3 kPa) (closed bars) for 24 hours. a) Monocytes were added to co-culture wells in 0.4 μm transwells. Total cell counts were carried out on the washed and trypsinised SMC using a Coulter counter. Bars represent mean +/- SEM, ***P<0.001, cells from 2 seperate vials studied n=6, one-way ANOVA or two-way ANOVA with Bonferonni post test. b) Cell free supernatants from normoxic and hypoxic monocytes were added to SMC and cultured for 24 hours. Total cell counts were analysed as above. Bars represent mean +/- SEM, ***P<0.001, n=4, one-way ANOVA with Bonferonni post test.

3.2.8 LIPOPOLYSACCHARRIDE HAS NO EFFECT ON THE ABILITY OF MONOCYTES TO INHIBIT HYPOXIC SMOOTH MUSCLE CELL PROLIFERATION

In pulmonary hypertension monocytes will be recruited to an acutely inflammatory pulmonary artery and thus be activated. To ensure that the co-culture model was representative of this, lipopolysaccharide (LPS), a potent TLR 4 agonist was used. LPS is known to activate the pro-inflammatory MyD88 pathway in monocytes leading to cytokine production and cell activation. LPS was used at 10 ng /ml which is the gold standard concentration when working with monocytes to activate a pro-inflammatory response (Figure 3.8). The experiment was carried out using at least 2 separate vials of cells over different passage numbers.

SMCs were seeded at 25,000 cells /well and cultured for 24 hours with and without monocytes and /or LPS following 24 hour oxygen equilibration and 48 hour serum starvation. Following 24 hour culture total cell counts were measured by Coulter counter. Monocytes stimulated with LPS were equally able to inhibit hypoxic SMC number as unstimulated monocytes (n=8).

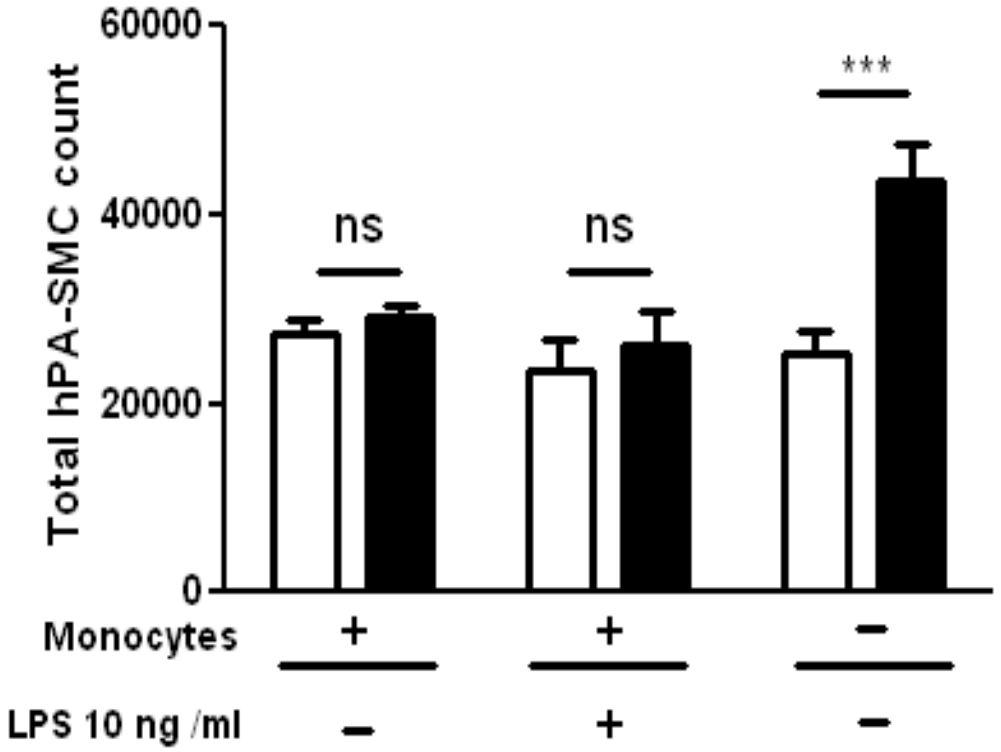

Figure 3.8 Lipopolysaccharide has no effect on the ability of monocytes to inhibit hypoxic smooth muscle cell proliferation

SMCs were seeded in 24 well plates at 25,000 cells /well and cultured in normoxia (19 kPa) (open bars) and hypoxia (3 kPa) (closed bars) for 24 hours prior to serum starvation. Plates were then maintained with and without monocytes (1 monocyte: 5 SMC) or LPS (10 ng/ml) stimulation. Total cell counts were calculated by Coulter counter. Bars represent mean +/- SEM, ***P<0.001, ns= not significant, cells from 2 seperate vials studied n=8, two-way ANOVA with Bonferonni post test.

3.2.9 SMOOTH MUSCLE CELL AND MONOCYTE CO-CULTURE PRO-INFLAMMATORY CYTOKINE EXPRESSION PROFILES

With the knowledge that hypoxic SMC proliferation can be modulated by monocyte supernatant, cell free supernatants were obtained from SMC and monocyte monocultures and co-cultures. Differences in expression between mono- and co-culture samples would give key insights into potential factors which could be eliciting inhibition of hypoxic SMC proliferation. Supernatant samples were then analysed by enzyme-linked immunosorbent assay (ELISA) for factors which monocytes were known to release such as IL- 1β, IL-1ra, IL-8, IL-6, IL-10, IFN-γ and RANTES. LPS at 10 ng /ml was used to create more physiologically relevant conditions and maximise monocyte activation and cytokine profiles.

Monocytes alone released undetectable levels of IL-8, this was unaffected by LPS stimulation or hypoxia. Interestingly, neither LPS stimulation nor hypoxia had any effect on IL-8 release from SMC alone (Figure 3.9 a). LPS stimulation almost doubled the expression of IL-8 from co-cultures compared to unstimulated co-cultures in each oxygen tension (n=6).

IL-6 release followed a similar pattern, stimulated co-cultures significantly increased IL-6 compared to unstimulated counterparts (n=6) (Figure 3.9 b). Under all conditions IL-1 β levels were below the limit of detection. This was also true of the TLR 3 downstream target IFN- γ, IL-1ra and the anti-inflammatory cytokine IL-10. The chemokine CCL5 also known as RANTES followed a similar pattern to the other pro-inflammatory cytokines and LPS stimulated co-cultures had significantly increased expression compared to unstimulated counterparts (n=6) (Figure 3.9 c).

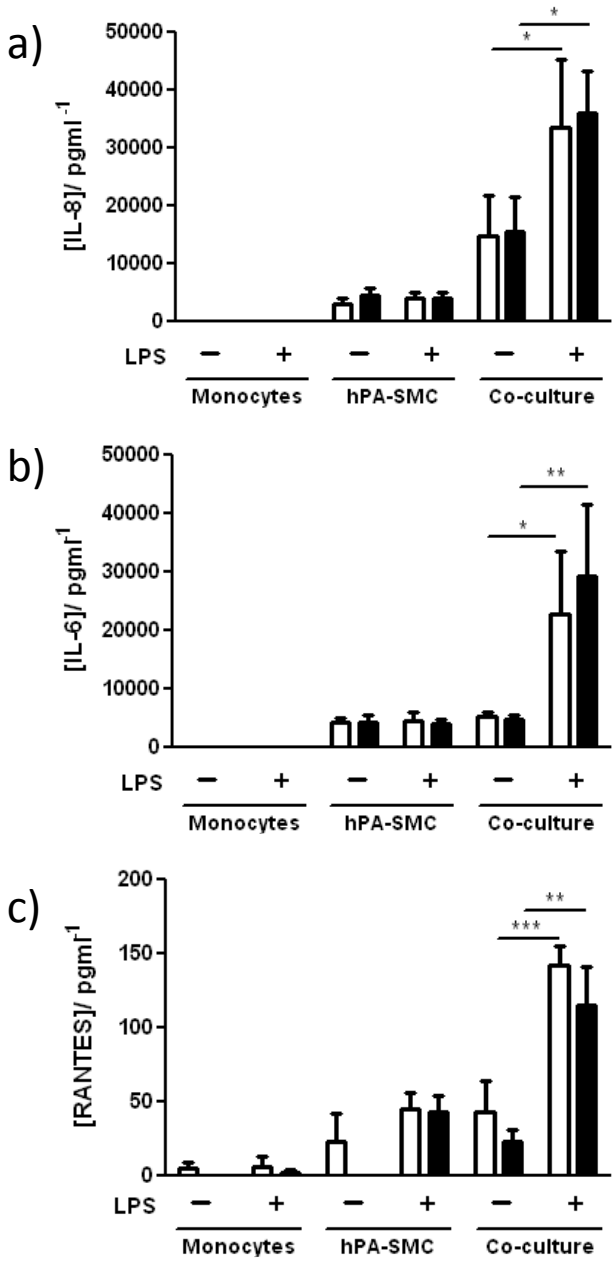

Figure 3.9 Pro-inflammatory cytokine profiles of smooth muscle cell and monocyte monoculture and co-cultures

Monocytes and SMC monocultures and co-cultures (1 monocyte: 5 SMC) were set up in normoxia (19 kPa) (open bars) and hypoxia (3 kPa) (closed bars). Cell free supernatants were collected from each condition with and without 10 ng/ ml LPS stimulation and analysed by sandwich ELSIA by the manufacturer's instructions. Values were calculated using log transformation and linear regression analysis for secreted expression of a) IL-8, b) IL-6 and c) RANTES. Bars represent mean +/- SEM, *P<0.05, **P<0.01, ***P<0.001, n=6, two-way ANOVA with Bonferonni post test.

3.2.10 EXPRESSION PROFILES OF DISEASE RELATED FACTORS

Being unable to find any pro-inflammatory cytokines or chemokines responsible for causing monocyte inhibition of SMC proliferation, disease linked factors were then examined. OPG, BMP4 and endothelin-1 are all factors shown to be increased in serum of patients with PAH. Each of the proteins has been shown to contribute to vascular remodelling and thus disease progression. Monocytes alone did not produce any OPG but SMC alone in both oxygen tensions produced the factor to similar levels (n=2). Stimulation had no effect on OPG release in either oxygen tension (Figure 3.10 a). Endothelin-1 and BMP4 were expressed below the limit of detection suggesting none of these factors could be responsible for monocyte inhibition of hypoxic SMC proliferation.

Another factor which has been shown to upregulated in remodelled pulmonary arteries and a known angiogenic factor is VEGF. This growth factor is also a HIF target gene so was used as a positive control for hypoxic samples. Hypoxia significantly increased VEGF levels compared to normoxic levels in SMC alone (n=6) and in SMC and monocyte co-cultures (n=6) providing indirect evidence of HIF activation in the culture system. LPS stimulation had no effect on VEGF expression (Figure 3.10 b). Monocytes stimulated with granulocyte macrophage colony stimulating factor (GM-CSF) were found to increase expression of the soluble VEGF receptor-1 also known as sFlt-1 (Eubank et al., 2012). It was postulated that in the culture system monocytes were activated and releasing sFlt-1 which was binding to the hypoxic induced VEGF from hypoxic SMCs preventing increase in cell number from co-culture samples. I went on to measure LPS stimulated monocyte release of sFlt-1 as well as in SMC alone and in monocyte and SMC co-culture. Normoxic monocytes alone produced no sFlt-1, hypoxia increased sFlt-1 levels and LPS further increased release but all values are below 150 pg/ ml which is the limit of detection (n=3) (Figure 3.10 c).

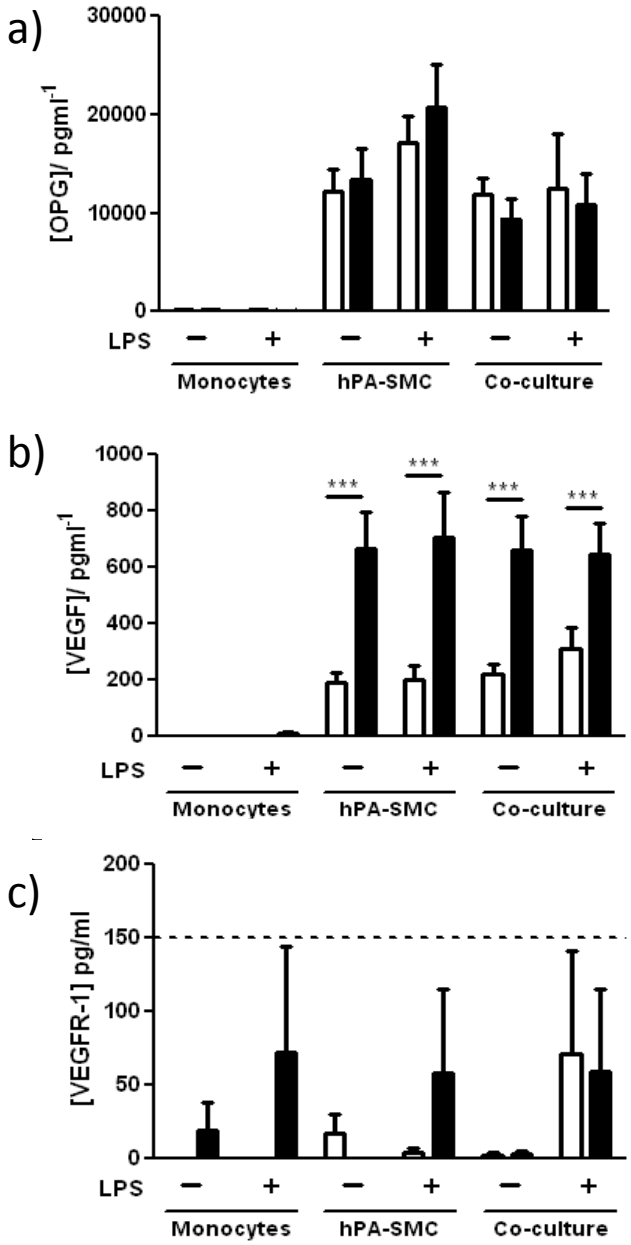

Figure 3.10 Expression profiles of disease related factors

SMCs and monocytes were grown in normoxia (19 kPa) (open bars) or hypoxia (3 kPa) (closed bars) for 24 hours as well as co-cultures of both cell types (1 monocyte: 5 SMC). Cell free supernatants were obtained from cultures with and without LPS (10 ng/ml) and analysed by ELISA according to the manufacturer's instructions. Values were calculated using log transformation and linear regression analysis for a) OPG (n=2), b) VEGF (n=6) and c) Flt-1 (n=3). Bars represent mean +/- SEM, ***P<0.001, two-way ANOVA with Bonferonni post test.

3.2.11 AORTIC SMOOTH MUSCLE CELL PRO-INFLAMMATORY CYTOKINE PROFILES

As the above results were contradictory to comparative data using aortic vascular SMCs (Morris et al., 2005), the validity of the results was investigated using aortic vascular SMCs in the same culture system. Cell free supernatants were obtained from human aortic vascular SMC and monocyte monocultures and co-cultures. Secreted IL-1 β, IL-6, IL-8 and VEGF were analysed by ELISA. As with pulmonary arterial SMC culture, LPS was used as an inflammatory stimulus to maximise the activation of the MyD88 pathway leading to increased pro-inflammatory cytokine release. There was no detectable IL-8 from monocytes alone in either oxygen tension with or without LPS stimulation. Neither LPS stimulation nor hypoxia had any effect on IL-8 release from SMC alone (Figure 3.11 a). Hypoxia significantly increased unstimulated co-culture IL-8 release compared with its normoxic counterpart (n=4). Stimulation further increased monocyte and SMC co-culture IL-8 release in hypoxia compared to normoxia (n=4). Monocytes alone produced no IL-6 while SMC alone in normoxia and hypoxia released equivalent levels of IL-6 (n=3). Stimulation had no effect on SMC monoculture release of IL-6 (n=4). Unstimulated co-culture IL-6 release was significantly increased compared to stimulated co-culture in normoxia (n=4) and hypoxia (n=4) (Figure 3.11 b). IL-1 β was detectable but limitations of the assay meant values were both low and variable (Figure 3.11 c). Again hypoxic secretion of VEGF was increased in hypoxia compared with normoxia. This was significant for hypoxic LPS stimulated co-culture compared to its normoxic counterpart (n=4) (Figure 3.11 d). These data closely resembled data previously published (Morris et al., 2005) suggesting that there is a real detectable difference in responsiveness between pulmonary artery SMCs and aortic vascular SMCs.

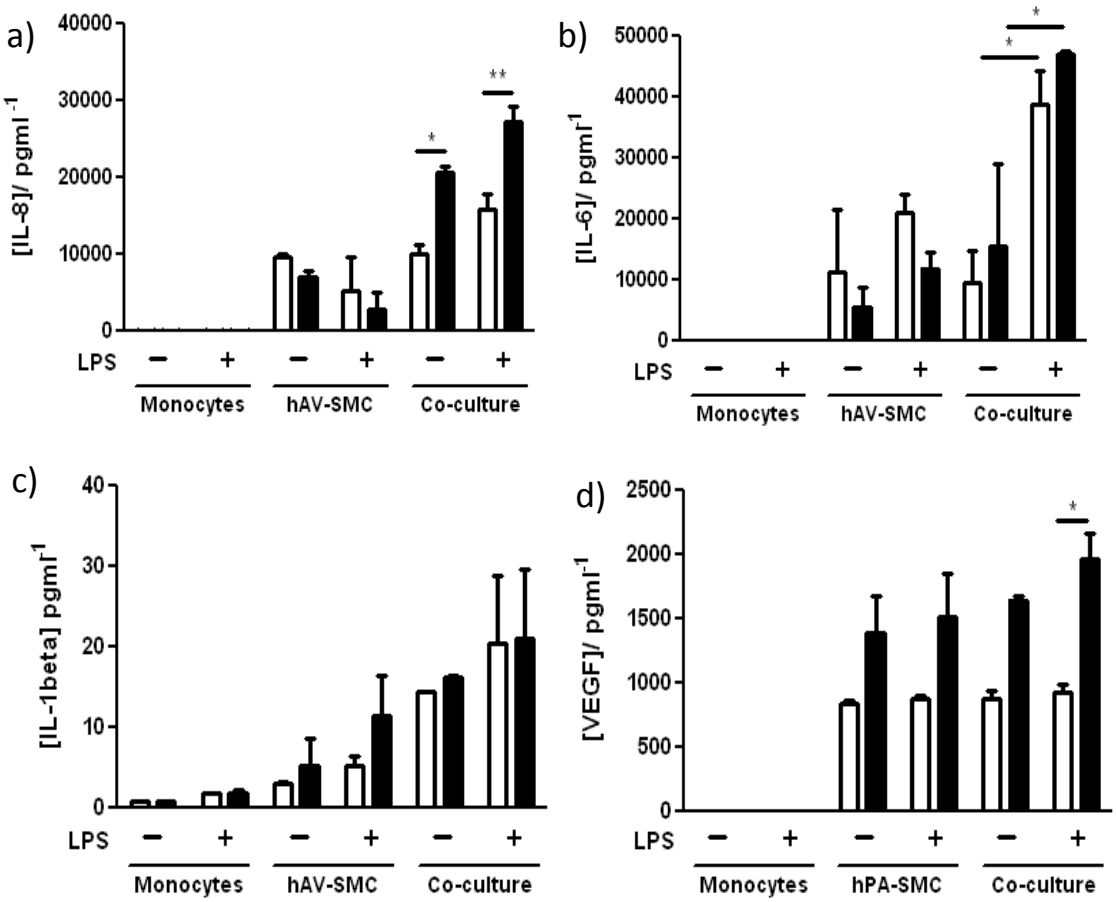

Figure 3.11 Aortic vascular smooth muscle cell pro-inflammatory cytokine profiles

Commercial aortic SMCs were cultured in normoxia (19 kPa) (open bars) and hypoxia (3 kPa) (closed bars) for 24 hours with and without monocytes (1 monocyte: 5 SMC). Cell free supernatants were obtained with and without LPS (10 ng/ml) stimulation and analysed by ELISA according to the manufacturer's instructions. Values were calculated using log transformation and linear regression analysis for a) IL-8 (n=4), b) IL-6 (n=4), c) IL-1 β (n=3) and d) VEGF (n=4). Bars represent mean +/- SEM, *P<0.05, **P<0.01, two-way ANOVA with Bonferonni post test.

3.2.12 Interleukin-1 receptor antagonist can inhibit hypoxic stimulated smooth muscle cell proliferation

Although IL- 1 was undetectable in culture supernatants by ELISA, the IL- 1 pathway may still have a role in monocyte inhibition of hypoxic SMC proliferation. IL- 1 is known t be difficult to detect by ELISA owing to the fact that it has both a short half life and is released early on during inflammation. Work by Professor Sabroe's group found that although they were unable to detect IL- 1 itself in culture supernatants they were able to modulate their phenotype by the addition of exogenous IL- 1ra showing a role for the IL- 1 pathway in their model. Therefore, to further investigate a role of the IL-1 pathway in the culture system above, SMC and monocyte cultures were pre-incubated with increase concentrations of a) exogenous human IL- 1ra (Anakinra) and b) its matched placebo (carrier fluid alone). This experiment was carried out using at least two different vials of pulmonary artery SMCs at different passages.

Hypoxic SMCs alone had significantly higher total cell counts than both their normoxic counterparts and hypoxic SMCs with monocytes (n=6) (Figure 3.12 a). Exogenous IL- 1ra at 0.75 ng/ ml led to a small reduction in hypoxic SMC number when cultured alone compared to hypoxic co-culture values and normoxic SMC number (n=4). Hypoxic SMC number was reduced further with addition of 1.5 ng/ ml IL- 1ra when compared to both hypoxia co-culture and normoxia alone (n=4). At 3 ng/ ml IL- 1ra hypoxic SMC number dropped to numbers similar to normoxic SMC alone and of hypoxic co-culture (n=6). Cultures incubated with IL-1ra at concentrations of more than 3 ng/ ml had a reduced hypoxic SMC number comparable to hypoxia co-culture and normoxia alone values.

To ensure the IL- 1ra carrier had no effect in the culture system, SMCs were grown both in normoxia and hypoxia with and without monocytes and either 3 ng/ ml or 50 ng/ ml Anakinra IL-1ra placebo. Exogenous placebo had no effect on total cell counts and in each condition, cell number in hypoxia alone was significantly higher than in either normoxia alone or hypoxia co-culture, (n=4).

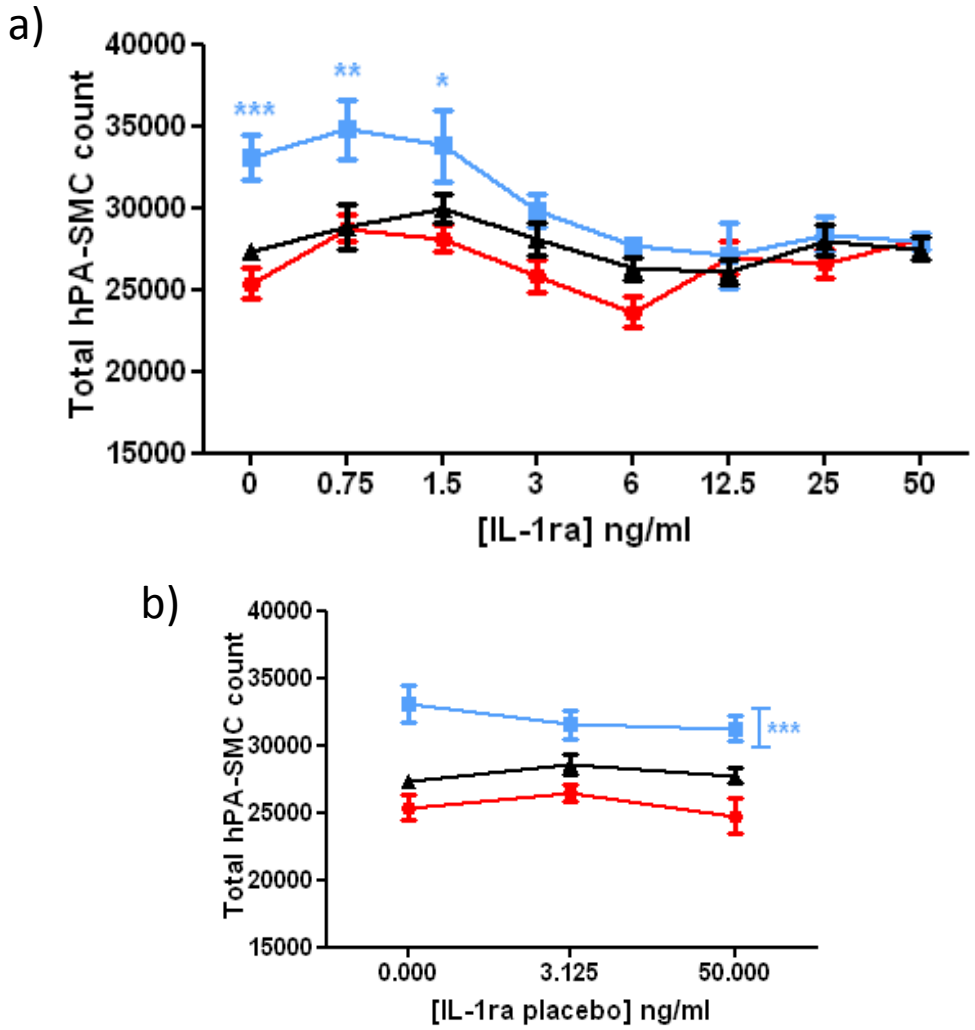

Figure 3.12 Exogenous IL-1ra can inhibit hypoxic stimulated smooth muscle cell proliferation

SMCs were cultured in normoxia (19 kPa) alone (black) and hypoxia (3 kPa) with (red) or without (blue) addition of monocytes (1 monocyte: 5 SMC). Each condition was pre incubated with increasing concentrations of a) IL-1ra or b) placebo for 30 mins prior to 24 hour culture. Total cell counts were performed by Coulter counter. Points represent mean +/- SEM a) *P<0.05, **P<0.01, ***P<0.001, cells from 2 seperate vials studied n=4 0.75 ng/ ml and 1.5 ng/ ml, n=6 other values, two-way ANOVA with Bonferonni post test. b) ***P<0.001, n=4, two-way ANOVA with Bonferonni post test.

3.2.13 Indirect evidence of Interleukin- 1 activity as measeured by Interleukin- 8 expression

Addition of exogenous IL- 1ra had a biological effect in the culture system but it was not known if this was due to interruption of the IL- 1 pathway. As we were unable to detect IL- 1 by ELISA, IL- 8 expression was used as an indirect measure of IL- 1 pathway activation. Both IL- 1β and IL- 8 release are induced by activation of the MyD88 pathway thus reduced activation of this pathway by IL- 1ra should mediate a reduction in IL-8..

SMC were grown in normoxia (19 kPa) and hypoxia (3 kPa) for 24 hours with or without pre-incubation with increase concentrations of exogenous IL- 1ra or placebo for 30 mins and with or without monocytes (1 monocyte: 5 SMC). Cell-free supernatants were then collected and analysed by ELISA for IL- 8 release.

Cell-free supernatants from a) SMC in normoxia alone (n=4), b) SMC in hypoxia alone (n=4) and c) SMC in hypoxia co-cultured with monocytes (n=4) had similar expression patterns of IL-8 (Figure 3.13). Each condition had a reduction in IL-8 with incubation of IL-1ra at concentrations of 3 ng/ ml or higher compared with no IL-1ra (n=4).

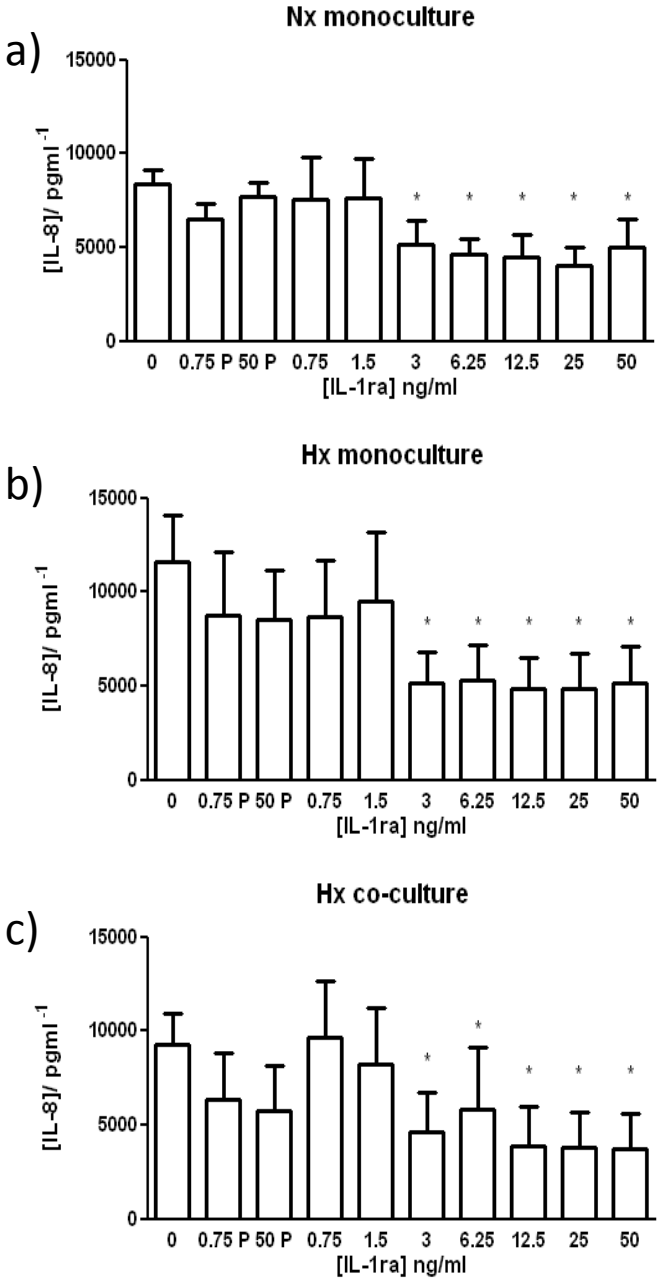

Figure 3.13 Indirect evidence of IL- 1 activity as measured by IL-8 expression
SMCs were seeded at 25,000 cells /well and plates left to equilibrate in normoxia (19 kPa) and hypoxia (3 kPa) for 24 hours. Following 48 hours serum starvation, plates were pre-incubated with increasing concentrations of exogenous IL-1ra for 30 mins prior to 24 hour culture with and without monocytes (1 monocyte: 5 SMC). Cell free supernatants were saved from samples cultured in a) normoxia alone, b) hypoxia alone and c) hypoxia with monocytes to be analysed by ELISA. Concentrations of interleukin-8 pg/ ml were calculated using log transformation and linear regression analysis. Bars represent mean +/- SEM, *P<0.05, n=4, one-way ANOVA with Bonferonni post test.

3.2.14 MONOCYTES CANNOT INHIBIT GROWTH FACTOR INDUCED SMOOTH MUSCLE CELL PROLIFERATION

Monocytes can inhibit hypoxic induced SMC proliferation but I was yet to determine if this is specific to hypoxia. To address this, the effect of monocytes on growth factor induced SMC proliferation was determined. The pro-angiogenic growth factor PDGF was used at increased concentrations to stimulate SMC proliferation.

SMCs were seeded at 25,000 cells /well with or without monocytes (1 monocyte: 5 SMC) and increase concentrations of PDGF following 48 hour serum starvation. After 24 hour culture total cell counts were performed by Coulter counter. SMC number significantly increased with addition of 3 ng/ ml PDGF in monoculture (n=4) and in co-culture (n=4) (Figure 3.14). This increase in cell number was maintained at 10 ng/ ml PDGF. Addition of monocytes had no effect on total cell counts at either concentration of PDGF.

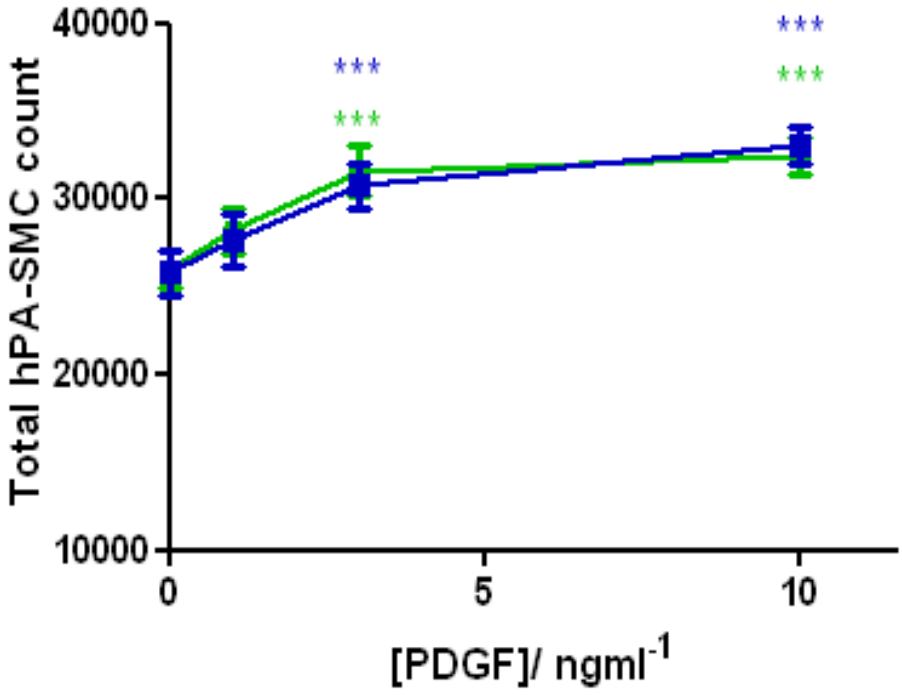

Figure 3.14 Monocytes cannot inhibit growth factor induced smooth muscle cell proliferation

SMCs were seeded at 25,000 cells /well before quiescence. Plates were then co-incubated with (blue) and without (green) monocytes (1 monocyte: 5 SMCs) and increasing concentrations of platelet derived growth factor (PDGF) for 24 hours. Total cell counts were performed by Coulter counter. Points represent mean +/- SEM, ***P<0.001, n=6, two-way ANOVA with Bonferonni post test.

3.3 DISCUSSION

In PAH, extracellular matrix deposition, endothelial dysfunction and aberrant channel formation lead to increase right ventricular pressure, poor oxygenation of the pulmonary vessels and eventually heart failure (Voelkel et al., 1995). Thickened medial layers underlie the vascular remodelling process however the trigger for this is still unknown. Much descriptive work has been done regarding phenotyping vascular changes associated with IPAH vessel remodelling but less is known about the role of the inflammatory component. It has been shown that these areas express the hypoxic inducible transcription factor HIF (Tuder et al., 2001) suggesting these areas may have localised hypoxia. With this in mind I was using physiological oxygen tensions of 3 kPa to gain a more reliable model for human conditions. Based on preliminary work in my methods a time frame of 24 hours was also selected (Chapter 2.4).

I found hypoxia significantly increases pulmonary arterial SMC total cell number. The effect of hypoxia on pulmonary arterial SMC is a source of much contention (Tamm et al., 1998) (Dempsey et al., 1991) (Eddahibi et al., 1999) (Cooper et al., 1999). Previous data from the Glasgow group has shown that SMC cultured in 1 % O_2 total cell numbers went up after 48 hours (Dempsey, 1991). Tamm *et al* have shown a significant increase in pulmonary arterial SMC proliferation after 48 hours in 3 % O_2 with 5 % FCS supplemented basal media (Tamm et al., 1998). This phenotype was mirrored using 5 % O_2 in serum starved conditions and in 1 % O_2 but 10 % FCS (Stotz et al., 2004) (Yang et al., 2002). These results seem to strengthen the observed phenotype, however, there is a body of data to suggest hypoxia leads to decreased or no change in pulmonary arterial SMC proliferation. These studies largely involved either serum starvation or complete anoxia (Eddahibi et al., 1999) (Cooper et al., 1999). Das's group have attributed the pro-proliferative SMC phenotype seen in PAH plexiform lesions to fibroblasts which potentiate the differentiation of SMC from a non-proliferating contractile phenotype to a proliferative synthetic one using *in vitro* cell culture models (Stenmark et al., 2002). Perhaps fibroblast contamination could account for some of the discrepancies in the data sets.

Cultured primary SMCs isolated by the Cambridge group showed the pleuripotency of pulmonary arterial SMC when in hypoxia. Initial exposure of SMCs from passage 1-3 to 3-4 kPa O_2 in media revealed inhibition of SMC proliferation as determined by [H^3]-thymidine incorporation. However, when these cells were maintained at low density in hypoxia for 1-2 weeks a hypoxic stimulated subpopulation was revealed (Yang et al., 2002). Similar to healthy pulmonary arterial SMCs obtained from commercial companies, these cells had a proliferative phenotype in hypoxia (5 % O_2) when in maintained culture. Unfortunately hypoxic growth rates of freshly isolated cells from commercial sources are unknown as each vial is received at passage 3. Reassuringly rates of proliferation as determined by total cell counts were similar for hypoxic commercial SMCs and hypoxic selected SMC subpopulations. Despite the different findings my robust data set supports the argument that hypoxia induces pulmonary artery SMC proliferation. These data may be useful to determine if local hypoxia is a trigger to SMC proliferation and thus vascular remodelling in disease.

Regardless of the difference in SMC number in either oxygen tension, I found that metabolic activity was preserved. I used the redox indicator alamarBlue® which is commonly used to confirm cell viability. With a high redox potential alamarBlue® can be preferentially reduced by cytochromes and electron acceptors in the electron transport chain without disturbing the pathway. Aerobic mitochondrial respiration requires high oxygen tensions for generation of ATP. Oxygen is essential to convert electron acceptors to their oxidised state therefore adequate oxygen concentrations are essential for efficient mitochondrial function. Hypoxia results in the build-up of electron acceptors in their reduced state, without re-oxidation production of ATP is decreased so cells revert to anaerobic glycolytic respiration. The direct affect to mitochondrial respiration caused by hypoxia may not only affect alamarBlue® reduction but also may mean the dye is not a reliable indicator of viability under conditions of oxygen limitation. I instead used the dye to indicate the relative metabolic activity when compared to killed controls and normalised for SMC number. The preserved metabolic activity in hypoxic SMCs compared to

normoxia despite an increase in hypoxic cell number may be due to the metabolic shift in SMCs as they revert to anaerobic glycolysis rather than aerobic respiration in hypoxia. Although monocytes have the ability to utilise mitochondrial respiration, they are described as facultative anaerobes. Also another key myeloid cell, the neutrophil, has been shown to be predominantly glycolytic even in oxygen abundant conditions. Therefore I was reassured to see that monocytes also displayed preserved metabolic activity in either oxygen tension. Uniquely I have also shown that, like the neutrophil, the monocyte exhibits a pro-survival phenotype in hypoxia.

As mentioned previously the medial layer of the pulmonary artery contains a heterogeneous population of SMCs. Frid *et al* have shown these consist of the non- proliferative 'contractile' state providing elasticity of vessels and extracellular matrix deposition the undifferentiated 'synthetic' state (Frid et al., 1994). The latter has a motile and proliferative phenotype and has been described within plexiform lesions of PAH pulmonary arteries (Worth et al., 2009). Due to the disparate nature of both these types of SMCs it was important to establish the type of SMCs used in my culture system and to ensure phenotypic switching was not occurring between oxygen tensions. I have successfully shown that both hypoxic and normoxic SMCs express the contractile SMC marker smooth muscle cell β actin and are negative for the synthetic SMC markers CD31 and Von Willebrand factor. These data not only suggest that the SMCs used are contractile but also that the cells are maintaining their phenotype in hypoxia.

My most important finding came with monocyte and SMC co-culture using a physiologically relevant ration of 1 monocyte to 5 SMCs. I found that hypoxic increase in total SMC number after 24 hours was abrogated with addition of monocytes. This finding formed the basis of my PhD suggesting perhaps monocytes have a regulatory role in the pulmonary vascular system may have a protective role against vascular remodelling by aiding repair mechanisms when recruited to sites of inflammation. The potential for this key finding to be altered in the disease setting will be investigated further using monocytes isolated from IPAH patients cultured with healthy SMC in Chapter 4.

Reduction of hypoxic SMC number by monocytes could be mediated either by monocytes inducing SMC apoptosis or monocytes reducing SMC proliferation. The former was investigated by measuring SMC apoptosis with and without monocyte co-culture via TUNEL assays. I found that decrease in hypoxic SMC number in the presence of monocytes was not due to increased apoptosis suggesting monocytes play a role in preventing hypoxic pulmonary arterial SMC proliferation rather than inducing SMC death. Whether this was a contact dependant phenomenon was yet to be established so 0.4 μm transwell inserts were used to separate SMCs from monocytes and it was shown that monocyte inhibition of hypoxic SMC proliferation was contact independent suggesting monocytes are secreting something which is inhibiting hypoxic SMC proliferation. I then went on to identify if this secreted factor is transferable and found that not only hypoxic monocyte supernatant could inhibit hypoxic SMC number but also normoxic monocyte supernatant. This finding suggests that monocytes are constitutively releasing a factor which is inhibiting hypoxic SMC proliferation. Identification of this unknown factor became the aim of the next series of experiments.

Monocytes are known to be a key source of cytokines and patient data from Humbert *et al* has shown that serum levels of IL- 6 and IL- 1 (both pro-inflammatory cytokines) are significantly increased in IPAH when compared to healthy controls (Humbert et al., 1995). The MCT rat model also showed increased levels of IL-6 in the lungs upon pulmonary hypertension onset (Voelkel et al., 1994). Monocyte derived cytokines may be responsible for regulating hypoxic SMC proliferation. The alteration of systemic cytokine concentrations in disease may account for disease progression. Both IL- 8 and IL- 1β have both been shown to directly regulate SMC proliferation and adhesion molecule expression with IL- 8 reducing VCAM-1 expression in rat vascular SMCs (Zhang et al., 2011) and IL- 1β causing SMC proliferation in both rat derived cells (Wang et al., 2011) and human SMCs (Kim et al., 2010)a. With this in mind cell-free supernatants from SMCs alone, monocytes alone and monocyte and SMC co-cultures were analysed for pro-inflammatory cytokines by ELISA.

In order to closely resemble physiological conditions the TLR4 agonist was used to apply an inflammatory insult. Monocytes are recruited to the vasculature in areas of inflammation thus LPS was used as it is a well studied inflammatory stimulus with known robust effects. To ensure LPS did not effect SMC numbers in either oxygen tension or monocyte ability to inhibit hypoxic SMC number LPS was added to the culture system and cell counts performed. I found that addition of LPS did not alter SMC proliferation or monocyte ability to inhibit hypoxic SMC proliferation. With regards to cytokine production I found induction of IL-6, IL-8 and RANTES in co-culture, this was increased with LPS stimulation but IL-1 β proved difficult to detect. These data did not indicate a potential target factor responsible for monocyte inhibition of hypoxic SMC number but cytokine values were all much lower than anticipated from previous work looking at aortic vascular SMCs (Morris et al., 2005). In order to confirm my ability to detect cytokines, experiments were repeated using aortic vascular SMCs. Having found aortic cytokine responses to be the same as predicted values previously published (Morris et al., 2005) I found when compared to aortic cells, pulmonary arterial SMC were much less responsive with a marked reduction in expression of most cytokines. Moreover, in contrast to aortic vascular SMC, pulmonary arterial SMC were also poorly responsive to LPS. Work by Dr. Lawrie's group identify further differences in lung versus systemic biology who found that whole body ApoE$^{-/-}$ /IL1-R1$^{-/-}$ double knock-out mice had an alternate active transcript of IL-1R1 in pulmonary vascular cells compared to systemic vascular cells (Lawrie et al., 2011). The difference in both cell types was further illustrated when comparing total cell count values. Aortic vascular SMC numbers were overall higher after 24 hour culture compared to their pulmonary artery counterparts. Moreover, oxygen tension had no effect on aortic vascular SMC number suggesting both hypoxic SMC proliferation and monocyte inhibition of SMC proliferation is specific to the pulmonary artery.

With the knowledge that patients with BMPRII mutations are more susceptible to developing PAH I looked at other members of the super family, namely TGF-β which is a known pro-proliferative cytokine. TGF- β has been shown by

Morrell's group to cause proliferation of IPAH patient pulmonary arterial SMC. Conversely, he found TGF- β caused inhibition of pulmonary arterial SMC proliferation in healthy controls (Hansmann et al., 2008). I found TGF- β to be expressed at very low levels which remained unchanged with co-culture. Another profile which is increased in sera of patients with IPAH compared to healthy controls and patients from elective orthopaedic preadmission clinic is the glycoprotein OPG. The protein plays a role in vascular cells by binding TNF-related apoptosis inducing ligand (TRAIL) thus preventing TRAIL binding death receptors and activating apoptosis (Emery et al., 1998). It is known that OPG has been directly linked to inflammation via the IL-1 pathway with IL-1 α and β themselves inducing OPG production in human pulmonary arterial SMC (Hofbauer et al., 1999) (Lawrie et al., 2008). Therefore secreted OPG levels were determined in the culture system however, there was no change in OPG expression either by LPS stimulation or by oxygen tension in SMC alone or in SMC and monocyte co-cultures.

Endothelin-1 expression is not only linked to PAH as a SMC pro-proliferative agent but it is also a HIF-2 α target gene which has been found in PAH plexiform lesions (Hickey et al., 2010). Surprisingly, ET-1 expression was maintained at very low levels in each oxygen tension and with co-culture. Despite the knowledge that SMC proliferate with response to ET-1, this phenomenon may be attributed to pulmonary artery endothelial cell production of ET-1. Further work surrounding this would be to carry out parallel co-cultures using the co-culture model with pulmonary arterial endothelial cells and monocytes. Reassuringly I saw up regulation of the HIF target gene VEGF in hypoxia compared to normoxia in each condition. This provided strong evidence that culture conditions were reliably hypoxic with increased HIF stabilisation and activity. Seeing as VEGF is a key SMC proliferative stimulus it was hypothesised that hypoxia was inducing SMC proliferation in a VEGF dependant manner and monocytes were able to inhibit this by releasing soluble VEGF receptor- 1 (sFlt-1) mopping up unbound VEGF. To test this hypothesis sFlt- 1 expression was measured in culture supernatants however sFlt- 1 could not be detected in either culture condition. Modulation of VEGF expression and the other growth

factors investigated may occur in disease suggesting an area of further work using cells from IPAH patients.

Although IL- 1 was undetectable by ELISA I cannot conclude that the pathway is not involved in monocyte inhibition of hypoxic SMC proliferation. Co-culture work from Morris *et al.* using aortic SMC and monocytes found no detectable IL-1β, however, indirect evidence of IL -1β activation was detected. Addition of IL-1 receptor antagonist (IL- 1ra) caused dose dependant reduction of IL- 8 release which is a downstream target of IL- 1 (Morris et al., 2005). I was unable to detect IL- 1 and saw no change in secreted levels of IL- 1ra, although, I am yet to define the intracellular concentrations of IL- 1ra. Copper and Beasley suggested the IL- 1 pathway played a role in hypoxic SMC proliferation by similar mechanisms to IL- 1α associated hypoxic fibroblast proliferation (Cooper et al., 1999). Work looking at healthy human vascular SMC from explants could not detect IL- 1α in supernatants but did find the cell-associated form was significantly increased in hypoxia. This increase in IL- 1α corresponded to an increase in vascular SMC proliferation. It is known that increased intracellular IL- 1α production can induce SMC migration and proliferation (Beasley et al., 1992). Moreover, hypoxia has been shown to increase IL- 1α protein and mRNA in both monocytes and endothelial cells (Koga et al., 1992) (Shreeniwas et al., 1992). However, the effect of hypoxia on SMC levels of IL- 1α is yet to be established.

In order to further elucidate a role for the IL- 1 pathway and IL- 1ra itself in SMC proliferation I used exogenous IL- 1ra and found dose dependant inhibition of hypoxic SMC proliferation. Reassuringly I found a reduction in IL- 8 release which was evident with IL- 1ra concentrations as low as 3 ng /ml indicating that addition of IL- 1ra in my model was having a biological effect. This may translate to disease progression as systemic administration of 10 μg /ml IL- 1ra by osmotic mini-pump to fat fed $ApoE^{-/-}$ /$IL\text{-}1R1^{-/-}$ double knock out mice significantly reduced development of PAH measured haemodynamically (Lawrie et al., 2011). IL- 1ra has previously been used as a protective agent for inflammatory PAH models. Work by Voelkel has shown that subcutaneous administration of 2 mg /kg IL- 1ra can significantly reduce MCT induced

increased mean pulmonary artery pressures but is unable to inhibit hypoxic induced increased mean pulmonary artery pressures in these same rats (Voelkel et al., 1993). He also shows induction of both IL- 1α and β mRNA and protein in pulmonary vessels from MCT PAH rats compared to chronic hypoxic rats (Voelkel et al., 1994). This work suggests that IL- 1α, β and receptor antagonist have no role in hypoxic vascular remodelling but does not address the selectivity of IL-1ra to the hypoxic proliferation response and forms the basis of a set of experiments in Chapter 4.

To address the specificity of monocyte inhibition of hypoxic SMC proliferation I used PDGF to induce SMC proliferation. PDGF is a potent SMC proliferative stimulus with reproducible predicable results (Ikeda et al., 1990) (Raines et al., 1989) (Tamm et al., 1998). I found monocytes were unable to inhibit PDGF induced SMC proliferation suggesting that monocyte inhibition of SMC proliferation only occurs for hypoxic induced SMC proliferation.

In conclusion I found that hypoxia significantly reduced apoptosis rates of monocytes and induced pulmonary artery SMC proliferation after 24 hour culture. My key finding came after co-culture of both cell types. Monocytes were able to inhibit hypoxic SMC proliferation and this inhibition was independent of both monocyte hypoxia and direct cell contact. This phenotype was specific to the pulmonary vasculature as aortic SMC had a different growth profile. Although I was unable to identify any pro-inflammatory cytokine or disease linked factor which may be mediating monocyte inhibition of hypoxic SMC proliferation, I found exogenous IL- 1ra could inhibit hypoxic SMC proliferation. However, selectivity of IL- 1ra for hypoxic proliferation is yet to be established. Furthermore, monocytes are unable to inhibit growth factor induced proliferation suggestion monocyte inhibition of SMC proliferation is specific to hypoxic induced proliferation.

4 MECHANISM OF HYPOXIC INHIBITION OF SMOOTH MUSCLE CELL PROLIFERATION

4.1 INTRODUCTION

The purpose of this chapter is to try and understand the potential mechanisms by which monocytes are inhibiting hypoxic SMC proliferation and the disease relevance of this finding. A very important pathway in PAH is the BMPR2 pathway with heterozygous mutations in BMPR2 found in about 60 % of patients with hereditary PAH patients (Chida et al., 2012) and in 27 % of sporadic cases of idiopathic disease (Rosenzweig et al., 2008). BMPR2 is a member of the TGF-β superfamily. It is already known that the cytokine TGF-β can induce proliferation in SMCs obtained from IPAH patient lung explants but has no effect on SMCs obtained from unused donor lungs with no vasculopathy (commercial SMC) proliferation (Morrell et al., 2001). The TGF-β pathway elicits it proliferative effects via the SMAD proteins SMAD 2 and SMAD 3. These proteins are phosphorylated upon TGF-β receptor activation and bind the co-SMAD protein, SMAD 4. Binding of the co-SMAD protein allows the complex to translocate to the nucleus leading to increase gene expression of proliferative mediators such as cyclin D (Chen et al., 2004) (Figure 4.1). Immunohistochemistry carried out on lung sections from patients with PAH compared to patients with secondary pulmonary hypertension or healthy unused donor lungs showed IPAH patient lung had decreased BMPR2 expression. Interactions between the TGF-β receptor and BMPR2 was suggested in these lung sections due to co-localisation of both these receptors, however, TGF-β receptor expression was preserved in each of the conditions (Atkinson et al., 2002). Like the TGF-β receptor, the BMPR2 pathway also elicits its effects via SMAD proteins, using SMAD 1, 5 and 8 to increase gene expression of anti-proliferative and apoptotic genes such as the DNA-binding protein inhibitor (Id-1) and Bcl-2 (Nakao et al., 1997) (Tamaki et al., 1998) (Figure 4.1).

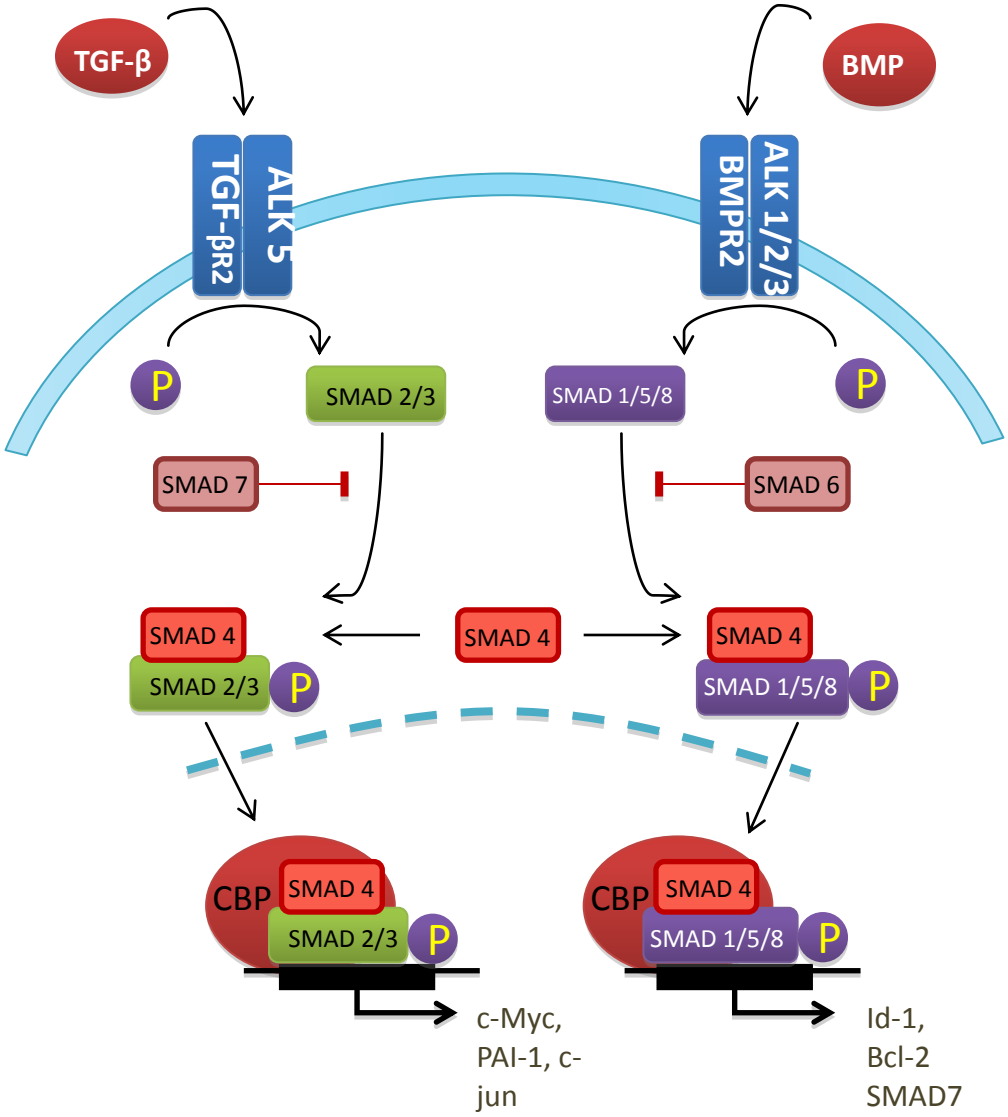

Figure 4.1 Cell signalling by the TGF- beta and BMPR2 pathway

Transforming growth factor- beta receptor 2 (TGF-βR2) and bone morphogenetic protein receptor 2 (BMPR2) dimerisation with activin receptor-like kinase 5 (ALK5) also known as transforming growth factor- beta receptor 1 (TGF-βR1) or ALK 1 /2 /3 respectively occurs upon ligand binding. Dimerisation leads to a phosphorylation cascade culminating in activation of receptor regulated SMAD 2 /3 with regards to TGF-β ligand binding and SMAD 1 /5 /8 with respect to BMP ligand activation. Phosphorylation of receptor regulated SMAD proteins allows binding of co-SMAD 4 and subsequent nuclear translocation. In the nucleus SMAD complexes bind CREB binding protein (CBP) allowing transcription of specific genes. TGF-β induces transcription of genes which contribute to cell cycle progression such as c-Myc whereas BMP results in anti-proliferative genes such as Id-1. Specific inhibitory SMADs regulate each pathway, SMAD 7 for TGF-β pathway and SMAD 6 for BMP pathway.

Both BMPR2 ligands, BMP 2 and 7 usually function to inhibit SMC proliferation. Previous work has shown that these ligands are ineffective in disease as this pathway is down regulated in PAH either by a dysfunctional receptor or dysregulation of the pathway members (Trembath et al., 2001) (Morrell et al., 2001). To further understand the importance of mutations in this pathway on my phenotype I obtained IPAH patient SMCs from Dr. Morrell (Papworth, Cambridge, UK) with a specific mutation in BMPR2 where residue 401 is replaced by a serine residue. In parallel I isolated monocytes from patients with IPAH and systemic sclerosis associated PAH to investigate if the circulating myeloid cells are different from healthy donor monocytes.

Chapter 3 showed that hypoxia leads to increased SMC numbers but it is still unknown how hypoxia leads to SMC proliferation. A potential pathway which may be implicated in hypoxic SMC proliferation is the HIF pathway. Not only has both protein and mRNA expression of the transcription factor been identified within IPAH lesions after vascular remodelling (Tuder et al., 2001) but also I have shown in Chapter 3 indirect evidence of HIF activation through increased protein expression of the HIF target gene VEGF. HIF is a heterodimer consisting of the ubiquitously expressed beta subunit and the oxygen sensitive alpha subunit. The HIF alpha subunit contains an ODDD consisting of a conserved sequence containing two preserved proline residues. When oxygen is readily available, specific PHD enzymes hydroxylate HIF and target it for degradation (Wykoff et al., 2000). The pan-hydroxylase inhibitor dimethyloxalylglycine (DMOG) inhibits PHD enzymes and thus stabilises HIF allowing its translocation to the nucleus. Pulmonary artery SMCs treated with DMOG have been shown to display enhanced proliferation with growth factor stimulation both by cell number and fluorescent DNA incorporation (Schultz et al., 2009), thus mimicking hypoxic proliferative effects in SMCs. Another indirect role of HIF in the pathogenesis of pulmonary hypertension was provided by work in the chronic hypoxia rat model. When these animals were administered 30 mg /kg dehydroepiandrosterone (DHEA), reduced vascular remodelling was observed compared to control rats administered PBS (Bonnet et al., 2003). Further work by Dessouroux *et al* found DHEA directly reduced

expression of HIF-1 alpha at the protein level in human pulmonary artery SMC suggesting a possible role of HIF in regulation of hypoxic induced pulmonary hypertension (Dessouroux et al., 2008).

During cellular hypoxia most cells switch from aerobic respiration to anaerobic glycolysis because oxygen is needed as the terminal electron acceptor in mitochondrial respiration. In aerobic respiration electrons are shunted through the mitochondrial membrane via Complex I, Complex II, coenzyme Q, Complex III, cytochrome *c* and Complex IV until being transferred to molecular oxygen allowing protons to be transferred across the mitochondrial membrane resulting in synthesis of 26-30 molecules of adenosine tri-phosphate (ATP) (Berg et al., 2006). In IPAH patient pulmonary artery endothelial cells, oxygen consumption was reduced when compared to healthy controls as measured by 5300A biological oxygen monitors and adapted polarographic oxygen electrodes. This was attributed to both a reduction in Complex IV activity seen spectrophotometrically, by MTT reduction and a reduction in total mitochondria numbers. With preserved ATP generation, a cellular switch to glycolysis was hypothesised (Xu et al., 2007). Myeloid cells are primarily glycolytic and are dependant on the HIF pathway for functional competence (Levene, 1912) (Kempner, 1939) (Walmsley et al., 2005) (Cramer et al., 2003). In order for all cells to function under oxidative stress and generate ATP the HIF pathway aids the switch to glycolysis with many glycolytic enzymes containing hypoxia response elements (HRE) in their promoter regions.

The metabolic switch from aerobic to anaerobic respiration also coincides with a change in redox potential. Hypoxic wild type mice have been found by using lucigen enhanced chemiluminescence technique to have an increase in superoxide activity (Liu et al., 2005). This is paralleled by an increase in hydroeicosatetraenoic acid (HETE) in patients with severe PAH (Bowers et al., 2004) and a decrease in antioxidant protein expression in IPAH patient lungs compared to unused donor lung (Masri et al., 2008). It is hypothesised that a reduction in antioxidant bioavailability coupled with changes in redox potential induced by hypoxia lead to the increase in ROS. Interestingly, inhibition of ROS by exogenous thrombin has been shown to reduce HIF-1 alpha protein levels in

vascular SMCs. This pathway may address why both mice with a whole body heterozygous deletion in HIF-1 and mice which have a deletion in one of the HIF-2 alpha alleles are protected from development of hypoxia induced pulmonary hypertension (Yu et al., 1999) (Brusselmans et al., 2003).

I propose to further investigate the role of the HIF pathway in both hypoxic SMC proliferation and monocyte inhibition of hypoxic SMC proliferation. Using monocytes obtained from PAH patients compared to healthy controls I will establish the disease specificity of monocyte inhibition of SMC proliferation. Monocytes will be isolated from both IPAH patients, patients with an inflammatory associated form of the disease (systemic sclerosis associated PAH) and healthy volunteers. I will also establish differences between IPAH patient SMCs and healthy commercial SMCs in the established co-culture model. Seeing as IPAH SMCs have a known BMPR2 mutation, I will investigate if knocking down BMPR2 will recapitulate IPAH SMC phenotypes in commercial SMCs. Moreover with the knowledge that hypoxia significantly increases ROS generation and that ROS confers SMC proliferation, I will identify if monocytes are eliciting their hypoxic inhibition of SMC proliferation by antioxidant release.

4.2 RESULTS

4.2.1 IPAH PATIENT MONOCYTES CANNOT INHIBIT HYPOXIC SMOOTH MUSCLE CELL PROLIFERATION

Having found that healthy monocytes can inhibit hypoxic SMC proliferation, the next question was is this altered in the disease setting? To establish if monocytes from patients with PAH can inhibit hypoxic SMC proliferation to the same order of magnitude as monocytes from healthy controls, monocytes were isolated from healthy controls, IPAH patients and patients with scleroderma associated PAH (another inflammatory form of the disease used as a control).

Healthy control SMCs were grown alone in hypoxia (3 kPa) or normoxia (19 kPa) for 24 hours prior to 48 hours quiescence. SMCs were cultured for a further 24 hours with or without monocytes isolated from peripheral blood at a ratio of 1 monocyte: 5 SMCs. Post-culture, cells were lifted and total cell counts were calculated by Coulter counter (Figure 4.2). Commercial healthy SMC number increased in hypoxia compared to normoxia (n=8). This increase in cell number was significantly reduced with co-culture of SMCs and healthy donor monocytes (n=8) (Figure 4.2.a).

In all conditions hypoxic monoculture caused a significant increase in total SMC number compared to normoxic monoculture. Monocytes isolated from patients with scleroderma associated PAH were also able to inhibit hypoxic SMC proliferation (n=12) (Figure 4.2.b). Our key finding was that monocytes isolated from IPAH patients were unable to inhibit hypoxic SMC proliferation (n=10) (Figure 4.2.c).

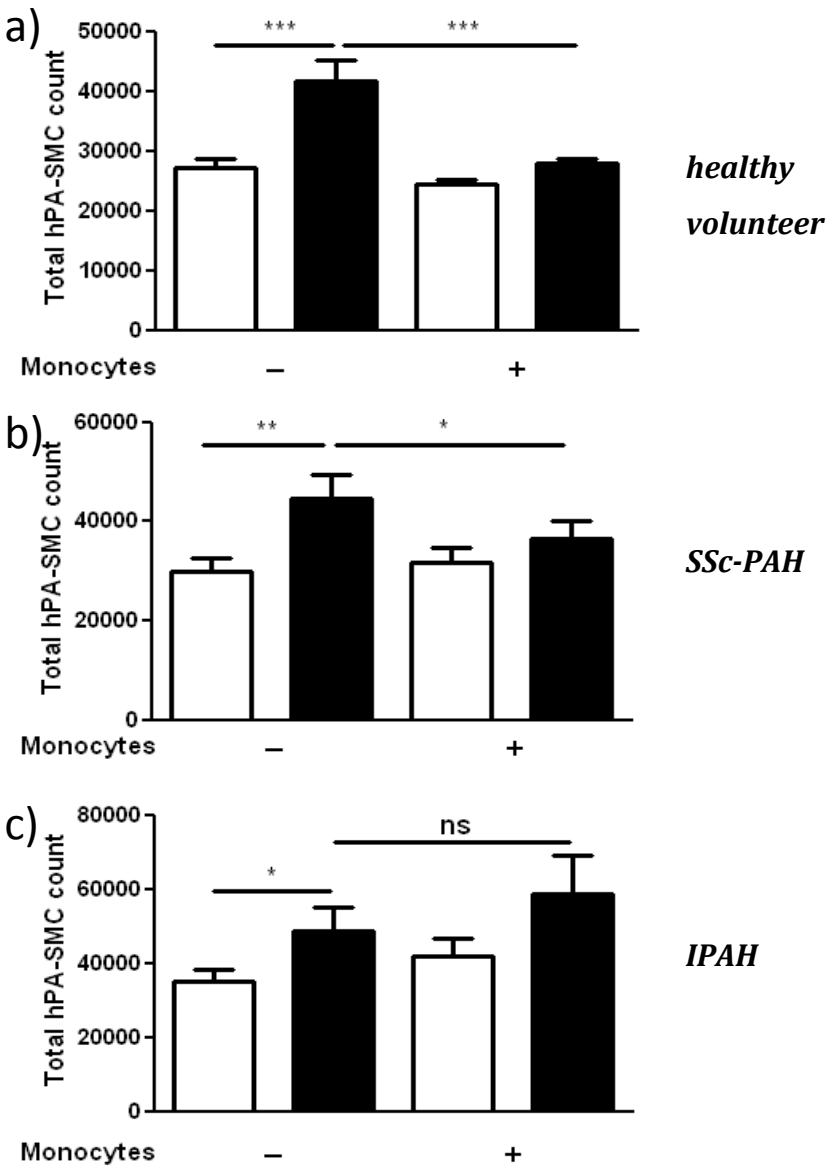

Figure 4.2 IPAH patient monocytes cannot inhibit hypoxic smooth muscle cell proliferation

SMCs were seeded at 25,000 cells /well and cultured in normoxia (19 kPa) (open bars) or hypoxia (3 kPa) (closed bars) for 24 hours prior to serum starvation. Plates were cultured for a further 24 hours in the presence and absence of monocytes isolated from peripheral blood of a) healthy volunteers, b) systemic sclerosis associated pulmonary artery hypertension patients (SSc-PAH) or c) IPAH at a ratio of 1 monocyte: 5 SMCs. Total cell counts were carried out by Coulter counter. Bars represent mean +/- SEM, *P<0.05, **P<0.01, ***P<0.001, ns= not significant, n=6 healthy volunteers, n=4 SSc-PAH, n=3 IPAH, one-way ANOVA with Bonferonni post test.

4.2.2 IPAH PATIENT SMOOTH MUSCLE CELLS HAVE AN INCREASED PROLIFERATIVE PHENOTYPE INDEPENDENT OF HYPOXIA AND MAINTAINED METABOLIC ACTIVITY

To establish if SMCs from patients have different growth profiles from SMCs obtained commercially from unused donor lungs with no known vasculopathy, SMCs obtained from a patient with IPAH were grown in normoxia (19 kPa) and hypoxia (3 kPa) with and without healthy donor monocytes. After 24 hour oxygen equilibration and 48 hour serum starvation cells are cultured for a further 24 hours with and without healthy donor monocytes.

Post-culture, SMCs were lifted and total cell counts were calculated by Coulter counter. Initial findings showed that IPAH patient SMC number after oxygen equilibration and quiescence was increased showing these SMC were proliferating during serum starvation. To control for this cells were recovered both before and after 24 hour mono- or co-culture. Therefore all results are expressed as % recovery i.e. (number of SMC after 24 hour culture /number of SMC before 24 hour culture) x 100. When recovery was taken into account for commercial healthy SMCs, hypoxia significantly increased SMC recovery but this was significantly reduced with co-culture with monocytes (n=5) (Figure 4.3.a). There was no change in % recovery for IPAH patient SMC in each culture condition (n=6) (Figure 4.3.b).

Reduction of alamarBlue® was used to measure metabolic activity and as an indirect measure of cell viability as described previously (Chapter 2.4.2). Cell free supernatants from IPAH patient SMC pre-incubated with the dye were compared with supernatants from 1 μg/ ml cycloheximide killed controls. Results are expressed as arbitrary units per 10,000 SMCs (Figure 4.3 c). When corrected for cell number there was no significant difference in relative metabolic activity in either oxygen tension (n=6).

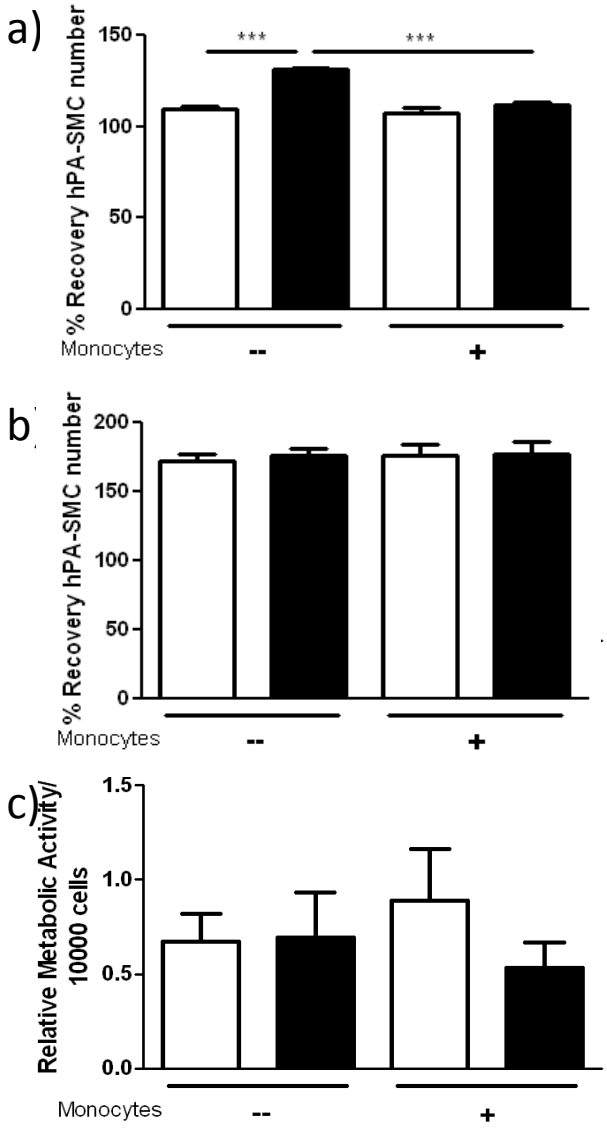

Figure 4.3 IPAH patient smooth muscle cells have an increased proliferative phenotype independent of hypoxia and preserved metabolic activity

SMCs obtained from an IPAH patient were seeded at 25,000 cells /well. Plates were cultured for 24 hours in normoxia (19 kPa) (open bars) or hypoxia (3 kPa) (closed bars) before serum starvation. Plates were cultured for a further 24 hours with and without the addition of monocytes (1 monocyte: 5 SMCs). After quiescence and after 24 hour culture cells were lifted and total cell counts were performed by Coulter counter. Cell numbers were expressed as % recovered after 24 hour culture for a) commercial SMC, n=5 and b) IPAH patient SMC, n=6. Bars represent mean +/- SEM, ***P<0.001, one-way ANOVA with Bonferonni post test. c) Relative metabolic activity was calculated by reduction of the redox indicator alamarBlue®. Results are normalised to cell number and bars represent mean +/- SEM, n=6.

4.2.3 IPAH PATIENT SMOOTH MUSCLE CELL VEGF EXPRESSION PROFILE

To account for the increased proliferative phenotype of IPAH patient SMCs compared to their healthy counterparts it was postulated that patient cells had increased HIF pathway activity. It was possible to use expression of the HIF target gene VEGF as an indirect indicator of HIF activity.

SMCs from IPAH patients were seeded at 25,000 cells /well and established in the co-culture model with and without the addition of 1 monocyte: 5 SMCs and /or LPS stimulation (10 ng /ml). Cell free supernatants were saved and analysed by ELISA for release of VEGF. SMCs from IPAH patients alone released approx. 1 1/2 times more VEGF than SMCs obtained commercially from explants donor lungs with no known vascular dysregulation (Figure 3.10). Contradictory to VEGF release from healthy commercial cells, VEGF release from IPAH SMCs was unaffected by oxygen tension or LPS stimulation (n=3). Co-culture with monocytes increased IPAH SMC VEGF release but this increase was not significantly different in either oxygen tension with or without LPS stimulation (Figure 4.4).

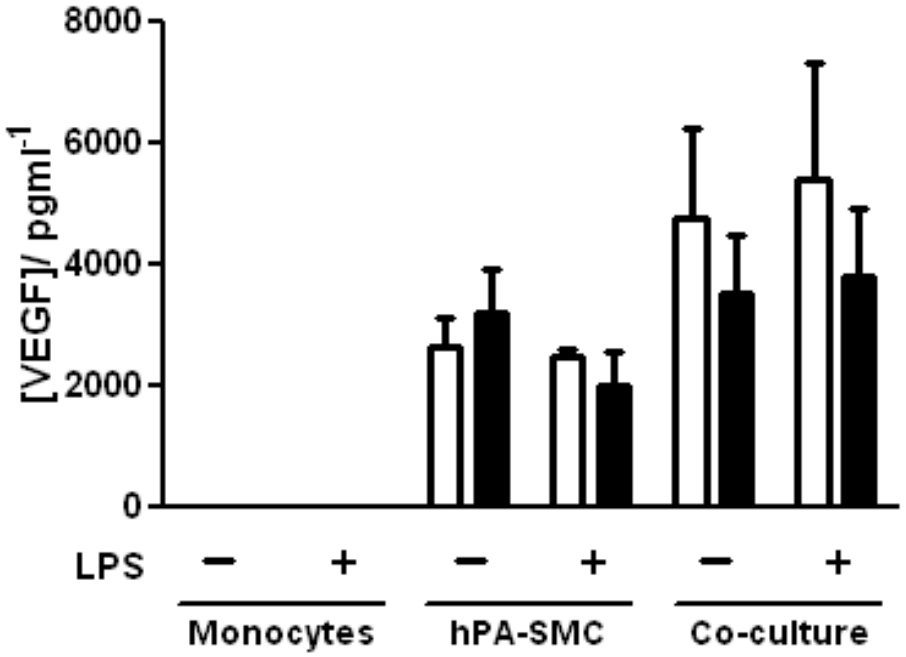

Figure 4.4 IPAH patient smooth muscle cell VEGF expression

IPAH patient SMCs were seeded at 25,000 cells /well and left to equilibrate in normoxia (19 kPa) (open bars) or hypoxia (3 kPa) (closed bars) for 24 hours before inducing senescence. Patient SMCs and healthy volunteer monocytes were then cultured alone for 24 hours as well as both cell types co-cultured together (1 monocyte: 5 SMCs). Cell free supernatants were obtained from cultures with and without LPS (10 ng /ml) stimulation and analysed by ELISA. Values were calculated using log transformation and linear regression analysis. All Bars represent mean +/- SEM, n=6.

4.2.4 THE PAN-HYDROXYLASE INHIBITOR DMOG CAUSES SMOOTH MUSCLE CELL PROLIFERATION WHICH IS NOT INHIBITED BY MONOCYTES

The mechanism by which monocytes can inhibit hypoxic SMC proliferation is unknown. However, it is known that SMCs must be hypoxic to reveal the phenotype therefore the mechanism may be HIF dependant. DMOG is a pan hydroxylase inhibitor thus inhibits activity of the prolyl hydroxylase enzymes which target HIF α subunits for degradation during abundant oxygen availability and stabilising HIF α protein expression. By determining whether monocytes can inhibit DMOG induced SMC proliferation we may be able to determine the hydroxylase dependence of monocyte inhibition of hypoxic SMC proliferation.

Healthy SMCs obtained commercially from unused donor lungs were seeded at 25,000 cells /well and placed in normoxia (19 kPa) for 24 hours prior to serum starvation. Cells were cultured for a further 24 hours with and without monocytes and increase concentrations of DMOG. Monocytes were isolated from peripheral blood of healthy volunteers and added at a ratio of 1 monocyte: 5 SMCs. After culture total cell counts were performed by Coulter counter. SMC number increased with increase concentrations of DMOG but monocytes had no effect on increase in cell number (n=10) (Figure 4.5).

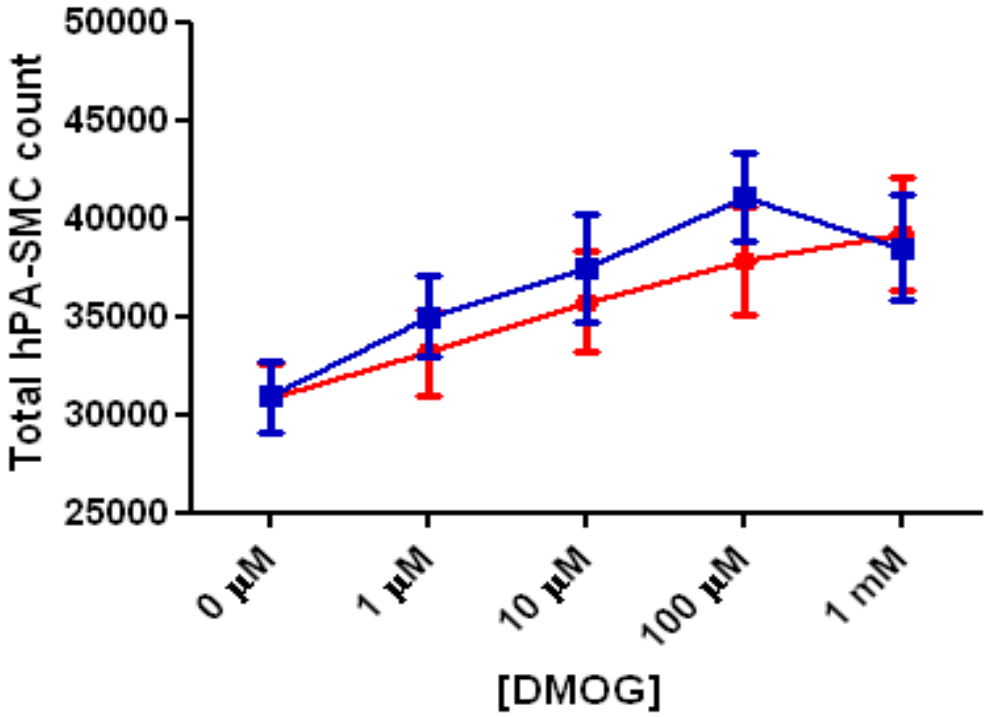

Figure 4.5 Monocytes cannot inhibit DMOG induced smooth muscle cell proliferation

Commercial SMCs were seeded at 25,000 cells /well and placed in normoxia (19 kPa) for 24 hours prior to serum starvation. Cells were then incubated with increase concentrations of DMOG for a further 24 hours with and without 1 monocyte: 5 SMCs. After culture, cells were washed and counted by Coulter counter. Graph shows SMC monoculture in blue and SMC and monocyte co-culture in red. Data points show mean +/- SEM, n=6.

4.2.5 MONOCYTE SUPERNATANTS PRE-INCUBATED WITH DMOG MAINTAIN THE ABILITY TO INHIBIT HYPOXIC SMOOTH MUSCLE CELL PROLIFERATION

Knowing that monocytes could not inhibit DMOG induced proliferation did not mean that monocyte inhibition of hypoxic SMC proliferation was HIF independent. DMOG may be adversely affecting the monocytes' ability to inhibit hypoxic proliferation. To investigate this further, cell free normoxic monocyte supernatants were obtained after 24 hour culture with and without 100 μM DMOG.

Meanwhile SMCs were seeded at 25,000 cells /well and were grown in normoxia (19 kPa) or hypoxia (3 kPa) for 24 hours before serum starvation. After quiescence cells were incubated for 24 hours with and without cell free supernatants. After culture, total cell counts were performed by Coulter counter. As shown previously (Figure 3.1) hypoxia significantly increased SMC number compared to normoxia. DMOG increased normoxic cell number (n=7) but hypoxia with DMOG significantly increased total cell counts compared to normoxic DMOG stimulation (n=7) (Figure 4.6). Monocyte supernatant inhibited hypoxic increase in cell number to normoxic levels (n=7). This was also true of DMOG treated monocyte supernatants (n=7) suggesting DMOG is not affecting monocytes' ability to inhibit SMC proliferation.

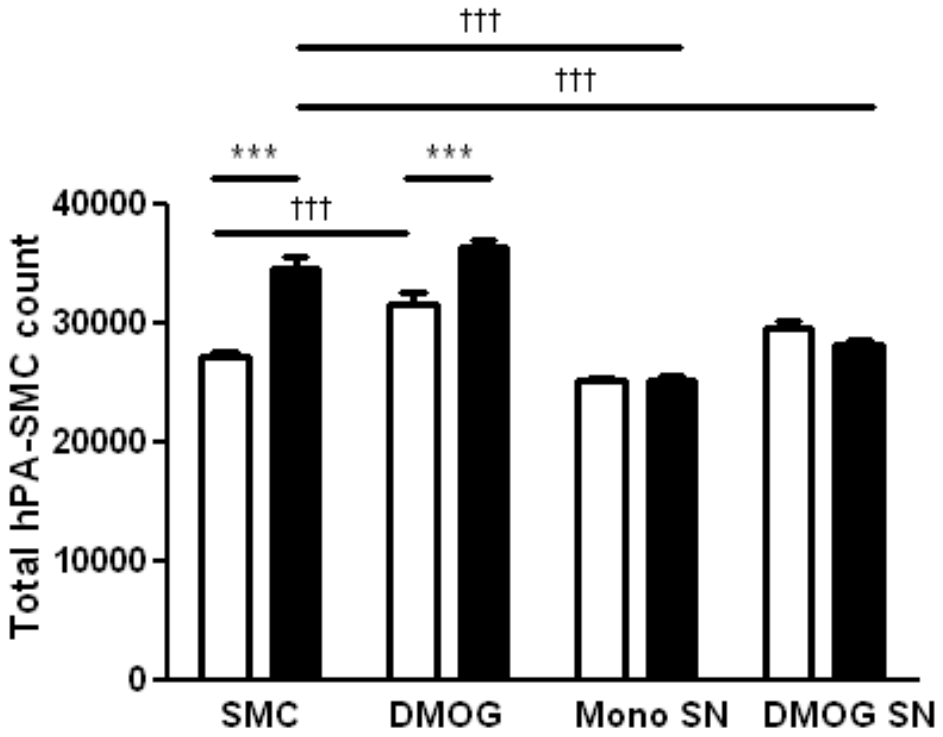

Figure 4.6 Monocyte supernatants pre-incubated with DMOG maintain the ability to inhibit hypoxic smooth muscle cell proliferation

Monocytes were resuspended at 0.1 x 10^6 /ml and incubated with and without DMOG (100 μM) for 24 hours before cell free supernatants were saved. SMCs were seeded at 25,000 cells /well and grown in normoxia (19 kPa) (open bars) or hypoxia (3 kPa) (closed bars) for 24 hour prior to serum starvation. SMCs were then cultured for a further 24 hours with and without supernatants. Total cell counts were calculated by Coulter counter. Bars represent mean +/- SEM, ***P<0.001, n=7, two-way ANOVA with Bonferonni post test, †††P<0.001, n=7 one-way ANOVA with Bonferonni post test.

4.2.6 Exogenous Interleukin- 1 receptor antagonist can inhibit DMOG induced smooth muscle cell proliferation

Having found that IL- 1ra could inhibit SMC proliferation I went on to try and establish the specificity of IL- 1ra to hypoxia by using DMOG. If IL- 1ra can inhibit DMOG induced SMC proliferation then it is likely that the IL- 1 pathway is not important in monocyte inhibition of hypoxic SMC proliferation as monocytes themselves cannot inhibit DMOG induced SMC proliferation. To ensure results were robust at least 2 different vials of healthy commercial SMCs were used at different passages.

SMCs were seeded at 25,000 cells /well and grown in normoxia for 24 hours prior to serum starvation. Plates were then cultured for a further 24 hours with and without 100 μM DMOG alone or with 10 ng /ml IL-1ra or 10 ng /ml IL-1ra placebo (IL-1ra carrier fluid alone). Total cell counts were performed after culture using a Coulter counter. A significant increase in cell number was observed with DMOG incubation compared to SMCs grown alone (n=12). This increase in cell number was significantly reduced with pre-incubation with 10 ng /ml IL-1ra but not its placebo (n=12) (Figure 4.7). These data suggest IL-1ra inhibition of SMC proliferation is not specific to monocyte inhibition of hypoxic SMC proliferation.

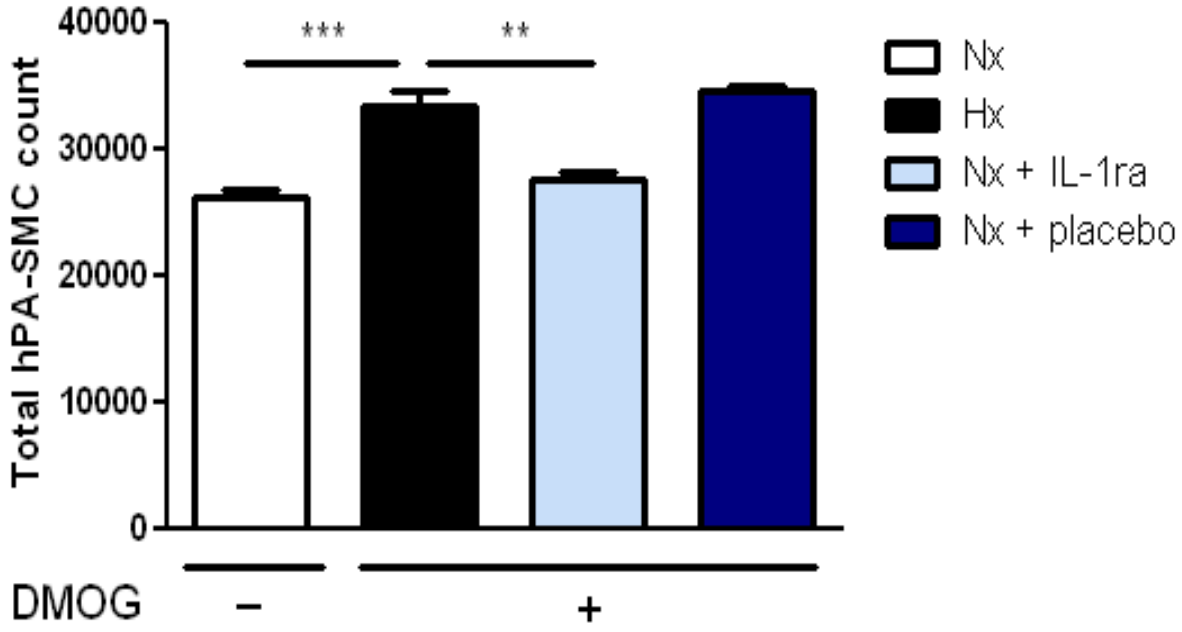

Figure 4.7 Exogenous IL-1ra can block DMOG induced smooth muscle cell proliferation

SMCs were seeded at 25,000 cells /well and following senescence, cells were incubated with and without 100 μM DMOG alone or with 10 ng/ ml IL-1ra or 10 ng/ ml IL-1ra placebo. Post-culture cells were washed and counted by Coulter counter. Bars represent mean +/- SEM, **P<0.01, ***P<0.001, n=12, one-way ANOVA with Bonferonni post test.

4.2.7 HIF-1 AND HIF-2 ALPHA PROTEIN REGULATION IN COMMERCIAL SMOOTH MUSCLE CELL AND MONOCYTE CO-CULTURES

Although monocytes were unable to inhibit DMOG induced SMC proliferation, due to DMOG being a non-specific pan-hydroxylase, the HIF independency of monocytes ability to inhibit SMC proliferation could not be confirmed. To further determine a role for the HIF pathway in both SMC proliferation and monocyte inhibition of hypoxic proliferation western blots were carried out on culture lysates for both HIF- 1 and HIF- 2α.

Commercial SMCs obtained from unused donor lungs with no known vasculopathies were cultured in normoxia (19 kPa) and hypoxia (3 kPa) for 24 hours with and without monocytes (1 monocyte: 5 SMCs) and /or DMOG (100 μM). Samples were then lysed and probed for both HIF- 1 and HIF- 2α protein expression on western blots. Blots were then analysed by densitometry normalising to corresponding actin expression.

SMCs alone had no HIF- 1α expression in normoxia however, both DMOG and hypoxia increased protein expression to similar levels (n=5) but monocytes had no inhibitory effect (n=5) (Figure 4.8). HIF- 1α has a predicted weight of 120 kDa and actin of 40 kDa. With regards to HIF- 2α expression which has a predicted weight of 120 kDa, normoxic SMCs alone expressed little HIF- 2α but this was increased with monocyte co-culture (n=5) this was also true in hypoxia (n=5). DMOG treatment significantly increased HIF- 2α expression in SMC alone (n=5) (Figure 4.9).

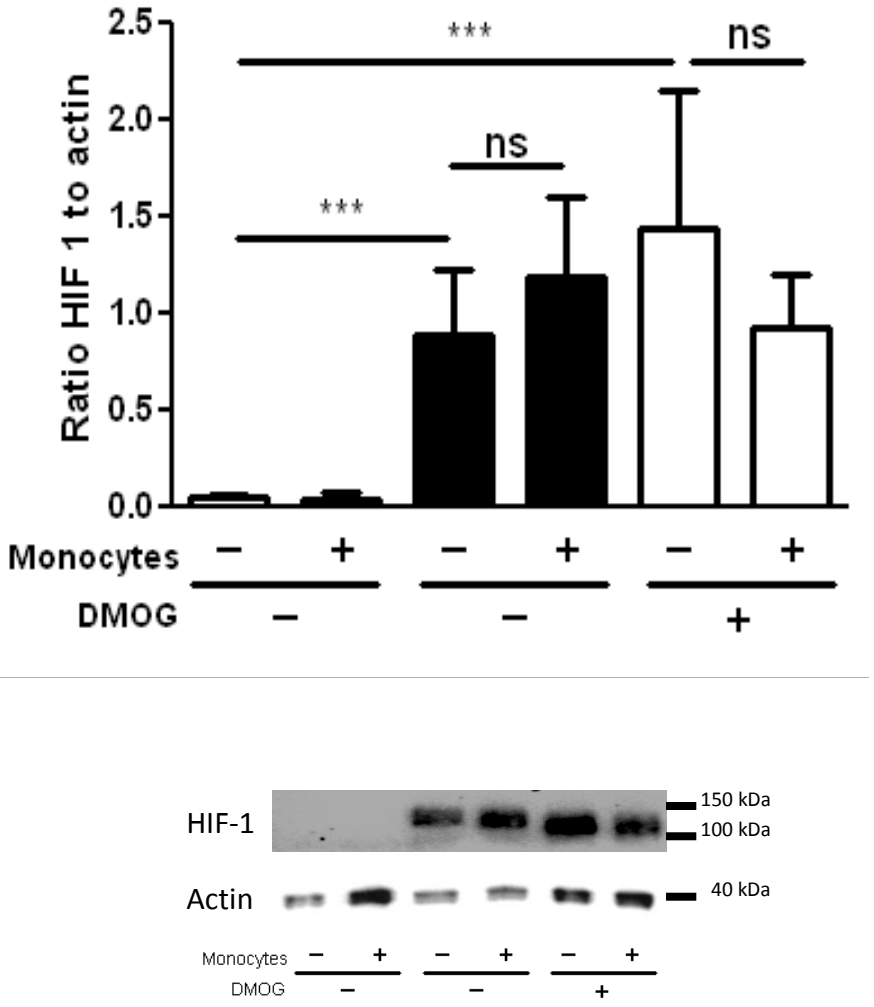

Figure 4.8 HIF- 1α expression is increased in commercial smooth muscle cells by hypoxia and DMOG

Commercial SMCs were seeded at 25,000 cells /well and cultured in normoxia (19 kPa) (open bars) or hypoxia (3 kPa) (closed bars) for 24 hours with and without monocytes (1 monocyte: 5 SMCs) and 100 μM DMOG. Post culture, cells were lysed and frozen at -80 °C before analysis by western blot. Graph represents densitometry results from five HIF- 1α (120 kDa) probed blots normalised to corresponding actin (40 kDa) expression. Bars represent mean +/- SEM, ***P<0.001, ns= not significant, students' *t*-test, n=5. Below shows representative western blot for HIF- 1α and actin loading control.

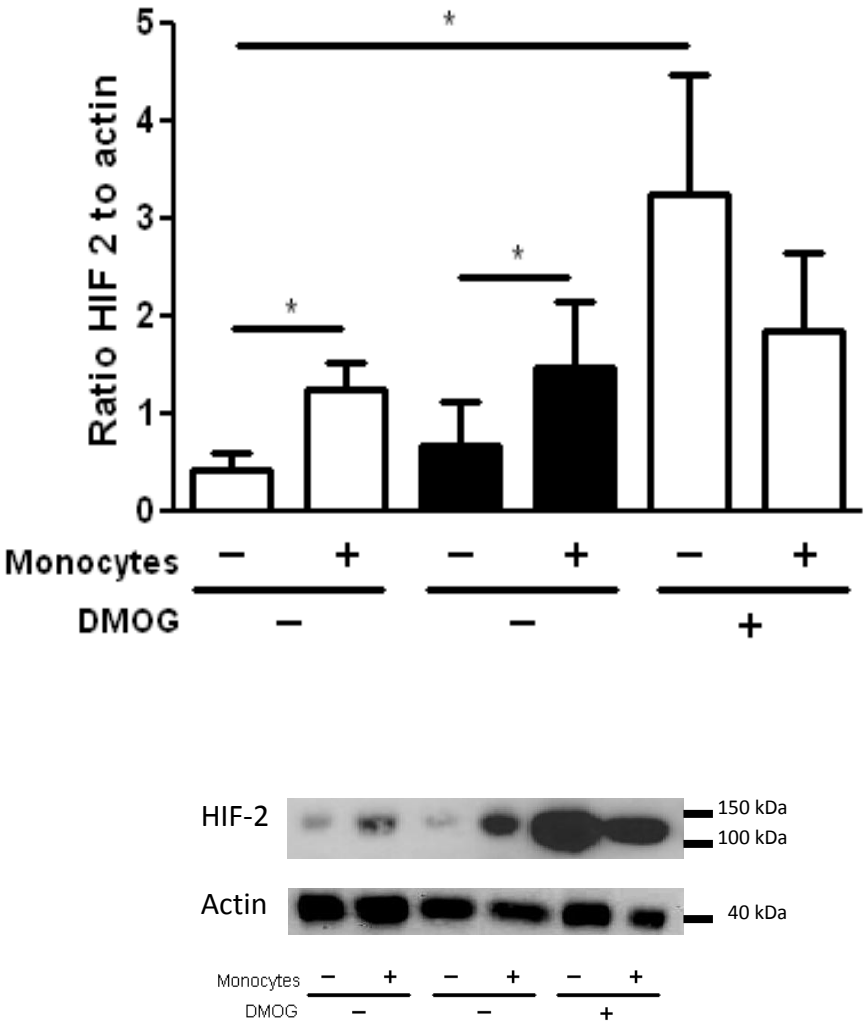

Figure 4.9 Expression of HIF- 2α is increased with co-culture in each oxygen tension and with DMOG stimulation

Commercial SMCs were seeded at 25,000 cells /well and cultured in normoxia (19 kPa) (open bars) or hypoxia (3 kPa) (closed bars) for 24 hours with and without monocytes (1 monocyte: 5 SMCs) and 100 μM DMOG. Post culture, cells were lysed and frozen at -80 °C before analysis by western blot. Graph represents densitometry results from five HIF- 2α (120 kDa) probed blots normalised to corresponding actin (40 kDa) expression. Bars represent mean +/- SEM, *P<0.05, n=5, students' *t*-test. Below shows representative western blot for HIF- 2α and actin loading control.

4.2.8 HIF-1 AND HIF-2 ALPHA PROTEIN EXPRESSION IN IPAH PATIENT SMOOTH MUSCLE CELL AND MONOCYTE CO-CULTURES

Having seen a difference in HIF- 2 protein expression with and without the addition of monocytes I went on to determine if SMCs from patients with IPAH showed any difference in HIF expression with and without monocyte co-culture. IPAH patient SMCs were cultured alone or with monocytes (1 monocyte: 5 SMCs) in normoxia (19 kPa) and hypoxia (3 kPa) with and without DMOG (100 μM). Samples were lysed and analysed by western blot for both HIF- 1 and HIF- 2α protein expression. Densitometry was used to quantify protein expression and results are normalised to corresponding actin expression. The predicted weights of both HIF α subunits are 120 kDa and actin is 40 kDa.

HIF- 1α expression was present at low levels in patient SMCs at low passages (from passage 4-5), however, the later passages (from passage 6-8) this was not seen. Taken together, the data showed little HIF- 1α protein expression in normoxia with and without monocytes. Hypoxia and DMOG significantly increased HIF- 1α protein levels in SMC alone when compared to normoxic SMC alone (n=6). Both hypoxia and DMOG significantly increased HIF- 1 expression in SMC and monocyte co-cultures compared to normoxic co-cultures (n=6) (Figure 4.10). Oxygen tension or DMOG stimulation had little effect on SMC expression of HIF- 2α. However there was a trend of increased HIF- 2α expression in SMC and monocyte co-culture compared to SMCs alone which was significant in normoxia (n=4) (Figure 4.11).

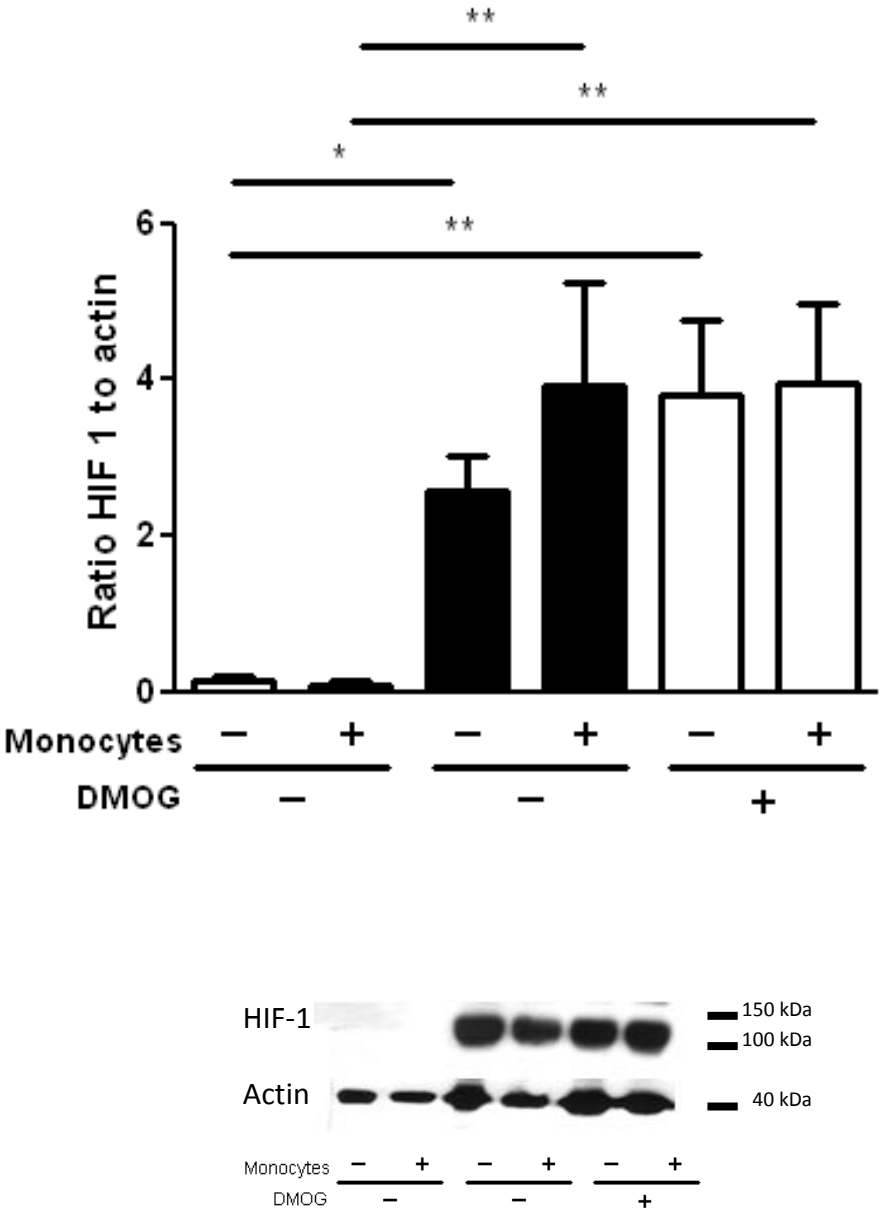

Figure 4.10 HIF-1 α expression is increased in hypoxia and with DMOG in IPAH patient smooth muscle cells

IPAH patient SMCs were seeded at 25,000 cells /well and cultured in normoxia (19 kPa) (open bars) or hypoxia (3 kPa) (closed bars) for 24 hours with and without monocytes (1 monocyte: 5 SMCs) and 100 μM DMOG. Post culture, cells were lysed and frozen at -80 °C before analysis by western blot. Graph represents densitometry results from six HIF- 1α probed blots normalised to corresponding actin expression. Bars represent mean +/- SEM, *P<0.05, **P<0.01, n=6, students' *t*-test. Below shows representative western blot for HIF- 1α and actin loading control.

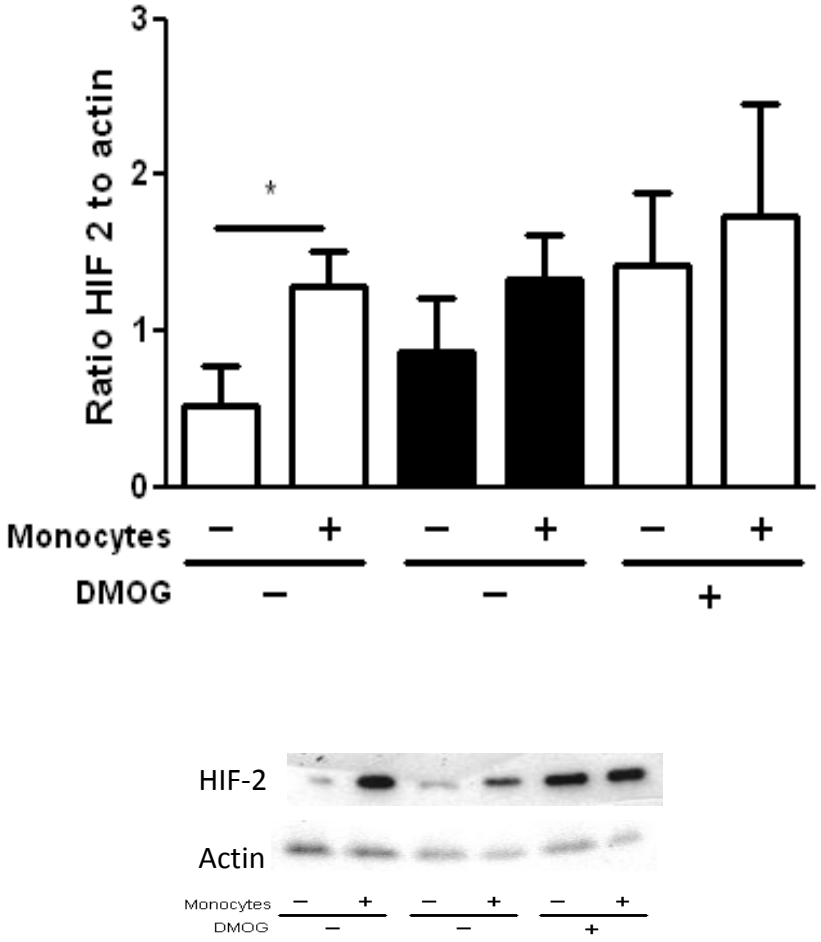

Figure 4.11 HIF- 2α expression in IPAH patient smooth muscle cells is preserved in each oxygen tension but increased with monocyte co-culture

IPAH patient SMCs were seeded at 25,000 cells /well and cultured in normoxia (19 kPa) (open bars) or hypoxia (3 kPa) (closed bars) for 24 hours with and without monocytes (1 monocyte: 5 SMCs) and 100 μM DMOG. Post culture, cells were lysed and frozen at -80 °C before analysis by western blot. Graph represents densitometry results from four HIF- 2α probed blots normalised to corresponding actin expression. Bars represent mean +/- SEM, *P<0.05, n=4, students' *t*-test. Below shows representative western blot for HIF- 2α and actin loading control.

4.2.9 HIF-1 ALPHA SIRNA TRANSFECTION IN COMMERCIAL AND IPAH PATIENT SMOOTH MUSCLE CELLS

The different effects of monocyte co-culture on commercial and IPAH patient hypoxic SMC HIF-1 expression was explored using siRNA targeting HIF- 1α to transfect both commercial and IPAH patient SMCs. These experiments would help identify any HIF- 1 dependence of monocyte inhibition of hypoxic SMC proliferation. Cells were seeded at 35,000 cells /well and either mock transfected, transfected with 2 μM scrambled siRNA or with HIF- 1α siRNA after which cells were incubated for 24 hours in normoxia (19 kPa) or hypoxia (3 kPa). Cell counts were performed by Coulter counter and lysates made for RNA isolation.

Commercial SMCs obtained from unused donor lungs displayed significantly increased cell number in hypoxic mock and scrambled siRNA transfected samples compared to normoxic counterparts (n=9) (Figure 4.12a). There was no significant difference in cell number in each oxygen tension when transfected with HIF- 1 siRNA. There was an increase in normoxic HIF- 1 siRNA transfected cell number compared to normoxic mock infected. While hypoxic HIF- 1 transfected cell numbers were unchanged when compared to hypoxic mock infected numbers.

This increase may be due to inefficient HIF- 1α knockdown. To establish transfection efficiency, real-time TaqMan PCR was used to quantify HIF- 1 RNA expression normalised to actin for each sample. For each experiment values were normalised to mock infected samples and expressed as % change from mock infected. In both normoxia and hypoxia HIF- 1α transfected samples had significantly less HIF- 1α expression when compared to scrambled controls (n=9) (Figure 4.12b) (n=9) (Figure 4.12c). HIF-2 siRNA had no effect on HIF-1 mRNA expression in each oxygen tension.

IPAH patient SMC number was maintained in hypoxia and normoxia for mock infected, scrambled siRNA transfected and HIF-1 α transfected samples (n=7) (Figure 4.13a). Transfection efficiency for all normoxic (Figure 4.13b) and hypoxic (Figure 4.13c) samples was determined by TaqMan real-time PCR. All samples were normalised to actin and each experiment normalised to mock infected samples. Data is expressed as % change from mock infected samples. In normoxia HIF- 1α expression was significantly reduced compared with scrambled siRNA transfected samples, this was also found in hypoxia (n=7). HIF-2 siRNA had no significant effect on HIF-1 mRNA in either oxygen tension.

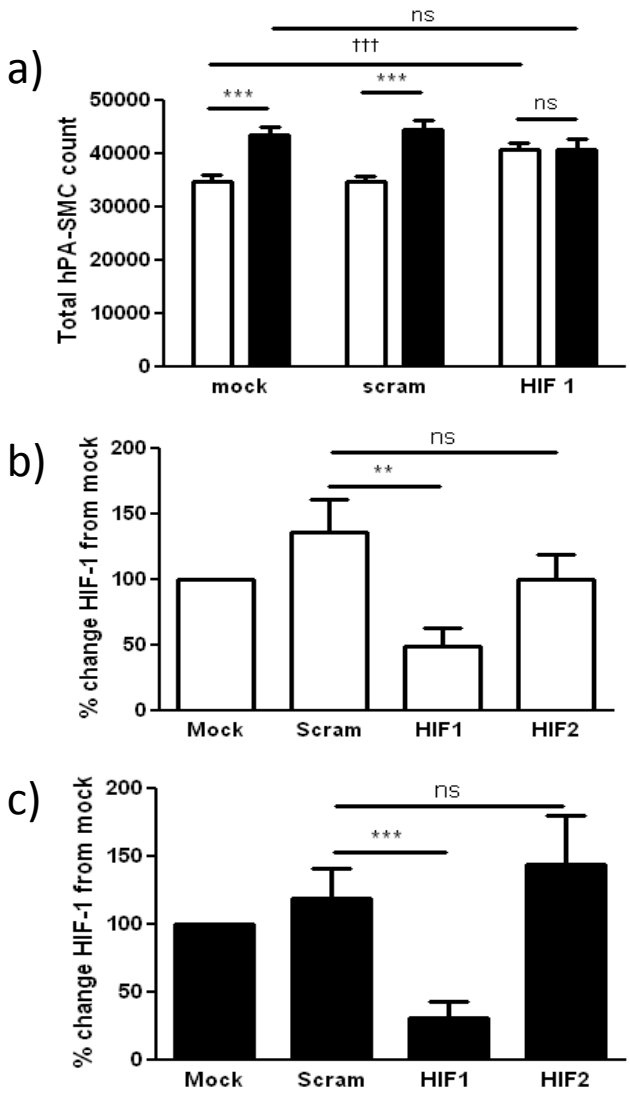

Figure 4.12 HIF- 1α knockdown increased normoxic commercial smooth muscle cell number but had no effect in hypoxia

Commercial SMCs were seeded at 35,000 cells /well and transfected with 2 μM siRNA targeting HIF- 1α. After transfection and 24 hour culture in normoxia (open bars) (19 kPa) and hypoxia (3 kPa) (closed bars) a) total cell counts were performed for mock infected, scrambled siRNA transfected and HIF- 1α siRNA transfected samples by Coulter counter. Bars represent mean +/- SEM, ***P<0.001, ns= not significant, cells from two separate vials studied n=9, two-way ANOVA with Bonferonni post test, †††P<0.001, ns= not significant, cells from two separate vials studied n=9, one-way ANOVA with Bonferonni post test. RNA expression of HIF- 1α normalised to actin as shown as % change from mock infected samples are shown for b) normoxic samples and c) hypoxic samples. Bars represent mean +/- SEM, **P<0.01, ***P<0.001, ns= not significant, n=9, students' *t*-test.

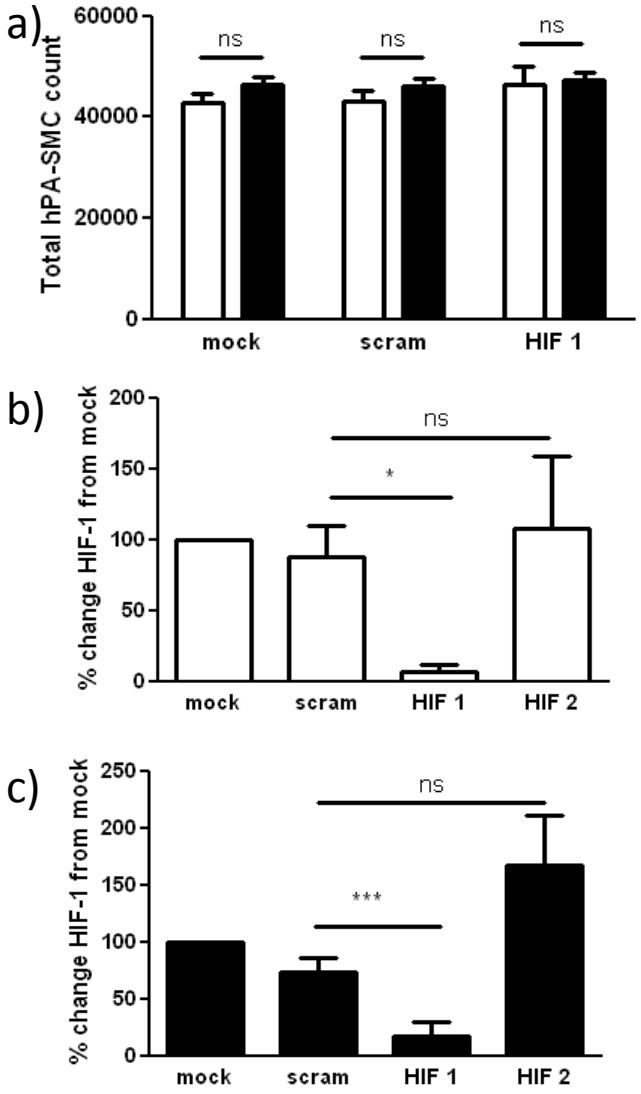

Figure 4.13 HIF- 1α did not change total IPAH smooth muscle cell number in either oxygen tension

IPAH patient SMCs were seeded at 35,000 cells /well and transfected with 2 μM siRNA targeting HIF- 1α. After transfection and 24 hour culture in normoxia (open bars) (19 kPa) and hypoxia (3 kPa) (closed bars) a) total cell counts were performed for mock infected, scrambled siRNA transfected and HIF- 1α siRNA transfected samples by Coulter counter. Bars represent mean +/- SEM, ***P<0.001, ns= not significant, n=7, two-way ANOVA with Bonferonni post test. RNA expression of HIF- 1α normalised to actin as shown as % change from mock infected samples are shown for b) normoxic samples and c) hypoxic samples. Bars represent mean +/- SEM, *P<0.05, ***P<0.001, ns= not significant, n=7, students' *t*-test.

4.2.10 HIF-2 ALPHA KNOCK-DOWN IN COMMERCIAL AND IPAH SMOOTH MUSCLE CELLS

Having observed a difference in HIF- 2 expression in both commercial and IPAH patient SMCs with and without monocytes I used siRNA targeting HIF- 2α in both commercial and IPAH patient SMCs to investigate the importance of HIF- 2α in SMC proliferation. Before transfection, cells were seeded at 35,000 cells /well and then mock transfected or transfected with 2 μM scrambled siRNA or with HIF- 2α siRNA. Plates were then incubated for 24 hours in normoxia (19 kPa) or hypoxia (3 kPa) after which cell counts were then performed by Coulter counter and lysates made for RNA isolation.

Commercial cells obtained from unused donor lungs with no vascular irregularities have a significantly increased cell number in hypoxia compared to normoxia in each transfection condition (n=7) (Figure 4.14a). Transfection efficiency was established at the RNA level by TaqMan PCR normalising to actin. For each experiment samples were normalised to mock infected samples and expressed as % change from mock infected. HIF- 2 siRNA significantly reduced normoxic and hypoxic HIF- 2 expression compared to scrambled controls (n=7) (Figure 4.14b), (n=7) (Figure 4.14c). HIF- 1 siRNA had no effect on HIF- 2 mRNA expression in either normoxia or hypoxia.

Cell numbers from IPAH patient SMC were unaffected by oxygen tension or transfection with HIF- 2α siRNA (n=7) (Figure 4.15a). TaqMan PCR was used to determine transfection efficiency of normoxic (Figure 4.15b) and hypoxic (Figure 4.15c) samples. Samples were normalised to actin and each experimental data point to mock infected sample. Data is expressed as % change from mock infected. HIF- 2α expression was significantly reduced in normoxic HIF- 2α transfected samples compared to samples transfected with scrambled siRNA (n=7). Hypoxic samples transfected with HIF- 2 siRNA had significantly reduced HIF- 2 mRNA expression compared to scrambled controls (n=7). HIF- 1 siRNA had no effect on HIF- 2 expression in either oxygen tension.

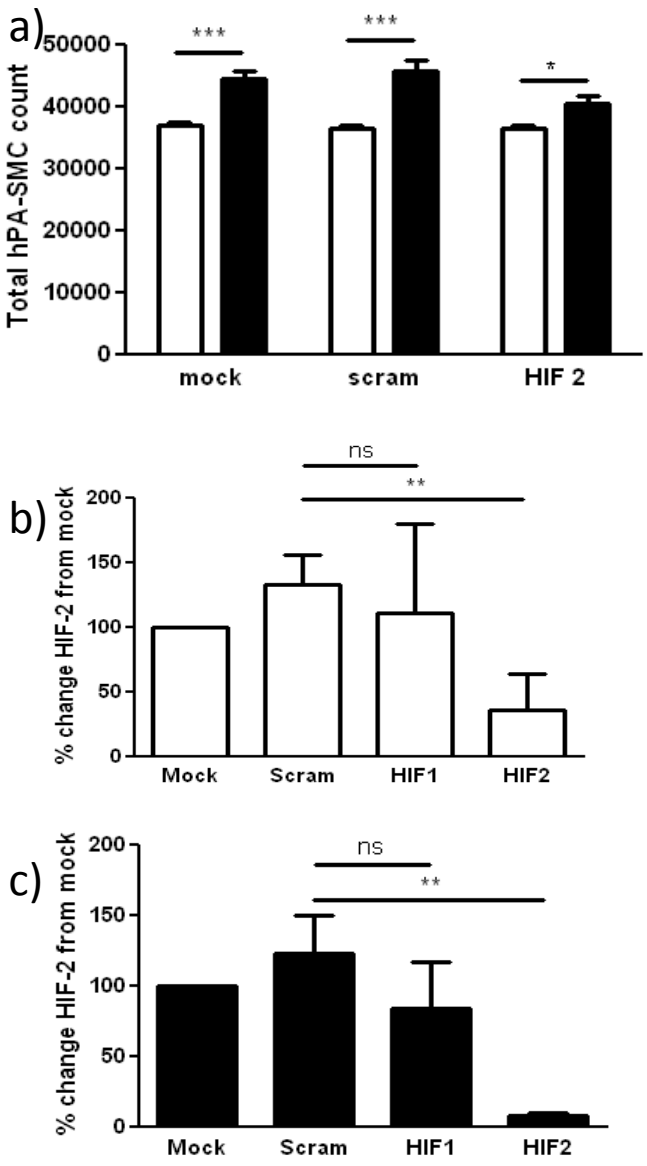

Figure 4.14 Knockdown of HIF- 2α in commercial smooth muscle cells did not change total cell counts

Commercial SMCs were seeded at 35,000 cells /well and transfected with 2 μM siRNA targeting HIF- 2α. After transfection and 24 hour culture in normoxia (open bars) (19 kPa) and hypoxia (3 kPa) (closed bars) a) total cell counts were performed for mock infected, scrambled siRNA transfected and HIF- 2α siRNA transfected samples by Coulter counter. Bars represent mean +/- SEM, *P<0.05, ***P<0.001, cells from two separate vials studied n=7, two-way ANOVA with Bonferonni post test. RNA expression of HIF- 2α normalised to actin as shown as % change from mock infected samples are shown for b) normoxic samples and c) hypoxic samples. Bars represent mean +/- SEM, **P<0.01, ns= not significant, n=7, students' *t*-test.

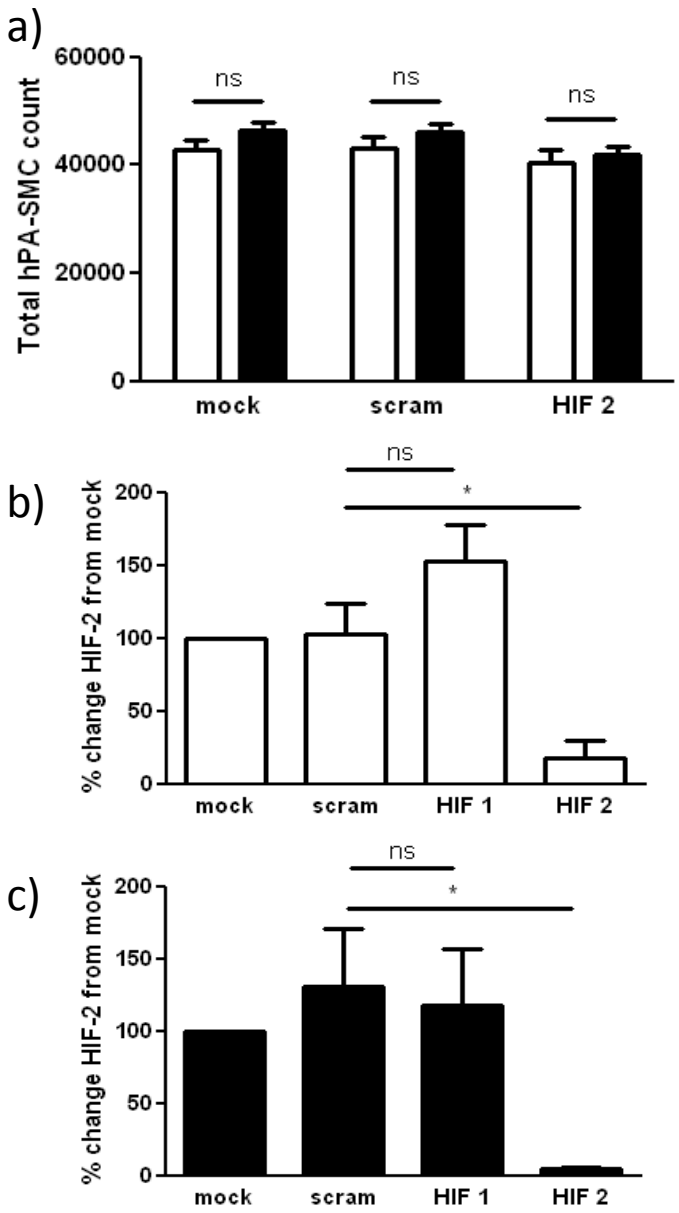

Figure 4.15 IPAH patient smooth muscle cell number was preserved with HIF- 2α knockdown

IPAH patient SMCs were seeded at 35,000 cells /well and transfected with 2 μM siRNA targeting HIF- 2α. After transfection and 24 hour culture in normoxia (open bars) (19 kPa) and hypoxia (3 kPa) (closed bars) a) total cell counts were performed for mock infected, scrambled siRNA transfected and HIF- 2α siRNA transfected samples by Coulter counter. Bars represent mean +/- SEM, ns= not significant, n=7, two-way ANOVA with Bonferonni post test. RNA expression of HIF- 2α normalised to actin as shown as % change from mock infected samples are shown for b) normoxic samples and c) hypoxic samples. Bars represent mean +/- SEM, *P<0.05, ns= not significant, n=7, students' *t*-test.

4.2.11 HIF-1 AND HIF-2 ALPHA DOUBLE KNOCK-DOWN IN PRIMARY SMOOTH MUSCLE CELLS

Having found differential roles for both HIF- 1 and HIF- 2α in normoxic commercial SMC proliferation and IPAH patient SMC proliferation I went on to transfect both commercial and IPAH patient SMCs with a mix of HIF- 1 and HIF- 2α siRNA at ratio of 1:1. The day before transfection, SMCs were seeded at 35,000 cells /well. The next day cells were either, mock transfected, transfected with 2 μM scrambled siRNA or transfected with a 1:1 mix of HIF- 1 and HIF- 2α siRNAs. After transfection cells were incubated for a further 24 hours in normoxia (19 kPa) or hypoxia (3 kPa). Post-culture total cell counts were then performed by Coulter counter and lysates made for RNA isolation.

In each condition hypoxia significantly increased commercial SMC number compared to normoxia. Co-transfection with both HIF- 1 and HIF- 2α siRNA had no effect on cell number in each oxygen tension (n=6) (Figure 4.16a). Relative HIF- 1 RNA expression was determined by TaqMan PCR to show transfection efficiency. TaqMan data showed a significant reduction in HIF- 1 and HIF- 2 expression in both normoxia and hypoxia for HIF- 1 and HIF- 2α siRNA co-transfected samples compared to scrambled siRNA transfected samples. All samples are normalised to actin and expressed as % change from mock infected (n=6) (Figure 4.16b) (n=6) (Figure 4.16c).

IPAH patient SMC total cell numbers were equivalent for both normoxic and hypoxic SMCs which were either mock transfected or transfected with non-targeting scrambled siRNA. Co-transfection with both HIF- 1 and HIF- 2α siRNA had no effect on total cell counts in either normoxia or hypoxia (Figure 4.17a). To determine efficiency of HIF- 1α knockdown TaqMan PCR was used. In both normoxia and hypoxia HIF- 1α expression was significantly reduced in co-transfected samples in normoxia and hypoxia compared to mock infected samples. Samples were normalised to actin and data from each experiment normalised to mock infected samples. Data is expressed as % change from mock infected (n=6) (Figure 4.17b). The expression of HIF- 2α was also determined by TaqMan real-time PCR. Data shows that co-transfection with both HIF- 1 and

HIF- 2α siRNAs significantly reduce HIF- 2α expression in both normoxia and hypoxia. Data is normalised to actin and expressed as % change from mock transfected samples (n=6) (Figure 4.17c).

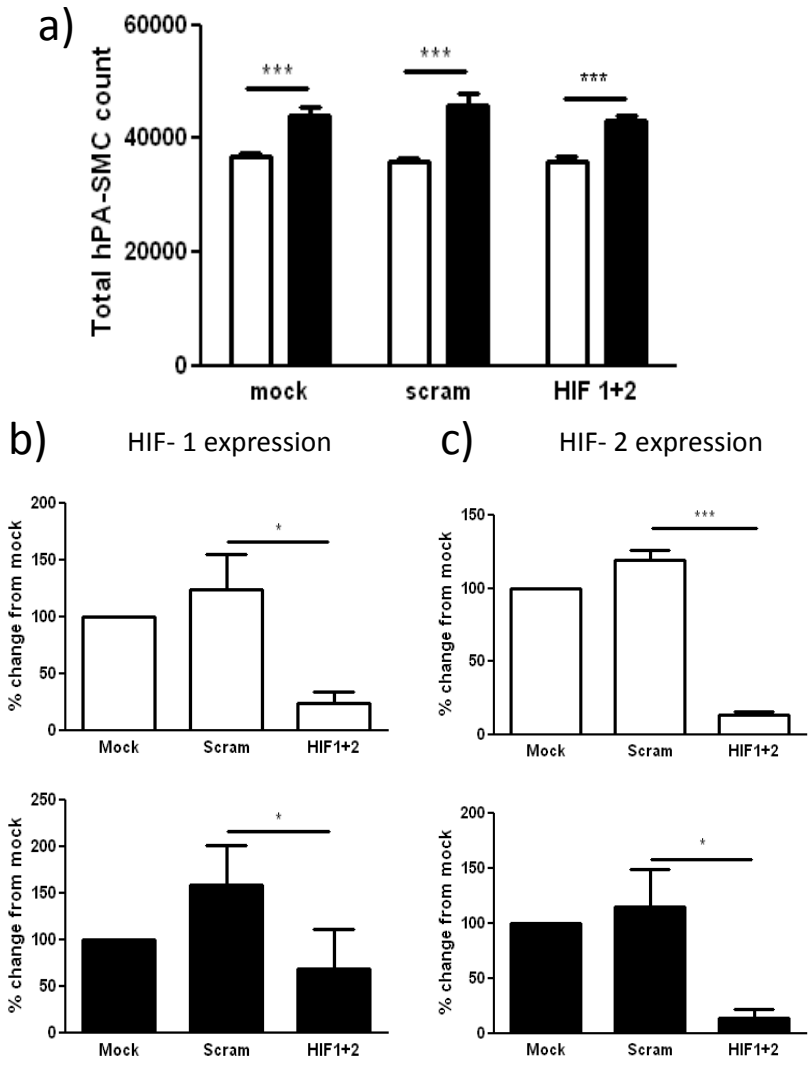

Figure 4.16 HIF- 1 and HIF- 2α co-transfection did not change total cell numbers in commercial smooth muscle cells

Commercial SMCs were seeded at 35,000 cells /well and transfected with 2 μM siRNA targeting both HIF- 1 and HIF- 2α. After transfection and 24 hour culture in normoxia (open bars) (19 kPa) and hypoxia (3 kPa) (closed bars) a) total cell counts were performed for mock infected, scrambled siRNA transfected and HIF siRNA transfected samples by Coulter counter. Bars represent mean +/- SEM, ***P<0.001, cells from two separate vials studied n=6, two-way ANOVA with Bonferonni post test. RNA expression of b) HIF- 1α and c) HIF- 2α normalised to actin as shown as % change from mock infected samples are shown for normoxic and hypoxic samples. Bars represent mean +/- SEM, *P<0.05, ***P<0.001, students' *t*-test.

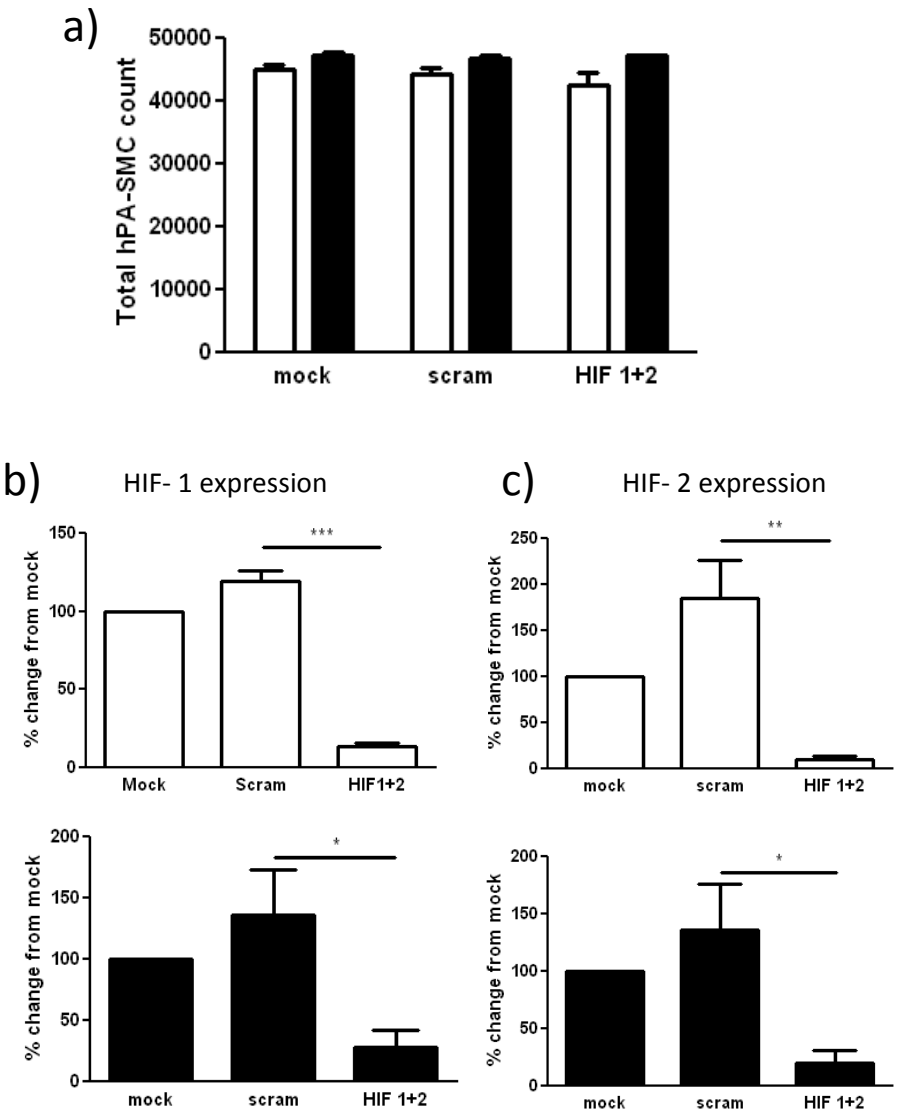

Figure 4.17 IPAH patient smooth muscle cell number was preserved with HIF-1 and HIF-2 α co-transfection

IPAH patient SMCs were seeded at 35,000 cells /well and transfected with 2 μM siRNA targeting both HIF- 1 and HIF- 2α. After transfection and 24 hour culture in normoxia (open bars) (19 kPa) and hypoxia (3 kPa) (closed bars) a) total cell counts were performed for mock infected, scrambled siRNA transfected and HIF siRNA transfected samples by Coulter counter. Bars represent mean +/- SEM, ***P<0.001, n=6, two-way ANOVA with Bonferonni post test. RNA expression of b) HIF- 1α and c) HIF- 2α normalised to actin as shown as % change from mock infected samples are shown for normoxic and hypoxic samples. Bars represent mean +/- SEM, *P<0.05, ***P<0.001, students' *t*-test.

4.2.12 Protein expression of HIF-1 and HIF-2 alpha in transfected commercial smooth muscle cells

Transfection efficiency at the RNA level has been shown to be effective. I then wanted to determine the consequence of RNA knockdown with regards to protein expression. SMCs obtained commercially as healthy cells with no vascular abnormalities were seeded at 35,000 cells /well and either mock infected or transfected with 2 μM siRNA. After transfection and 24 hour culture in either normoxia (19 kPa) or hypoxia (3 kPa) protein lysates were made for analysis by western blot. Blots were then analysed by densitometry normalising to corresponding actin expression.

SMCs had no HIF- 1α expression in normoxia so transfection had no effect on normoxic HIF- 1α expression. Hypoxia increased HIF- 1α expression in both mock and scrambled siRNA transfected cells. Transfection with HIF- 1α siRNA significantly reduced HIF-1 protein expression (n=4) (Figure 4.18). HIF- 2α protein expression was more stable in normoxia and HIF- 2 siRNA significantly reduced expression compared to mock and scrambled siRNA transfected samples (n=4). HIF- 2α protein was expressed highly in both hypoxic mock and scrambled siRNA samples but this was dramatically reduced in HIF- 2α siRNA transfected samples (n=4) (Figure 4.19).

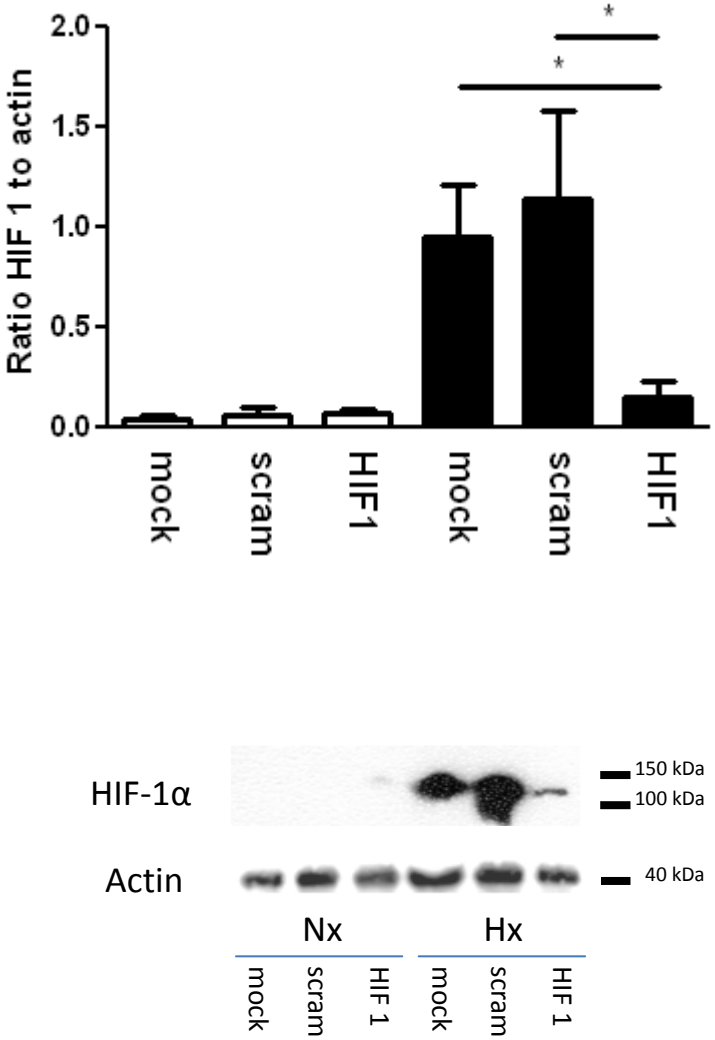

Figure 4.18 HIF- 1α siRNA transfection in commercial smooth muscle cells reduced HIF- 1α protein expression in hypoxia

Commercial SMCs were seeded at 35,000 cells /well and either mock transfected or transfected with 2 μM siRNA targeting HIF- 1 or non-targeting siRNA. After transfection and 24 hour culture in normoxia (open bars) (19 kPa) and hypoxia (3 kPa) (closed bars) cells were lysed. Graph represents densitometry results from four HIF-1α probed blots normalised to corresponding actin expression. Bars represent mean +/- SEM, *P<0.05, **P<0.01, n=4, students' *t*-test. Below shows a representative western blot for HIF- 1 and actin loading control. HIF- 1α has a predicted weight of 120 kDa and actin of 40 kDa.

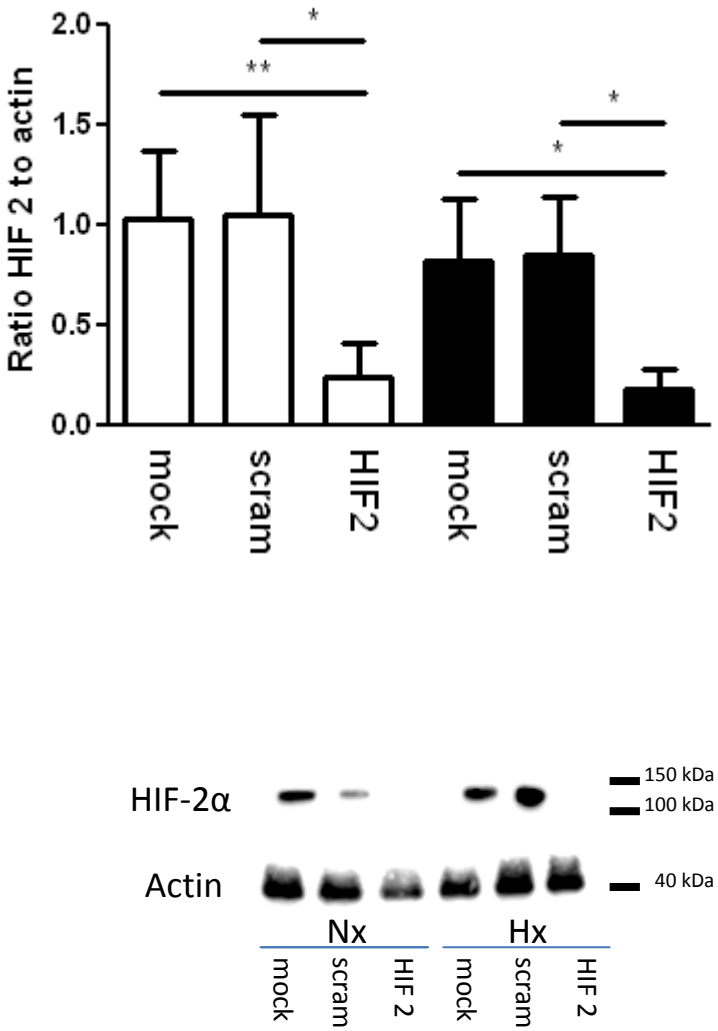

Figure 4.19 Protein expression of HIF- 2α was reduced in commercial smooth muscle cells with HIF - 2α siRNA transfection

Commercial SMCs were seeded at 35,000 cells /well and either mock transfected or transfected with 2 μM siRNA targeting HIF- 2α or non-targeting siRNA. After transfection and 24 hour culture in normoxia (open bars) (19 kPa) and hypoxia (3 kPa) (closed bars) cells were lysed. Graph represents densitometry results from four HIF-2α probed blots normalised to corresponding actin expression. Bars represent mean +/- SEM, *P<0.05, n=4, students' *t*-test. Below shows a representative western blot for HIF- 2 and actin loading control. HIF- 2α has a predicted weight of 120 kDa and actin of 40 kDa.

4.2.13 Protein expression of HIF-1 and HIF-2 alpha in HIF- 1 and HIF- 2 alpha siRNA transfected IPAH patient smooth muscle cells

IPAH patient SMC transfection efficiency at the protein level was determined next. IPAH patient SMCs were seeded at 35,000 cells /well and either mock infected or transfected with 2 μM scambled siRNA or 2 μM siRNA targeting either HIF- 1α or HIF- 2α. After transfection and 24 hour culture in normoxia (19 kPa) or hypoxia (3 kPa), protein lysates were made for analysis by western blot. Blots were then analysed by densitometry normalising to corresponding actin expression.

Patient SMC HIF-1 protein expression was very low in normoxia so transfection with HIF-1 siRNA had no effect. Hypoxia increased HIF- 1α protein expression and this was significantly reduced with HIF- 1α transfection (n=4) (Figure 4.20). HIF- 2α protein expression was present at similar levels in normoxia and hypoxia. HIF- 2 siRNA significantly reduced HIF-2 protein compared to mock and scrambled siRNA counterparts in normoxia (n=4) and hypoxia (n=4) (Figure 4.21).

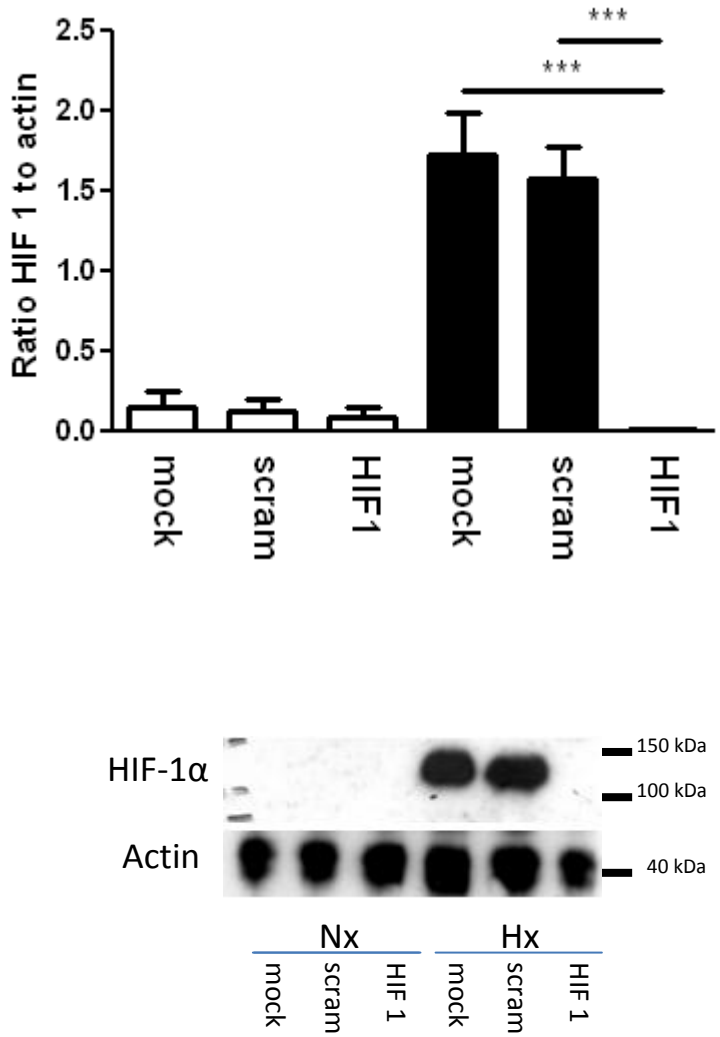

Figure 4.20 Hypoxic increase in IPAH patient smooth muscle cell HIF- 1α expression was lost with HIF- 1α siRNA transfection

IPAH patient SMCs were seeded at 35,000 cells /well and transfected with 2 μM siRNA targeting HIF- 1 or non-targeting scrambled siRNA. After transfection and 24 hour culture in normoxia (open bars) (19 kPa) and hypoxia (3 kPa) (closed bars) cells were lysed. Graph represents densitometry results from four HIF- 1α probed blots normalised to corresponding actin expression. Bars represent mean +/- SEM, *P<0.05, **P<0.01, n=4, students' *t*-test. Below shows a representative western blot for HIF- 1 and actin loading control. HIF- 1α has a predicted weight of 120 kDa and actin of 40 kDa.

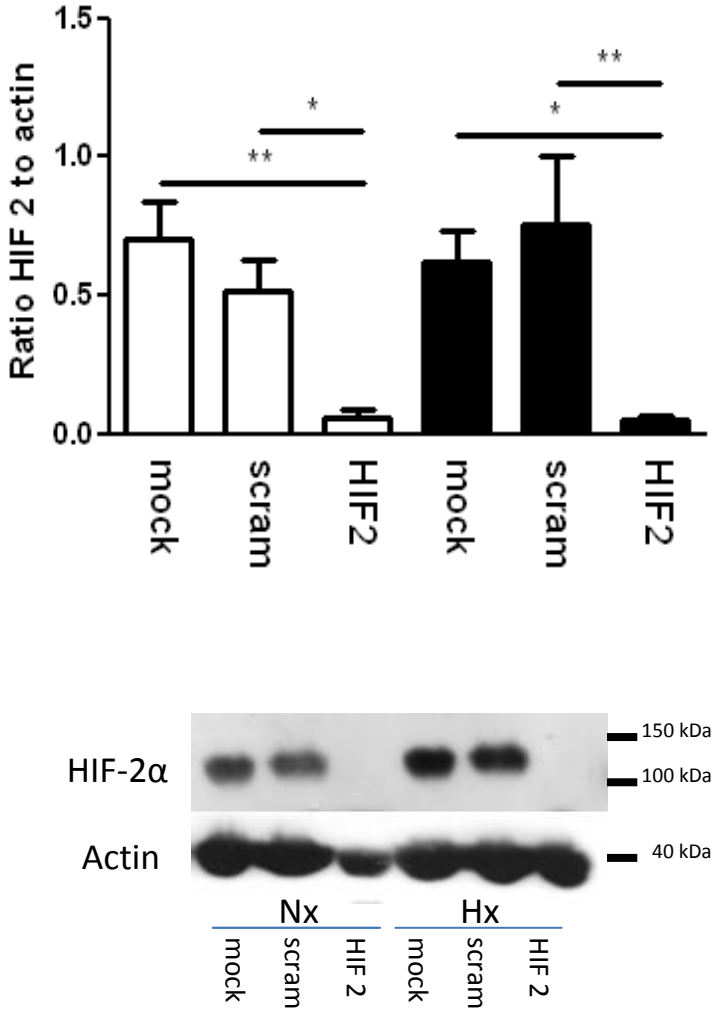

Figure 4.21 Protein expression of HIF-2α was abolished in both oxygen tensions with HIF-2α siRNA transfection in IPAH patient smooth muscle cells

IPAH patient SMCs were seeded at 35,000 cells /well and transfected with 2 μM siRNA targeting HIF- 2 or non-targeting scrambled siRNA. After transfection and 24 hour culture in normoxia (open bars) (19 kPa) and hypoxia (3 kPa) (closed bars) cells were lysed. Graph represents densitometry results from four HIF- 2α probed blots normalised to corresponding actin expression. Bars represent mean +/- SEM, *P<0.05, **P<0.01, n=4, students' t-test. Below shows a representative western blot for HIF- 2 and actin loading control. HIF- 2α has a predicted weight of 120 kDa and actin of 40 kDa.

4.2.14 BMPR2 KNOCKDOWN IN COMMERCIAL SMOOTH MUSCLE CELLS RECAPITULATED THE IPAH PATIENT SMOOTH MUSCLE CELL PHENOTYPE

The vial of IPAH patient SMCs I used had a known mutation in BMPR2. This mutation has a serine substitution from the leucine at residue 401 in the kinase domain of the protein making it functionally inactive. The inactive BMPR2 protein is thought to be responsible for the SMC hyperproliferative phenotype therefore siRNA transfection of healthy commercial SMCs targeting BMPR2 should induce an IPAH patient SMC phenotype.

To test this hypothesis, commercially available healthy SMCs with no known vascular abnormalities were transfected with siRNA targeting BMPR2. Commercial SMCs were seeded at 35,000 cells /well and were either, mock transfected, transfected with 2 μM scrambled siRNA or 2 μM siRNA targeting BMPR2. Post-transfection plates were cultured for 24 hours in normoxia (19 kPa) or hypoxia (3 kPa) and total cell counts performed.

Transfection with BMPR2 significantly increased normoxic cell number when compared to mock infected samples. This increase was unaffected by co-culture with monocytes (n=6) (Figure 4.22a). Transfection efficiency was calculated by TaqMan PCR. Samples were normalised to actin and expressed as % change from mock infected. BMPR2 siRNA significantly reduced BMPR2 expression when compared to scrambled siRNA transfected samples (n=6) (Figure 4.22b).

Total cell counts of transfected SMCs in hypoxia were unaffected by either transfection condition or co-culture with monocytes (n=6) (Figure 4.23a). Efficiency of transfection was calculated by real-time TaqMan PCR and normalised to actin. All data is expressed as % change from mock transfected. BMPR2 transfection significantly reduced BMPR2 expression compared to scrambled siRNA transfection (n=6) (Figure 4.23b).

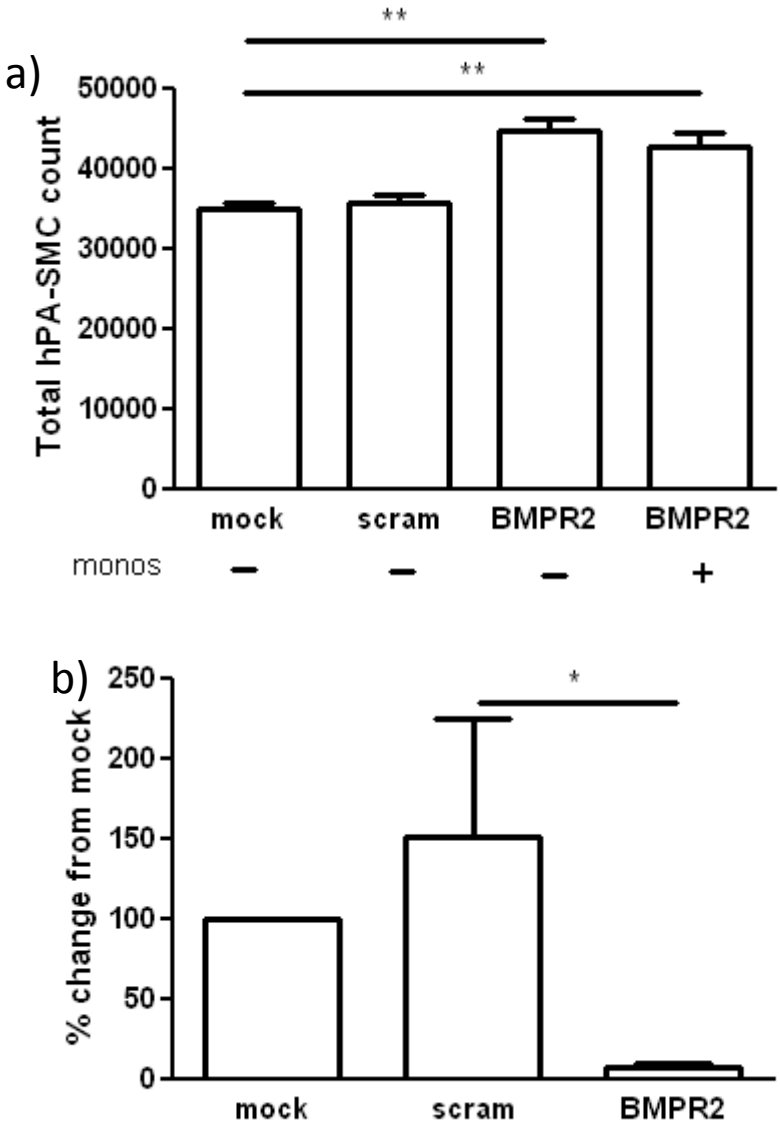

Figure 4.22 BMPR2 siRNA transfection increased normoxic smooth muscle cell number and monocyte co-culture did not inhibit this increase

Commercial SMCs were seeded at 35,000 cells /well and transfected with 2 μM siRNA targeting BMPR2. After transfection and 24 hour culture in normoxia (19 kPa) a) total cell counts were performed for mock infected, scrambled siRNA transfected and BMPR2 siRNA transfected samples by Coulter counter. Bars represent mean +/- SEM, **P<0.01, n=6 experiments, one-way ANOVA with Bonferonni post test. b) RNA expression of BMPR2 normalised to actin as shown as % change from mock infected. Bars represent mean +/- SEM, *P<0.05, students' *t*-test.

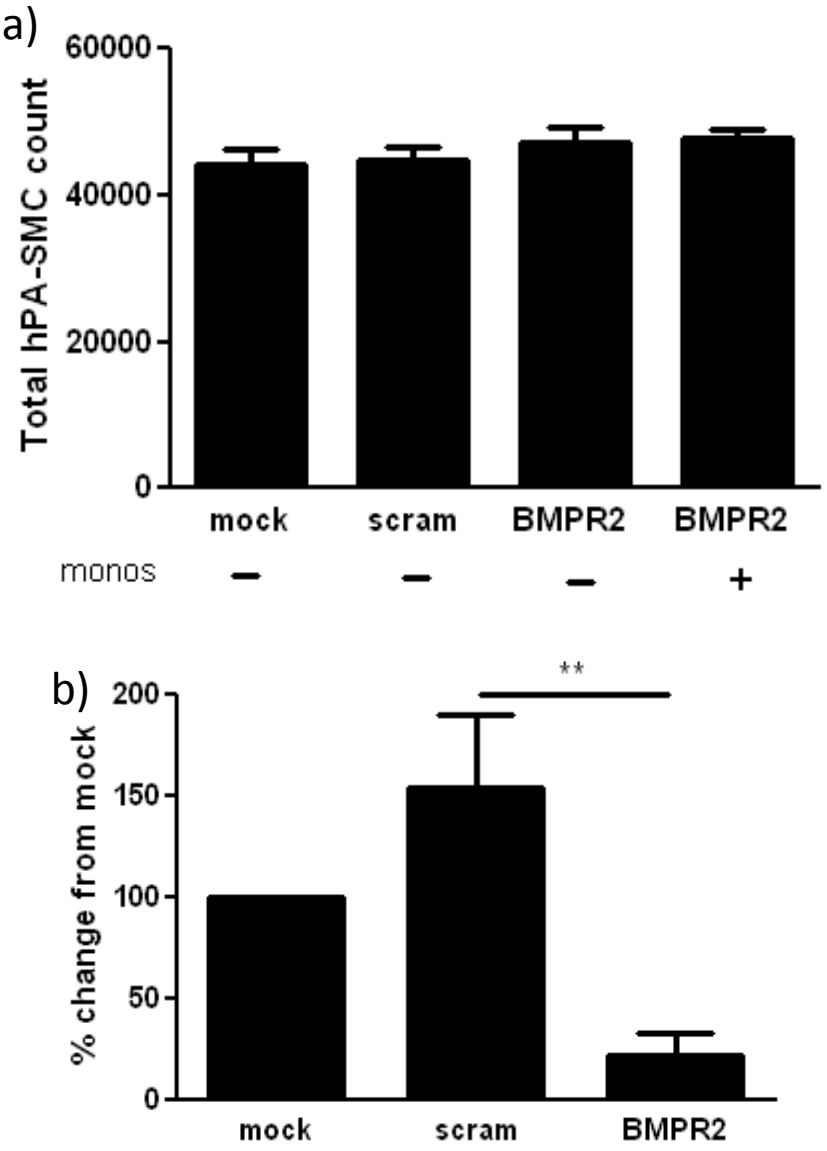

Figure 4.23 Hypoxic smooth muscle cell number was preserved with and without BMPR2 siRNA transfection

Commercial SMCs were seeded at 35,000 cells /well and transfected with 2 μM siRNA targeting BMPR2. After transfection and 24 hour culture in hypoxia (3 kPa) a) total cell counts were performed for mock infected, scrambled siRNA transfected and BMPR2 siRNA transfected samples by Coulter counter. Bars represent mean +/- SEM. b) RNA expression of BMPR2 normalised to actin as shown as % change from mock infected. Bars represent mean +/- SEM, **P<0.01, students' *t*-test.

4.2.15 Smooth muscle cell number is preserved with co-incubation with Trolox

With the discovery that hypoxic SMC proliferation was HIF independent other hypoxic regulated pathways which were able to affect SMC proliferation were investigated. One possibility was that hypoxic induced ROS was driving proliferation and monocyte derived antioxidants were able to neutralise ROS dependant SMC proliferation. To test the hypothesis that ROS were inducing hypoxic SMC proliferation I used the vitamin E analogue and antioxidant Trolox in the hope that this would reduce hypoxic SMC number by preventing oxidation.

Healthy commercial SMCs were seeded at 25,000 cells /well and cultured in normoxia (Nx) (19 kPa) and hypoxia (Hx) (3 kPa) prior to serum starvation. Plates were cultured for a further 24 hours with increase concentrations of Trolox. Total cell counts were then performed by Coulter counter. Total cell numbers were significantly increased in hypoxia compared to normoxia (n=3). Increase concentrations of Trolox had no additive effect on total cell numbers (Figure 4.24).

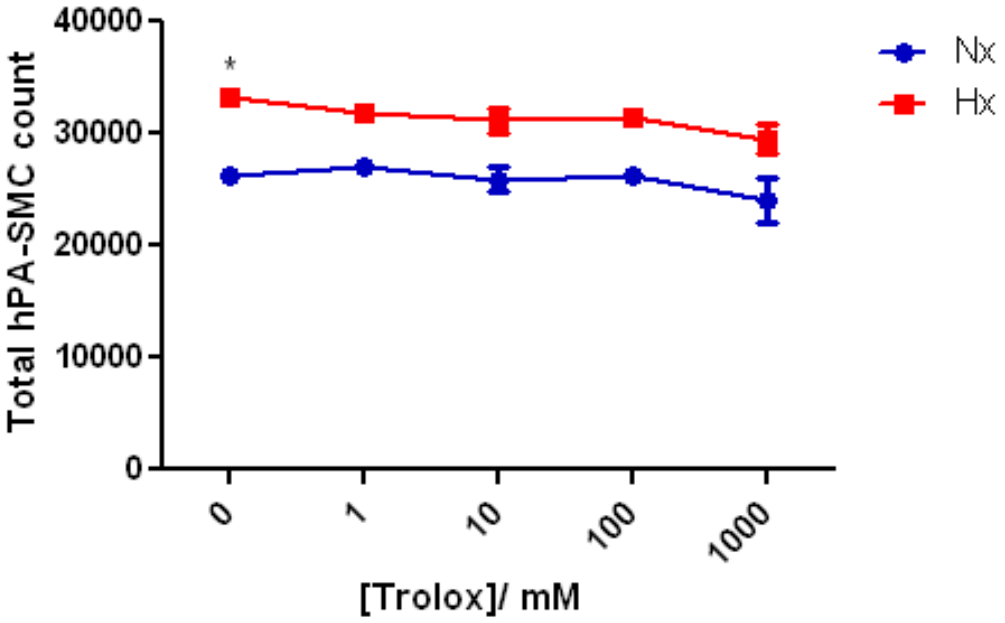

Figure 4.24 Smooth muscle cell numbers are unchanged by incubation with increase concentrations of Trolox

SMCs were seeded at 25,000 cells /well and cultured in normoxia (Nx) (19 kPa) and hypoxia (Hx) (3 kPa) prior to serum starvation. Cells were then cultured for a further 24 hours with increase concentrations of Trolox. After culture, cells were washed and counted by Coulter counter. Graph shows normoxic cultures in blue and hypoxic cultures in red. Data points show mean +/- SEM, *P<0.05, n=3, one-way ANOVA with Bonferonni post test.

4.3 DISCUSSION

Despite the discovery of mutations in BMPR2 predisposing to PAH, the specific triggers of PAH and the cause of BMPR2 mutation independent cases are unknown. However, immune cell infiltration is often found surrounding both concentric and plexiform lesions formed in developed PAH. Despite the presence of these cells being increased in areas of vascular remodelling and monocytes being found to extravate diseased endothelium the exact role of these cells in PAH disease progression is yet to be established. I have shown that monocytes isolated from peripheral blood of patients with IPAH are unable to inhibit hypoxic SMC proliferation. This is not true of monocytes obtained from patients with an inflammatory associated form of the disease. Systemic sclerosis is an autoimmune disease characterised by increased inflammation and collagen deposition. Systemic sclerosis associated PAH has many similarities to IPAH both with its vascular remodelling and inflammatory component. Similar to IPAH, in many cases of systemic sclerosis associated PAH, an increase in TGF-β pathway activation is observed. However, monocytes from systemic sclerosis associated PAH patients were able to inhibit hypoxic SMC proliferation showing that monocyte inability to inhibit hypoxic SMC proliferation is specific to sporadic forms of the disease. Moreover, the inability of IPAH monocytes to inhibit hypoxic SMC proliferation suggests that the circulating myeloid cells display an altered phenotype to myeloid cells from healthy controls.

This is supported by work from Bull *et al*. who found differences in gene expression for PBMCs obtained from IPAH patients and associated forms of the disease compared to healthy controls. The group analysed PBMCs obtained from IPAH patients, associated PAH patients and healthy volunteers. Using Affymetrix array chips a microarray was carried out on lysates of each cohort analysing about 6,000 genes. After analysis approximately 3,000 genes were identified to be comparable in all subjects. Unsurprisingly, cluster analysis showed a strong linkage in gene expression of IPAH and associated PAH samples compared to the healthy controls. This was validated in a second set of

samples; excitingly this second validation led to discovery of a key difference between IPAH patient PBMCs and associated PAH PBMCs. IPAH patient PBMC expression of the herpes virus entry mediator encoding gene HVEM was dramatically increased compared to diseased and healthy volunteer controls further suggesting circulating IPAH mononuclear cells are uniquely changed in disease (Bull et al., 2004). Despite PBMCs being studied monocytes in isolation have not been studied in PAH with regards to number, function and phenotype, monocytes have been shown to be altered in other cardiovascular diseases. For example monocytes isolated from patients with atherosclerosis presented with increased migration compared to monocytes from healthy controls (Bath et al., 1991). With the knowledge that the pulmonary vasculature is very different from the systemic vasculature as illustrated in my work in Chapter 3, it is unlikely that processes in atherlerosclerosis are the same in PAH development. However, data from other cardiovascular diseases could give important mechanistic insights into potential pathways involved in PAH progression.

There is little data phenotyping monocytes with regards to IPAH, however, by using data from other closely related cell types we may gain key insights to mechanisms which support the theory that monocytes may have an altered phenotype in IPAH compared to healthy. Another circulating cell type derived from the same hematopoietic stem cell as the monocyte is the $CD34^{+}CD133^{+}$ endothelial progenitor cell. Isolation of these cells from IPAH patient PBMCs showed an increase in circulating $CD34^{+}CD133^{+}$ cell number when compared to healthy controls (Farha et al., 2011). Evidence that these endothelial progenitors derive from a common cell lineage to monocytes and macrophages was provided in 2000. It was found that plate purified macrophages isolated from healthy volunteer blood could de-differentiate into endothelial like cells. With growth factor stimulation these cells could form tubes in Matrigel™ like mature endothelial cells as well as expressing endothelial cell markers such as von Willebrand Factor suggesting that endothelial cell progenitors could be derived from myeloid lineage (Schmeisser et al., 2001). A later publication isolated PBMCs from healthy volunteer buffy coats and successfully propagated pleuripotent stem cells. These stem cells had the ability to differentiate into

colony forming endothelial cells identifying a potential origin for endothelial cell progenitors (Zhao et al., 2003). Not only have circulating $CD34^{+}CD133^{+}$ endothelial cell progenitor numbers been shown to be increased in IPAH patients when compared to healthy controls but also despite similar baseline haematological profiles, $CD34^{+}CD133^{+}$ endothelial cell progenitor cells were more proliferative in IPAH patients when compared to controls (Farha et al., 2011) (Toshner et al., 2009). Severe combined immunodeficiency mice on a non-obese diabetic background (NOD SCID) injected with endothelial progenitor cells isolated from patients with IPAH produced vascular lesions and showed an increased proliferative phenotype (Asosingh et al., 2008). The increase in endothelial progenitor cell number has been postulated to be used as a biomarker for cardiovascular disease as peripheral blood from patients at different cardiovascular disease states with no history of cardiovascular disease compared to healthy controls had an increase in $CD34^{+}CD133^{+}$ cell number (Hill et al., 2003). Monocytes themselves although maintained in number between IPAH and healthy cohorts may have an altered phenotype which is yet to be established with regards to functional competence and protein or gene expression.

In addition to showing monocytes cells are altered in disease, I have shown that IPAH patient SMCs have an altered phenotype. I have found that SMCs from IPAH patients had a hyper-proliferative phenotype in normoxia to 5 % serum. Hypoxia had no additive effect on SMC proliferation with both oxygen tensions giving similar total cell counts. Unlike with commercial SMC, monocytes are unable to inhibit patient SMC proliferation. Previous work on IPAH patient SMCs found them to proliferate to hypoxia in serum starved conditions (Yang et al., 2002). Although I didn't observe this, I think that my cells were already at maximum proliferation after 24 hours in 5 % serum so I was unable to see uplift in hypoxia. With a known BMPR2 mutation in IPAH SMCs, the inability of monocytes to inhibit patient SMC proliferation may mean that monocyte inhibition of hypoxic proliferation is independent of the BMPR2 and SMAD 1/5/8 pathway. Combining both IPAH patient monocytes and SMCs will be important to further understand the disease phenotype.

To ensure my culture system was hypoxic I measured the pO_2 of my culture supernatants but also secreted VEGF expression was used as a positive control. As a HIF target gene its expression was reassuringly increased in healthy hypoxic SMC supernatant samples compared to their normoxic counterparts. However, in my patient samples both normoxic and hypoxic expression of VEGF was equivalent. Moreover, in each culture condition VEGF expression was at least 2 fold higher then in healthy cells. One possible explanation for the differential growth phenotypes of diseased and healthy cells could be attributed to this difference in HIF pathway activation. In order to understand the role of the HIF pathway in hypoxic SMC proliferation the pan-hydroxylase enzyme DMOG was used to stabilise the oxygen sensitive domain of HIF- 1α. I found that HIF stabilisation with DMOG increased SMC proliferation and healthy monocytes were unable to inhibit DMOG- induced SMC proliferation. Work by Schultz, *et al.* found that DMOG inhibited growth factor induced proliferation in pulmonary artery SMC as shown by a reduction in $[H]^+$ thymidine incorporation. Contradictory to my findings, in control cells treated with 100 μM DMOG there was no increase in SMC proliferation. However, SMC proliferation is very sensitive to serum availability and these cultures were in 1 % FCS which can reduce proliferation with regards to cell number and cyclin A expression (Schultz et al., 2009). Taken together, these findings suggested that HIF stability is important for SMC proliferation but monocyte inhibition of proliferation is independent of the HIF stability. However perhaps the chemical was adversely affecting monocytes' ability to inhibit hypoxic SMC proliferation, to address this I pre-treated the monocytes with DMOG and cell-free supernatants applied to both normoxic and hypoxic SMCs. I proved that cell-free supernatants from monocytes pre-treated with DMOG were still able to inhibit hypoxic SMC proliferation. Despite these data, the non-specific nature of DMOG means I cannot conclusively show that monocyte inhibition of hypoxic SMC proliferation is HIF independent. Moreover they may be DMOG carryover in the supernatant samples. What I can conclude from my experiments using DMOG as a proliferative stimulus is that IL- 1ra inhibition of SMC proliferation is not specific for hypoxia. Unlike monocytes, exogenous IL-1ra can inhibit both

hypoxic SMC proliferation and DMOG induced proliferation suggesting it is a more global regulator of SMC proliferation.

To further address the HIF specificity of hypoxic SMC proliferation and inhibition of proliferation by monocyte co-culture I performed western blot analysis on SMC after 24 hour culture with and without monocytes. Although I found no change in HIF- 1α in SMC with or without monocytes, I did see an increase in HIF- 1α with hypoxia or DMOG. With regards to HIF- 2α, I found monocyte and SMC co-culture increased HIF- 2α expression compared to SMC monoculture in either oxygen tension but not with DMOG. This suggests that monocyte inhibition of SMC proliferation is HIF- 1α independent. However, it is still unknown if HIF- 2α has a role in monocyte inhibition of SMC proliferation or if HIF is important for hypoxic SMC proliferation. Using siRNA targeting both HIF- 1 and HIF- 2α I found that knockdown of HIF- 1α induced normoxic SMC proliferation but this was not so in IPAH patient SMC. Moreover, knockdown of HIF- 1α did not induce a compensatory increase in HIF- 2α. Knock down of HIF- 2 had no effect on SMC proliferation in each oxygen tension for both commercial and IPAH patient SMC. Despite the increase in HIF- 2α protein seen in monocyte and SMC co-culture, HIF- 2α has no effect on SMC proliferation suggesting SMC increase in HIF- 2α protein is affecting SMCs in a proliferation independent manner. Given that both HIF- 1 and HIF- 2α have differential roles on cell cycle progression (Henze and Acker, 2010) (Schultz et al., 2005), an imbalance of either subunit may switch a senescent cell to progress through the cell cycle. This is illustrated by the fact that growth factor induced pulmonary artery SMC is inhibited with successful knockdown of HIF- 1α but siRNA targeting HIF- 2α has no effect on cell number in these same cells (Schultz et al., 2005). In human pulmonary artery SMCs, knockdown of HIF- 2α leads to a reduction in activity of the transcription factor forkhead box M1 (FoxM1). This reduction in turn leads to a reduction in the cell cycle mediators aurora A kinase and cyclin D1 (Raghavan et al., 2012). This would suggest that HIF- 2 siRNA would reduce hypoxic SMC number but this is not seen in my work suggesting hypoxic SMC proliferation is driven by a different mechanism.

In relation to cancer there is evidence of a differential role for both HIF- 1 and HIF- 2α. Immunohistochemistry on non-small cell lung cancer tissues show a change in regulation and expression of HIF- 1 and HIF- 2α during tumour progression (Wu et al., 2011). In lung sections from patients undergoing surgery for emphysema the remodelled lung vessels showed increased HIF- 1 stabilisation showing indirect evidence of the hypoxic microenvironment. These areas also showed an increase in proliferation cellular nuclear antigens as well as an increase in active caspase 3. These data were reproduced *in vitro* using $CoCl_2$ as a HIF stabiliser on vascular SMCs. In different subpopulations of the vascular cells, proliferation, apoptosis and HIF expression was different, again suggesting differential roles for the HIFs in different cell populations (Howard et al., 2012).

Hypoxia induces both HIF- 1 and HIF- 2 stabilisation and pulmonary artery SMC proliferation in male Sprague-dawley rats which then go on to develop pulmonary hypertension. This increase in both HIF subtypes also parallels and increase in ROS and intracellular Ca^{2+} (Zhang et al., 2012). The drug fluoxetine, a serotonin reuptake inhibitor, reduces hypoxic induction of HIF- 1α in MCT injected rats exposed to chronic hypoxia. This also leads to a reduction in ROS illustrating the close linkage between HIF- 1 expression and redox states of cells (Han et al., 2012). To determine whether hypoxia increased ROS in my culture system and thus induced hypoxic SMC proliferation, I used the antioxidant Trolox. Using increased concentrations of the vitamin E analogue Trolox I showed that monocyte inhibition of hypoxic proliferation was not due to monocytes release of an antioxidant by showing Trolox had no effect on hypoxic SMC proliferation.

In conclusion I have shown that monocytes from IPAH patients are unable to inhibit hypoxic SMC proliferation and IPAH SMCs have an enhanced proliferative phenotype. I have shown that IL-1ra inhibition of SMC proliferation is not selective for hypoxia and the hypoxic SMC proliferation is HIF independent but there may be a role for the HIF pathway in monocyte inhibition of SMC proliferation. Further work would be to analyse the consequence of IPAH monocyte and IPAH SMC co-culture to further understand

the effect of disease on both vascular and circulating cells. In order to understand the mechanism of monocyte inhibition of hypoxic SMC proliferation I would like to explore other HIF independent pathways such as calcium channel regulation and iron bioavailability as explored in Chapter 5 and possibly investigate the inhibitory feedback effects of HIF- 3α in vascular SMCs (Augstein et al., 2011). It would also be interesting to investigate the role of the more mature $CD16^+$ monocyte subset in PAH with regards to cell number and function. This monocyte subset is thought to have a more patrolling and regulatory role while $CD14^+$ monocytes are first recruited to sites of inflammation and injury. However, no work has been done to investigate differential monocyte subset recruitment to vessels without inflammation so it is not known if either subset has a regulatory role in vessel homeostasis but an inflammatory role with stimulus.

5 GENERAL DISCUSSION

PAH is a devastating vascular disease characterised by SMC hypertrophy and hyperplasia as well as endothelial cell dysregulation. Concentric lesion formation leads to narrowing and occlusion of the small pulmonary arteries leading to increased right ventricular pressure and eventually right heart failure. Endothelial aberrant growth can also lead to lesion development in the form of plexiform lesions. These have been found to have increased inflammatory cell infiltrates as well as inflammatory cytokines themselves being increased in serum from patients with the disease. The remodelled pulmonary vessels also stain positive for HIF which is a key mediator for myeloid cell function and an indirect indicator that these areas are hypoxic (although the exact oxygen tensions of the vessels are unknown). For these reasons I wanted to investigate SMC and monocyte co-cultures in normoxia and hypoxia with the hypothesis that monocytes can regulate SMC inhibition in a HIF dependant manner. Further to this to determine if IPAH patient monocytes and SMCs behave differentially to their healthy counterparts.

My data showed that SMC number increased in hypoxia compared to normoxia and that this increase was specific to the pulmonary vasculature as aortic vascular SMCs were unaffected by hypoxia. Despite the robustness of my cell count data it is still not known if increase in SMC number is due to proliferation. Using TUNEL assays it was established that differences in total hypoxic SMC counts with and without monocytes were not attributed to increase in apoptosis with hypoxic co-culture. However, to confirm differences in total cell counts were due to proliferation further work could be done. A traditional assay used for determining proliferation is measuring radioisotope labelled thymidine incorporation. During cell division labelled thymidine is incorporated into replicated DNA allowing the divided cells to be counted on scintillation β counters. Having specific normoxic radioisotope work areas and only one hypoxic workstation the ability to carry out both hypoxic and radioactive work was restricted. Another assay which works on the same principle to radio labelled thymidine is 5-bromo-2-deoxyuridine (BrdU)

incorporation. Fluorescent antibody labelling of BrdU in permeabilised SMCs can then be measured on flow cytometry with propidium iodide staining which labels all DNA to calculate proportions of proliferating cells. A further flow based assay is CellTrace™ CFSE or carboxyfluorescein diacetate, succinimidyl ester. This compound enters cells where, once internalised, is cleaved to give a fluorescent product. This fluorescence is then halved when the cell divides allowing visualisation of division peaks representing each generation on a flow cytometer. Seeing as the increase in SMC number by hypoxia compared to normoxia is less than two fold the division index was too low to calculate division and thus proliferation by these methods. However, by showing there is not an increase in apoptosis in hypoxic co-cultures it is unlikely that increase in cell number is not due to SMC proliferation.

Importantly healthy donor monocytes were able to inhibit hypoxic increase in cell number independently to direct cell contact and monocyte hypoxia. Suggesting monocytes are constitutively releasing a factor to regulate vascular tone. The initiating factor of IPAH development has not been identified but it is known that pro-inflammatory cytokines are increased in disease. It would be interesting to establish if circulating monocytes have protective role on vascular homeostasis which is altered upon disease onset or if the circulating myeloid cell baseline phenotypes are different in people predisposed to the disease. Due to the small number of monocytes (5,000) used in each co-culture experiment it was difficult to recover monocytes to phenotype post co-culture. The cell permeable dye alamarBlue® was used to determine relative metabolic activity of monocytes post-culture, however, due to this redox indicator being hypoxia sensitive it was not a reliable assay. Monocyte survival was explored using TUNEL assay on transwell fixed monocytes but again small numbers of monocytes used in each experiment meant reliable counts were unable to be obtained. One way to combat this problem would be to upscale the experiment using larger wells and transwell inserts which could be an area of future work to phenotype monocytes after co-culture.

Analysis of culture supernatants for proinflammatory cytokines and disease linked factors was unable to yield a potential factor which monocyte inhibition

of hypoxic SMC proliferation may be attributed to. If monocytes are releasing a molecule which is inhibiting hypoxic SMC proliferation then it would be expected that supernatants from hypoxic SMC mono- and co-cultures would have differential compound content. If time allowed culture supernatants could be analysed by mass spectrometry in order to identify differences in hypoxic monoculture and hypoxic co-culture supernatants. Having focused on ELISA analysis we have not explored the whether non-protein factors may be eliciting monocyte inhibition of hypoxic SMC proliferation. By boiling culture supernatants it is possible to denature proteins therefore if monocyte inhibition of SMC proliferation is still observed it may be attributed to a lipid or another non-protein factor. However, cytokine profiles were not initially investigated to identify potential target molecules. Profiles were used to phenotype the co-culture model in order to directly compare to published work in aortic vascular SMCs.

HIV is a retrovirus which infects immune cells leading to acquired immunodeficiency syndrome. As therapeutics and prognosis have improved for HIV patients, an increase in HIV induced pulmonary hypertension has been observed in patients with chronic HIV load. The underlying mechanisms of this disease subset are yet to be established however, pathogenesis follows similar characteristics to other subsets of PAH (Lederman, 2008). With this in mind instead of using the bacterial wall product and TLR4 agonist to maximise cytokine responses in monocyte and SMC cultures it may be useful to use a TLR3 agonist. Unlike TLR4 which responds to bacterial ligands, TLR3 recognises double stranded DNA as produced by viruses. Polyinosinic-polycytidylic acid also known as poly(I:C) is such an agonist. Poly(I:C) is a viral mimic of double stranded DNA which activates TLR3 on SMCs. This could be an area of future work and would lead to better understanding of the development of HIV induced PAH.

A promising pathway involved in inducing SMC proliferation that can be altered by monocytes is the IL- 1 pathway. My data showed exogenous IL- 1ra can modulate hypoxic SMC proliferation potentially implicating IL- 1ra as mediating monocyte inhibition of SMC proliferation. However, further exploration found

IL- 1ra could block DMOG induced SMC proliferation. Having found that monocytes were unable to block DMOG induced SMC proliferation and being unable to detect any IL- 1ra in monocyte culture supernatants it is unlikely that monocyte inhibition of SMC proliferation is due to IL- 1ra. Although monocytes were able to inhibit SMC proliferation, the specificity of monocyte inhibition to hypoxic induced proliferation was yet to be identified. With this in mind PDGF was used to stimulate SMC proliferation. Seeing as monocytes were unable to inhibit both growth factor and DMOG induced SMC proliferation it is likely that monocyte inhibition of proliferation is specific to hypoxic induced SMC proliferation.

My key finding is that IPAH patient monocytes are unable to inhibit hypoxic SMC proliferation suggesting that circulating monocytes have an altered phenotype in disease. This is an important finding because it seems to be specific for IPAH. Monocytes obtained from patients with PAH associated with an immune disorder, systemic sclerosis (SSc), are equally able to inhibit hypoxic SMC proliferation as healthy monocytes. It is important to note that all IPAH patients were treatment naive but this was not the case for SSc associated PAH patients. SSc is a chronic disease and many patients have progressed disease before the onset of PAH therefore obtaining a treatment naive cohort is difficult. If time allowed I would have liked to obtain more patients and better age and sex match the SSc associated PAH patients, IPAH patients and healthy volunteer cohorts. To further explore the theory that the circulating monocytes from IPAH patients are altered compared to disease and healthy controls, functional analysis could be done on the freshly isolated cells. Small yields of monocytes obtained after peripheral blood isolation prevented extensive phenotyping to be carried out. Despite this both RNA and protein from each patient has been stored with analysis postponed until potential targets to investigate are identified. One suggestion would be to investigate protein expression of both $CD14^+$ and $CD16^+$ markers. It is not known which subset predominates in IPAH or if circulating numbers of either subset is altered in disease. Moreover, it would be interesting to know if subset numbers are altered between each subgroup of PAH.

Not only do monocytes display an altered phenotype in IPAH but also IPAH SMCs are found to be hyper proliferative compared to their healthy counterparts. Patient SMCs showed enhanced proliferation in serum which was unaltered in hypoxia or by monocyte co-culture emphasising the importance of phenotyping diseased SMCs post-culture. Examination of freshly thawed cells showed that IPAH SMCs stained positive for the contractile SMC indication β-smooth muscle cell actin. Unfortunately post-culture cells were lifted for cell counts or lysed therefore preventing identification of SMC phenotype post-culture. IPAH patient SMC proliferation is likely due to BMPR2 dysregulation coupled with increased TGF-β pathway activation as these cells have a mutated BMPR2 so the balance between both pathways will be altered. These data suggest that both the BMPR2 and TGF-β pathway are important for controlling SMC proliferation but that these pathways act independently of hypoxic induced SMC proliferation. Also these pathways are unlikely to be the cause of monocyte inhibition of SMC proliferation as monocytes cannot modulate patient SMC proliferation.

HIF dependence of SMC proliferation was investigated using siRNA targeting HIF- 1α, HIF- 2α or both together. My data showed that hypoxic SMC proliferation was independent of the HIF pathway but I am yet to establish if monocyte inhibition of hypoxic SMC proliferation is HIF dependant. Being unable to transfect human monocytes themselves this question is more difficult to address. One possible solution would be to use an *in vivo* transgenic murine model. With the availability of a myeloid specific HIF knock out mouse it is possible to culture pulmonary arterial SMCs in hypoxia and normoxia with and without HIF knockout monocytes. However, the difficulty arises with human and mouse interactions. It is arguable how biologically relevant mouse monocytes are to human SMCs. Ideally mouse pulmonary arterial SMCs could be cultured and found to respond to hypoxia as human SMCs. Thus co-cultures of both mouse monocytes and SMCs could be phenotyped. Moreover murine models of PAH have been difficult to create with mouse vessels being particularly resistant to vascular remodelling as characteristic of PAH.

Therefore the question of HIF dependence of monocyte inhibition of SMC proliferation is still unknown.

Although it has been much documented that hypoxia induces SMC proliferation the mechanism is still unknown. It is known that hypoxia impairs potassium channel function. Dysregulation of voltage dependant potassium channels (K_v) leads to decreased potassium influx and so release of intracellular calcium ion stores. This is perpetuated by chloride ion influx by voltage dependant chloride channels (Cl_v). As seen by growth factor induced SMC proliferation intracellular calcium has an important role in controlling SMC proliferation. To reset the balance of intracellular calcium, activity of both calcium regulated chloride channel (Cl_{Ca}) and calcium regulated potassium channel (K_{Ca}) is needed. These channels increase efflux of chloride ions and influx of potassium ions respectively. Monocytes may function to regain intracellular balance reducing hypoxic SMC proliferation in healthy SMCs but much work is needed to explore this option. Patch-clamp techniques could be used to identify membrane potentials and channel activity in SMC monocultures and monocyte supernatant treated SMC monocultures in both oxygen tensions to identify differences in channel functions.

Interestingly IPAH patients have been found to be deficient in iron with reduced serum ferritin. This is also true of other forms of PAH such as associated with Chuvash polycythemia and secondary pulmonary hypertension to congenital heart disease (Sable, 2012). The importance of iron and hypoxia in pulmonary hypertension was emphasised by work from Smith *et al* who found healthy volunteers exposed to 8 hours of isocarpic hypoxia developed increased pulmonary arterial pressure. Infusion of 4 g per 70 kg body mass of an iron chelator (desferrioxamine mesylate) for 8 hours exacerbated pulmonary arterial pressures upon hypoxic exposure. But supplemented iron in the form of 200 mg iron(III)- hydroxide sucrose significantly reduced pulmonary arterial pressures upon hypoxia exposure (Smith, 2008). An essential co-factor for the HIF- α regulators prolyl hydroxylases (PHDs) is iron so deficiency may constitute increase HIF activity. Although systemic vascular HIF activity has not been measured in IPAH patients, an increase in HIF expression both at the

mRNA and protein level is seen in IPAH patient diseased vessels. If monocytes are releasing iron and iron reduces vascular remodelling thus reduces SMC proliferation then this pathway may be responsible for monocyte inhibition of SMC proliferation. This theory could be explained by monocyte expression of CD163, a haemoglobin scavenger receptor. The CD163 receptor allows monocytes to breakdown haemoglobin into heme leading to subsequent isolation of iron by heme oxidase (Kong, 2012). Seeing as monocyte isolations are not 100 % pure, residual red blood cells may be recycled by monocytes allowing release of iron. This theory could be explored by supplementing hypoxic SMC culture with exogenous iron in order to establish the effects of iron on hypoxic SMC proliferation.

In conclusion I found that pulmonary arterial SMCs proliferate to hypoxia and that this is inhibited by healthy monocyte co-culture in a HIF and contact independent manner. Further to this, IPAH patient monocytes and SMCs had an altered phenotype compared to healthy controls. Much is unknown with regards to the development of IPAH therefore this work is important for discovering insights to disease progression. Better understanding of the disease could lead to development of better targeted therapeutics in a view to improve patient prognosis.

6 BIBLIOGRAPHY

AHMED, F. 2010. Profile of Gregg L. Semenza. *Proceedings of the National Academy of Sciences,* 107**,** 14521-14523.

AHN, Y. T., KIM, Y. M., ADAMS, E., LYU, S. C., ALVIRA, C. M. & CORNFIELD, D. N. 2012. Hypoxia-inducible factor-1alpha regulates KCNMB1 expression in human pulmonary artery smooth muscle cells. *Am J Physiol Lung Cell Mol Physiol.* 302, (3), L352-L359.

ALDRED, M. A., VIJAYAKRISHNAN, J., JAMES, V., SOUBRIER, F., GOMEZ-SANCHEZ, M. A., MARTENSSON, G., GALIE, N., MANES, A., CORRIS, P., SIMONNEAU, G., HUMBERT, M., MORRELL, N. W. & TREMBATH, R. C. 2006. BMPR2 gene rearrangements account for a significant proportion of mutations in familial and idiopathic pulmonary arterial hypertension. *Hum Mutat,* 27**,** 212-3.

ARCHER, S. L., SOUIL, E., DINH-XUAN, A. T., SCHREMMER, B., MERCIER, J. C., EL YAAGOUBI, A., NGUYEN-HUU, L., REEVE, H. L. & HAMPL, V. 1998. Molecular identification of the role of voltage-gated K+ channels, Kv1.5 and Kv2.1, in hypoxic pulmonary vasoconstriction and control of resting membrane potential in rat pulmonary artery myocytes. *J Clin Invest,* 101**,** 2319-30.

ASOSINGH, K., ALDRED, M. A., VASANJI, A., DRAZBA, J., SHARP, J., FARVER, C., COMHAIR, S. A., XU, W., LICINA, L., HUANG, L., ANAND-APTE, B., YODER, M. C., TUDER, R. M. & ERZURUM, S. C. 2008. Circulating angiogenic precursors in idiopathic pulmonary arterial hypertension. *Am J Pathol.* 172, (3), 615-627.

ATKINSON, C., STEWART, S., UPTON, P. D., MACHADO, R., THOMSON, J. R., TREMBATH, R. C. & MORRELL, N. W. 2002. Primary pulmonary hypertension is associated with reduced pulmonary vascular expression of type II bone morphogenetic protein receptor. *Circulation,* 105**,** 1672-8.

AUGSTEIN, A., POITZ, D. M., BRAUN-DULLAEUS, R. C., STRASSER, R. H. & SCHMEISSER, A. 2011. Cell-specific and hypoxia-dependent regulation of human HIF-3alpha: inhibition of the expression of HIF target genes in vascular cells. *Cell Mol Life Sci,* 68**,** 2627-42.

BALABANIAN, K., FOUSSAT, A., DORFMULLER, P., DURAND-GASSELIN, I., CAPEL, F., BOUCHET-DELBOS, L., PORTIER, A., MARFAING-KOKA, A., KRZYSIEK, R., RIMANIOL, A. C., SIMONNEAU, G., EMILIE, D. & HUMBERT, M. 2002. CX(3)C chemokine fractalkine in pulmonary arterial hypertension. *Am J Respir Crit Care Med,* 165**,** 1419-25.

BARST, R. J., MCGOON, M. D., ELLIOTT, C. G., FOREMAN, A. J., MILLER, D. P. & IVY, D. D. 2012. Survival in childhood pulmonary arterial hypertension: insights from the registry to evaluate early and long-term pulmonary arterial hypertension disease management. *Circulation.* 125, (1), 113-22.

BATH, P. M., GLADWIN, A. M. & MARTIN, J. F. 1991. Human monocyte characteristics are altered in hypercholesterolaemia. *Atherosclerosis,* 90**,** 175-81.

BEPPU, H., ICHINOSE, F., KAWAI, N., JONES, R. C., YU, P. B., ZAPOL, W. M., MIYAZONO, K., LI, E. & BLOCH, K. D. 2004. BMPR-II heterozygous mice have mild pulmonary hypertension and an impaired pulmonary vascular remodeling response to prolonged hypoxia. *Am J Physiol Lung Cell Mol Physiol.* 287, (6), L1241-47.

BERG, J. M., TYMOCZKO, J. L. & STRYER, L. 2006. Section: Metabolism, chapter 18 oxidative phosphorylation, chapter 16 glycolysis *In:* HADLER, G. L. (ed.) *Biochemistry 6th edition.* New York, NY, USA: Tenney, S.

BONNET, S., DUMAS-DE-LA-ROQUE, E., BEGUERET, H., MARTHAN, R., FAYON, M., DOS SANTOS, P., SAVINEAU, J. P. & BAULIEU, E. E. 2003. Dehydroepiandrosterone

(DHEA) prevents and reverses chronic hypoxic pulmonary hypertension. *Proc Natl Acad Sci U S A.* 100, (16), 9488-93.

BORREGAARD, N. & HERLIN, T. 1982. Energy metabolism of human neutrophils during phagocytosis. *J Clin Invest,* 70**,** 550-7.

BOWERS, R., COOL, C., MURPHY, R. C., TUDER, R. M., HOPKEN, M. W., FLORES, S. C. & VOELKEL, N. F. 2004. Oxidative stress in severe pulmonary hypertension. *Am J Respir Crit Care Med.* 169, (6), 764-7.

BRUSSELMANS, K., COMPERNOLLE, V., TJWA, M., WIESENER, M. S., MAXWELL, P. H., COLLEN, D. & CARMELIET, P. 2003. Heterozygous deficiency of hypoxia-inducible factor-2alpha protects mice against pulmonary hypertension and right ventricular dysfunction during prolonged hypoxia. *J Clin Invest,* 111**,** 1519-27.

BULL, T. M., COLDREN, C. D., MOORE, M., SOTTO-SANTIAGO, S. M., PHAM, D. V., NANA-SINKAM, S. P., VOELKEL, N. F. & GERACI, M. W. 2004. Gene microarray analysis of peripheral blood cells in pulmonary arterial hypertension. *Am J Respir Crit Care Med.* 170, (8), 911-9.

BURKE, B., GIANNOUDIS, A., CORKE, K. P., GILL, D., WELLS, M., ZLEGLER-HEITBROCK, L., LEWIS, C. E., 2003. Hypoxia-induced gene expression in human macrophages. *Am J Pathol.,* 163, 1233-1243.

BURTON, V. J., HOLMES, A. M., CIUCLAN, L. I., ROBINSON, A., ROGER, J. S., JARAI, G., PEARCE, A. C. & BUDD, D. C. 2011. Attenuation of leukocyte recruitment via CXCR1/2 inhibition stops the progression of PAH in mice with genetic ablation of endothelial BMPR-II. *Blood.* 118, (17), 4750-8.

CARMELIET, P., FERREIRA, V., BREIER, G., POLLEFEYT, S., KIECKENS, L., GERTSENSTEIN, M., FAHRIG, M., VANDENHOECK, A., HARPAL, K., EBERHARDT, C., DECLERCQ, C., PAWLING, J., MOONS, L., COLLEN, D., RISAU, W. & NAGY, A. 1996. Abnormal blood vessel development and lethality in embryos lacking a single VEGF allele. *Nature,* 380**,** 435-9.

CHAMBERLAIN, J., EVANS, D., KING, A., DEWBERRY, R., DOWER, S., CROSSMAN, D. & FRANCIS, S. 2006. Interleukin-1beta and signaling of interleukin-1 in vascular wall and circulating cells modulates the extent of neointima formation in mice. *Am J Pathol,* 168**,** 1396-403.

CHAVAKIS, E., CHOI, E. Y. & CHAVAKIS, T. 2009. Novel aspects in the regulation of the leukocyte adhesion cascade. *Thromb Haemost.* 102, (2), 191-7.

CHAZOVA, I., LOYD, J. E., ZHDANOV, V. S., NEWMAN, J. H., BELENKOV, Y. & MEYRICK, B. 1995. Pulmonary artery adventitial changes and venous involvement in primary pulmonary hypertension. *Am J Pathol,* 146**,** 389-97.

CHEN, D., ZHAO, M. & MUNDY, G. R. 2004. Bone morphogenetic proteins. *Growth Factors.* 22, (4), 233-41.

CHEN, Y. R., DAI, A. G., HU, R. C. & JIANG, Y. L. 2006. Differential and reciprocal regulation between hypoxia-inducible factor-alpha subunits and their prolyl hydroxylases in pulmonary arteries of rat with hypoxia-induced hypertension. *Acta Biochim Biophys Sin (Shanghai),* 38**,** 423-34.

CHIDA, A., SHINTANI, M., NAKAYAMA, T., FURUTANI, Y., HAYAMA, E., INAI, K., SAJI, T., NONOYAMA, S. & NAKANISHI, T. 2012. Missense Mutations of the BMPR1B (ALK6) Gene in Childhood Idiopathic Pulmonary Arterial Hypertension. *Circ J.* 76, (7), 1804.

CHO, W. K., LEE, C. M., KANG, M. J., HUANG, Y., GIORDANO, F. J., LEE, P. J., TROW, T. K., HOMER, R. J., SESSA, W. C., ELIAS, J. A. & LEE, C. G. 2013. IL-13 receptor alpha2-arginase 2 pathway mediates IL-13-induced pulmonary hypertension. *Am J Physiol Lung Cell Mol Physiol.* 304, (2), L112-24.

CHOWDHURY, R., MCDONOUGH, M. A., MECINOVIC, J., LOENARZ, C., FLASHMAN, E., HEWITSON, K. S., DOMENE, C. & SCHOFIELD, C. J. 2009. Structural basis for

binding of hypoxia-inducible factor to the oxygen-sensing prolyl hydroxylases. *Structure.* 17, (7), 981-9.

COGAN, J., AUSTIN, E., HEDGES, L., WOMACK, B., WEST, J., LOYD, J. & HAMID, R. 2012. Role of BMPR2 alternative splicing in heritable pulmonary arterial hypertension penetrance. *Circulation.* 126, (15), 1907-16.

COGAN, J. D., PAUCIULO, M. W., BATCHMAN, A. P., PRINCE, M. A., ROBBINS, I. M., HEDGES, L. K., STANTON, K. C., WHEELER, L. A., PHILLIPS, J. A., 3RD, LOYD, J. E. & NICHOLS, W. C. 2006. High frequency of BMPR2 exonic deletions/duplications in familial pulmonary arterial hypertension. *Am J Respir Crit Care Med.* 174, (5), 590-8.

COOL, C. D., STEWART, J. S., WERAHERA, P., MILLER, G. J., WILLIAMS, R. L., VOELKEL, N. F. & TUDER, R. M. 1999. Three-dimensional reconstruction of pulmonary arteries in plexiform pulmonary hypertension using cell-specific markers. Evidence for a dynamic and heterogeneous process of pulmonary endothelial cell growth. *Am J Pathol,* 155**,** 411-9.

COOPER, A. L. & BEASLEY, D. 1999. Hypoxia stimulates proliferation and interleukin-1alpha production in human vascular smooth muscle cells. *Am J Physiol,* 277**,** H1326-37.

CRAMER, T., YAMANISHI, Y., CLAUSEN, B. E., FORSTER, I., PAWLINSKI, R., MACKMAN, N., HAASE, V. H., JAENISCH, R., CORR, M., NIZET, V., FIRESTEIN, G. S., GERBER, H. P., FERRARA, N. & JOHNSON, R. S. 2003. HIF-1alpha is essential for myeloid cell-mediated inflammation. *Cell.* 112, (5), 645-57.

DAVIES, A. O. 1986. Effects of endogenous redox-active compounds on coupling of human beta 2-adrenergic receptors. *Am J Med Sci,* 292**,** 257-63.

DEMPSEY, E. C., DAS, M., FRID, M. G., XU, Y. & STENMARK, K. R. 1998. Hypoxic growth of bovine pulmonary artery smooth muscle cells: dependence on synergy, heterogeneity, and injury-induced phenotypic change. *Chest,* 114**,** 29S-30S.

DEMPSEY, E. C., MCMURTRY, I. F., O'BRIEN, R. F. 1991. Protein kinase C activation allows pulmonary artery smooth muscle cells to proliferate to hypoxia. *AJP-Lung Physiol,* 260, (2), L136-L145.

DESSOUROUX, A., AKWA, Y. & BAULIEU, E. E. 2008. DHEA decreases HIF-1alpha accumulation under hypoxia in human pulmonary artery cells: potential role in the treatment of pulmonary arterial hypertension. *J Steroid Biochem Mol Biol.* 109, (1-2), 81-9.

DORFMULLER, P., CHAUMAIS, M. C., GIANNAKOULI, M., DURAND-GASSELIN, I., RAYMOND, N., FADEL, E., MERCIER, O., CHARLOTTE, F., MONTANI, D., SIMONNEAU, G., HUMBERT, M. & PERROS, F. 2011. Increased oxidative stress and severe arterial remodeling induced by permanent high-flow challenge in experimental pulmonary hypertension. *Respir Res.* 12, 119.

DORFMULLER, P., PERROS, F., BALABANIAN, K. & HUMBERT, M. 2003. Inflammation in pulmonary arterial hypertension. *Eur Respir J,* 22**,** 358-63.

EDDAHIBI, S., FABRE, V., BONI, C., MARTRES, M. P., RAFFESTIN, B., HAMON, M. & ADNOT, S. 1999. Induction of serotonin transporter by hypoxia in pulmonary vascular smooth muscle cells. Relationship with the mitogenic action of serotonin. *Circ Res,* 84**,** 329-36.

ELBARGHATI, L., MURDOCH, C., LEWIS. C. E., 2008. Effects of hypoxia on transcription factor expression in human monocytes and macrophages. *Immunobiol.* 213, 899-908.

EMERY, J. G., MCDONNELL, P., BURKE, M. B., DEEN, K. C., LYN, S., SILVERMAN, C., DUL, E., APPELBAUM, E. R., EICHMAN, C., DIPRINZIO, R., DODDS, R. A., JAMES, I. E., ROSENBERG, M., LEE, J. C. & YOUNG, P. R. 1998. Osteoprotegerin is a receptor for the cytotoxic ligand TRAIL. *J Biol Chem,* 273**,** 14363-7.

EUBANK, T. D., RODA, J. M., LIU, H., O'NEIL, T. & MARSH, C. B. 2011. Opposing roles for HIF-1alpha and HIF-2alpha in the regulation of angiogenesis by mononuclear phagocytes. *Blood.* 117, (1), 323-32.

FARHA, S., ASOSINGH, K., XU, W., SHARP, J., GEORGE, D., COMHAIR, S., PARK, M., TANG, W. H., LOYD, J. E., THEIL, K., TUBBS, R., HSI, E., LICHTIN, A. & ERZURUM, S. C. 2011. Hypoxia-inducible factors in human pulmonary arterial hypertension: a link to the intrinsic myeloid abnormalities. *Blood*. 117, (13), 3485-93.

FARTOUKH, M., EMILIE, D., LE GALL, C., MONTI, G., SIMONNEAU, G. & HUMBERT, M. 1998. Chemokine macrophage inflammatory protein-1alpha mRNA expression in lung biopsy specimens of primary pulmonary hypertension. *Chest,* 114**,** 50S-51S.

FERRARA, N., CARVER-MOORE, K., CHEN, H., DOWD, M., LU, L., O'SHEA, K. S., POWELL-BRAXTON, L., HILLAN, K. J. & MOORE, M. W. 1996. Heterozygous embryonic lethality induced by targeted inactivation of the VEGF gene. *Nature,* 380**,** 439-42.

FOGG, D. K., SIBON, C., MILED, C., JUNG, S., AUCOUTURIER, P., LITTMAN, D. R., CUMANO, A. & GEISSMANN, F. 2006. A clonogenic bone marrow progenitor specific for macrophages and dendritic cells. *Science.* 311, (5757), 83-7.

FREYHAUS, H., DAGNELL, M., LEUCHS, M., VANTLER, M., BERGHAUSEN, E. M., CAGLAYAN, E., WEISSMANN, N., DAHAL, B. K., SCHERMULY, R. T., OSTMAN A., KAPPERT, K., ROSENKRANS, S. 2011. Hypoxia enhanses platelet-derived growth factor signaling in the pulmonary vasculature by down-regulation of protein tyrosine phosphatases. *Am J Resp Crit Care Med,* 183, (8), 1092-102.

FRID, M. G., ALDASHEV, A. A., DEMPSEY, E. C. & STENMARK, K. R. 1997. Smooth muscle cells isolated from discrete compartments of the mature vascular media exhibit unique phenotypes and distinct growth capabilities. *Circ Res,* 81**,** 940-52.

FRID, M. G., BRUNETTI, J. A., BURKE, D. L., CARPENTER, T. C., DAVIE, N. J., REEVES, J. T., ROEDERSHEIMER, M. T., VAN ROOIJEN, N. & STENMARK, K. R. 2006. Hypoxia-induced pulmonary vascular remodeling requires recruitment of circulating mesenchymal precursors of a monocyte/macrophage lineage. *Am J Pathol.* 168, (2), 659-69.

FRID, M. G., LI, M., GNANASEKHARAN, M., BURKE, D. L., FRAGOSO, M., STRASSHEIM, D., SYLMAN, J. L. & STENMARK, K. R. 2009. Sustained hypoxia leads to the emergence of cells with enhanced growth, migratory, and promitogenic potentials within the distal pulmonary artery wall. *Am J Physiol Lung Cell Mol Physiol.* 297, (6), L1059-72.

GAINE, S. P. & RUBIN, L. J. 1998. Primary pulmonary hypertension. *Lancet,* 352**,** 719-25.

GALE, D. P., HARTEN, S. K., REID, C. D., TUDDENHAM, E. G. & MAXWELL, P. H. 2008. Autosomal dominant erythrocytosis and pulmonary arterial hypertension associated with an activating HIF2 alpha mutation. *Blood.* 112, (9), 919-21.

GEIGER, R., BERGER, R. M., HESS, J., BOGERS, A. J., SHARMA, H. S. & MOOI, W. J. 2000. Enhanced expression of vascular endothelial growth factor in pulmonary plexogenic arteriopathy due to congenital heart disease. *J Pathol.* 191, (2), 202-7.

GERTLER, J. P., PERRY, L., L'ITALIEN, G., CHUNG-WELCH, N., CAMBRIA, R. P., ORKIN, R. & ABBOTT, W. M. 1993. Ambient oxygen tension modulates endothelial fibrinolysis. *J Vasc Surg.* 18, (6), 939-45.

GLEADLE, J. M., MOLE, D. R. & PUGH, C. W. 2006. Hypoxia-inducible factors: where, when and why? *Kidney Int,* 69**,** 15-7.

HALL, S., BROGAN, P., HAWORTH, S. G. & KLEIN, N. 2009. Contribution of inflammation to the pathology of idiopathic pulmonary arterial hypertension in children. *Thorax.* 64, (9), 778-83.

HAN, D. D., WANG, Y., ZHANG, X. H., LIU, J. R. & WANG, H. L. 2012. Fluoxetine protects against monocrotaline-induced pulmonary arterial remodeling by inhibition of

hypoxia-inducible factor-1alpha and vascular endothelial growth factor. *Can J Physiol Pharmacol,* 90**,** 445-54.

HANSMANN, G., DE JESUS PEREZ, V. A., ALASTALO, T. P., ALVIRA, C. M., GUIGNABERT, C., BEKKER, J. M., SCHELLONG, S., URASHIMA, T., WANG, L., MORRELL, N. W. & RABINOVITCH, M. 2008. An antiproliferative BMP-2/PPARgamma/apoE axis in human and murine SMCs and its role in pulmonary hypertension. *J Clin Invest,* 118**,** 1846-57.

HASSOUN, P. M., PASRICHA, P. J., TEUFEL, E., LEE, S. L. & FANBURG, B. L. 1989. Hypoxia stimulates the release by bovine pulmonary artery endothelial cells of an inhibitor of pulmonary artery smooth muscle cell growth. *Am J Respir Cell Mol Biol,* 1**,** 377-84.

HENZE, A. T. & ACKER, T. 2010. Feedback regulators of hypoxia-inducible factors and their role in cancer biology. *Cell Cycle.* 9, (14), 2749-63.

HICKEY, M. M., RICHARDSON, T., WANG, T., MOSQUEIRA, M., ARGUIRI, E., YU, H., YU, Q. C., SOLOMIDES, C. C., MORRISEY, E. E., KHURANA, T. S., CHRISTOFIDOU-SOLOMIDOU, M. & SIMON, M. C. 2010. The von Hippel-Lindau Chuvash mutation promotes pulmonary hypertension and fibrosis in mice. *J Clin Invest,* 120**,** 827-39.

HILGENDORF, I. & SWIRSKI, F. K. 2012. Making a difference: monocyte heterogeneity in cardiovascular disease. *Curr Atheroscler Rep,* 14**,** 450-9.

HILL, J. M., ZALOS, G., HALCOX, J. P., SCHENKE, W. H., WACLAWIW, M. A., QUYYUMI, A. A. & FINKEL, T. 2003. Circulating endothelial progenitor cells, vascular function, and cardiovascular risk. *N Engl J Med.* 348, (7), 593-600.

HIROSE, S., HOSODA, Y., FURUYA, S., OTSUKI, T. & IKEDA, E. 2000. Expression of vascular endothelial growth factor and its receptors correlates closely with formation of the plexiform lesion in human pulmonary hypertension. *Pathol Int.* 50, (6), 472-9.

HOFBAUER, L. C., LACEY, D. L., DUNSTAN, C. R., SPELSBERG, T. C., RIGGS, B. L. & KHOSLA, S. 1999. Interleukin-1beta and tumor necrosis factor-alpha, but not interleukin-6, stimulate osteoprotegerin ligand gene expression in human osteoblastic cells. *Bone.* 25, (30), 255-9.

HOWARD, L. S., CROSBY, A., VAUGHAN, P., SOBOLEWSKI, A., SOUTHWOOD, M., FOSTER, M. L., CHILVERS, E. R. & MORRELL, N. W. 2012. Distinct responses to hypoxia in subpopulations of distal pulmonary artery cells contribute to pulmonary vascular remodeling in emphysema. *Pulm Circ.* 2, (2), 241-9.

HUANG, J., WOLK, J. H., GEWITZ, M. H. & MATHEW, R. 2012. Caveolin-1 expression during the progression of pulmonary hypertension. *Exp Biol Med* 237, (8), 956-65.

HUMBERT, M., MONTI, G., BRENOT, F., SITBON, O., PORTIER, A., GRANGEOT-KEROS, L., DUROUX, P., GALANAUD, P., SIMONNEAU, G. & EMILIE, D. 1995. Increased interleukin-1 and interleukin-6 serum concentrations in severe primary pulmonary hypertension. *Am J Respir Crit Care Med,* 151**,** 1628-31.

HUMBERT, M., MORRELL, N. W., ARCHER, S. L., STENMARK, K. R., MACLEAN, M. R., LANG, I. M., CHRISTMAN, B. W., WEIR, E. K., EICKELBERG, O., VOELKEL, N. F. & RABINOVITCH, M. 2004. Cellular and molecular pathobiology of pulmonary arterial hypertension. *J Am Coll Cardiol,* 43**,** 13S-24S.

IKEDA, U., IKEDA, M., OOHARA, T., KANO, S. & YAGINUMA, T. 1990. Mitogenic action of interleukin-1 alpha on vascular smooth muscle cells mediated by PDGF. *Atherosclerosis,* 84**,** 183-8.

IRANI, K., XIA, Y., ZWEIER, J. L., SOLLOTT, S. J., DER, C. J., FEARON, E. R., SUNDARESAN, M., FINKEL, T. & GOLDSCHMIDT-CLERMONT, P. J. 1997. Mitogenic signaling mediated by oxidants in Ras-transformed fibroblasts. *Science,* 275**,** 1649-52.

ITOH, T., NAGAYA, N., ISHIBASHI-UEDA, H., KYOTANI, S., OYA, H., SAKAMAKI, F., KIMURA, H. & NAKANISHI, N. 2006. Increased plasma monocyte

chemoattractant protein-1 level in idiopathic pulmonary arterial hypertension. *Respirology.* 11, (2), 158-63.

JAMES, W. R. & THOMAS, A. J. 1968. The effect of hypoxia on the heart and pulmonary arterioles of mice. *Cardiovasc Res,* 2**,** 278-83.

JIANG, B., XU, S., BRECHER, P., COHEN, R. A. 2002. Growth factors enhance interleukin-1 beta-induced persistant activation of nuclear factor- kappa B in rat vascular smooth muscle cells. *Arterioscler Thromb Vasc Biol,* 22, (11), 1811-1816.

KEMPNER, W. 1939. THE NATURE OF LEUKEMIC BLOOD CELLS AS DETERMINED BY THEIR METABOLISM. *J Clin Invest,* 18**,** 291-300.

KIM, H. J., KIM, M. Y., HWANG, J. S., LEE, J. H., CHANG, K. C., KIM, J. H., HAN, C. W. & SEO, H. G. 2010. PPARdelta inhibits IL-1beta-stimulated proliferation and migration of vascular smooth muscle cells via up-regulation of IL-1Ra. *Cell Mol Life Sci,* 67**,** 2119-30.

KOGA, S., OGAWA, S., KUWABARA, K., BRETT, J., LEAVY, J. A., RYAN, J., KOGA, Y., PLOCINSKI, J., BENJAMIN, W., BURNS, D. K. & ET AL. 1992. Synthesis and release of interleukin 1 by reoxygenated human mononuclear phagocytes. *J Clin Invest,* 90**,** 1007-15.

KREISEL, D., NAVA, R. G., LI, W., ZINSELMEYER, B. H., WANG, B., LAI, J., PLESS, R., GELMAN, A. E., KRUPNICK, A. S. & MILLER, M. J. 2010. In vivo two-photon imaging reveals monocyte-dependent neutrophil extravasation during pulmonary inflammation. *Proc Natl Acad Sci* 107, (42), 18073-8.

KROTOVA, K., PATEL, J. M., BLOCK, E. R. & ZHARIKOV, S. 2010. Hypoxic upregulation of arginase II in human lung endothelial cells. *Am J Physiol Cell Physiol.* 299, (6), C1541-8.

KUHTREIBER, W. M., LANZA, R. P., BEYER, A. M., KIRKLAND, K. S. & CHICK, W. L. 1993. Relationship between insulin secretion and oxygen tension in hybrid diffusion chambers. *ASAIO J,* 39**,** M247-51.

LAIRD, A. D., CHRISTENSEN, J. G., LI, G., CARVER, J., SMITH, K., XIN, X., MOSS, K. G., LOUIE, S. G., MENDEL, D. B. & CHERRINGTON, J. M. 2002. SU6668 inhibits Flk-1/KDR and PDGFRbeta in vivo, resulting in rapid apoptosis of tumor vasculature and tumor regression in mice. *FASEB J.* 16, (7), 681-90.

LARSEN, K. O., YNDESTAD, A., SJAASTAD, I., LOBERG, E. M., GOVERUD, I. L., HALVORSEN, B., JIA, J., ANDREASSEN, A. K., HUSBERG, C., JONASSON, S., LIPP, M., CHRISTENSEN, G., AUKRUST, P. & SKJONSBERG, O. H. 2011. Lack of CCR7 induces pulmonary hypertension involving perivascular leukocyte infiltration and inflammation. *Am J Physiol Lung Cell Mol Physiol.* 301, (1), L50-9.

LAWRIE, A., HAMEED, A. G., CHAMBERLAIN, J., ARNOLD, N., KENNERLEY, A., HOPKINSON, K., PICKWORTH, J., KIELY, D. G., CROSSMAN, D. C. & FRANCIS, S. E. 2011. Paigen diet-fed apolipoprotein E knockout mice develop severe pulmonary hypertension in an interleukin-1-dependent manner. *Am J Pathol.* 179, (4), 1693-705.

LEVENE, G. M. M. 1912. The action of leucocytes on glucose. Journal Biological Chemistry , 11, 361-370a.

LI, Q. F., WANG, X. R., YANG, Y. W. & LIN, H. 2006. Hypoxia upregulates hypoxia inducible factor (HIF)-3alpha expression in lung epithelial cells: characterization and comparison with HIF-1alpha. *Cell Res.* 125, (8), 1381-8.

LIU, J. Q., ERBYNN, E. M. & FOLZ, R. J. 2005. Chronic hypoxia-enhanced murine pulmonary vasoconstriction: role of superoxide and gp91phox. *Chest.* 128, (6), 5945-5965.

LUND, N., DE ASLA, R. J., CLADIS, F., PAPADAKOS, P. J. & THORBORG, P. A. 1995. Dopexamine hydrochloride in septic shock: effects on oxygen delivery and oxygenation of gut, liver, and muscle. *J Trauma,* 38**,** 767-75.

MACHADO, R. D., ALDRED, M. A., JAMES, V., HARRISON, R. E., PATEL, B., SCHWALBE, E. C., GRUENIG, E., JANSSEN, B., KOEHLER, R., SEEGER, W., EICKELBERG, O.,

OLSCHEWSKI, H., ELLIOTT, C. G., GLISSMEYER, E., CARLQUIST, J., KIM, M., TORBICKI, A., FIJALKOWSKA, A., SZEWCZYK, G., PARMA, J., ABRAMOWICZ, M. J., GALIE, N., MORISAKI, H., KYOTANI, S., NAKANISHI, N., MORISAKI, T., HUMBERT, M., SIMONNEAU, G., SITBON, O., SOUBRIER, F., COULET, F., MORRELL, N. W. & TREMBATH, R. C. 2006. Mutations of the TGF-beta type II receptor BMPR2 in pulmonary arterial hypertension. *Hum Mutat,* 27**,** 121-32.

MAGGIORINI, M. 2003. Cardio-pulmonary interactions at high altitude. Pulmonary hypertension as a common denominator. *Adv Exp Med Biol,* 543**,** 177-89.

MAKINO, Y., KANOPKA, A., WILSON, W. J., TANAKA, H. & POELLINGER, L. 2002. Inhibitory PAS domain protein (IPAS) is a hypoxia-inducible splicing variant of the hypoxia-inducible factor-3alpha locus. *J Biol Chem.* 277, (36), 32405-8.

MARTIN, I., HUMBERT, M., MARFAINQ-KOKA, A., CAPRON, F., WOLF, M., MEYER, D., SIMONNEAU, G., ANGLES-CANO, E. 2002. plasminogen activation by blood monocytes and alveolar macrophagesin primary pulmonary hypertension. *Blood Coaquil Fibrinolysis.* 13, (5), 417-422.

MASRI, F. A., COMHAIR, S. A., DOSTANIC-LARSON, I., KANEKO, F. T., DWEIK, R. A., ARROLIGA, A. C. & ERZURUM, S. C. 2008. Deficiency of lung antioxidants in idiopathic pulmonary arterial hypertension. *Clin Transl Sci.* 1, (2), 99-106.

MASSON, N., SINGLETON, R. S., SEKIRNIK, R., TRUDGIAN, D. C., AMBROSE, L. J., MIRANDA, M. X., TIAN, Y. M., KESSLER, B. M., SCHOFIELD, C. J. & RATCLIFFE, P. J. 2012. The FIH hydroxylase is a cellular peroxide sensor that modulates HIF transcriptional activity. *EMBO Rep.* 13,(3), 251-7.

MAUS, U. A., WAELSCH, K., KUZIEL, W. A., DELBECK, T., MACK, M., BLACKWELL, T. S., CHRISTMAN, J. W., SCHLONDORFF, D., SEEGER, W. & LOHMEYER, J. 2003. Monocytes are potent facilitators of alveolar neutrophil emigration during lung inflammation: role of the CCL2-CCR2 axis. *J Immunol,* 170**,** 3273-8.

MCGLOTHLIN, D. 2012. Classification of pulmonary hypertension. *Heart Fail Clin.* 8, (3), 301-17.

MCLAUGHLIN, V. V., PRESBERG, K. W., DOYLE, R. L., ABMAN, S. H., MCCRORY, D. C., FORTIN, T. & AHEARN, G. 2004. Prognosis of pulmonary arterial hypertension: ACCP evidence-based clinical practice guidelines. *Chest.* 126, 78S-92S.

MEYRICK, B. & REID, L. 1978. The effect of continued hypoxia on rat pulmonary arterial circulation. An ultrastructural study. *Lab Invest,* 38**,** 188-200.

MILHOAN, K. A., LANE, T. A. & BLOOR, C. M. 1992. Hypoxia induces endothelial cells to increase their adherence for neutrophils: role of PAF. *Am J Physiol,* 263**,** H956-62.

MORRELL, N. W., YANG, X., UPTON, P. D., JOURDAN, K. B., MORGAN, N., SHEARES, K. K. & TREMBATH, R. C. 2001. Altered growth responses of pulmonary artery smooth muscle cells from patients with primary pulmonary hypertension to transforming growth factor-beta(1) and bone morphogenetic proteins. *Circulation,* 104**,** 790-5.

MORRIS, G. E., WHYTE, M. K., MARTIN, G. F., JOSE, P. J., DOWER, S. K. & SABROE, I. 2005. Agonists of toll-like receptors 2 and 4 activate airway smooth muscle via mononuclear leukocytes. *Am J Respir Crit Care Med.* 171, (8), 814-22.

MORTON, A. C., ARNOLD, N. D., GUNN, J., VARCOE, R., FRANCIS, S. E., DOWER, S. K. & CROSSMAN, D. C. 2005. Interleukin-1 receptor antagonist alters the response to vessel wall injury in a porcine coronary artery model. *Cardiovasc Res,* 68**,** 493-501.

NAKAO, A., AFRAKHTE, M., MOREN, A., NAKAYAMA, T., CHRISTIAN, J. L., HEUCHEL, R., ITOH, S., KAWABATA, M., HELDIN, N. E., HELDIN, C. H. & TEN DIJKE, P. 1997. Identification of Smad7, a TGFbeta-inducible antagonist of TGF-beta signalling. *Nature,* 389**,** 631-5.

NISHIMAKI, T., AOTSUKA, S., KONDO, H., YAMAMOTO, K., TAKASAKI, Y., SUMIYA, M. & YOKOHARI, R. 1999. Immunological analysis of pulmonary hypertension in connective tissue diseases. *J Rheumatol,* 26**,** 2357-62.

PAK, O., ALDASHEV, A., WELSH, D. & PEACOCK, A. 2007. The effects of hypoxia on the cells of the pulmonary vasculature. *Eur Respir J,* 30**,** 364-72.

PASSLICK, B., FLIEGER, D. & ZIEGLER-HEITBROCK, H. W. 1989. Identification and characterization of a novel monocyte subpopulation in human peripheral blood. *Blood,* 74**,** 2527-34.

PENALOZA, D. & ARIAS-STELLA, J. 2007. The heart and pulmonary circulation at high altitudes: healthy highlanders and chronic mountain sickness. *Circulation.* 115, (9), 1132-46.

PERCY, M. J., ZHAO, Q., FLORES, A., HARRISON, C., LAPPIN, T. R., MAXWELL, P. H., MCMULLIN, M. F. & LEE, F. S. 2006. A family with erythrocytosis establishes a role for prolyl hydroxylase domain protein 2 in oxygen homeostasis. *Proc Natl Acad Sci U S A,* 103**,** 654-9.

PEYSSONNAUX, C., CEJUDO-MARTIN, P., DOEDENS, A., ZINKERNAGEL, A. S., JOHNSON, R. S., NIZET, V. 2007. Essential role of hypoxia inducible transcription factor 1 alpha in development of LPS-induced sepsis. *J Immunol.* 78, 7516-19.

POST, J. M., HUME, J. R., ARCHER, S. L. & WEIR, E. K. 1992. Direct role for potassium channel inhibition in hypoxic pulmonary vasoconstriction. *Am J Physiol,* 262**,** C882-90.

RAGHAVAN, A., ZHOU, G., ZHOU, Q., IBE, J. C., RAMCHANDRAN, R., YANG, Q., RACHERLA, H., RAYCHAUDHURI, P. & RAJ, J. U. 2012. Hypoxia-induced pulmonary arterial smooth muscle cell proliferation is controlled by forkhead box M1. *Am J Respir Cell Mol Biol.* 46, (4), 431-6.

RAINES, E. W., DOWER, S. K. & ROSS, R. 1989. Interleukin-1 mitogenic activity for fibroblasts and smooth muscle cells is due to PDGF-AA. *Science,* 243**,** 393-6.

ROSENZWEIG, E. B., MORSE, J. H., KNOWLES, J. A., CHADA, K. K., KHAN, A. M., ROBERTS, K. E., MCELROY, J. J., JUSKIW, N. K., MALLORY, N. C., RICH, S., DIAMOND, B. & BARST, R. J. 2008. Clinical implications of determining BMPR2 mutation status in a large cohort of children and adults with pulmonary arterial hypertension. *J Heart Lung Transplant.* 27, (6), 668-79.

RUBIN, L. J. 1997. Primary pulmonary hypertension. *N Engl J Med,* 336**,** 111-7.

RUIS J., GURNA, M., SCHACHTRUP, C., AKASSOGLOU, K., ZINKERNAGEL, A. S., NIZET, V., JOHNSON, R. S., HADDAD,, G. G., KARIN, M., 2003. NF-kappaB links innate immunity to the hypoxic response through transcriptional regulation of HIF-1 alpha. *Nature,* 453, (7198), 807-11.

SAKAO, S., TARASEVICIENE-STEWART, L., WOOD, K., COOL, C. D. & VOELKEL, N. F. 2006. Apoptosis of pulmonary microvascular endothelial cells stimulates vascular smooth muscle cell growth. *Am J Physiol Lung Cell Mol Physiol,* 291**,** L362-8.

SASU, S. & BEASLEY, D. 2000. Essential roles of IkappaB kinases alpha and beta in serum- and IL-1-induced human VSMC proliferation. *Am J Physiol Heart Circ Physiol,* 278**,** H1823-31.

SAXENA, A., RAUCH, U., BERG, K. E., ANDERSSON, L., HOLLENDER, L., CARLSSON, A. M., GOMEZ, M. F., HULTGARDH-NILSSON, A., NILSSON, J. & BJORKBACKA, H. 2011. The vascular repair process after injury of the carotid artery is regulated by IL-1RI and MyD88 signalling. *Cardiovasc Res.* 91, (2), 350-7.

SCHMEISSER, A., GARLICHS, C. D., ZHANG, H., ESKAFI, S., GRAFFY, C., LUDWIG, J., STRASSER, R. H. & DANIEL, W. G. 2001. Monocytes coexpress endothelial and macrophagocytic lineage markers and form cord-like structures in Matrigel under angiogenic conditions. *Cardiovasc Res.* 49, (3), 671-80.

SCHULTZ, K., MURTHY, V., TATRO, J. B. & BEASLEY, D. 2009. Prolyl hydroxylase 2 deficiency limits proliferation of vascular smooth muscle cells by hypoxia-

inducible factor-1{alpha}-dependent mechanisms. *Am J Physiol Lung Cell Mol Physiol.* 296, (6), L921-7.

SCHULTZ, K., RASMUSSEN, L. M. & LEDET, T. 2005. Expression levels and functional aspects of the hyaluronan receptor CD44. Effects of insulin, glucose, IGF-I, or growth hormone on human arterial smooth muscle cells. *Metabolism.* 54, (3), 287-95.

SEMENZA, G. L. 2000. HIF-1: mediator of physiological and pathophysiological responses to hypoxia. *J Appl Physiol,* 88**,** 1474-80.

SHREENIWAS, R., KOGA, S., KARAKURUM, M., PINSKY, D., KAISER, E., BRETT, J., WOLITZKY, B. A., NORTON, C., PLOCINSKI, J., BENJAMIN, W. & ET AL. 1992. Hypoxia-mediated induction of endothelial cell interleukin-1 alpha. An autocrine mechanism promoting expression of leukocyte adhesion molecules on the vessel surface. *J Clin Invest,* 90**,** 2333-9.

SMITH, T. G., BALANOS, G. M., CROFT, Q. P., TALBOT, N. P., DORRINGTON, K. L., RATCLIFFE, P. J. & ROBBINS, P. A. 2008. The increase in pulmonary arterial pressure caused by hypoxia depends on iron status. *J Physiol,* 586**,** 5999-6005.

STEINER, M. K., SYRKINA, O. L., KOLLIPUTI, N., MARK, E. J., HALES, C. A. & WAXMAN, A. B. 2009. Interleukin-6 overexpression induces pulmonary hypertension. *Circ Res.* 104, (2), 236-44.

STENMARK, K. R., DAVIE, N., FRID, M., GERASIMOVSKAYA, E. & DAS, M. 2006. Role of the adventitia in pulmonary vascular remodeling. *Physiology* 21, 134-45.

SUNDERKOTTER, C., NIKOLIC, T., DILLON, M. J., VAN ROOIJEN, N., STEHLING, M., DREVETS, D. A. & LEENEN, P. J. 2004. Subpopulations of mouse blood monocytes differ in maturation stage and inflammatory response. *J Immunol,* 172**,** 4410-7.

TALATI, M., WEST, J., BLACKWELL, T. R., LOYD, J. E. & MEYRICK, B. 2010. BMPR2 mutation alters the lung macrophage endothelin-1 cascade in a mouse model and patients with heritable pulmonary artery hypertension. *Am J Physiol Lung Cell Mol Physiol.* 299, (3), L363-73.

TAMAKI, K., SOUCHELNYTSKYI, S., ITOH, S., NAKAO, A., SAMPATH, K., HELDIN, C. H. & TEN DIJKE, P. 1998. Intracellular signaling of osteogenic protein-1 through Smad5 activation. *J Cell Physiol.* 117, (2), 355-63.

TARASEVICIENE-STEWART, L., KASAHARA, Y., ALGER, L., HIRTH, P., MC MAHON, G., WALTENBERGER, J., VOELKEL, N. F. & TUDER, R. M. 2001. Inhibition of the VEGF receptor 2 combined with chronic hypoxia causes cell death-dependent pulmonary endothelial cell proliferation and severe pulmonary hypertension. *The FASEB Journal,* 15**,** 427-438.

THOMAS, R. & LIPSKY, P. E. 1994. Human peripheral blood dendritic cell subsets. Isolation and characterization of precursor and mature antigen-presenting cells. *J Immunol,* 153**,** 4016-28.

TORSNEY, E., HU, Y. & XU, Q. 2005. Adventitial progenitor cells contribute to arteriosclerosis. *Trends Cardiovasc Med.* 15, (2), 64-8.

TOSHNER, M., VOSWINCKEL, R., SOUTHWOOD, M., AL-LAMKI, R., HOWARD, L. S., MARCHESAN, D., YANG, J., SUNTHARALINGAM, J., SOON, E., EXLEY, A., STEWART, S., HECKER, M., ZHU, Z., GEHLING, U., SEEGER, W., PEPKE-ZABA, J. & MORRELL, N. W. 2009. Evidence of dysfunction of endothelial progenitors in pulmonary arterial hypertension. *Am J Respir Crit Care Med.* 180, (8), 780-7.

TOUYZ, R. M. & SCHIFFRIN, E. L. 2004. Reactive oxygen species in vascular biology: implications in hypertension. *Histochem Cell Biol,* 122**,** 339-52.

TSAPOURNIOTI, S., MYLONIS, I., HATZIEFTHIMIOU, A., IOANNOU, M. G., STAMATIOU, R., KOUKOULIS, G. K., SIMOS, G., MOLYVDAS, P. A., PARASKEVA, E., 2013. TNFa induces expression of HIF-1a mRNA and protein but inhibits hypoxic stimulation of HIF-1 transcriptional activity in airway smooth muscle cells. *J Cell Physiol.* 228, (8), 1745-53.

TSOUKNOS, A., NASH, G. B. & RAINGER, G. E. 2003. Monocytes initiate a cycle of leukocyte recruitment when cocultured with endothelial cells. *Atherosclerosis,* 170**,** 49-58.

TUDER, R. M., GROVES, B., BADESCH, D. B. & VOELKEL, N. F. 1994. Exuberant endothelial cell growth and elements of inflammation are present in plexiform lesions of pulmonary hypertension. *Am J Pathol,* 144**,** 275-85.

VOELKEL, N. F. & TUDER, R. 1994. Interleukin-1 receptor antagonist inhibits pulmonary hypertension induced by inflammation. *Ann N Y Acad Sci,* 725**,** 104-9.

VOELKEL, N. F., TUDER, R. M., BRIDGES, J. & AREND, W. P. 1994. Interleukin-1 receptor antagonist treatment reduces pulmonary hypertension generated in rats by monocrotaline. *Am J Respir Cell Mol Biol,* 11**,** 664-75.

WALLACE, C. S. & TRUSKEY, G. A. 2010. Direct-contact co-culture between smooth muscle and endothelial cells inhibits TNF-alpha-mediated endothelial cell activation. *Am J Physiol Heart Circ Physiol.* 299, (2), H338-46.

WALMSLEY, S. R., PRINT, C., FARAHI, N., PEYSSONNAUX, C., JOHNSON, R. S., CRAMER, T., SOBOLEWSKI, A., CONDLIFFE, A. M., COWBURN, A. S., JOHNSON, N. & CHILVERS, E. R. 2005. Hypoxia-induced neutrophil survival is mediated by HIF-1alpha-dependent NF-kappaB activity. *J Exp Med.* 201, (1), 105-15.

WANG, G. L., JIANG, B. H., RUE, E. A. & SEMENZA, G. L. 1995. Hypoxia-inducible factor 1 is a basic-helix-loop-helix-PAS heterodimer regulated by cellular O2 tension. *Proceedings of the National Academy of Sciences,* 92**,** 5510-5514.

WANG, Z., KONG, L., KANG, J., VAUGHN, D. M., BUSH, G. D., WALDING, A. L., GRIGORIAN, A. A., ROBINSON, J. S., JR. & NAKAYAMA, D. K. 2011. Interleukin-lbeta induces migration of rat arterial smooth muscle cells through a mechanism involving increased matrix metalloproteinase-2 activity. *J Surg Res.* 169, (2), 328-96.

WEBER, C., BELGE, K. U., VON HUNDELSHAUSEN, P., DRAUDE, G., STEPPICH, B., MACK, M., FRANKENBERGER, M., WEBER, K. S. & ZIEGLER-HEITBROCK, H. W. 2000. Differential chemokine receptor expression and function in human monocyte subpopulations. *J Leukoc Biol,* 67**,** 699-704.

WIENER, L., SANTAMORE, W. P., VENKATASWAMY, A., PLZAK, L. & TEMPLETON, J. 1982. Postoperative monitoring of myocardial oxygen tension: experience in 51 coronary artery bypass patients. *Clin Cardiol,* 5**,** 431-5.

WONG, H. R., FINDER, J. D., WASSERLOOS, K., LOWENSTEIN, C. J., GELLER, D. A., BILLIAR, T. R., PITT, B. R. & DAVIES, P. 1996. Transcriptional regulation of iNOS by IL-1 beta in cultured rat pulmonary artery smooth muscle cells. *Am J Physiol,* 271**,** L166-71.

WU, S. N. 2003. Large-conductance Ca2+- activated K+ channels:physiological role and pharmacology. *Curr Med Chem,* 10**,** 649-61.

WU, X. H., QIAN, C. & YUAN, K. 2011. Correlations of hypoxia-inducible factor-1alpha/hypoxia-inducible factor-2alpha expression with angiogenesis factors expression and prognosis in non-small cell lung cancer. *Chin Med J (Engl),* 124**,** 11-8.

WYKOFF, C. C., PUGH, C. W., MAXWELL, P. H., HARRIS, A. L. & RATCLIFFE, P. J. 2000. Identification of novel hypoxia dependent and independent target genes of the von Hippel-Lindau (VHL) tumour suppressor by mRNA differential expression profiling. *Oncogene,* 19**,** 6297-305.

XU, W., KOECK, T., LARA, A. R., NEUMANN, D., DIFILIPPO, F. P., KOO, M., JANOCHA, A. J., MASRI, F. A., ARROLIGA, A. C., JENNINGS, C., DWEIK, R. A., TUDER, R. M., STUEHR, D. J. & ERZURUM, S. C. 2007. Alterations of cellular bioenergetics in pulmonary artery endothelial cells. *Proc Natl Acad Sci U S A.* 104, (4), 1342-7.

YANG, X., SHEARES, K. K., DAVIE, N., UPTON, P. D., TAYLOR, G. W., HORSLEY, J., WHARTON, J. & MORRELL, N. W. 2002. Hypoxic induction of cox-2 regulates

proliferation of human pulmonary artery smooth muscle cells. *Am J Respir Cell Mol Biol,* 27**,** 688-96.

YOSHIDA, Y., TANAKA, S., UMEMORI, H., MINOWA, O., USUI, M., IKEMATSU, N., HOSODA, E., IMAMURA, T., KUNO, J., YAMASHITA, T., MIYAZONO, K., NODA, M., NODA, T. & YAMAMOTO, T. 2000. Negative regulation of BMP/Smad signaling by Tob in osteoblasts. *Cell,* 103**,** 1085-97.

YU, A. Y., SHIMODA, L. A., IYER, N. V., HUSO, D. L., SUN, X., MCWILLIAMS, R., BEATY, T., SHAM, J. S., WIENER, C. M., SYLVESTER, J. T. & SEMENZA, G. L. 1999. Impaired physiological responses to chronic hypoxia in mice partially deficient for hypoxia-inducible factor 1alpha. *J Clin Invest,* 103**,** 691-6.

YUAN, X. J., WANG, J., JUHASZOVA, M., GAINE, S. P. & RUBIN, L. J. 1998. Attenuated K+ channel gene transcription in primary pulmonary hypertension. *Lancet,* 351**,** 726-7.

ZHANG, Y., TALWAR, A., TSANG, D., BRUCHFELD, A., SADOUGHI, A., HU, M., OMONUWA, K., CHENG, K. F., AL-ABED, Y. & MILLER, E. J. 2012. Macrophage migration inhibitory factor mediates hypoxia-induced pulmonary hypertension. *Mol Med.* 18, (1), 215-23.

ZHANG, Z., CHU, G., WU, H. X., ZOU, N., SUN, B. G. & DAI, Q. Y. 2011. IL-8 reduces VCAM-1 secretion of smooth muscle cells by increasing p-ERK expression when 3-D co-cultured with vascular endothelial cells. *Clin Invest Med,* 34**,** E138-46.

ZHAO, Y., GLESNE, D. & HUBERMAN, E. 2003. A human peripheral blood monocyte-derived subset acts as pluripotent stem cells. *Proc Natl Acad Sci U S A.* 100, (5), 2426-31.

ZIEGLER-HEITBROCK, H. W., PASSLICK, B. & FLIEGER, D. 1988. The monoclonal antimonocyte antibody My4 stains B lymphocytes and two distinct monocyte subsets in human peripheral blood. *Hybridoma,* 7**,** 521-7.

7 APPENDICES

7.1 Appendix I

Cytokine	Coating Ab stock	Coating Ab dilution	Standard stock	Standard dilution	Biotinylated Ab stock	Biotinylated Ab dilution
Interleukin-8	stock 720 µg /ml	use at 4 µg /ml, 55.5 µl in 10 ml	stock 100 ng /ml	use at 2000 pg/ml, 10 µl in 500 µl	stock 3.6 µg /ml	use at 20 ng /ml, 55.5 µl in 10 ml
Interleukin-6	stock 360 µg /ml	use at 2 µg /ml, 55.5 µl in 10 ml	stock 120 ng /ml	use at 600 pg /ml, 2.5 µl in 500 µl	stock 9 µg /ml	use at 50 ng /ml, 55.5 µl in 10 ml
Interleukin-1β	stock 720 µg /ml	use at 4 µg /ml, 55.5 µl in 10 ml	stock 75 ng /ml	use at 250 pg /ml, 2 in 20 dilution then 17 µl in 500 µl	stock 36 µg /ml	use at 200 ng /ml, 55.5 µl in 10 ml
Interleukin-10	stock 360 µg /ml	use at 2 µg /ml, 55.5 µl in 10 ml	stock 95 ng /ml	use at 2000 pg/ml, 10.5 µl in 500 µl	stock 27 µg /ml	use at 150 ng /ml, 55.5 µl in 10 ml
RANTES	stock 180 µg /ml	use at 1 µg /ml, 55.5 µl in 10 ml	stock 120 ng /ml	use at 1000 pg /ml, 4.2 µl in 500 µl	stock 3.6 µg /ml	use at 20 ng /ml, 55.5 µl in 10 ml
VEGF	stock 180 µg /ml	use at 1 µg /ml, 55.5 µl in 10 ml	stock 110 ng /ml	use at 2000 pg /ml, 9 µl in 500 µl	stock 18 µg /ml	use at 100 ng /ml, 55.5 µl in 10 ml
VEGFR1	stock 720 µg /ml	use at 4 µg /ml, 55.5 µl in 10 ml	stock 440 ng /ml	use at 10,000 pg /ml, 11.4 µl in 500 µl	stock 27 µg /ml	use at 150 ng /ml, 55.5 µl in 10 ml
BMP4	stock 360 µg /ml	use at 2 µg /ml, 55.5 µl in 10 ml	stock 80 ng /ml	use at 1000 pg /ml, 6.25 µl in 500 µl	stock 180 µg /ml	use at 1 µg /ml, 55.5 µl in 10 ml
OPG	stock 360 µg /ml	use at 2 µg /ml, 55.5 µl in 10 ml	stock 105 ng /ml	use at 4000 pg /ml, 19 µl in 500 µl	stock 36 µg /ml	use at 200 ng /ml, 55.5 µl in 10 ml
TGF-β	stock 360 µg /ml	use at 2 µg /ml, 55.5 µl in 10 ml	stock 220 ng /ml	use at 2000 pg /ml, 4.55 µl in 500 µl	stock 54 µg /ml	use at 300 ng /ml, 55.5 µl in 10 ml

ELISA antibody concentrations as according to manufacturers' instructions (R&D Systems Inc.).

7.2 Appendix II

> 99 % Glycerol (Sigma-Aldrich Ltd)	3 ml
Deionised water	4800 µl
1 M Tris-HCl (pH 7.4) (Bio-Rad Laboratories)	100 µl
100 mM sodium orthovanadate	100 µl
10 % SDS (Sigma-Aldrich Ltd)	1 ml
Protease inhibitors in water (Hoffmann-La Roche Ltd)	1 ml
Total volume	**10 ml**

Recipe for making sodium orthovanadte protein lysis buffer

7.3 Appendix III

Resolving Gel

8 % Gel	1 gel	2 gels	3 gels	4 gels
Water	8 ml	12 ml	16 ml	20 ml
40 % Acrylamide (Bio-Rad Laboratories Ltd.)	3 ml	4.5 ml	6 ml	7.5 ml
1.5 M Tris-Hcl pH 8 (Bio-Rad Laboratories Ltd.)	3.8 ml	5.7 ml	7.6 ml	9.5 ml
20 % SDS (Sigma-Aldrich Ltd.)	7.5 µl	112.5 µl	150 µl	187.5 µl
20 % APS	150 µl	225 µl	300 µl	375 µl
TEMED (Bio-Rad Laboratories Ltd.)	6 µl	9 µl	12 µl	15 µl

Stacking Gel

8 % Gel	1 gel	2 gels	3 gels	4 gels
Water	3 ml	6 ml	9 ml	12 ml
40 % Acrylamide (Bio-Rad Laboratories Ltd.)	620 µl	1240 µl	1860 µl	2480 µl
0.5 M Tris-Hcl pH 6.8 (Bio-Rad Laboratories Ltd.)	1260 µl	2520 µl	3780 µl	5040 µl
20 % SDS (Sigma-Aldrich Ltd.)	25 µl	50 µl	75 µl	100 µl
20 % APS	50 µl	100 µl	150 µl	200 µl
TEMED (Bio-Rad Laboratories Ltd.)	5 µl	10 µl	15 µl	20 µl

Recipes for making 8 % SDS- PAGE gels

7.4 Appendix IV

10 x Running buffer stocks

Glycine (Fisher Scientific)	190 g
Tris Base (Fisher Scientific)	30.3 g
20 % SDS (Sigma-Aldrich Ltd.)	50 ml
deionised water	to 1 litre

Dilute to 1 x solution before use

Recipe for making running buffer for western blots

7.5 Appendix V

10 x Transfer buffer stocks

Glycine (Fisher Scientific)	14.5 g
Tris Base (Fisher Scientific)	29 g
20 % SDS (Sigma-Aldrich Ltd.)	9.25 ml
deionised water	to 400 ml

immediately before use make 1 x solution

10 x transfer buffer	100 ml
Methanol (VWR International Ltd.)	200 ml
deionised water	700 ml

Recipe for making transfer buffer for Western blots

7.6 Appendix VI

Antibody	Dilution
HIF-1 α (Novus Biologicals, LLC), NB100-105, mouse monoclonal	1 in 500, 8 µl in 4 ml 5 % Marvel in TBS-Tween
HIF-2 α (Novus Biologicals, LLC), NB100-132, mouse monoclonal	1 in 200, 20 µl in 4 ml 5 % Marvel in TBS-Tween
Actin (Sigma-Aldrich Ltd.), A2668, rabbit polyclonal	1 in 1000, 4 µl in 4 ml 5 % Marvel in TBS-Tween

Western blot antibodies and dilutions used